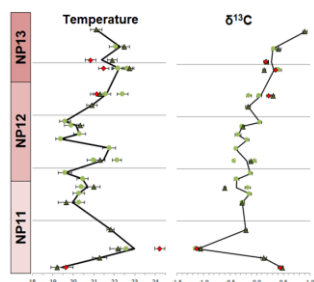


# Isotopic study of the early Eocene paleoecology and paleoenvironment in Aktulagay

The Aktulagay Section, Kazakhstan



**Steven TESSEUR**

Supervisor: Prof. R.P. Speijer  
[KU Leuven](#)

Co-supervisor: Prof. P. Claeys  
[VUB](#)

Co-supervisor: Prof. E. Steurbaut  
[KBIN](#)

Mentors: A. Deprez and S. D'haenens  
[KU Leuven](#)

Thesis presented in  
 fulfillment of the requirements  
 for the degree of Master of Science  
 in de geologie



© Copyright by KU Leuven

Without written permission of the promotors and the authors it is forbidden to reproduce or adapt in any form or by any means any part of this publication. Requests for obtaining the right to reproduce or utilize parts of this publication should be addressed to KU Leuven, Faculteit Wetenschappen, Geel Huis, Kasteelpark Arenberg 11 bus 2100, 3001 Leuven (Heverlee), Telephone +32 16 32 14 01.

A written permission of the promotor is also required to use the methods, products, schematics and programs described in this work for industrial or commercial use, and for submitting this publication in scientific contests.





## Preface

The main goal of this paper was to identify the microhabitat of several early Eocene species and to study the early Eocene Paleoenvironment in the northern Peri-Tethys. I chose this subject above others because of my general interest in the geological history and my particular interest for isotopic data. I am pleased with the result of my work and did not regret my choice.

I would therefore like to thank my supervisor Prof. Robert P. Speijer for entrusting me with this subject and for his continuous support during the entire year.

I further want to thank my co-promoter Prof. Philippe Claeys for allowing me to use the mass spectrometer at the VUB.

I want to thank my mentor Arne Deprez for frequently aiding me with the foraminifer taxonomy, for his assistance with SEM-imaging and especially for frequently losing card games during the lunch breaks.

I want to thank my mentor Simon D'haenens for his aid with the foraminifer taxonomy and particularly for his aid with the mass spectrometer at the VUB. I also want to thank him for his optimism and for his interest in my research.

I want to thank my 'not official' mentor Peter Stassen, for his aid with foraminifer taxonomy, his constructive (sometimes destructive) criticism and especially his amusing everlasting pessimism. (It was awesome to learn from him in August 2012 that I wouldn't make the deadline of June 2013, I guess he was right).

I further want to thank Arne Deprez, Simon D'haenens and Peter Stassen for the interesting (and amusing) discussions we had. Our debates demonstrated that for each scientific problem at least 4 different hypotheses exist.

I want to thank Maïté Van Rampelbergh for kindly assisting me with the mass spectrometer at the VUB.

I want to thank other people that supported me during the year, especially my friend Arnaud Vander Velpen who had similar stress symptoms and occupations. I also want to thank my friends Eric Schouteden, Jeroen Van Woensel, Maarten Panis, Sien Benoit and An Van de Winkel for their support.

Finally I want to thank my mom for providing me with sufficient organic matter and fluids to sustain my brain, my dog for being my dog (it has no specific function), my dad for being my dad (his function is rather gaming related) and DJs Headhunterz, Wildstylez, Ran-D, Noisecontrollers, Frontliner, Digital Punk, Scope, Coone, Psyko Punkz, Zatox, Chain reaction, Alpha Twins, Isaac, Crypsis, Tatanka, D-Block, S-te-fan, Brennan Heart, Adaro, Gunz fo Hire, Neilio, TNT, Zhangar, Da Tweekaz, The Viper, The Playah, Scary Clowns and Radical Redemption for improving my environmental conditions especially between 22:00 and 4:00.

## Abstract

The early Eocene paleoclimate is known for its extraordinary warm temperatures, especially during the EECO. However very limited data is currently available to study the world paleotemperature distribution. In addition many questions exist concerning the habitats of the foraminifers that lived in the early Eocene. Habitats are often predicted based on morphology but this has been demonstrated to be only accurate 75% of the time (Buzas *et al.*, 1993). The paleoecology and the paleoenvironment of the early Eocene were investigated in this study based on a section belong in to the outer shelf setting (at 125 to 200 m paleodepth) within the Northern Peri-Tethys. This study provides 140 isotopic measurements for both  $\delta^{13}\text{C}$  and  $\delta^{18}\text{O}$  of planktic and benthic foraminifers. The isotopes can be used to predict paleotemperatures and to predict the microhabitat of foraminifers. The foraminifers were derived from 24 samples from the Alashen Formation and the Aktulagay Formation of the Aktulagay Section in West Kazakhstan spread over the biostratigraphic interval NP11 to middle NP13 (ca. 54-50 Ma). The preservation of the foraminifers was verified with binocular microscopy and SEM-imaging and was confirmed to be generally very good for the benthic foraminifers and good to moderate for the planktic foraminifers. Based on the  $\delta^{13}\text{C}$  results *Anomalinoidea acutus*, *Anomalinoidea rubiginosis*, *Anomalinoidea zitteli*, *Cibicidoides cf. rigidus*, *Cibicidoides decoratus* and *Cibicidoides rigidus* were identified as epibenthic species. *Cibicidoides cf. decoratus*, *Cibicidoides sp. 1*, *Lenticulina spp.*, *Marginulinopsis spp.*, *Nuttallides truempyi*, *Percultazonaria sp. 1*, *Pyramidulina sp. 1*, *Spiroloculina sp. 1*, *Stainforthia sp. 1* and *Turrilina brevispira* were identified as either epibenthic or shallow endobenthic species. *Alabamina midwayensis*, *Allomorphina sp. 1*, *Anomalinoidea cf. praeacutus*, *Aragonia aragonensis*, *Bulimina (aff.) midwayensis*, *Bulimina kugleri*, *Loxostomoides applinae*, *Oridorsalis plummerae*, *Pulsiphonina prima*, *Ramulina sp. 1*, *Stilostomella sp. 1*, *Uvigerina elongata* and *Valvulineria scrobiculata* were identified as shallow endobenthic species and *Bulimina aksuatica*, *Bulimina cf. thanetensis*, *Coryphostoma spp.*, *Dentalina sp. 1* and *Nodosaria sp. 1* were identified as deep endobenthic species. Furthermore the  $\delta^{18}\text{O}$  and the  $\delta^{13}\text{C}$  results of *Lenticulina spp.*, *Marginulinopsis spp.*, *Nodosaria sp. 1* and *Percultazonaria sp. 1* were considered strongly affected by kinetic disequilibrium calcite precipitation, a hypothesis that was already proposed for *Lenticulina spp.* by Wendler *et al.* (2013). The isotopic results further indicated that *Anomalinoidea acutus*, *Coryphostoma spp.*, *Turrilina brevispira* and *Uvigerina elongata* were tolerant to low oxygen conditions while other species like *Bulimina aksuatica*, *Cibicidoides cf. decoratus* and *Loxostomoides applinae* were rather unsuccessful competing with other species under low oxygen conditions. Finally strong indications were presented to reject the hypothesis that a pH gradient within the sediment has significant influence on the  $\delta^{18}\text{O}$  values of foraminifers (proposed by e.g. Bemis *et al.*, 1998; Schmiedel *et al.*, 2004; Friedrich *et al.*, 2006; Wendler *et al.*, 2013), which is in support of e.g. McCorkle *et al.* (1997) and Fontanier *et al.* (2008). It was concluded that  $\delta^{18}\text{O}$  is mainly a reflection of their food preference and vital effects instead of their microhabitat. Concerning the paleoenvironment, the paleotemperature at the sea floor was estimated to vary between 19 °C and 24 °C ( $\pm 1.8$  °C). The thermocline temperatures were estimated to be 0 °C to 2.5 °C higher. The mixed layer temperature could

not be estimated due to the high ( $\pm 9$  °C) uncertainty on the temperature predictions which is mainly a consequence of the unknown salinity. The highest seafloor temperatures were associated with the nearby presence of a hyperthermal (likely ETM2) and with the EECO. The seafloor  $\delta^{13}\text{C}$  record revealed a gradual increasing  $\delta^{13}\text{C}$  trend from middle NP11 to middle NP 13 ( $\Delta\delta^{13}\text{C} = 1\text{‰}$ ) in Aktulagay which was considered a reflection of the global deep sea  $\delta^{13}\text{C}$  trend after comparison with Cramer *et al.* (2009). In conclusion this study provides microhabitat and oxygen tolerance information of several benthic foraminifers that can aid in the reconstruction of the paleoassemblages and the paleoenvironment, furthermore our study provides data for paleotemperature reconstructions of the Peri-Tethyan Region. Finally our results discourage the use of  $\delta^{18}\text{O}$  for habitat interpretations and discourage the use of isotopic measurements of *Lenticulina spp.*, *Marginulinopsis spp.*, *Nodosaria sp. 1* and *Percultazonaria sp. 1* for paleoenvironmental reconstructions.

## Samenvatting

Het paleoklimaat van het vroege Eoceen is gekend voor de bijzonder warme temperaturen, vooral tijdens de EECO. Slechts een beperkte hoeveelheid data is vandaag beschikbaar om de vroeg Eocene temperatuur distributie van onze planeet te bestuderen. Daarnaast zijn er nog veel vragen in verband met de habitat van verscheidene benthische foraminiferen die leefden tijdens het vroege Eoceen. Hun habitats worden vaak afgeleid van hun schaal morfologie maar Buzas *et al.* (1993) toonde reeds aan dat dit slechts accuraat is voor 75% van de soorten. Zowel de paleoecologie als het paleomilieu tijdens het vroege Eoceen werden in deze studie onderzocht op een locatie die behoorde tot het vroegere continentaal plat (125 tot 200 m waterdiepte) van de noordelijke Peri Tethys. Deze studie omvat 140 isotopen metingen van zowel  $\delta^{13}\text{C}$  als  $\delta^{18}\text{O}$  op benthische en planktische foraminiferen. Deze isotopen werden gebruikt om paleotemperaturen in deze regio te reconstrueren en om de microhabitats van de benthische foraminiferen te bestuderen. De foraminiferen zijn afkomstig van 24 stalen verspreid over de Alashan Formatie en de Aktulagay Formatie in de Aktulagay Sectie van West Kazachstan. Deze formaties behoren tot het biostratigrafisch interval NP11 tot midden NP13 (ca. 54-50 Ma). De preservatie van de foraminiferen werd gecontroleerd met behulp van een binoculaire microscoop en SEM-foto's. De preservatie van de benthische foraminiferen werd in het algemeen als zeer goed beschouwd. De preservatie van planktische foraminiferen werd eerder aanzien als matig tot goed. Gebaseerd op de  $\delta^{13}\text{C}$  resultaten werden *Anomalinoidea rubiginosa*, *Anomalinoidea zitteli*, *Cibicidoides cf. rigidus*, *Cibicidoides decoratus* en *Cibicidoides rigidus* geïdentificeerd als epibenthische soorten. *Cibicidoides cf. decoratus*, *Cibicidoides sp. 1*, *Lenticulina spp.*, *Marginulinopsis spp.*, *Nuttallides truempyi*, *Percultazonaria sp. 1*, *Pyramidulina sp. 1*, *Spiroloculina sp. 1*, *Stainforthia sp. 1* en *Turrilina brevispira* werden geïdentificeerd als ofwel epibenthische ofwel ondiep endobenthische soorten. *Alabama midwayensis*, *Allomorphina sp. 1*, *Anomalinoidea cf. praeacutus*, *Aragonia aragonensis*, *Bulimina (aff.) midwayensis*, *Bulimina kugleri*, *Loxostomoides applinae*, *Oridorsalis plummerae*, *Pulsiphonina prima*, *Ramulina sp. 1*, *Stilostomella sp. 1*, *Uvigerina elongata* en *Valvulineria scrobiculata* werden geïdentificeerd als ondiep endobenthische soorten en *Bulimina aksuatica*, *Bulimina cf. thanetensis*, *Coryphostoma spp.*, *Dentalina sp. 1* en *Nodosaria sp. 1* werden geïdentificeerd als diep endobenthische soorten. Verder werd geconcludeerd dat de  $\delta^{18}\text{O}$  en de  $\delta^{13}\text{C}$  resultaten van *Lenticulina spp.*, *Marginulinopsis spp.*, *Nodosaria sp. 1* en *Percultazonaria sp. 1* sterk beïnvloed zijn door kinetische disequilibrium precipitatie. Deze hypothese werd reeds voorgesteld voor *Lenticulina spp.* door Wendler *et al.* (2013). Daarnaast toonden de resultaten aan dat *Anomalinoidea acutus*, *Coryphostoma spp.*, *Turrilina brevispira* en *Uvigerina elongata* tolerant zijn voor lage zuurstof gehalten terwijl andere soorten zoals *Bulimina aksuatica*, *Cibicidoides cf. decoratus* en *Loxostomoides applinae* niet langer succesvol zijn onder deze omstandigheden om te concurreren met andere soorten. Tenslotte werden er sterke aanwijzingen gevonden om de hypothese te verwerpen dat de pH gradient in het sediment een sterke invloed heeft op de  $\delta^{18}\text{O}$  waarden van de foraminiferen (Deze hypothese was voorgesteld door onder andere Bemis *et al.*, 1998; Schmiedl *et al.*, 2004; Friedrich *et al.*, 2006; Wendler *et al.*, 2013), het verwerpen van deze hypothese is in lijn met de conclusies van McCorkle *et al.* (1997) en

Fontanier *et al.* (2008). Er werd geconcludeerd dat  $\delta^{18}\text{O}$  hoofdzakelijk vitale effecten en voedselvoorkeur reflecteerd.

In verband met het paleomilieu werden bodemwatertemperaturen voorspeld variërend tussen 19 °C en 24 °C ( $\pm 1.8$  °C). De thermocline temperaturen werden 0 °C tot 2.5 °C hoger geschat. Een accurate temperatuursvoorspelling van het oppervlakte water bleek onmogelijk door de hoge onzekerheid ( $\pm 9$  °C) die gerelateerd is aan de onbekende saliniteit. De hoogste bodemwater temperaturen werden geassocieerd met de nabijheid van een hyperthermaal (waarschijnlijk ETM2) en met de EECO. De  $\delta^{13}\text{C}$  waarden van het bodemwater toonden een gradueel stijgende  $\delta^{13}\text{C}$  trend van midden NP11 tot midden NP 13 ( $\Delta\delta^{13}\text{C} = 1\text{‰}$ ) in Aktulagay. Dit werd beschouwd als een weerspiegeling van de globale diepzee  $\delta^{13}\text{C}$  trend op basis van een vergelijking met de data van Cramer *et al.* (2009).

In conclusie biedt deze studie informatie omtrent de microhabitat en de zuurstofgehalte tolerantie van verschillende benthische foraminiferen. Deze kunnen helpen in de reconstructie van paleoassemblages en van het paleomilieu. Bovendien biedt deze studie temperatuur data aan die kan gebruikt worden voor het genereren van paleotemperatuurreconstructies van de Peri-Tethys Regio. Ten slotte ontmoedigen de resultaten het gebruik van  $\delta^{18}\text{O}$  waarden voor de habitat interpretatie van foraminiferen en ontmoedigen de resultaten het gebruik van isotopen metingen van *Lenticulina spp.*, *Marginulinopsis spp.*, *Nodosaria sp. 1* and *Percultazonaria sp. 1* voor paleomilieu reconstructies.

## **List of abbreviations**

CIE = Carbon Isotope Excursion

e.c. = equilibrium calcite

EECO = Early Eocene Climatic Optimum

ETM = Eocene Thermal Maximum

DIC = Dissolved Inorganic Carbon

NP11 = Nannoplankton zone 11

POM = Primary Organic Membrane

sp. = species (singular)

spp. = species (plural)

sw = seawater

# Table of Contents

Preface .....	I
Abstract .....	II
Samenvatting.....	IV
List of abbreviations .....	VI
1 Introduction.....	1
2 Aktulagay and the Tethyan region .....	3
2.1 Geographical and geological position of Aktulagay .....	3
2.2 Tectonic and paleogeographic history of the Tethyan Region .....	4
2.2.1 Introduction.....	4
2.2.2 The Carboniferous.....	4
2.2.3 The Permian .....	5
2.2.4 The Triassic and the Jurassic.....	6
2.2.5 The Cretaceous .....	7
2.2.6 The Cenozoic Era & the Ypresian .....	7
2.3 The paleoclimate .....	10
2.3.1 The paleotemperature during the Ypresian.....	10
2.3.2 Hyperthermal events .....	13
2.4 Lithology and lithostratigraphy.....	15
2.4.1 Introduction.....	15
2.4.2 Unit A (The Alashen Formation) based on King <i>et al.</i> (submitted).....	16
2.4.3 Unit B (Aktulagay Formation) based on King <i>et al.</i> (submitted) .....	16
2.4.4 Unit C (Tolagaysor Formation) based on King <i>et al.</i> (submitted).....	16
2.4.5 Parasequences and omission surfaces.....	16
2.5 Biostratigraphy.....	19
2.5.1 Introduction.....	19
2.5.2 Biostratigraphy.....	19
2.5.3 Correlating Biostratigraphy into an age model .....	19
2.6 Paleontology.....	24

2.6.1	Dinoflagellate cysts.....	24
2.6.2	Calcareous nannofossils.....	24
2.6.3	Ostracods.....	24
2.6.4	Echinoids, fish remains, bivalves and gastropods (Pteropods).....	24
2.6.5	Shark and ray teeth .....	25
2.6.6	Planktic foraminifers .....	27
2.6.7	Benthic foraminifers .....	27
3	The isotopic signature of foraminifers .....	29
3.1	Introduction .....	29
3.2	Parameters determining the $\delta^{13}\text{C}$ signature .....	29
3.2.1	Temperature .....	29
3.2.2	Geochemistry: DIC and the pH.....	29
3.2.3	Vital effects .....	30
3.2.4	Food preference (benthic foraminifers) .....	30
3.2.5	Symbionts & irradiance levels (planktic foraminifers).....	31
3.3	Parameters determining the $\delta^{18}\text{O}$ signature.....	31
3.3.1	Temperature .....	31
3.3.2	Geochemistry: salinity and the pH.....	31
3.3.3	Vital effects .....	32
3.4	Other parameters.....	32
3.4.1	The sampled time interval and the sample size .....	32
3.4.2	Post depositional alteration or contamination.....	32
4	Material and methods.....	33
4.1	Sampling and preparation.....	33
4.2	Work strategy.....	34
4.2.1	Isotope paleoecology.....	34
4.2.2	The isotopic record .....	34
4.3	Scanning Electron Microscopy (SEM) .....	36
4.4	The Finnigan Mass Spectrometer DeltaPlus .....	36



4.5	Correcting the isotopic measurements and their standard deviations .....	37
4.5.1	Accuracy .....	37
4.5.2	Precision .....	37
4.6	Results – the section .....	39
4.6.1	The range of the $\delta^{13}\text{C}$ and $\delta^{18}\text{O}$ data .....	39
4.6.2	The $\delta^{13}\text{C}$ and $\delta^{18}\text{O}$ results over the section.....	39
5	Diagenesis & contamination.....	43
5.1	Introduction .....	43
5.2	Diagenesis of benthic foraminifers .....	44
5.2.1	Introduction .....	44
5.2.2	Results .....	44
5.2.3	<i>Anomalinoides acutus</i> .....	46
5.2.4	Other benthic foraminifers .....	48
5.2.5	Discussion .....	50
5.2.6	Summary .....	52
5.3	Diagenesis of planktic foraminifers.....	54
5.3.1	Introduction .....	54
5.3.2	Results .....	54
5.3.3	Discussion .....	55
5.3.4	The effect on $\delta^{13}\text{O}$ .....	63
5.3.5	The effect on $\delta^{13}\text{C}$ .....	65
5.3.6	Summary .....	65
5.4	Contamination .....	66
5.4.1	Introduction .....	66
5.4.2	Prevention of contamination.....	66
5.4.3	Direction of the error.....	67
5.4.4	The experiment.....	71
5.4.5	The results of the experiment.....	71
5.4.6	Summary .....	71

6	Isotope paleoecology .....	73
6.1	Results .....	73
6.1.1	The $\delta^{13}\text{C}$ values .....	73
6.1.2	The $\delta^{18}\text{O}$ values .....	74
6.1.3	The isotopic values of genera.....	74
6.2	Discussion.....	80
6.2.1	Microhabitat identification .....	80
6.2.2	Complications .....	88
6.2.3	Morphologic microhabitat interpretation .....	94
6.3	Summary.....	98
7	The epibenthic isotopic record .....	99
7.1	Introduction .....	99
7.2	Isotopic variability within a sample .....	99
7.3	Equilibrium calcite and correction factors .....	104
7.3.1	<i>Cibicidoides decoratus</i> .....	104
7.3.2	<i>Anomalinooides acutus</i> .....	104
7.3.3	<i>Anomalinooides zitteli</i> .....	105
7.4	The seafloor temperature predictions .....	108
7.5	The epibenthic $\delta^{13}\text{C}$ record .....	111
7.6	Discussion.....	112
7.6.1	Identification of CIEs and hyperthermals .....	112
7.6.2	The global $\delta^{18}\text{O}$ trend .....	112
7.6.3	The global $\delta^{13}\text{C}$ trend.....	113
7.6.4	Comparison with the isotopic data from the Kheu River Section .....	114
7.7	Summary.....	118
8	The endobenthic record .....	119
8.1	Results .....	119
8.1.1	$\Delta\delta^{13}\text{C}$ values .....	119
8.1.2	$\Delta\delta^{18}\text{O}$ values.....	119

8.2	Discussion .....	125
8.2.1	Suboxic conditions at 15.95 m .....	125
8.2.2	Rejection of the pH-microhabitat relation hypothesis .....	126
8.2.3	The microhabitat of <i>Uvigerina elongata</i> and <i>Bulimina aksuatica</i> in subunit A2 .....	129
8.2.4	The influence of hyperthermals on the foraminifer assemblage .....	129
8.2.5	<i>Pulsiphonina prima</i> .....	130
8.2.6	The consequence of migration .....	130
8.3	Summary .....	130
9	The planktic isotopic record .....	133
9.1	Ontogenetic effects and the $\delta^{18}\text{O}_{e.c}$ derived from planktic foraminifers .....	133
9.2	The $\delta^{18}\text{O}_{sw}$ prediction and the salinity of the mixed layer .....	134
9.2.1	Prediction based on Zachos <i>et al.</i> (1994) .....	135
9.3	The $\delta^{18}\text{O}_{sw}$ prediction and the salinity at the thermocline .....	138
9.4	Results .....	138
9.4.1	$\delta^{13}\text{C}$ .....	138
9.4.2	$\delta^{18}\text{O}$ and temperature .....	138
9.5	Discussion planktic foraminifer isotopic values .....	141
9.5.1	Seasonality .....	141
9.5.2	Productivity variation and fluvial water influence .....	143
9.5.3	Secondary Calcite .....	143
9.5.4	The temperature predictions .....	144
9.6	Summary .....	144
10	Conclusion .....	147
11	References .....	149
	Appendix I. : Measurements - Benthic species .....	157
	Appendix II. : Measurements - Planktic species .....	161
	Appendix III. : Preservation issues observed with binocular microscope .....	162
	Appendix IV. : Natural isotopic variability of epibenthic specimen .....	163
	Appendix V. : $\delta^{13}\text{C}$ correlation of <i>Cibicoides decoratus</i> and <i>Anomalinoidea acutus</i> .....	164

Appendix VI. : $\delta^{18}\text{O}$ correlation of <i>Cibicidoides decoratus</i> and <i>Anomalinoidea acutus</i> .....	164
Appendix VII. : $\delta^{13}\text{C}$ correlation of <i>Anomalinoidea acutus</i> and <i>Anomalinoidea zitteli</i> .....	165
Appendix VIII. : $\delta^{13}\text{C}$ correlation of <i>Cibicidoides decoratus</i> and <i>Anomalinoidea zitteli</i> .....	165
Appendix IX. : $\delta^{18}\text{O}$ correlation of <i>Anomalinoidea acutus</i> and <i>Anomalinoidea zitteli</i> .....	166
Appendix X. : $\delta^{18}\text{O}$ correlation of <i>Cibicidoides decoratus</i> and <i>Anomalinoidea zitteli</i> .....	166
Appendix XI. The clustered species of Deprez <i>et al.</i> (2012) .....	167
Appendix XII. Taxonomy.....	168

# 1 Introduction

The Ypresian [56.0 - 47.8 Ma (Gradstein *et al.*, 2012)] is the oldest stage of the Eocene series. It is known as the warmest period of the Cenozoic Era and is characterized by the occurrence of several hyperthermals which are short term global warming events. In this study the isotopic signatures ( $\delta^{18}\text{O}$  and  $\delta^{13}\text{C}$ ) of foraminifer tests will be measured. Foraminifers are small organisms that can either have a planktic habitat or a benthic habitat. Planktic species are subdivided into mixed layer species and thermocline species (living deeper). Benthic species live at the seafloor and are subdivided into epibenthic (living on or within the first centimeter of sediment) and endobenthic species (living deeper). The isotopic signature of a foraminifer test mainly reflects its (micro)habitat, its metabolism, the water temperature and the water chemistry. Therefore isotopic measurements are a valuable tool for paleoenvironmental reconstructions because they provide information about the water chemistry and temperature over the entire water column. Furthermore the isotopes are a valuable tool for paleoecology to determine the microhabitats of the benthic foraminifers. Because endobenthic and epibenthic species react differently on changing environmental parameters (e.g. the oxygen level), knowledge about the benthic microhabitats is required to interpret the relative abundance of these benthic species. In absence of isotopic data the microhabitat of benthic species is often derived from their test morphology. However the study of Buzas *et al.* (1993) demonstrated that a morphologic interpretation is only accurate 75% of the time. An isotopic study provides a more accurate determination of the microhabitat. During the Early Eocene, the Aktulagay hills of West Kazakhstan were located in the northeastern part of the Peri-Tethys Ocean, an ocean that extended from Italy to Kazakhstan. The sediments in Aktulagay were part of the outer shelf of the East European platform. In this study foraminifers from the Aktulagay hills will be isotopically studied ( $\delta^{18}\text{O}$  and  $\delta^{13}\text{C}$ ) over the biostratigraphic interval NP11 to middle NP13 (King *et al.*, submitted). Limited shelf studies of the biostratigraphic interval NP11-NP13 are currently available and most isotopic studies are limited to bulk  $\delta^{13}\text{C}$  measurements. These bulk  $\delta^{13}\text{C}$  measurements do not provide the same accuracy and precision as species specific measurements to reconstruct the paleoenvironment. The Aktulagay section has been studied before by King *et al.* (submitted), Deprez (2012) and Deprez *et al.*, (submitted). King *et al.* (submitted) provided a detailed lithologic description, a study of many types of macro- (shark teeth, pteropods ...), micro- (dinoflagellate cysts, foraminifers...) and nannofossils and a detailed biostratigraphy. Deprez (2012) and Deprez *et al.*, (submitted) studied the benthic foraminifer assemblage and determined the relative abundance of several benthic species over the section. The first objective of this study is to determine the benthic foraminifer microhabitats based on their isotopic signatures. For this part of the study many different species will be measured in 3 different samples. These 3 samples were taken from 3 different biofacies defined by Deprez (submitted) that represent different foraminifer assemblages and paleoenvironments. The second objective is to create isotopic records over the section in order to study the changing the paleoenvironment of the northern Peri Tethys Region during the Ypresian. The records will be generated for planktic species that lived in the mixed layer waters, (sub)thermocline planktic

species that lived in deeper waters, epibenthic species that lived on the sediment surface and endobenthic species that lived within the sediment. The  $\delta^{18}\text{O}$  records of both benthic and planktic foraminifers will be used to reconstruct the paleotemperature over the paleowatercolumn. The  $\delta^{13}\text{C}$  record provides information about the organic carbon flux and changes in the foraminifer microhabitat. The results of this study should provide microhabitat information for several benthic foraminifers that can aid in the reconstruction of the paleoassemblages. In addition the paleotemperature data from Aktulagay should aid future paleotemperature reconstructions of the Peri-Tethyan Region.

## 2 Aktulagay and the Tethyan region

### 2.1 Geographical and geological position of Aktulagay

The Aktulagay section is located in the western part of the Aktobe Province in West Kazakhstan at  $47^{\circ}32'31.47''\text{N}$  &  $55^{\circ}09'13.75''\text{E}$  (Figure 1). It is found 200 km northeast of the Caspian Sea and 100 km northeast of the nearest town Qulsary. On a geological map (Figure 2), the Aktulagay section is found at the southwestern boundary of hills composed of Mesozoic-Paleozoic sediments. The western hills are dominated by Jurassic and Cretaceous sediments while the eastern hills are dominated by Paleozoic sediments. The hills are cut by several rivers that eventually reach the Caspian Sea in the southwest. South and the west of the hills the landscape is mainly dominated by Quaternary plains.



Figure 1. Position Aktulagay on geographic map (Microsoft Corporation, 2013).

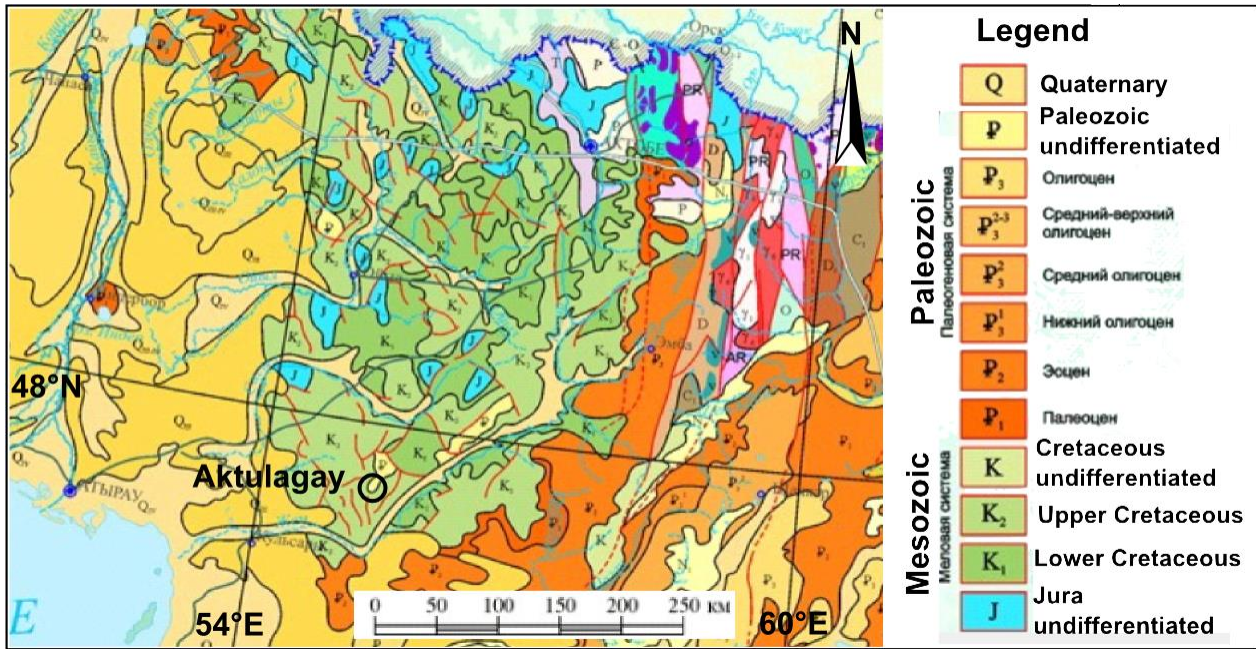


Figure 2. Projection of Aktulagay on the geological map (Geological map of Kazakhstan).

## 2.2 Tectonic and paleogeographic history of the Tethyan Region

### 2.2.1 Introduction

The tectonic and the paleogeographical history of the Tethyan region is long and complex. This paragraph will sketch this history with focus on the major events. More specific events concerning the Pre-Caspian Basin will be highlighted because Aktulagay was part of this basin for a major part of its history.

### 2.2.2 The Carboniferous

During the Carboniferous, the continental plates Kazakhstania and Siberia migrated towards Laurussia (composed of Baltica and Laurentia) until the plates collided at the end of the Carboniferous (Figure 3). The orogenesis pursued till the Trias and the Ural mountain range was formed north of Aktulagay (Gaetani *et al.*, 2003). Meanwhile, the tectonic movements caused continuous subsidence of Pre-Caspian Basin from the Devonian till the Early Permian. In this basin carbonates and clastic sediments were deposited at the margins while black shales and turbidites were deposited at larger the depths. Molasse deposits are also found on the margins of the basin related to the development of the Urals (Ulmishek, 2003). During Carboniferous time the ocean to the southwest of Kazakhstania was referred to as the Paleotethys Ocean (Scotese, 2001).



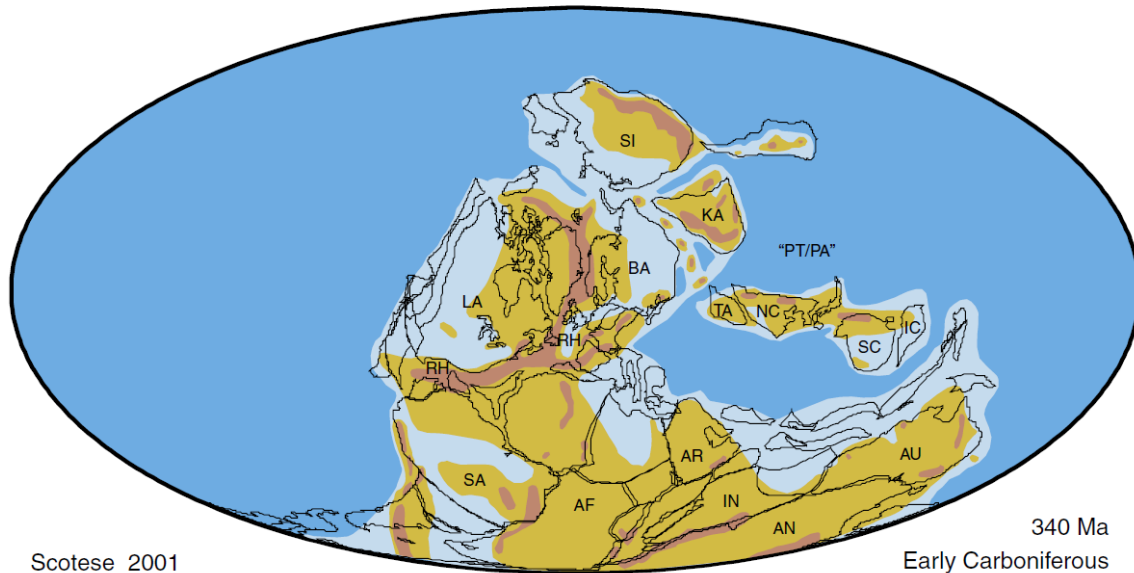


Figure 3. Early Carboniferous Pangea reconstruction. The figure shows the tectonic situation prior to the collision of Siberia and Kazakhstan with Laurussia (Baltica + Laurentia).  
 Legend: AF = Africa; AN = Antarctica; AU = Australia; AR = Arabia; **BA = Baltica**; IN = India; **KA = Kazakhstan**; LA = Laurentia; NC = North China; “PT/PA” = “Paleotethys/Paleoasian Ocean”; RH = former Rheic Ocean; SA = South America; SC = South China; **SI = Siberia**; TA = Tarim (Scotese, 2001).

### 2.2.3 The Permian

During the Permian, Laurasia and Gondwana dextrally sheared along each other (Gaetani *et al.*, 2003 & Muttoni *et al.*, 2009). In the meantime the Neotethys Ocean opened along the eastern margin of Gondwana and the Paleotethys Ocean started to subduct along the southern margin of Laurasia. Aktulagay is located near the southern border of Laurasia and positioned in the Pre-Caspian basin. (Figure 5) (Gaetani *et al.*, 2003). During the Permian the Pre-Caspian basin loses connection to the Paleotethys Ocean due to continued continental collision. This disconnection leads to the massive deposition of evaporites (mainly salts) (Ulmishek, 2003). During the late Permian the subduction zone also encompassed the region south of Aktulagay (Muttoni *et al.*, 2009). Several volcanic arcs and back arc basins came to existence in e.g. the Caucasus and Caspian Regions (Gaetani *et al.*, 2003).

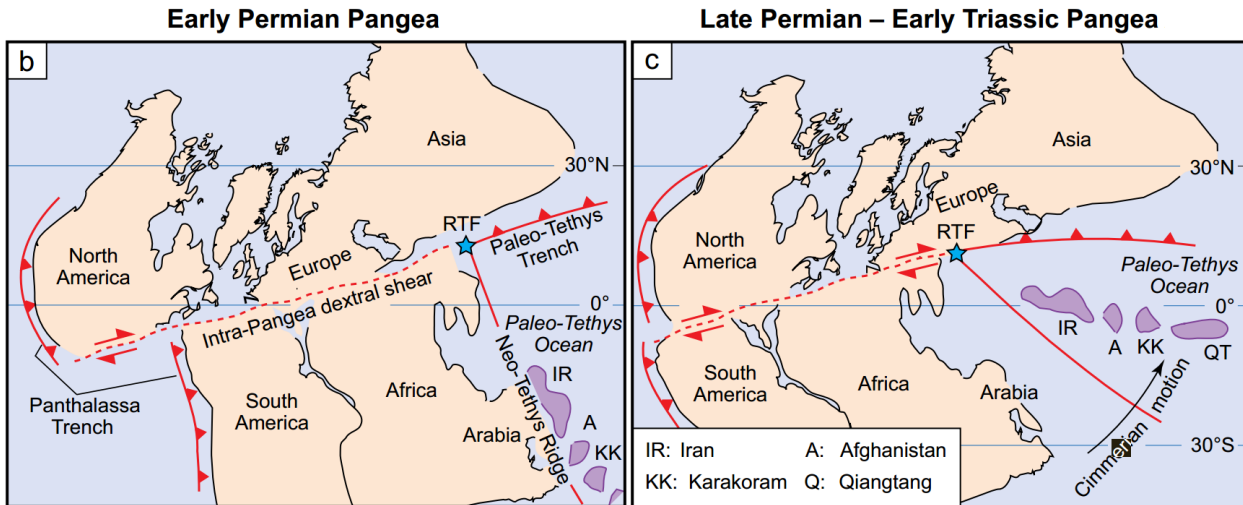


Figure 4. Tectonic history during the Permian, map from Muttoni *et al.* (2009).

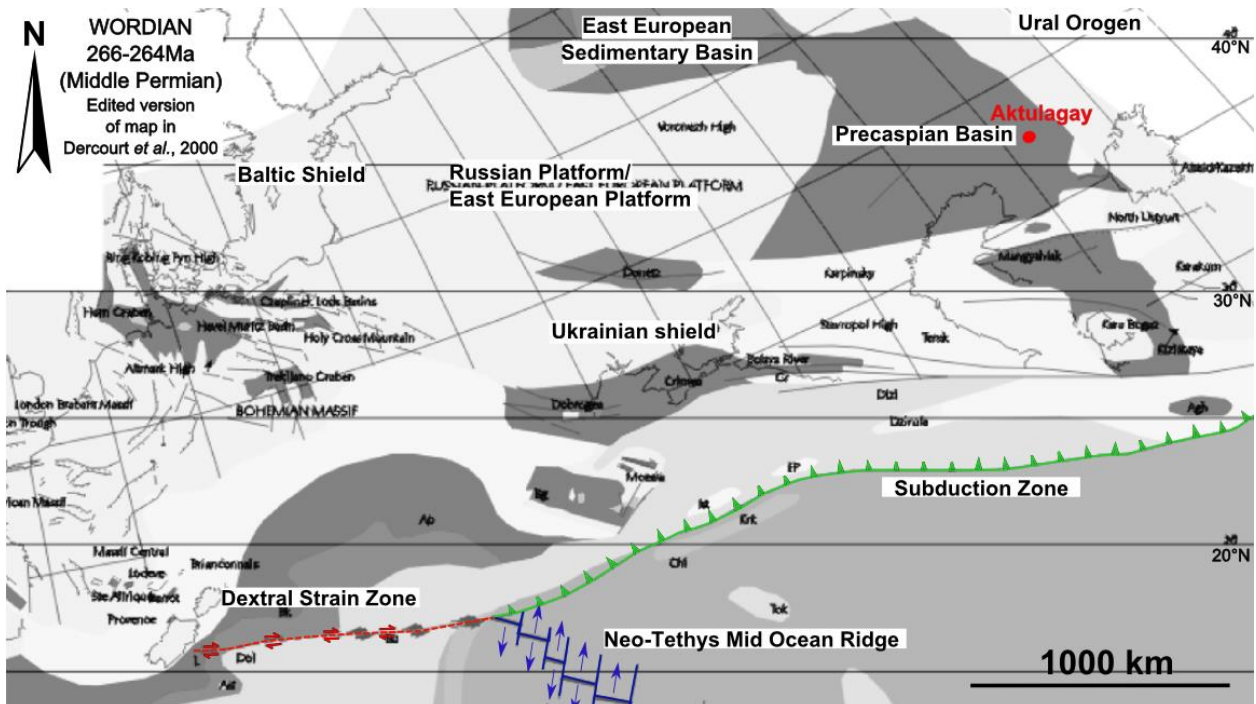


Figure 5. Paleogeographic map of the northern Tethyan Region during the Middle Permian. Original map from Dercourt *et al.* (2000). Some features were highlighted and Aktulagay is marked.

### 2.2.4 The Triassic and the Jurassic

Subduction continued during the Triassic and Jurassic time periods and convergence remained dominant in the western part of the Tethys region. This resulted in the formation of island arcs and back arc basins. Nevertheless the breakup of Pangea started and extension started along the “Tornquist-Teisseyre line” (in East Europe) and the “North African line” (Gaetani *et al.*, 2003).

During the Triassic, the Precaspian basin knows a rapid subsidence. The sediments in the basin are dominantly continental debris. But carbonates, evaporates (salt domes), shales and marls are also present in some parts of the basin. The subsidence came to an end in the Jurassic (Ulmishek, 2003).

During the Jurassic, sea level significantly rose and caused a widespread transgression in the Tethyan region. At the Middle Jurassic, Tethyan waters connected with Boreal waters and the Barents-Petchora (North Siberia) region became connected to the Tethyan Region. This later connection was possible by flooding of the foreland basins of the Urals. The Jurassic transgression caused a widespread deposition of shallow carbonate platforms on the continental shelves (Gaetani *et al.*, 2003).

### **2.2.5 The Cretaceous**

During the Cretaceous the onset towards the Alpine Orogeny started. A connection of the North Sea with the Tethys Region existed in periods with maximum sea level, although it was sometimes disturbed by orogenic activity (Gaetani *et al.*, 2003). High sea level in combination with subsidence caused a wide marine transgression on the African Continent, covering e.g. former Tunisia, Libya and Egypt (Gaetani *et al.*, 2003).

### **2.2.6 The Cenozoic Era & the Ypresian**

During the Cenozoic era, the Peri-Tethyan regions were progressively cut off marine connections. Nevertheless due to the extremely high sea level in the Early Eocene, a connection of the Tethys Ocean with the North Sea could still be established across the Polish basin (Figure 6 & Figure 8) (Gaetani *et al.* 2003; Steurbaut, 2011; King *et al.*, submitted). Furthermore the Turgai Strait was still open in the Early Eocene and allowed a connection between the Tethyan Region and the Arctic sea. This connection could possibly lead to the inflow of colder water in the Tethyan region. Whether or not this is the case, it is still unresolved whether the Aktulagay region was directly influenced by the currents in the Turgai Strait. The Mugodzhary High, a continental bulge 200 km east of Aktulagay was suggested in the map of Decourt *et al.* (2000). If this Mugodzhary High existed, Aktulagay would have had a rather isolated position in the Tethyan Basin. There is however no consensus over the existence of this large continental bulge during the Ypresian. For example, Steurbaut (2011) suggests the presence of the Orsk Channel in his map (Figure 7), which separates the Mugodzhary High from the large European Platform and allows a more direct connection from Aktulagay to the Turgai Strait. Either way, the deposition of clay west of the Mugodzhary High, north of Aktulagay would indicate limited currents during the Ypresian (Figure 8). In Aktulagay marls and clays were deposited during the Ypresian and not far south of Aktulagay limestones can be found (Decourt *et al.*, 2000). The paleodepth of Aktulagay during the Ypresian was estimated at 125-200 m by Deprez (submitted).

Later in the Cenozoic the sea-level drops and the Turgai Strait finally closes at ~29 Ma in the Oligocene (Hou *et al.*, 2011). From the Oligocene and onwards the Peri-Tethyan basins of West and Central Europe underwent basin inversion (Gaetani *et al.*, 2003).

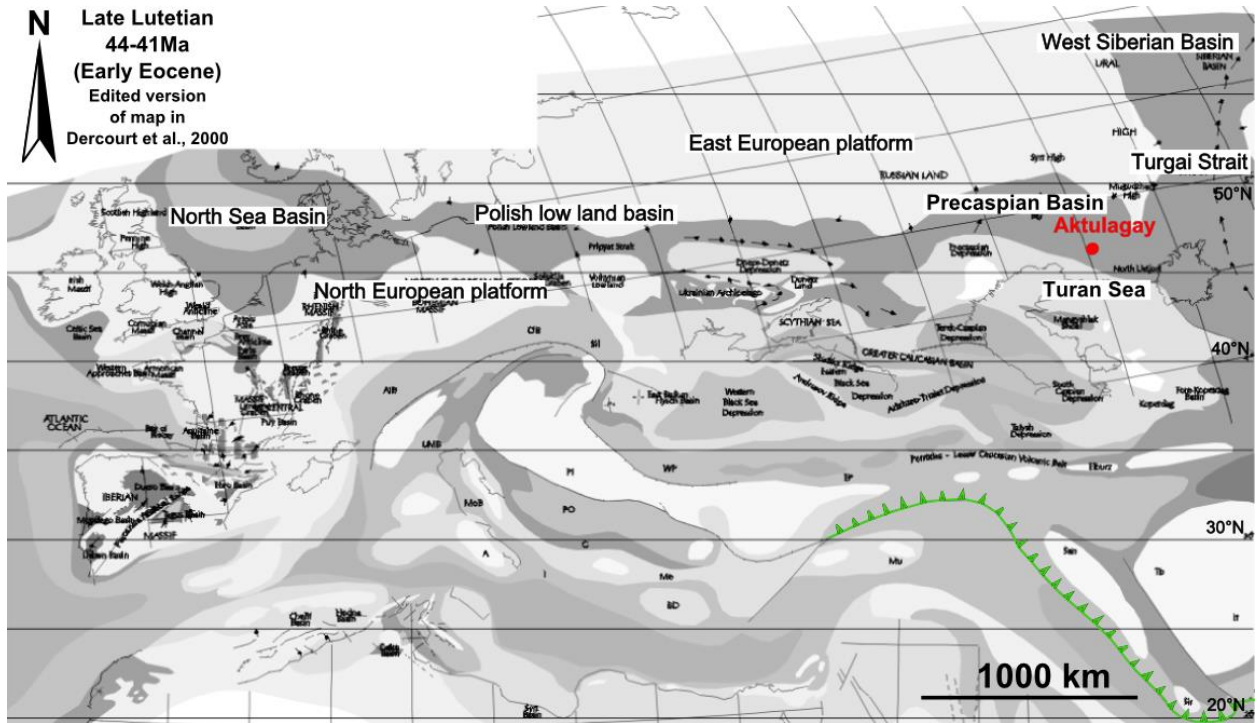


Figure 6. Paleogeographic map of the northern Tethyan Region during the Early Eocene. Original map from Dercourt *et al.* (2000). Some features were highlighted and Aktulagay is marked.

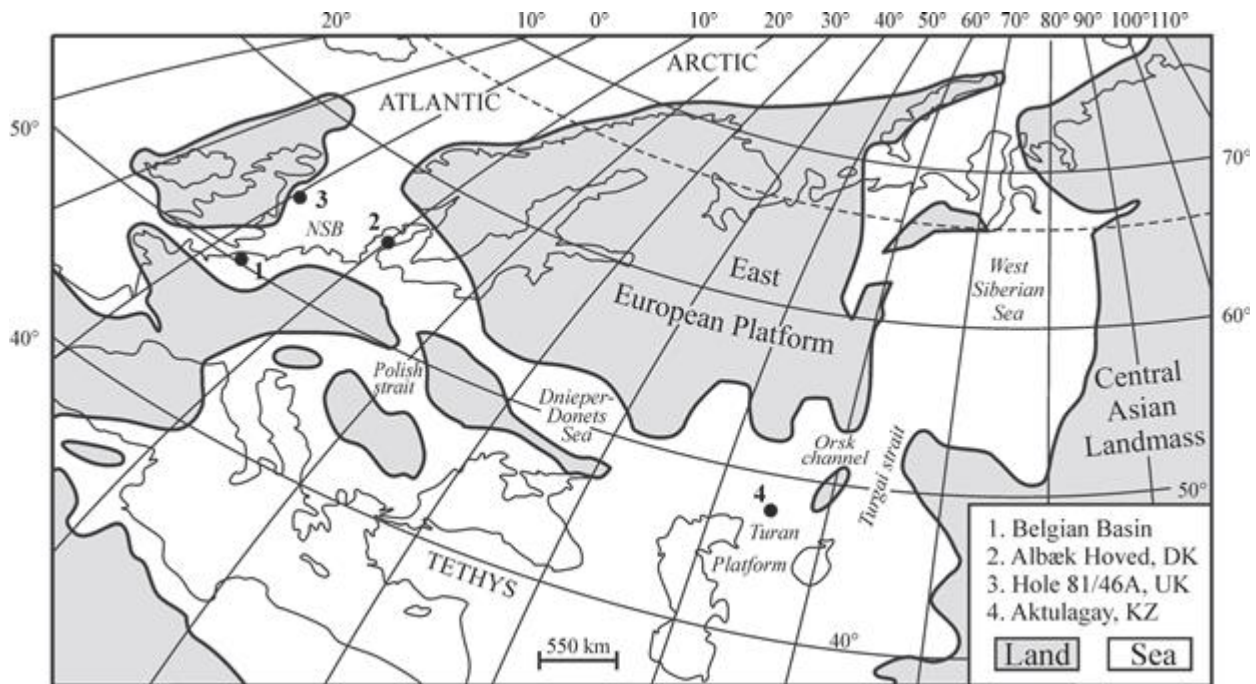


Figure 7. Paleogeographic map during the Ypresian from Steurbaut (2011), with the location of the Aktulagay Section.



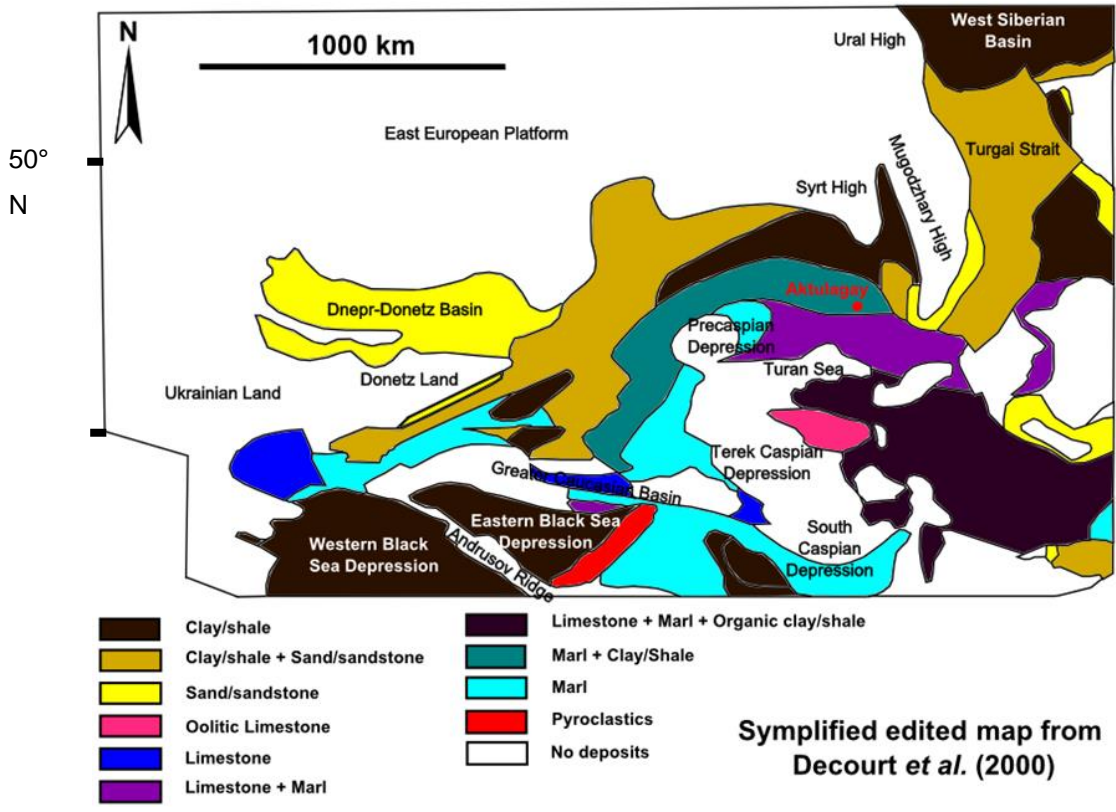
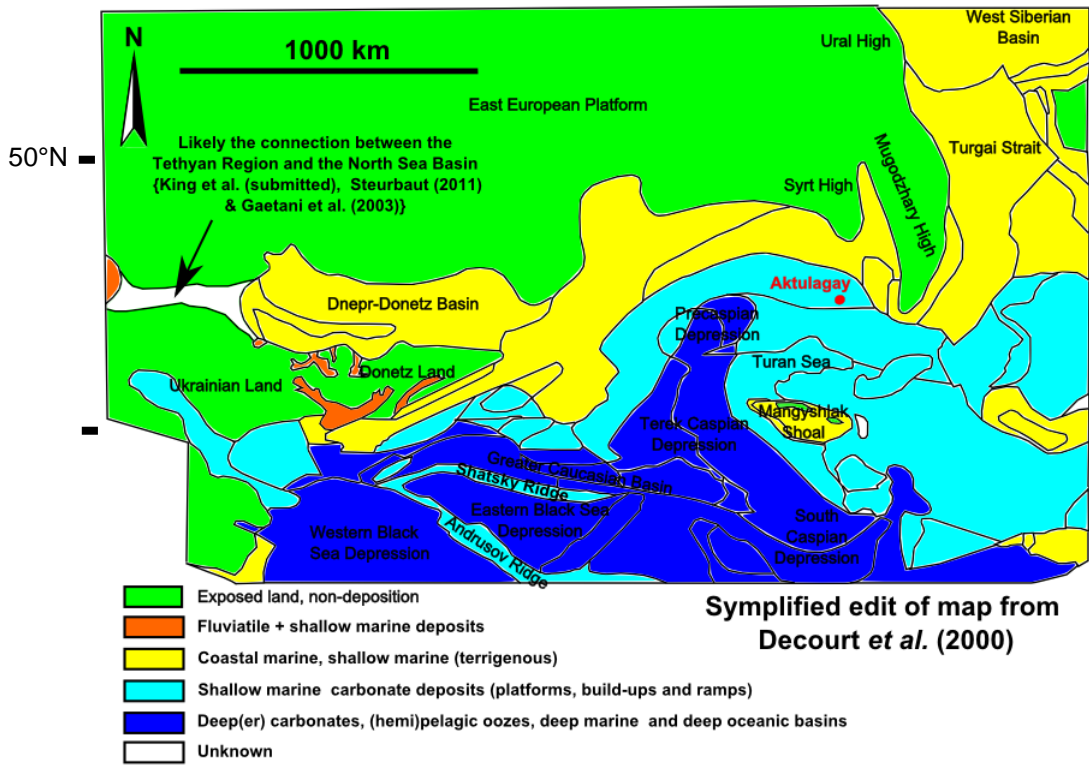


Figure 8. Maps of the northern Tethyan Region from Early/Middle Ypresian. Both maps are based on a map from Decourt *et al.* (2000). The upper map demonstrates the geographical interpretation, while the lower map gives an overview of the lithology in the Tethys Region.

## 2.3 The paleoclimate

### 2.3.1 The paleotemperature during the Ypresian

Based on a variety of geochemical and paleontological proxies, the Ypresian [56.0 - 47.8 Ma (Gradstein *et al.*, 2012)] is known as the warmest stage in the Cenozoic Era (Figure 9). Maximum temperatures were reached during the Early Eocene Climatic Optimum (EECO) at 52 to 50 Ma. In the Early Eocene the global ice volume was assumed negligible (Wise *et al.*, 1991; Zachos *et al.*, 1994; Pearson *et al.*, 2007; Huber and Caballero, 2011; Roberts *et al.*, 2011). This assumption is supported by several proxies like the absence of ice rafting debris records (Wise *et al.*, 1991 & Zachos *et al.*, 1994) and the high latitude occurrence of frost intolerant fauna and flora (e.g. Huber & Caballero, 2011; Keating-Bitonti *et al.*, 2011).

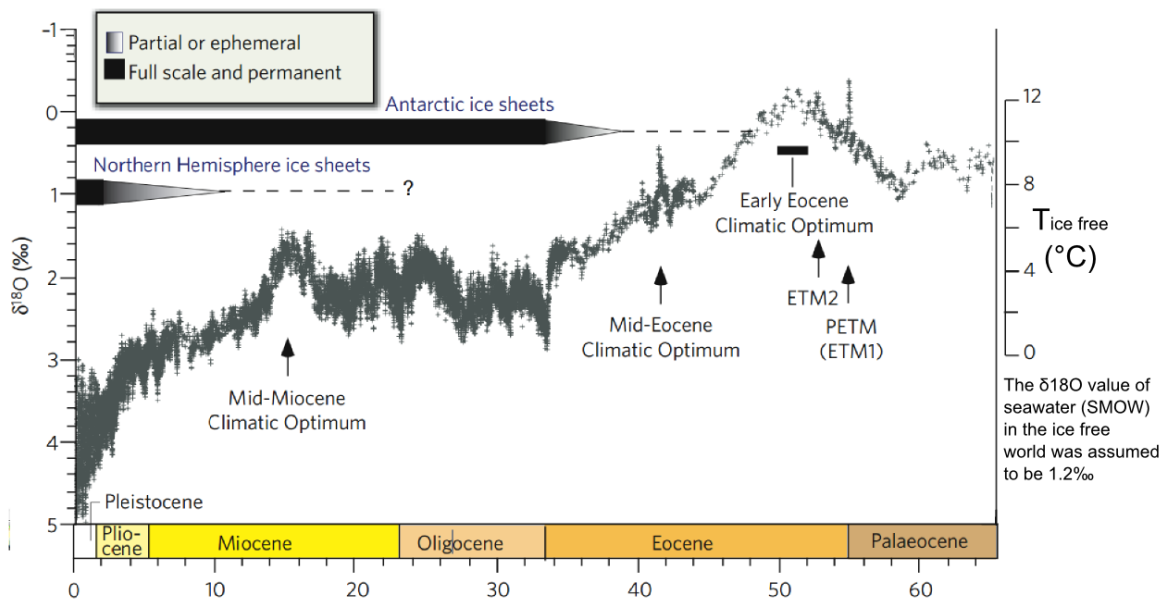


Figure 9. Figure from Zachos *et al.* (2008). This curve represents a global deep-sea benthic foraminifers (mainly *Cibicidoides* spp. and *Nuttallides* spp.)  $\delta^{18}\text{O}$  record, based on records from the Deep Sea Drilling Project and the Ocean Drilling Program sites. The temperature prediction is only valid for the ice-free world. Note that the precise time scale no longer matches the scale of Gradstein *et al.*, 2012.

The Early Eocene is characterized by extremely high temperatures at higher latitudes. For example Hollis *et al.* (2009) reported SST estimates of  $\sim 30^\circ\text{C}$  at  $55^\circ\text{S}$  based on a planktic foraminifer  $\delta^{18}\text{O}$  record in New Zealand and Bijl *et al.* (2009) calculated SST of  $\sim 34^\circ\text{C}$  at  $65^\circ\text{S}$  based on  $\text{TEX}_{86}$  at the East Tasman Plateau. An overview of calculated Early Eocene SST is plotted in Figure 10. Despite the estimation of very high temperatures at high latitudes, marine and terrestrial proxies at equatorial regions suggested temperatures only slightly higher than the modern temperatures. This suggested an extremely low equator-to-pole temperature gradient during the Early Eocene (Keating-Bitonti *et al.*, 2011 and Huber & Caballero, 2011). This low equator-to-pole temperature gradient was hard to explain and many hypotheses were proposed involving e.g. enhanced greenhouse gas forcing, large lakes, polar stratospheric clouds, increased heat transport, altered orbital parameters, topography, ocean gateways,

vegetation, etc. (Huber & Caballero, 2011). Despite these efforts, the produced MAT (mean annual temperature) models encountered problems in the order of 10-20 °C (Huber and Caballero, 2011).

In the past 10 years the question has risen whether the older temperature predictions are correct. There is an increasing support for the assumption that some of the tropical temperature predictions based on planktic foraminifers have been diagenetically altered towards lower temperatures (e.g. Pearson *et al.*, 2001, Sexton *et al.*, 2006, Huber & Caballero, 2011 and Roberts *et al.*, 2011). Furthermore it has been proposed that floral physiognomic techniques were misinterpreted because they would be insensitive to temperatures much higher than modern temperatures (Head *et al.*, 2009 and Huber & Caballero, 2011). Many terrestrial proxy records would have originated from regions with significant paleoelevation (Smith *et al.*, 2009 and Huber & Caballero, 2011). More recent tropical data for the Eocene epoch of Pearson *et al.* 2001, estimated tropical sea surface temperatures to be at least in the order of 28-32 °C instead of the older tropical temperature predictions in the order of 15-23 °C. The higher tropical temperatures are in support for a less extreme equator-pole-gradient. Pearson *et al.* (2001) and Huber & Caballero (2011) point at the importance of greenhouse gases for the explanation of the high temperatures. With this in mind, Huber & Caballero (2011) modeled Early Eocene world surface air temperatures (by assuming amplified CO<sub>2</sub> concentrations) mainly based on Leaf margin analysis (Figure 11). Roberts *et al.* (2011) also modeled SST during the Early Eocene. Their modeled results were compared with Early Eocene temperature data derived from Mg/Ca ratio measurements of foraminifer calcite and TEX<sub>86</sub>-index measurements (Figure 12). Unfortunately at higher latitudes the models clearly fail to predict the higher temperatures.

The isotopic measurements in this thesis will allow estimations of seawater temperatures of the Northern Tethys Region. Foraminifer isotopic data of the Ypresian is scarce in general. The largest Early Eocene data records are derived from ocean settings gathered by Deep Sea Drilling Projects (e.g. core 689 from Kennett & Stott (1990) or cores 883 & 884 from Pak and Miller (1995)) but data from outer shelf settings like Aktulagay is rare. Furthermore most Early Eocene foraminifer isotopic measurements focus on events like the PETM and not on the general long term trends. Finally bulk isotopic records are also available and more abundant than foraminifer isotopic studies, but bulk isotope studies cannot provide the same isotopic precision as foraminifer calcite studies. This is because the bulk isotopic values have an increased number of parameters that can cause deviations that are not temperature related (e.g. the ratio surface water species/thermocline species). Furthermore it is harder to prevent bias of secondary calcite in Bulk isotopic values. It is therefore clear that the data of this thesis will make a valuable addition to the global dataset of foraminifer isotopic data.

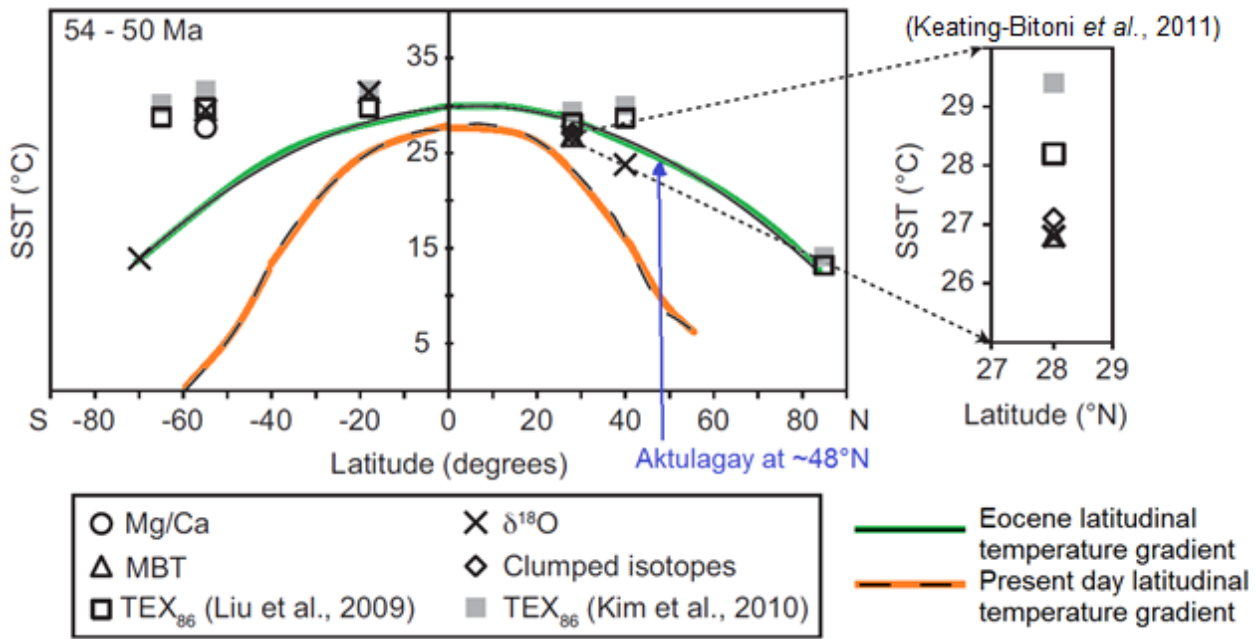


Figure 10. The equator-to-pole mean sea surface temperature gradient Reconstruction from Keating-Bitonti *et al.* (2011), based on data of Sluijs *et al.* (2006); Zachos *et al.* (2006); Pearson *et al.* (2007); Bijl *et al.* (2009); Hollis *et al.* (2009); Creech *et al.* (2010) and Keating-Bitonti *et al.* (2011).

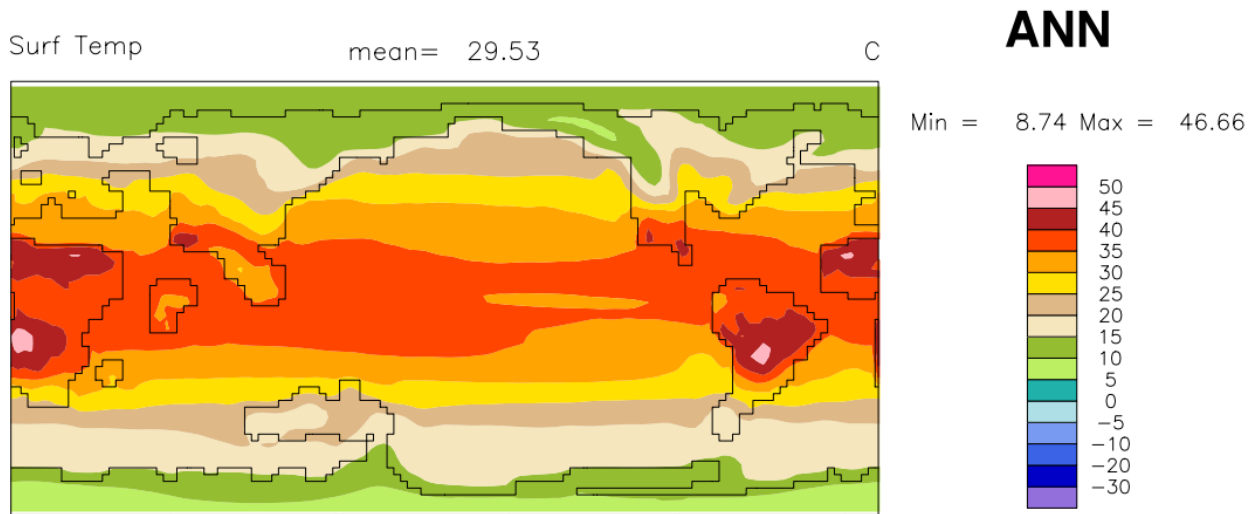


Figure 11. Map modeled by Huber & Caballero (2011), showing the average annual mean surface temperatures during the Early Eocene. Their model primarily relies on LMA or Leaf Margin Analysis, in which they use macroflora proxies to estimate paleotemperature. The whole list of proxy data sources can be found in Huber & Caballero (2011).



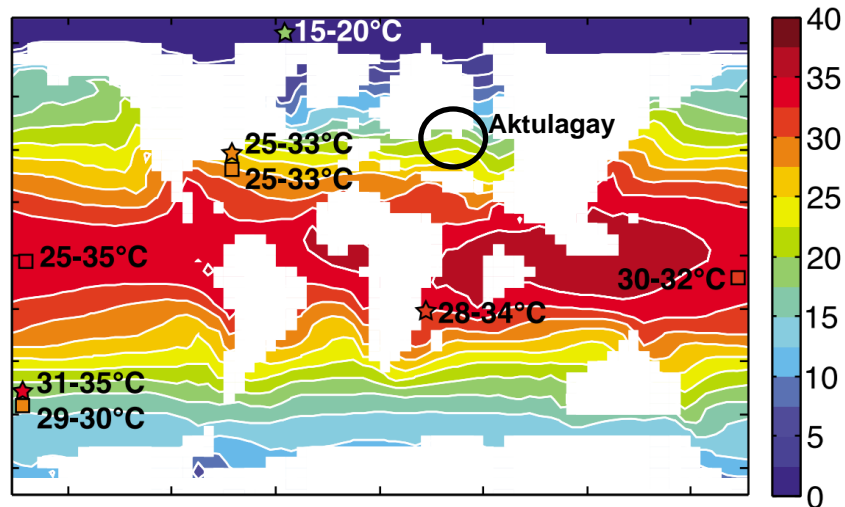


Figure 12. The mean annual sea-surface temperatures (°C) from the Early Eocene are simulated in this map. The result was compared with data from marine temperature proxies: Mg/Ca of foraminifer calcite (squares) and the TEX<sub>86</sub>-index (stars). The location of Aktulagay is marked on the map. (Figure from Roberts *et al.*, 2011).

### 2.3.2 Hyperthermal events

Beside the overall high temperatures, brief time intervals of even more extreme temperatures occurred during the Early Eocene. These time intervals lasted only a few tens of thousands of years and are known as hyperthermals (Zachos *et al.*, 2008). These hyperthermals are associated with Carbon Isotope Excursions (CIEs) towards more depleted values and are considered the result of a short time atmospheric CO<sub>2</sub> (&CH<sub>4</sub>) concentration increases (e.g. Zachos *et al.*, 2008; Huber & Caballero, 2011). The most extreme and best studied hyperthermal of the Cenozoic is the Paleocene-Eocene Thermal Maximum (PETM). The global temperature would have risen by more than 5 °C and more than 2000 Gt CO<sub>2</sub> would have entered the ocean and atmospheric system (Zachos *et al.*, 2008). These extreme temperatures also coincide with important paleontological events including deep-sea benthic foraminifer extinction (Vandenberghe *et al.*, 2012). Other hyperthermal events following the PETM are the Eocene Thermal Maximum 2 (ETM2 or H1) which is approximately 2 million years later and Eocene Thermal Maximum 3 (also referred to as the X-event or the K-event). These events have similar isotopic excursions as PETM, although they are less pronounced (Vandenberghe *et al.*, 2012). Some authors claim that these CIE events are related to the Milankovitch cycles or more specific to maxima in the eccentricity cycle (Cramer *et al.*, 2003; Lourens *et al.*, 2005). These CIEs are not necessarily hyperthermal events. Cramer *et al.* (2003) identifies a series of CIEs based on Bulk δ<sup>13</sup>C values of 4 deep-sea cores. They defined the following CIEs; A, B1, B2, C1, C2, D1, D2, E1, E2, F, G, H1, H2; I1, I2, K and L. From which H1 corresponds to ETM2 and K corresponds to ETM3 (Figure 13). The relation between CIEs and the eccentricity cycle has not been generally accepted (Vandenberghe *et al.*, 2012).

It is likely that the hyperthermal events and CIEs are recorded in the Aktulagay section. However, due to the low sampling resolution of approximately 1 sample per meter and the absence of samples from sapropelic layers (organic rich clay layers) that might be associated with such events, there is a significant

chance most of the CIEs lay in-between samples. Nevertheless, the larger CIEs (like ETM2) have impact over larger time intervals and could be recorded.

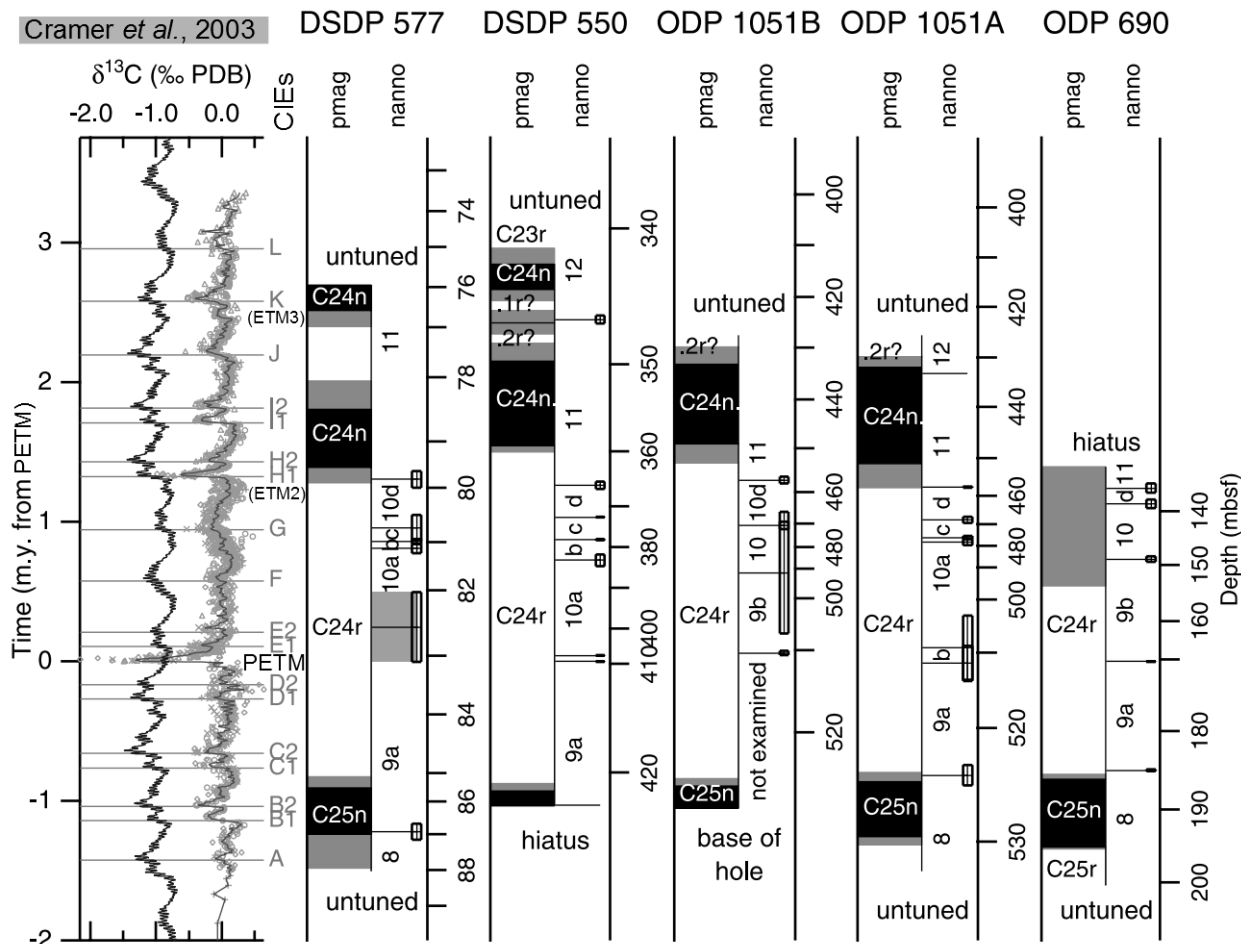


Figure 13. The identification of CIEs in the Paleocene and the Early Eocene by Cramer *et al.* (2003). Their isotopic values are based on the  $\delta^{13}\text{C}$  bulk isotopic values (‰ PDB) of DSDP 577, DSDP 550, ODP 1051A, ODP 1051B and ODP 690. "pmag" stands for magnetic polarity zonation (black: normal, white: inverse, grey: uncertain) and "nanno" for nannofossil biostratigraphic (sub)zonal boundaries

## 2.4 Lithology and lithostratigraphy

### 2.4.1 Introduction

The Aktulagay Section (Figure 14) was originally studied and sampled by King *et al.* (submitted). Consequently the description of the lithology of the section in this thesis is entirely based on their publication. The Aktulagay Section consists of the white chalks of the Upper Cretaceous (Maastrichtian) at the bottom, the clayey to marly sediments of the Eocene (Ypresian, Lutetian and possibly Bartonian) above and the Middle Miocene (Sarmatian) limestone at the top. The Eocene sediments were further subdivided into Units A, B, C and D by King *et al.* (submitted). They linked these units to Formations described in the regional literature with Unit A being the Alashen Formation, Unit B the Aktulagay Formation (defined by King *et al.* (submitted)), Unit C the Tolagaysor Formation and Unit D the Sangruk Formation. The isotopic study of this thesis is limited to Units A and B of the Ypresian. The samples were already studied by Deprez *et al.* (2012) and Deprez (Submitted). Therefore the same sample numbering is applied. Heights in the thesis are expressed as height with respect to the Maastrichtian-Ypresian unconformity. A litholog of the entire section is given in Figure 15 and a more detailed litholog of Unit A and B is given in Figure 16.

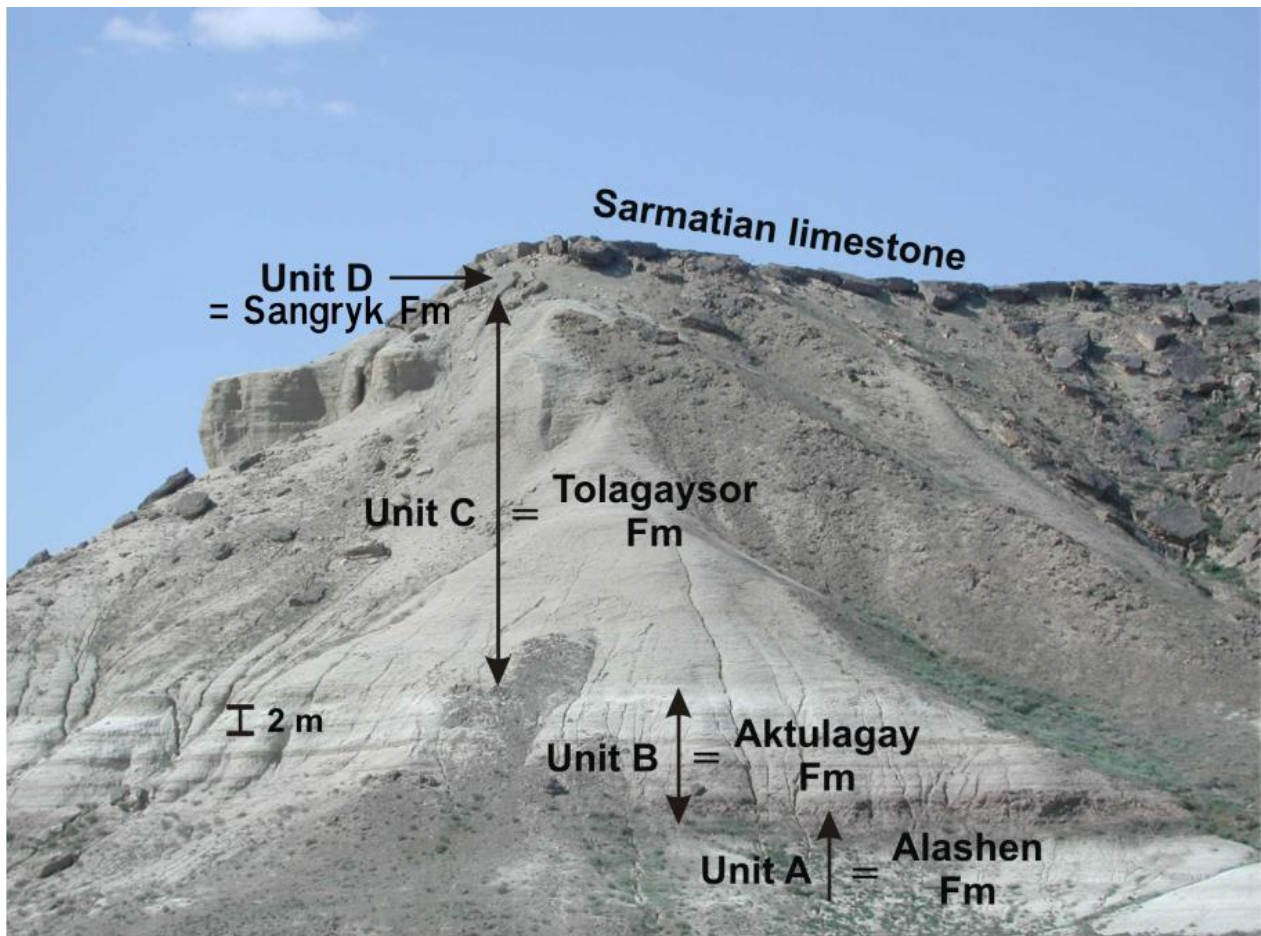


Figure 14. Picture of the Aktulagay section (Steurbaut, 2011)

## **2.4.2 Unit A (The Alashen Formation) based on King *et al.* (submitted)**

### **2.4.2.1 Subunit A1 (0 to 0.20 m)**

Subunit A1 consists of grey green clay. The basal contact with the underlying Maastrichtian chalk is sharp.

### **2.4.2.2 Subunit A2 (0.20 to 10.0 m)**

The contact between A1 and A2 is abrupt and interburrowed. Small phosphatic grains are found at the base of A2. Subunit A2 consists mainly of calcareous (foraminifer rich) clay. Only at the interval between 5.65 m and 6.80 m the clay is darker and less calcareous. 13 intensely interburrowed surfaces were identified in the subunit.

### **2.4.2.3 Subunit A3 (10.0 m to 13.45 m)**

Subunit A3 is composed of marl and chalk. The lower part of the subunit has the highest carbonate content in the Eocene part of the Section. The basal contact is an interburrowed surface and another interburrowed surface is found higher in the Unit.

## **2.4.3 Unit B (Aktulagay Formation) based on King *et al.* (submitted)**

### **2.4.3.1 Subunit Unit B1 (13.45 m 16.22 m)**

Subunit B1 consists dominantly of light brown, slightly calcareous to non-calcareous clay. There are also greenish clay layers present which are thought to have been partially secondarily decalcified. The base of the unit is defined by a thin black sapropelic clay layer. 3 other black sapropelic clay beds and a single light brown fissile clay bed are found higher in subunit B1. The contacts between the sapropelic beds and the clays are sharp, except for one where it is an interburrowed omission surface. Deprez *et al.* (submitted) qualitatively observed a higher organic matter content in the 3 samples (17, 18 and 19) from unit B1 than in samples of unit A and subunit B2 with the exceptions of sample 13 and 14.

### **2.4.3.2 Subunit Unit B2 (16.22 m to 23.57 m)**

Subunit B2 consists of carbonate rich sediments similar to those of Unit A. The contact between B1 and B2 is an interburrowed surface. 4 sapropelic black clay layers and 5 light brown fissile clay layers are found in subunit B2 similar to those of subunit B1.

## **2.4.4 Unit C (Tolagaysor Formation) based on King *et al.* (submitted)**

The base of subunit C1 (23.57 m to 27.25 m) is marked by a sharp decrease in carbonate content and the presence of quartz grains (mainly silt fraction). The lower part of Unit C2 is more clay rich. At 28.9 m the clay content decreases again and at 56 m the first quartz grains with sand fraction are observed.

## **2.4.5 Parasequences and omission surfaces**

Several interburrowed surfaces were recognized by King *et al.* (submitted). They assumed that these surfaces represent omission surfaces. Furthermore they recognized minor depositional parasequences in subunit A2 that are characterized by an upward decrease in carbonate content (from marl to calcareous

clay). [A parasequence is defined as a relatively conformable succession of genetically related beds or bedsets bounded by marine flooding surfaces (Mulholland, 1998).] They interpreted the interburrowed contacts between these parasequence as flooding surfaces. They further suggested that these parasequences might represent Milankovitch cycles.

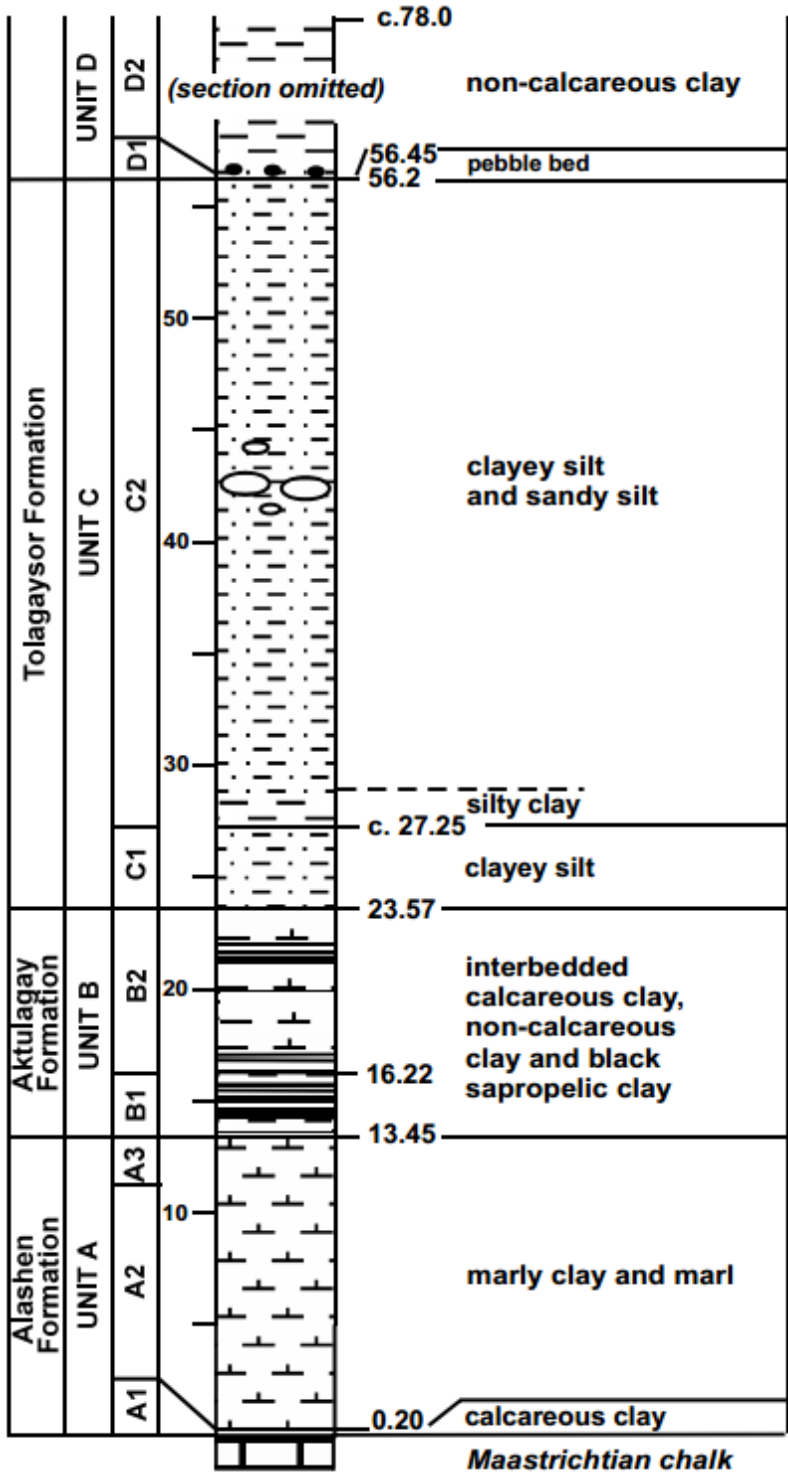


Figure 15. Schematic litholog of the entire Aktulagay section made by King *et al.* (submitted)

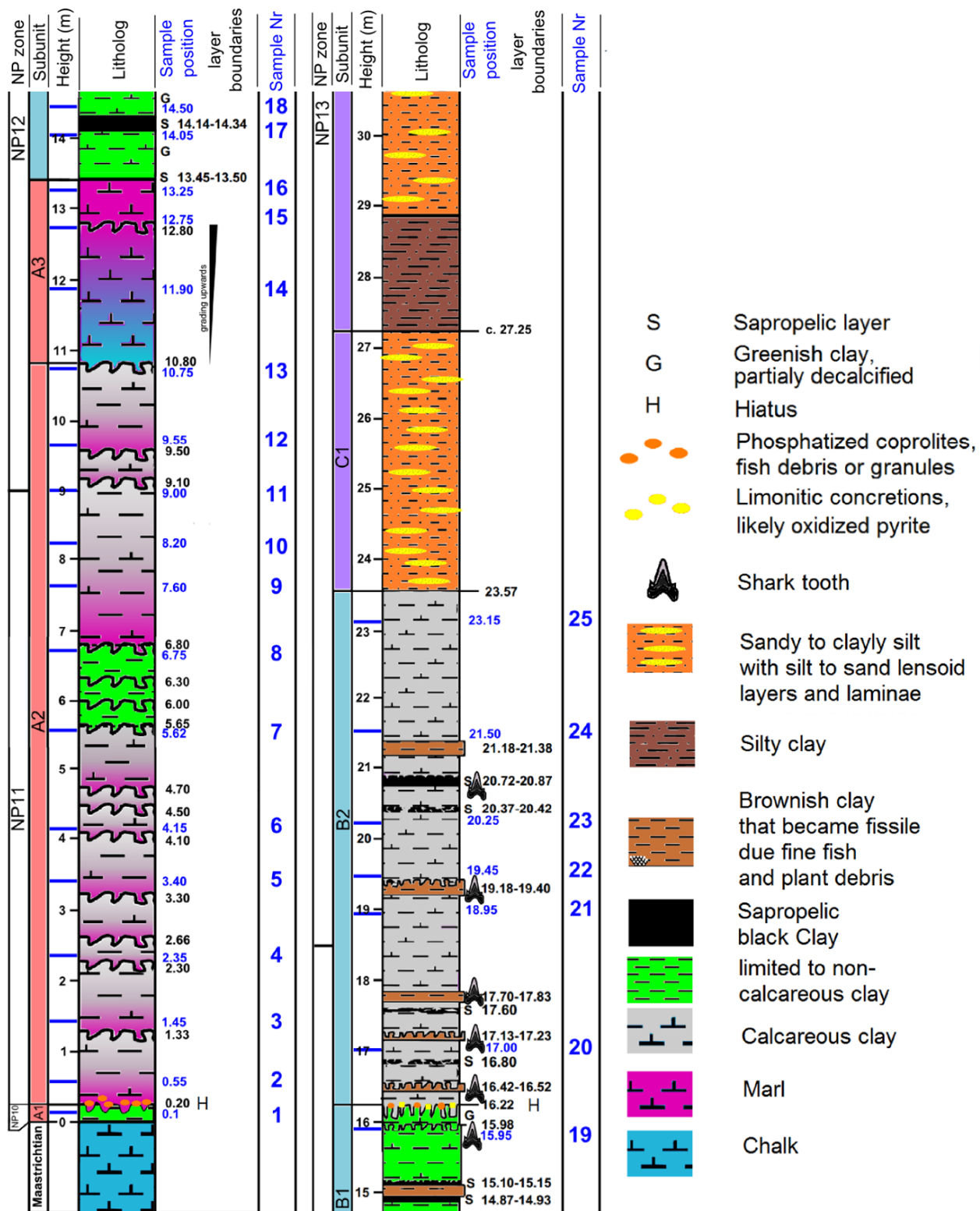


Figure 16. Slightly modified litholog of the Aktulagay section. The original litholog was made by King *et al.* (submitted). The positions of the samples are marked.

## 2.5 Biostratigraphy

### 2.5.1 Introduction

Several omission surfaces and 2 hiatuses were recognized in unit A and B (King *et al.*, submitted). In theory the term omission surface is applied for a discontinuity surface of the most minor nature. In practice the term means that the time gap could not be demonstrated based on the biostratigraphy of King *et al.* (submitted). Their biostratigraphic interpretation is based on nannofossils and dinoflagellate cysts and can be found in Figure 17 and Figure 18 respectively.

### 2.5.2 Biostratigraphy

According to King *et al.* (submitted), subunit A1 belongs to middle NP10. Between subunits A1 and A2 a significant hiatus occurs. It is associated with the abrupt lithologic change and the concentration of phosphate granules at the base of A2. The presence of the hiatus is demonstrated by dinoflagellate cyst biostratigraphy. The hiatus comprises 2 Dinoflagellate zones; The *Wetzeliella astra* Zone and The *Wetzeliella meckelfeldensis* Zone. The lowermost part of NP 11 is considered present in Aktulagay based on nannofossil biostratigraphy (King *et al.*, submitted). Nevertheless biostratigraphy of lower A2 is complicated by reworking of sediment between 0.20 and 0.50 m. The presence of *Tribraehiatus orthostylus* in association with the absence of *Tribraehiatus contortus* would indicate the base of NP11. Furthermore the consistent presence of *Tribraehiatus orthostylus*, *Discoaster multiradiatus* and the high frequency of *Micrantholithus spp.* would indicate the presence of the lowermost part of NP11 (King *et al.*, submitted). In subunit A2 King *et al.* (submitted) identified almost all nannofossil subzones from the much more expanded succession of the North Sea Basin. They conclude that therefore no significant hiatuses are present in this interval. The lower boundary of NP12, defined by the first occurrence of *Discoaster lodoensis*, is positioned at 9.0 m (King *et al.* (submitted). In unit A3 and B1 no hiatuses are reported, the sediments belong to NP12 (King *et al.*, submitted). Between B1 and B2 a significant hiatus occurs. King *et al.* (submitted) report the co-occurrence of 8 first occurrences at the base of B2. The hiatus encompasses Subzones VII and VIIIa when correlated with the North Sea basin (King *et al.*, submitted & Steurbaut, 1998). No further hiatuses were found in B2 and King *et al.* (submitted) did not find biostratigraphic indications for a hiatus between B2 and C1. In B2 the transition of NP12 to NP13 was defined with the last occurrence of *Tribraehiatus orthostylus*.

### 2.5.3 Correlating Biostratigraphy into an age model

The studied time interval can be estimated studied based on the NP-zones. Deprez (2012) based his time estimates of the Aktulagay Section on Luterbacher *et al.* (2004). In this study a more recent publication is available; Vandenberghe *et al.* (2012). When comparing both publications the difference is striking (Figure 19 and Figure 20). In Luterbacher *et al.* (2004), the duration of NP11, NP12 and NP13 correspond to 0.9 myr, 1.6 myr and 2.2 myr respectively while in Vandenberghe *et al.* (2012), NP11, NP12 and NP13 correspond to 0.5 myr, 3.2 myr and 1.3 myr. Therefore if the dates of Luterbacher *et al.* (2004) are applied,

NP12 is almost 2 times the duration of NP11, but when the dates of Vandenberghe *et al.* (2012) are applied, NP12 is 6 times the duration of NP11. The uncertainty is thus too great to predict the size of the hiatuses or the sedimentation rates over the section. It will be avoided translate section height into time. A rough estimate based on both publications is that Unit A and B encompass a time period of 3 to 4 million years. It is also apparent that a correlation of the NP zones with magnetostratigraphic records is rather tricky.



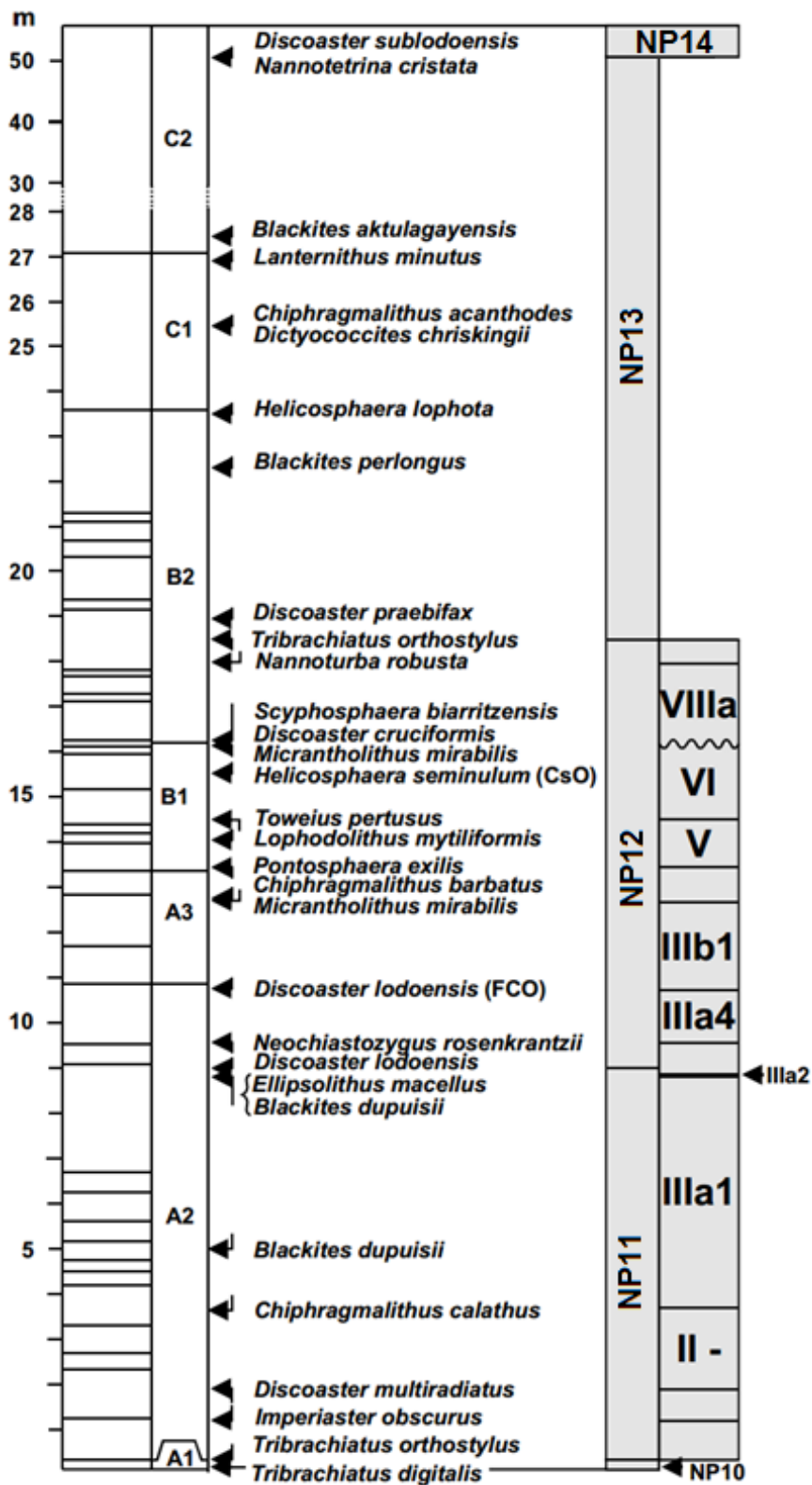


Figure 17. Position of first occurrences, first consistent occurrences (FCOs) and last occurrences of nannofossil species. To the right the corresponding Nannofossil zones and the subzones that were defined in the North Sea Basin (King *et al.*, submitted).

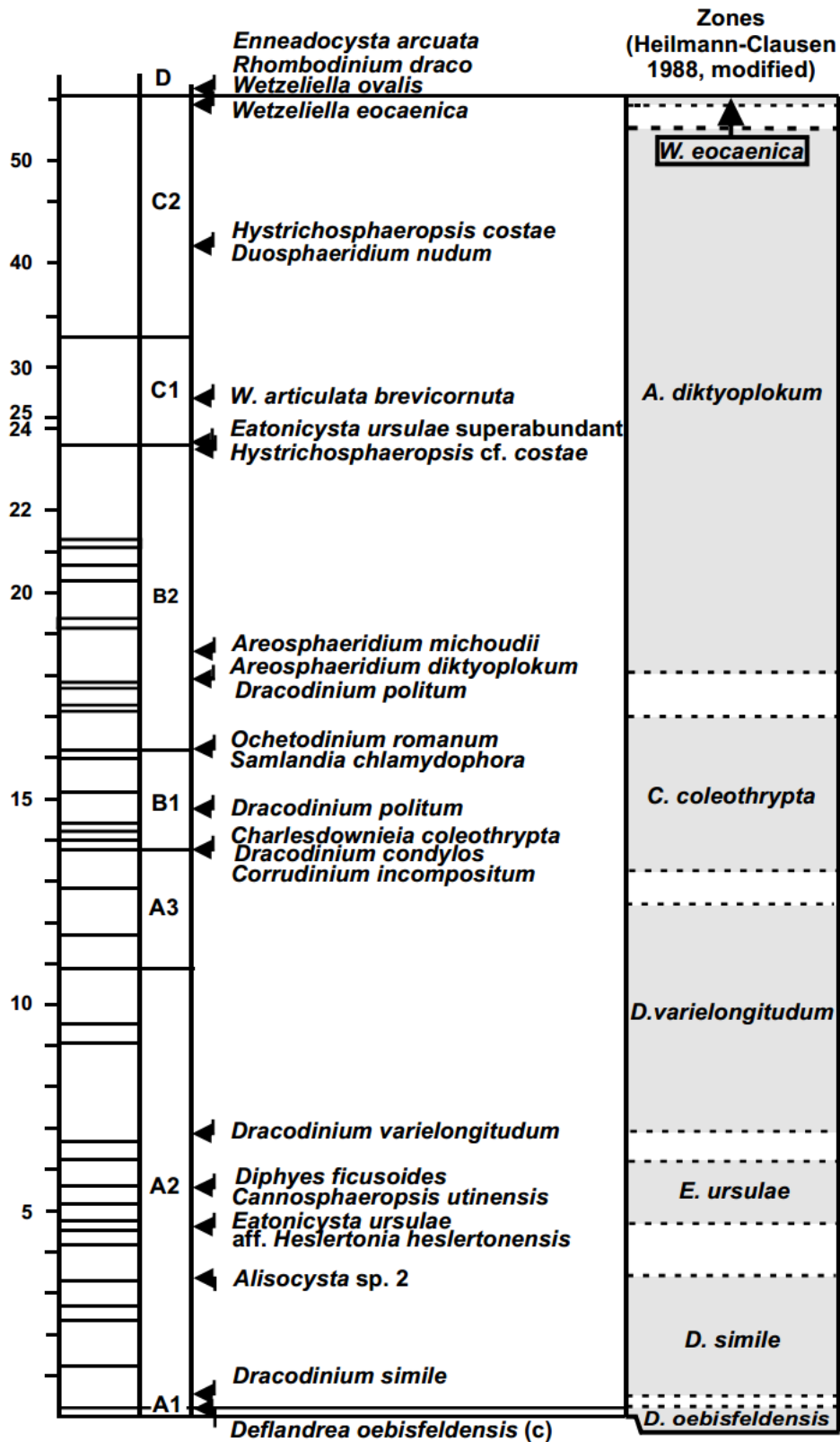


Figure 18. The identification of dinoflagellate cyst events and zones (King *et al.*, submitted).



## 2.6 Paleontology

### 2.6.1 Dinoflagellate cysts

The dinoflagellate cyst diversity is high over units A and B. From 0 to 7 m there is a relative increase in *Spiniferites spp.* and a relative decrease in *Areoligera spp.* The abundance of dinoflagellate cysts varies over the section although Deprez *et al.* (submitted) noted an exceptional abundance at 19.45 m and 20.25 m and the relative high abundance of the genera *Cordosphaeridium*.

According to King *et al.* (submitted), the relative increase in *Spiniferites spp.* suggests the deepening of the basin with a Maximum Flooding Surface (MFS) at 7 m. Deprez (submitted) linked the high abundance of dinoflagellate cysts and the high relative abundance of the genera *Cordosphaeridium* to more brackish water in the interval.

### 2.6.2 Calcareous nannofossils

Unit A is dominated by *Toweius spp.* and *Coccolithus pelagicus*. Nevertheless the interval 0.20 to 2.25 m contains increased numbers of *Micrantholithus spp.* Above 3.7 m till the upper part of Unit A, there are no significant changes in the nannoplankton assemblage except for some individual species blooms. In subunit B1, nannofossils are less diverse and less abundant. They are even virtually absent in the middle part of B1. In this interval there is a relative higher occurrence of *Imperiaster obscurus* and *Micrantholithus mirabili*. Subunit B2 has a rich and diverse assemblage of nannofossils, *Pontosphaera spp.*, *Coccolithus pelagicus*, *Discoaster spp.* and *Blackites creber* are relatively abundant.

According to King *et al.* (submitted), *Toweius spp.* and *Coccolithus pelagicus*, suggest fully marine setting with normal salinities in unit A. The increase of *Micrantholithus spp.* at 0.20 to 2.25 m points towards more coastal influence (King *et al.*, submitted). The higher occurrence of *Imperiaster obscurus* and *Micrantholithus mirabili* in subunit B1 would reflect shallower water in proximity of the coastline. Finally, *Pontosphaera spp.*, *Coccolithus pelagicus*, *Discoaster spp.* and *Blackites creber* in unit B2 are considered near shore species by King *et al.* (submitted).

### 2.6.3 Ostracods

Ostracods are almost absent in subunit A1 but are rather abundant in subunits A2 and A3. There is a sudden strong decrease in ostracod diversity in subunit B1. In B2 their diversity is restored (Figure 21).

### 2.6.4 Echinoids, fish remains, bivalves and gastropods (Pteropods)

Echinoid debris and fish debris (scales and bones) are consistently found over the units A, B and C.

Fish remains are also found concentrated in the brown clay intervals together with plant debris. Mollusc moulds, nuculids bivalves and small pectinid bivalves are found in unit A2. Small bivalves have an increased abundance between 12.80 m and 13.45 m. Pteropods occur only sporadically over units A, C and subunit B1, but have an increased abundance in subunit B2.

### **2.6.5 Shark and ray teeth**

Shark and ray teeth have an increased dominance in 6 levels of the section. These levels are found in unit B. According to King *et al.* (submitted) it was hard to identify the precise levels from which the assemblages originate but they note that their collecting levels correspond closely to the light brown clay intervals. The species encountered are dominated by *Xiphodolamia spp.* and *Otodus spp.*

The dominance of *Xiphodolamia spp.* is considered a very unusual shark fauna, it would indicate moderately deep water, a high productivity environment and little or no benthos (King *et al.*, submitted).

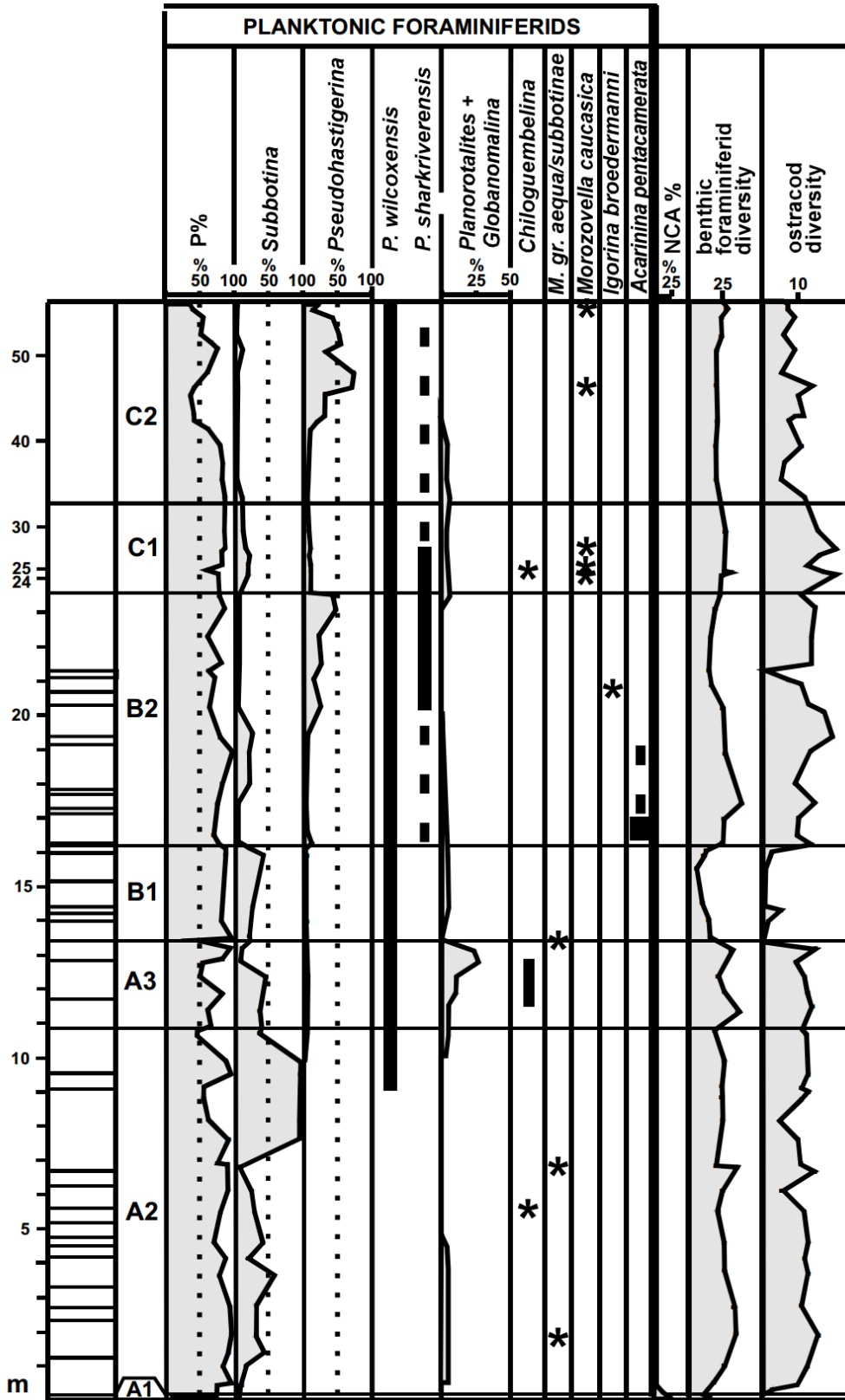


Figure 21. Summary figure of King *et al.* (submitted) concerning planktic foraminifers, benthic foraminifers and ostracods.

## 2.6.6 Planktic foraminifers

The planktic foraminifer percentage (P%, relative to the total number of foraminifers) has been examined by both King *et al.* (submitted) and Deprez *et al.* (submitted) (Figure 22). Their results sometimes differ up to 20%. This is related to the fact that King *et al.* (submitted) only counted foraminifers from the 120 to 250µm fraction while Deprez *et al.* (submitted) counted foraminifers from the >63µm size fraction. Furthermore King *et al.* (submitted) has studied more samples. Some observations they had in common are the extremely low P% value in A1 and a generally high P% (mostly >70%) in unit A2 and A3. Significant decreases of P% are recorded at 10.75 m and 20.25 m. Moderate increases of P% are found at 9.55 m and 13.25 m in both datasets. The data of Deprez *et al.* (2012) also suggest higher P% between 0.5 and 5 m and a decrease of P% at 20.25 m. An interesting observation of King *et al.* (submitted) is the remarkable dominance (>90%) of *Subbotina spp.* over the planktic foraminifer genera between 7.6 and 9.9 m (Figure 21). Since the abundance is usually limited to <50% of the planktic foraminifer assemblage. They also note the progressive increase in planktic foraminifer genera *Planorotalites* and *Chiloguembelina* in subunit A3 and the progressive increase in planktic foraminifer genus *Pseudohastigerina* in the upper part of subunit B2 (Figure 21). King *et al.* (submitted) suggest the increased P% reflect more marine settings and that a decrease in P% can be the result of more brackish water input. The increase of *Pseudohastigerina*, *Planorotalites* and *Chiloguembelina* are considered indications of shallowing in the upper part of A3 and B2. The final interpretation of King *et al.* (submitted) concerning water depth can be found in Figure 23.

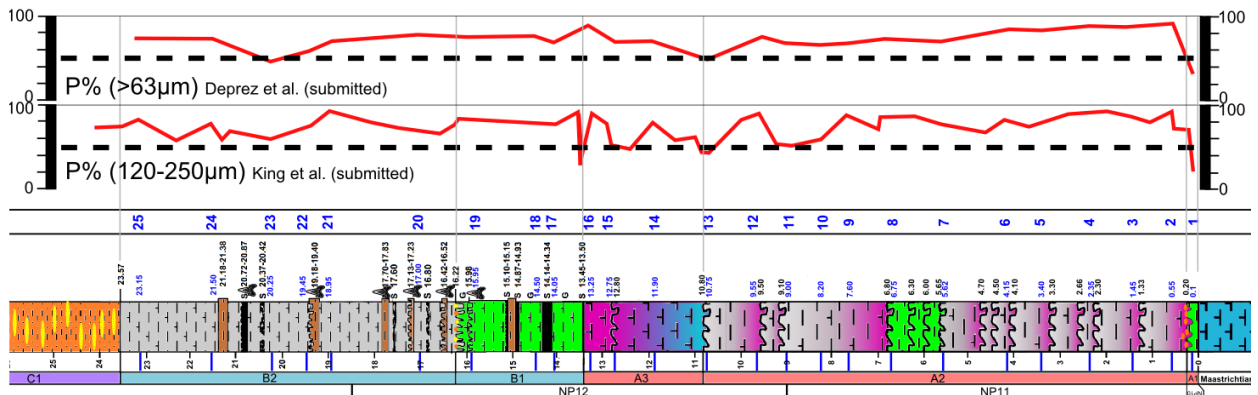
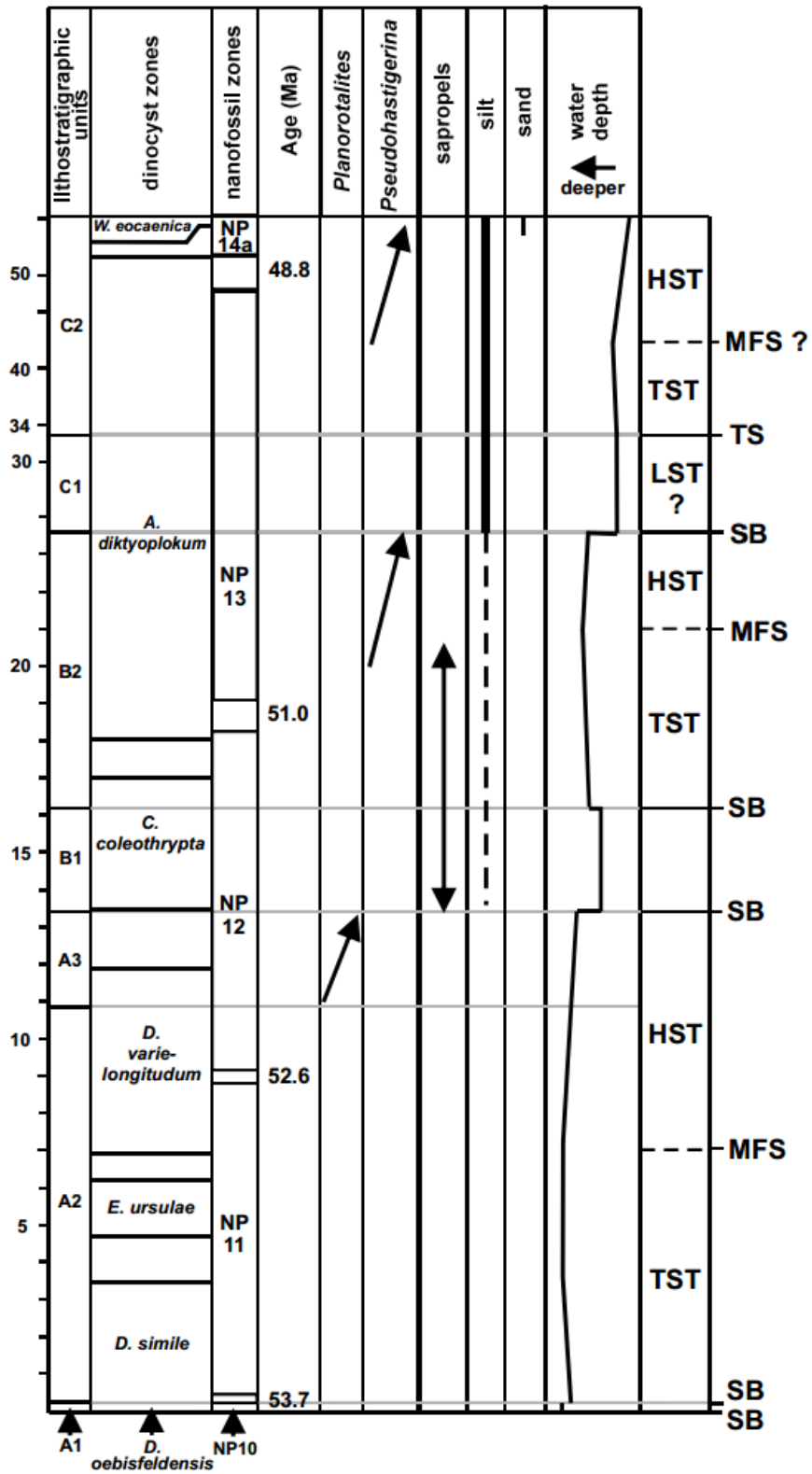


Figure 22. The percentage planktic foraminifers calculated by King *et al.* (submitted) and Deprez *et al.* (submitted). The complete lithocolumn with legend can be found in Figure 16.

## 2.6.7 Benthic foraminifers

Benthic foraminifer assemblages were studied quantitatively over the section by Deprez *et al.* (submitted). They found interesting abrupt changes in the abundance of certain species. Patterns that stand out are e.g. *Epistominella minuta*, and *Pulsiphonina prima*, where the abundance varies from hardly present to over 30% of the benthic foraminifer population. The relative abundances determined by Deprez *et al.* (submitted). These relative abundance patterns are rather unique for each species.



**Figure 23.** Summary figure of King *et al.* (submitted) and their interpretation of the water depth at Aktulagay. HST: highstand systems tract. LST: lowstand systems tract. MFS: maximum flooding surface. TS: transgressive surface. TST: transgressive sequence tract. SB: sequence boundary. Age of nanofossil zone boundaries is based on Luterbacher *et al.* (2004).



## 3 The isotopic signature of foraminifers

### 3.1 Introduction

To understand the absolute and the relative values of the isotopic signature of foraminifers, this chapter will give an overview of parameters that are known to determine the isotopic signature.

The isotopic signature measured is influenced by the (micro)habitat in which the individual foraminifers lived (the temperature, geochemistry and the amount & quality of the organic matter available for consumption), their symbionts (only relevant for planktonic foraminifers), vital effects (type of metabolism, variability between foraminifers of the same species, ontogenetic effects), the time interval that the sample represents, the amount of specimens that were required for 1 measurement and finally post depositional alteration (recrystallization, precipitation, filling & dissolution).

### 3.2 Parameters determining the $\delta^{13}\text{C}$ signature

#### 3.2.1 Temperature

The direct effect of temperature is its influence on the kinetics of the isotopic exchange reaction between solid carbonate and dissolved bicarbonate. Changes in temperature therefore cause changes in the equilibrium isotope fractionation (Emrich *et al.*, 1970; Cooke and Rohling, 2001). Emrich *et al.* (1970) calculated that the solid carbonate phase is relatively more enriched in  $^{13}\text{C}$  when the temperature decreases ( $-0.063 \pm 0.008\text{‰ } ^\circ\text{C}^{-1}$ ). The effect is rather small and most authors consider  $\delta^{13}\text{C}$  insensitive to temperature.

#### 3.2.2 Geochemistry: DIC and the pH

The  $\delta^{13}\text{C}$  signature measured in foraminifer tests tracks the variations in the  $\delta^{13}\text{C}$  signature of the total amount of dissolved inorganic carbon ( $\delta^{13}\text{C}_{\text{DIC}}$ ) in the ocean (Bemis *et al.*, 2000). Therefore foraminifers are used as a proxy for changes in the global carbon cycle. On a smaller scale, the difference between  $\delta^{13}\text{C}$  of planktic and benthic foraminifers provides information about the strength of the biological pump and about the surface to deep water  $\delta^{13}\text{C}$  gradient (Bemis *et al.*, 2000). Within the sediment a strong  $\delta^{13}\text{C}_{\text{DIC}}$  depth gradient exists in the pore water towards more depleted values. This gradient exists due to the microbial oxidation of particulate organic matter (POM) rich in  $^{12}\text{C}$ . In deep sea water the majority of the oxidation occurs within the upper few centimeters (McCorkle *et al.*, 1985; Papadimitriou *et al.*, 2004). Due to the  $\delta^{13}\text{C}_{\text{DIC}}$  gradient, there is a general relation between the living depth of the foraminifer and their  $\delta^{13}\text{C}$  signature. This has been illustrated by e.g. Rathburn *et al.* (1996). It is one of the main reasons why epibenthic species can be distinguished from endobenthic species based on their  $\delta^{13}\text{C}$  values.

Although there is in general a relation with depth, the relation is considered to be poor due to other parameters like food preference and vital effects (Rathburn *et al.*, 1996; Basak *et al.*, 2009).

The pH is mainly affected by the seawater carbonate ion concentration  $[\text{CO}_3^{2-}]$ . Studies on planktic foraminifers (e.g. Spero *et al.*, 1997) indicate a more depleted  $\delta^{13}\text{C}$  signal when the pH increases, although the cause is not well understood (Friedrich *et al.*, 2006 & Katz *et al.*, 2010).

According to Friedrich *et al.* (2006) the effect of pH on the benthic foraminifer community isotopic values has never been demonstrated even though significant pH-depth gradients have been measured on pore waters of marine sediments.

### 3.2.3 Vital effects

One of the most important vital effects is the ontogenetic effect. The ontogenetic effect is the effect of changing isotopic value during growth. This effect has been demonstrated for both planktic and benthic foraminifers. In both cases,  $\delta^{13}\text{C}$  moves towards more positive values during growth. The largest effect exists for mixed layer dwelling planktic foraminifers (e.g. *Acarinina spp.*). Smaller effects exist for thermocline dwelling foraminifers (e.g. *Subbotina spp.*) and endobenthic foraminifers (e.g. *Uvigerina spp.*) (Schumacher *et al.*, 2010; Edgar *et al.*, 2012). Several hypotheses were proposed to explain this effect like the change in microhabitat during life or the higher metabolic rates in juvenile specimens (Spero and Lea, 1996; Cooke and Rohling, 2001; Schumacher *et al.*, 2010; Edgar *et al.*, 2012). The influence of ontogenetic effect can be limited by respecting a limited size fraction for isotopic measurements (e.g. Rathburn *et al.*, 1996; Schumacher *et al.*, 2010).

Another vital effect is the type and rate of the metabolism. When a specimen has a higher respiration rate, it incorporates more respired  $\text{CO}_2$  into its test. This would result in a reduction of  $\delta^{13}\text{C}$ . Furthermore if the specimen experiences stages of rapid test calcification (kinetic effect), it results in even more depleted  $\delta^{13}\text{C}$  values (Mackensen *et al.*, 2000). Differences in metabolisms are one of the reasons why isotopic offsets between species occur. Finally some (endo)benthic species can apply anaerobic metabolisms which might also affect their  $\delta^{13}\text{C}$  signature (Moodley *et al.*, 1998; Risgaard-Petersen, 2006).

### 3.2.4 Food preference (benthic foraminifers)

Rathburn *et al.* (1996), Jorissen *et al.* (2007) and Basak *et al.* (2009) suggest that some benthic species respond differently to the input of various types of food particles than others. They suggest that food preferences exist. The main difference is made between the consumption of labile organic matter and the consumption of refractory organic matter (Carney *et al.*, 1989; Jorissen *et al.*, 2007). Labile organic matter is easily aerobically remineralised over time spans of days to weeks. It consists of fresh marine organic matter and phytodetritus. On the contrary the refractory organic matter takes longer time spans (months to years) to be consumed. This refractory organic matter finds its origin in aged organic matter and is often delivered by lateral sea currents. These later lateral advection currents are especially important in ocean margin settings. The consumption of refractory organic matter is anaerobic and it is mainly consumed by the endobenthic foraminifers. Rathburn *et al.* (1996) and Basak *et al.* (2009) suggest that food preference is one of the reasons why the  $\delta^{13}\text{C}_{\text{calcite}}$ -depth relation is often not respected for endobenthic species.

### 3.2.5 Symbionts & irradiance levels (planktic foraminifers)

Many planktic foraminifers that dwell at the ocean mixed layer contain symbionts. Symbionts preferentially remove  $^{12}\text{C}$  from the microenvironment for photosynthesis and therefore cause the foraminifers to have enriched  $\delta^{13}\text{C}$  test values. (Bemis *et al.*, 2000) The magnitude of the enrichment is related to the solar irradiance levels. Bemis *et al.* (2000) compared  $\delta^{13}\text{C}$  for foraminifers that lived under solar irradiance levels of 20–30  $\mu\text{mol photons}\cdot\text{m}^{-2}$  with foraminifers that lived under solar irradiance levels exceeding 386  $\mu\text{mol photons}\cdot\text{m}^{-2}$  (Note; 386  $\mu\text{mol photons}\cdot\text{m}^{-2}$  corresponds to the maximum symbiont photosynthesis rate). For symbiotic foraminifer *Orbulina universa*, they observed a +1‰ shift in  $\delta^{13}\text{C}$  due to the higher irradiance levels.

## 3.3 Parameters determining the $\delta^{18}\text{O}$ signature

### 3.3.1 Temperature

Temperature changes influence the equilibrium isotope fractionation between solid carbonate and dissolved bicarbonate. This effect is significant for  $\delta^{18}\text{O}$  and therefore  $\delta^{18}\text{O}$  is used as a tool to reconstruct paleotemperature. In foraminifer studies the most applied equation is the equation of Erez and Luz (1983), because their equation is based on planktic foraminifer calcite:

$$T(^{\circ}\text{C}) = 17.0 - 4.52 \cdot (\delta^{18}\text{O}_{\text{calcite}} - \delta^{18}\text{O}_{\text{seawater}}) + 0.03 \cdot (\delta^{18}\text{O}_{\text{calcite}} - \delta^{18}\text{O}_{\text{seawater}})^2 \quad (\text{Erez \& Luz 1983})$$

This equation shows that higher temperatures correspond with more depleted  $\delta^{18}\text{O}_{\text{calcite}}$  values (approximately  $-0.22\text{‰}\cdot^{\circ}\text{C}^{-1}$ ).

### 3.3.2 Geochemistry: salinity and the pH

The salinity of seawater is linked to the global ice volume, the balance between evaporation and precipitation and the mixing of different water masses. Therefore salinity is indirectly related to  $\delta^{18}\text{O}_{\text{seawater}}$ . Variation in the global ice volume strongly affects  $\delta^{18}\text{O}_{\text{seawater}}$ , since  $^{16}\text{O}$  is preferentially incorporated in ice. Fortunately the Early Eocene is considered an ice free world (Zachos *et al.*, 1994; Pearson *et al.*, 2007) and this therefore facilitates global  $\delta^{18}\text{O}_{\text{seawater}}$  prediction compared to most Cenozoic studies.

More regional effects are precipitation and evaporation. These parameters can influence the  $\delta^{18}\text{O}$  of surface water. The influence can become significant in extreme weather conditions like monsoons and droughts (Cooke and Rohling, 2001). Planktic species that preferentially build their test in one season and species that live only over short time spans are most vulnerable to these effects. It can be one of the reasons for a significant difference in  $\delta^{18}\text{O}$  between species or between specimens of the same species, reflecting strong seasonality. Finally salinity is also affected by the mixing of different water masses. If ocean water masses mix the effect on salinity remains limited. On the other hand if the seawater mixes with fresh water the effect on salinity can be very large. Since fresh water floats over salt seawater, the influence is mainly limited to the  $\delta^{18}\text{O}$  signature of mixed layer dwellers. Fresh water mixing is mainly a risk for continental margin settings like Aktulagay.

The study of Spero *et al.* (1997) demonstrates that the  $\delta^{18}\text{O}$  signature of planktic foraminifer calcite becomes more depleted with increasing pH. This is explained by the observation that the  $\delta^{18}\text{O}$  signature of  $\text{HCO}_3^-$  is relatively more enriched in  $^{18}\text{O}$  than the signature of  $\text{CO}_3^{2-}$ . An increase in pH corresponds with an increase in the  $[\text{CO}_3^{2-}]/[\text{HCO}_3^-]$  ratio and therefore corresponds with an increase in the consumption of  $\text{CO}_3^{2-}$  by planktic foraminifers (Spero *et al.*, 1997, Bemis *et al.*, 2000 and Katz *et al.*, 2010).

### 3.3.3 Vital effects

As explained for  $\delta^{13}\text{C}$ , the ontogenetic effect is the effect of changing isotopic value during growth. The effect can also exist for  $\delta^{18}\text{O}$  although it is less pronounced and often negligible for smaller benthic foraminifers. According to Cooke and Rohling (2001) the ontogenetic effect for mixed layer dwelling planktic foraminifers is considered an effect of migration of the specimens in the water column during their life time. However the data of Spero and Lea (1996) rather suggests the effect is related to metabolic rates. An increasing  $\delta^{18}\text{O}$  trend with growth has also been demonstrated for endobenthic *Uvigerina* species by Schumacher *et al.* (2010). In conclusion a limited size fraction range is preferred for both  $\delta^{13}\text{C}$  and  $\delta^{18}\text{O}$  to constrain the ontogenetic effect.

## 3.4 Other parameters

### 3.4.1 The sampled time interval and the sample size

A sample represents a certain time interval in which the above parameters varied. This time interval becomes significantly larger for sediments that were strongly bioturbated. Measurements that encompass multiple specimens have a time averaging effect while measurements of one specimen risk to only represent the circumstances of much smaller timeframes (months/years). Furthermore the various parameters can strongly fluctuate seasonally in ocean surface water, which has a significant effect on the isotopic signal of mixed layer dwelling foraminifers.

### 3.4.2 Post depositional alteration or contamination

The original measurement can be strongly modified by post depositional alteration or contamination. If secondary calcite precipitates on the test or if the test recrystallizes, the original signal can be lost. The effect of recrystallization and precipitation mainly depend on the fluid properties that caused it (geochemical composition and temperature). A contamination risk of the isotopic signal is the occurrence of bulk material within or on the foraminifer test.

## 4 Material and methods

### 4.1 Sampling and preparation

The Aktulagay section was sampled and described by Christopher King and David J Ward in 2000. Additional samples were taken in 2001 and 2003 (Steurbaut, 2011; King *et al.*, submitted). Deprez (2012) prepared 36 of the samples for micropaleontological analyses and 24 of these prepared samples were isotopically analyzed in this study. The sample preparation procedure is described here:

In order to disintegrate the clay within the samples, the preparation started with the immersion of the samples into cups filled with distilled water. Thereafter, the samples were dried in the oven at 50 °C. Next, the samples were immersed in a soda solution (50 g/l) and they were covered to prevent contamination. The samples remained in the soda for a day in order to further disintegrate the clay in the sample. After a day the soda color was noted as indication for the amount of organic matter in the sample.

Now that the clay was disintegrated, a first sample was washed through 2 successive sieves form respectively 2 mm and 63 µm. The 2 mm sieve was washed with tap water above the 63 µm sieve to remove any remaining particles (<2 mm) adhering to the sieve. Thereafter the sample in the 63 µm sieve was further washed with tap water until the water that passes through the sieve became clear. This indicated that clay and silt particles were no longer passing through. After wet sieving the >63 µm fraction, the sample was cast into a cup together with distilled water. The use of distilled water instead of tap water prevented contamination of the sample with secondary calcite. Before restarting the sieving procedure with the next sample, the sieves were emerged into methylene blue. This caused any remaining fossil fragments to gain a blue color so that they could be recognized as lab contamination. After staining, tap water was used to remove the methylene blue from the sieve and the sieving procedure could be restarted with the next sample. Finally all the samples were dried at 50 °C for a couple of days.

For this thesis 24 samples were dry sieved into the following fractions: 63-125 µm, 125-180 µm, 250-300 µm and >300 µm. From these fractions different foraminifer species were handpicked, using a binocular microscope, a pencil and distilled water. Information about the preservation, the fraction, the amount and an estimation of the mass of the foraminifers were written down for every measurement (Appendix I & Appendix II). The mass was measured using a microbalance with a precision of 0.001 mg or was estimated based on previous measurements of the same species. Information about the mass was necessary since the mass spectrometer requires a CO<sub>2</sub> pressure between 500 and 1150 µbar for high precision. The amount of CO<sub>2</sub> produced during the reaction of the sample with the acid is related to the carbonate mass. An appropriate carbonate mass was estimated to be between 35 and 65 µg. The amount of foraminifers required for one measurement could vary from a single fragment (e.g. *Pyramidulina sp1*, >300 µm fraction) up to a hundred foraminifers (*Pulsiphonina prima*, 63-125 µm fraction). After the specimens were picked, they were immersed in an ultrasonic bath to remove adhering particles. In case

fossils were not cleaned in an ultrasonic bath due to being very fragile and/or rare fossils, it was noted in the description of the measurement (Appendix I & Appendix II).

## 4.2 Work strategy

### 4.2.1 Isotope paleoecology

Three samples were chosen for an extensive study of the benthic foraminifer assemblage. The chosen samples were 13, 17 and 22 at 10.75 m, 14.05 m and 19.45 m respectively.

These samples were chosen because:

- They represent the 3 biofacies I, II and III defined by Deprez (submitted) (Figure 24). These biofacies represent different benthic foraminifer assemblages and environmental settings.
- No secondary calcite or recrystallization features were recognized.
- Sufficient material is available to measure less abundant foraminifers.

The goal was to measure as many different species as possible to determine their microhabitats. Due time constraints, species were preferentially gathered in the larger size fractions (125+  $\mu\text{m}$ ). Two exceptions were *Pulsiphonina prima* and *Uvigerina elongata* that had to be gathered in the 63-125  $\mu\text{m}$  size fraction. These exceptions were made because these species are an important part of the foraminifer assemblage with relative abundances up to 29.4 % and 15.8 % respectively (Deprez *et al.*, submitted; Figure 24). It was further chosen to only measure non agglutinated foraminifers with calcite tests. Some species were measured in all three samples to allow an isotopic correlation between the samples and to verify the consistence of their relative isotopic signature/microhabitat.

### 4.2.2 The isotopic record

The study of the section involves the generation of an epibenthic record, an endobenthic record, a thermocline planktic record and a mixed layer planktic record. These four isotopic records would generate information about these four microhabitats. The epibenthic record was considered the most important and gained full priority. After the ecological study the benthic species representing the epibenthic and the endobenthic microhabitat were chosen. For the planktic species it was assumed that the genera *Subbotina* and *Parasubbotina* represent a thermocline microhabitat while the genera *Acarinina* represent a mixed-layer microhabitat (Pearson *et al.*, 2006). For the benthic record it was possible to make species specific records, but for the planktic record this was not possible. Nevertheless it was attempted to identify the measured species. For all the long term records it was attempted to respect the size fractions to limit possible isotopic variation due ontogenetic effects.

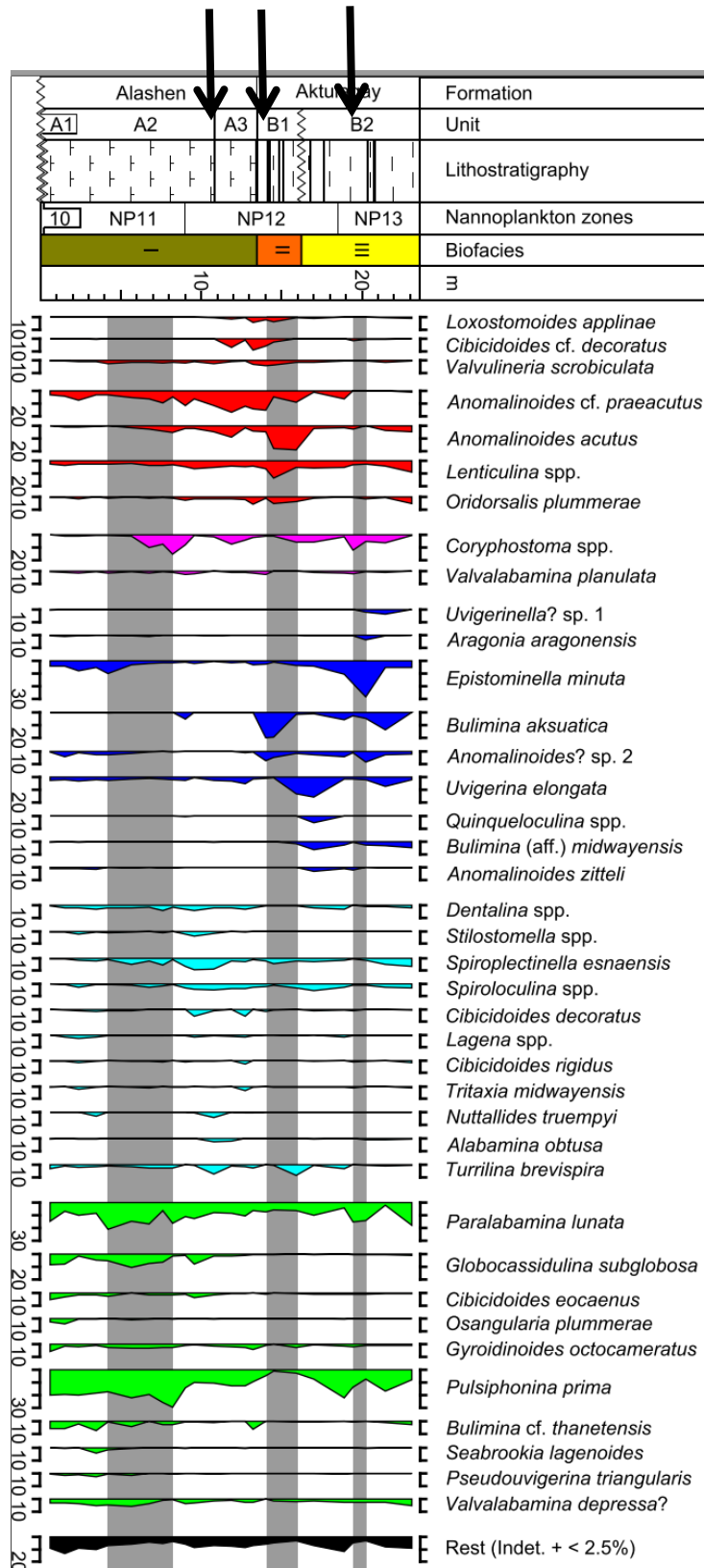


Figure 24. Edited figure from Deprez *et al.* (submitted). The arrows mark the chosen samples for the comprehensive isotopic ecological study. Sample 13 at 10.75 m represents biofacies I. Sample 17 at 14.05 m represents biofacies II. Sample 22 at 19.45 m represents biofacies III.

### 4.3 Scanning Electron Microscopy (SEM)

In order to verify the preservation and to help with the identification of some species, SEM-images were taken. In this study a Jeol JSM-6400 was used as scanning electron microscope. The foraminifers were placed on a stub and gold coated before they were examined under the SEM. This conductive coating prevented the specimens from charging by the electron beam.

### 4.4 The Finnigan Mass Spectrometer DeltaPlus

The Mass Spectrometer applied to measure both the oxygen ( $\delta^{18}\text{O}$ ) and the carbon ( $\delta^{13}\text{C}$ ) stable isotope ratios is the Finnigan Mass Spectrometer DeltaPlus. The Mass Spectrometer was made available by Prof. Dr. Ph. Claeys of the Vrije universiteit Brussel (VUB). The Finnigan Mass Spectrometer Delta Plus XP is a Continuous flow Isotope Ratio Mass Spectrometer (CF-IRMS). It operates on Isodat software (Version 2.0). The Finnigan Mass Spectrometer DeltaPlus can measure approximately 24 samples every 24 hours (excluding standards). The setup of the carousel is shown in Figure 25.

The Mass Spectrometer operates in the 2 lines at once. The 2 empty vials mark the starting and end position of each line. The procedure starts with a test of the acid in both lines. This test is necessary because the acid in the lines can oxidize during the time the Mass Spectrometer is inactive. Oxidized acid loses its effectiveness in dissolving the carbonate and needs to be removed during the acid test. After the acid test, the Mass Spectrometer starts with the measurement of the isotopic values of an International Standard (NBS 19) on both lines. NBS 19 is the international calcite standard material made in laboratories with known  $\delta^{18}\text{O}$  ( $-2.2\pm 0.02\text{‰}$ ) and  $\delta^{13}\text{C}$  ( $1.95\pm 0.01\text{‰}$ ) values relative to VPDB (Vienna Pee Dee Belemnite). The measured values of the standards are used to calibrate the measurements of the samples and to correct for systematic errors made by the mass spectrometer. Then as shown in Figure 25, the device continues to measure cyclically samples and standards until all vials in the carousel are empty. After measuring, the vials were cleaned in an ultrasonic bath of milli-Q water for two hours. Afterwards the vials are cleaned with acetone and dried.

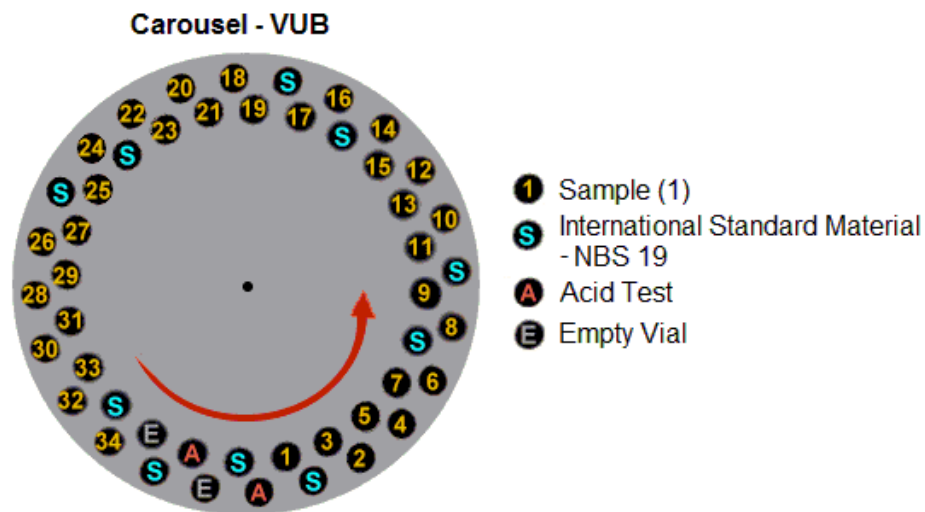


Figure 25. Set up of the Carousel in preparation of a measurement at the VUB.



## 4.5 Correcting the isotopic measurements and their standard deviations

All measurements were corrected with the workingstandards (NBS-19) that were measured in the same sequence. For every 8 samples, 2 working standards were measured. Both accuracy and precision are corrected with the working standards.

### 4.5.1 Accuracy

Accuracy is the extent in which an average measurement deviates from its true value. The accuracy was estimated by calculating the mean of the workingstandards and by determining the deviation from the known VPDB value. The calculated accuracies for  $\delta^{13}\text{C}$  varied from  $-0.024\text{‰}$  to  $+0.016\text{‰}$  and were in general smaller than those for  $\delta^{18}\text{O}$  varying from  $-0.028\text{‰}$  to  $+0.106\text{‰}$ . An example for an accuracy correction is given in Table 1.

### 4.5.2 Precision

The precision of a measurement can be expressed as the standard deviation relative to the true VPDB value. The standard deviation of an individual measurement is a combination of:

- The uncertainty of an individual measurement determined by the measuring device. ( $\sigma_{\text{measurement}}$ , e.g. influenced by the generated CO<sub>2</sub> pressure, leakage,...)
- The uncertainty that a workingstandard represents the VPDB value after the accuracy correction. ( $\sigma_{\text{workingstandard}}$ )
- The uncertainty that the true value of the workingstandards represent the exact value of VPDB ( $\sigma_{\text{workingstandard/VPDB}}$ ). These values are given by the workingstandard manufacturer. The official  $\delta^{18}\text{O}$  and  $\delta^{13}\text{C}$  values of the standard NBS-19 are respectively  $-2.20 \pm 0.01$  and  $1.95 \pm 0.02$ .

Analogous to Nørgaard *et al.* (1999), the combined standard deviation  $\sigma_{\text{measurement/VPDB}}$  can be calculated in the following way;

$$\sigma_{\text{measurement/VPDB}} = \sqrt{[(\sigma_{\text{measurement}})^2 + (\sigma_{\text{workingstandard}})^2 + (\sigma_{\text{workingstandard/VPDB}})^2]}$$

An example for a precision correction is given in Table 1.

Example for accuracy and precision corrections (*Cibicidoides decuratus* at 7.60 m).

Accuracy correction:

$$\delta^{13}\text{C}_{\text{measurement}} = -0.138\text{‰}$$

$$\delta^{18}\text{O}_{\text{measurement}} = -2.492\text{‰}$$

$$\delta^{13}\text{C}_{\text{workingstandard average}} = 1.943\text{‰}$$

$$\delta^{18}\text{O}_{\text{workingstandard average}} = -2.295\text{‰}$$

$$\delta^{13}\text{C}_{\text{VPDB}} = 1.950\text{‰}$$

$$\delta^{18}\text{O}_{\text{VPDB}} = -2.200\text{‰}$$

$$\text{Correction} = +0.007\text{‰}$$

$$\text{Correction} = +0.095$$

$$\delta^{13}\text{C}_{\text{corrected measurement}} = -0.131\text{‰}$$

$$\delta^{18}\text{O}_{\text{corrected measurement}} = -2.397\text{‰}$$

Precision Correction:

$$\sigma_{\text{measurement}, \delta^{13}\text{C}} = 0.024\text{‰}$$

$$\sigma_{\text{measurement}, \delta^{18}\text{O}} = 0.048\text{‰}$$

$$\sigma_{\text{workingstandard}, \delta^{13}\text{C}} = 0.025\text{‰}$$

$$\sigma_{\text{workingstandard}, \delta^{18}\text{O}} = 0.034\text{‰}$$

$$\sigma_{\text{workingstandard/VPDB}, \delta^{13}\text{C}} = 0.010\text{‰}$$

$$\sigma_{\text{workingstandard/VPDB}, \delta^{18}\text{O}} = 0.020\text{‰}$$

$$\sigma_{\text{measurement/VPDB}, \delta^{13}\text{C}} = 0.036\text{‰}$$

$$\sigma_{\text{measurement/VPDB}, \delta^{18}\text{O}} = 0.062\text{‰}$$

Table 1. Example of the measurement corrections for accuracy and precision.

## 5 Results – the section

### 5.1 The range of the $\delta^{13}\text{C}$ and $\delta^{18}\text{O}$ data

Based on the results of the ecological study, the epibenthic record is based on *Cibicidoides decoratus*, *Anomalinooides acutus* and *Anomalinooides zitteli*. The endobenthic record is based on *Uvigerina elongata* and *Bulimina aksuatica*. The thermocline planktic record is based on *(Para)Subbotina spp.* and the mixed layer planktic record is based on *Acarinina spp.* The choice of these species will be justified in the discussion section. All the data is plotted in Figure 26. Figure 26The figure demonstrates that the benthic data, the thermocline planktic data and the mixed layer planktic data can easily be distinguished based on their isotopic ranges. For  $\delta^{13}\text{C}$  the benthic data ranges from -5.1‰ to 0.7‰, the thermocline planktic data ranges from -0.3‰ to 1.5‰ and the mixed layer planktic data ranges from 2.1‰ to 4.8‰. For  $\delta^{18}\text{O}$  the benthic data ranges from -3.6‰ to -1.6‰, the thermocline planktic data ranges from -4.1‰ to -3.5‰ and the mixed layer planktic data ranges from -7.0‰ to -4.0‰.

### 5.2 The $\delta^{13}\text{C}$ and $\delta^{18}\text{O}$ results over the section

The  $\delta^{13}\text{C}$  and  $\delta^{18}\text{O}$  data is plotted over the section in Figure 27 and Figure 28. This data has not yet been corrected for vital effects and the data with preservation/contamination problems has not yet been evaluated. Therefore a detailed description of the data will follow after the data has been corrected and the preservation is evaluated.

### Overview of all measurements

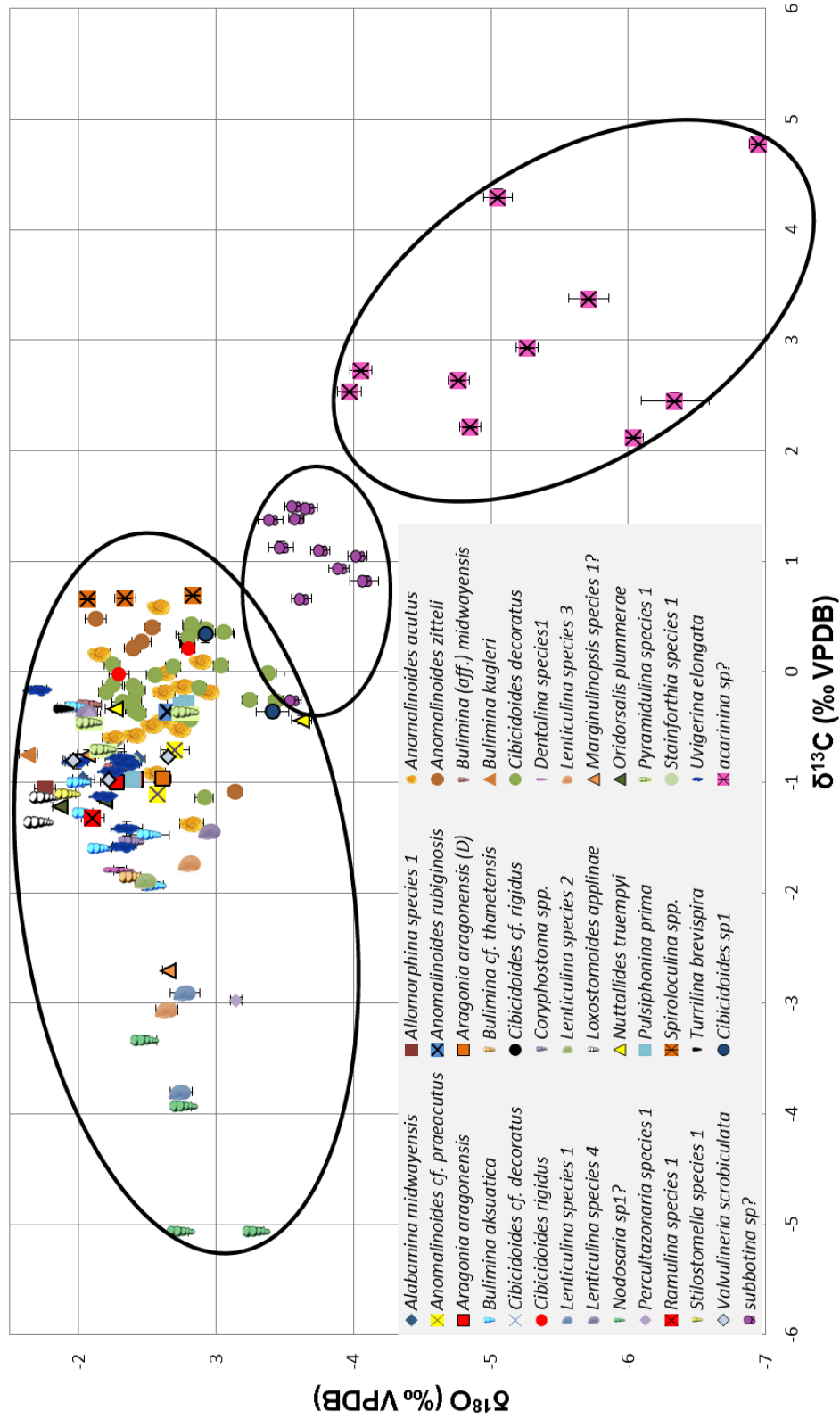
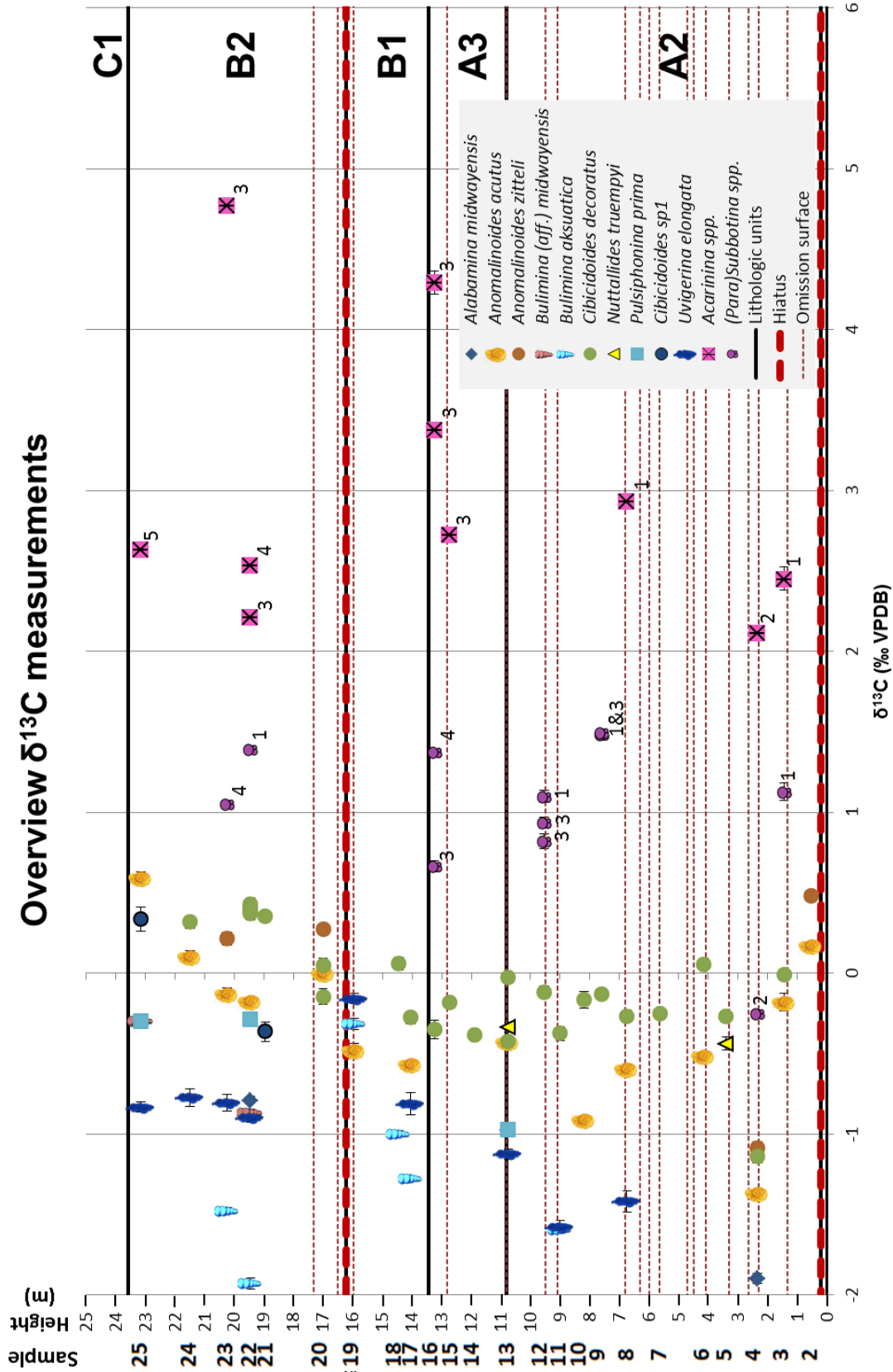
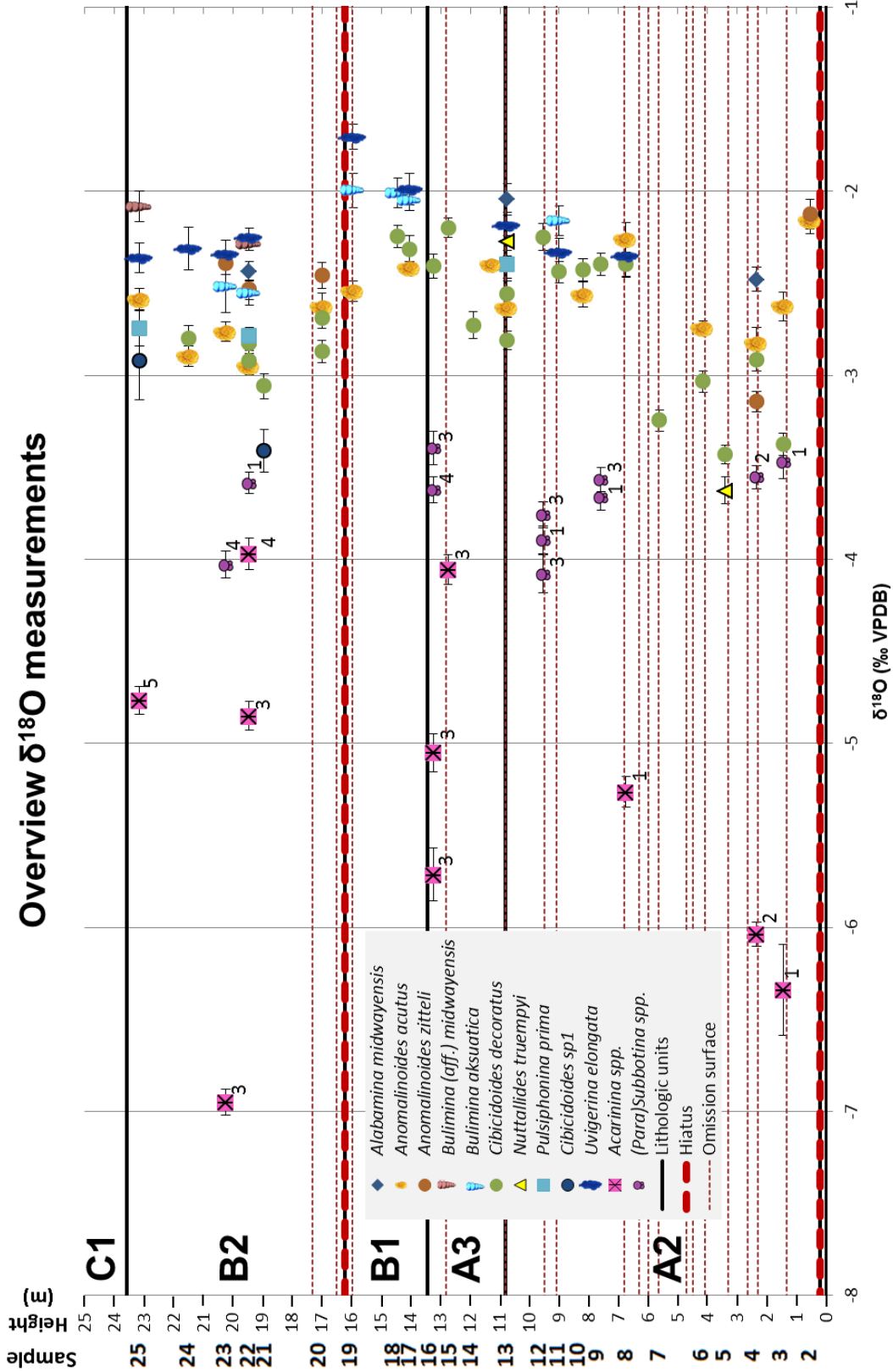


Figure 26. Overview of all  $\delta^{13}\text{C}$  &  $\delta^{18}\text{O}$  data of the 25 samples and the bulk data of Deprez (2012). The benthic data, the thermocline planktic data and the mixed layer planktic data can easily be distinguished based on their isotopic values.



**Acarinina sp. 1:** *Acarinina esnehensis*, **Acarinina sp. 2:** *Acarinina cuneicamerata*, **Acarinina sp. 3:** *Acarinina medizai*,  
**Acarinina species 4: ?**, **Acarinina species 5: ?**, **Subbotina sp. 1:** *Subbotina patagonica*, **Subbotina, sp. 2:** *Parasubbotina pseudowilsoni*, **Subbotina**  
**sp. 2: ?** *Subbotina enaricae* 4: *Subbotina vancouveris* (Daaren et al. 2006)

Figure 27. Overview of the  $\delta^{13}\text{C}$  measurements over the section. The lithologic units, omission surfaces and hiatuses were marked based on the litholog of King *et al.* (Submitted).



**Acarinina sp. 1:** *Acarinina esnehensis*, **Acarinina sp. 2:** *Acarinina cuneicamerata*, **Acarinina sp. 3:** *Acarinina medizai*,  
**Acarinina species 4:** ?, **Subbotina sp. 1:** *Subbotina patagonica*, **Subbotina, sp. 2:** *Parasubbotina pseudowilsoni*,  
**Subbotina sp. 3:** ? **Subbotina species 4:** *Subbotina vernaensis* (Pearson *et al.* 2006)

## 6 Diagenesis & contamination

### 6.1 Introduction

Diagenesis is known to alter the isotopic signature of foraminifer calcite. According to Sexton *et al.* (2006), “the cool tropic paradox” (D’Hondt and Arthur, 1996) during the Cretaceous and the Eocene was likely primarily caused by diagenesis. Therefore diagenesis is a problem for accurate paleoclimatic reconstructions and a good evaluation of the measured foraminifer calcite is considered crucial. Further possible contamination due the presence of bulk material should also be examined. Therefore this chapter focusses on preservation and contamination problems. The first goal of this chapter is to determine which isotopic measurements are affected significantly by diagenesis and/or contamination. The second goal is to estimate the direction and the magnitude of the deviation.

In this study SEM-images were applied to examine the preservation. The method allows to judge the (relative) significance and the type of the diagenesis/contamination problem. SEM-images are frequently used in literature for this purpose. Some studies attempted to link diagenetic features observed in the SEM-images to the deviation in the isotopic signature. This was done for planktic foraminifers and to a lesser degree for benthic foraminifers by Sexton *et al.* (2006) and Sexton & Wilson (2009) respectively.

Observations concerning the preservation and contamination under the binocular microscope are summarized in Appendix III.

## 6.2 Diagenesis of benthic foraminifers

### 6.2.1 Introduction

The preservation of the benthic foraminifers in the Aktulagay section is variable over the section. Furthermore the preservation within the samples is not always uniform. To judge the preservation SEM-images were applied. According to Sexton and Wilson (2009), benthic foraminifers are in general observed to be more robust to diagenetic alteration than planktic foraminifers. This is explained as a consequence of two aspects. First of all early diagenesis in pore waters would occur at a similar temperature as the water temperature in which the benthic foraminifers secreted their test. Secondly many benthic foraminifer species have more heavily calcified tests than most planktic foraminifers, causing them to be more robust to diagenesis (Sexton and Wilson, 2009).

### 6.2.2 Results

#### 6.2.2.1 *Cibicidoides decoratus*

*Cibicidoides decoratus* is a species that was measured over most of the section. Figure 29 demonstrates several SEM-pictures of specimens from several different samples. In the left column of Figure 29, some examples are given of specimens with excellent preservation of samples 4, 20 and 22. Their outer test wall and the cross section appear to be unaltered. However the cross section is hard to judge due imperfect breaking of the tests. In Figure 29J a lineation is sometimes observed on the test wall. In the right column of Figure 29 examples of foraminifers are given where clear indications for diagenesis were noticed under the binocular microscope. The main indication was a decrease in transparency of the test, which was very subtle for the photographed specimens of Sample 4 and Sample 10 (Figure 29C;R). For other specimens of Sample 3, 5, 6, 7 and 21 the decrease in test transparency was often obvious and the secondary crystals were sometimes visible with the binocular microscope (e.g. Figure 29G;K). In Figure 30 the cross section of a less transparent specimen from Sample 5 is enlarged. The SEM-image suggests that recrystallization occurred at the inner test wall and possibly more central of the test wall. It is possible that the larger crystals found on the inner wall of the specimen of Sample 6 (Figure 29G) represent a subsequent stage of continued recrystallization. It is remarkable that the outer test wall of the example from Sample 6 appears to be rather smooth and well preserved. While examples from samples 4 and 10 have tiny secondary crystals growing on their outer test walls but still possess smooth inner test walls (Figure 29C;R).



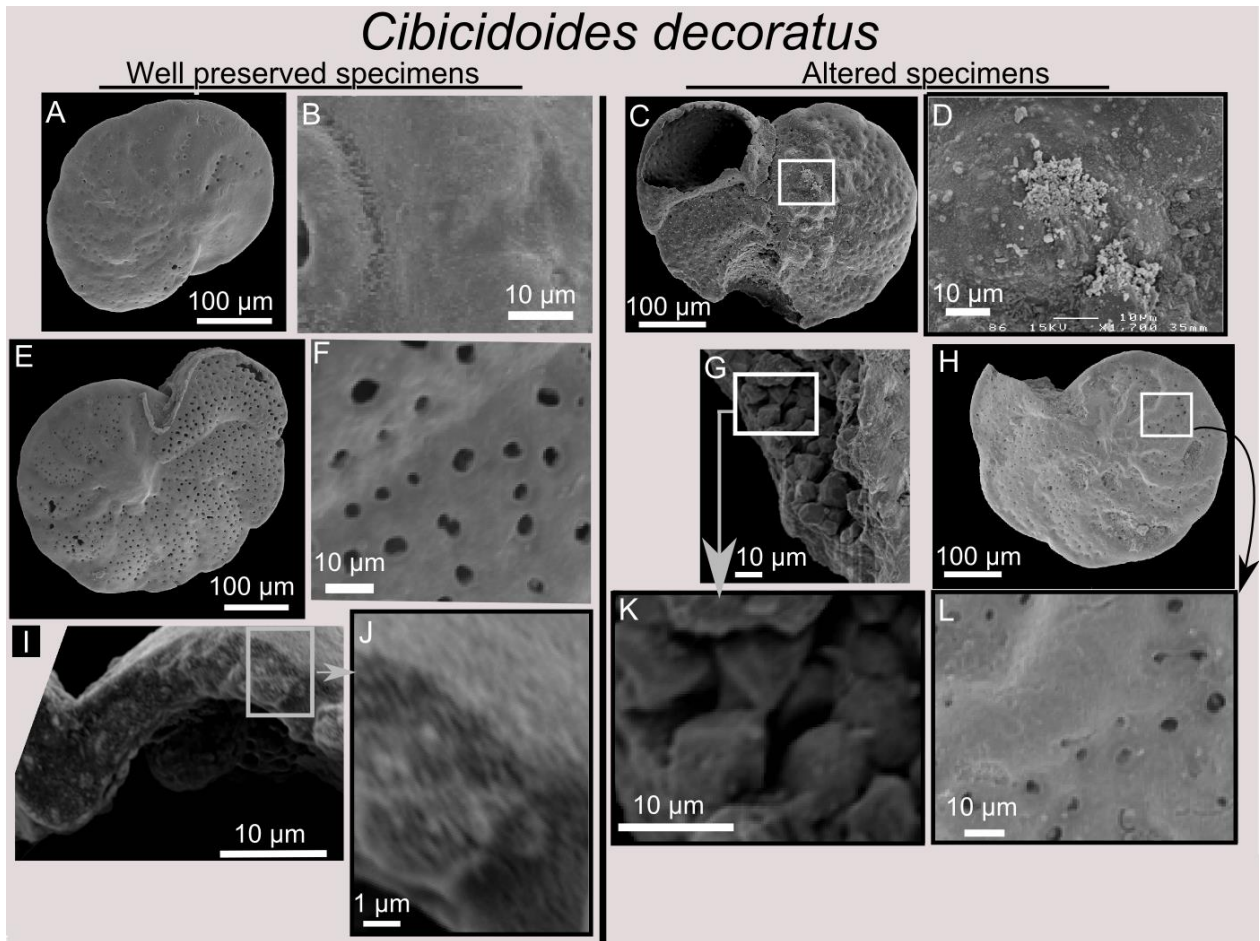


Figure 29. SEM-images of *Cibicidoides decoratus* specimens from several samples to discuss the preservation. The left column presents specimens with no signs of recrystallization/secondary calcite. The right column presents specimens affected by diagenesis. Figure A, B, C and D are all specimens from Sample 4. A demonstrates a smooth test wall. B is a close-up of A. C demonstrates an apparently well preserved specimen, but a close up in D demonstrates the occurrence of small secondary crystals that indicate the start of recrystallization. Therefore the preservation within Sample 4 is not uniform. E and F are images of a specimen from Sample 20 with no indications for diagenesis. G and H are pictures of a specimen in Sample 6 that was not transparent under the binocular microscope. In G the secondary calcite crystals are very large (up to 10  $\mu\text{m}$  in diameter). H reveals that despite the large secondary crystals within the foraminifer, the outer test wall demonstrates no clear sign of diagenesis. I and J demonstrate a cross section of a specimen from Sample 20. In I the inner test wall appears rather homogeneous. In J a lamination feature is recognized, it is unclear whether this is related to the original test structure or related to dissolution. M is a well preserved specimen from Sample 22. N and O are images of a specimen from Sample 5. This specimen was less transparent under the binocular microscope. In N the difference with the better preserved specimens is not obvious although some of the test textures appear to be fading. In the cross section indications are found of recrystallization (magnified in Figure 30). P and O demonstrate a well preserved specimen of Sample 22. R, S and T are images from a specimen in Sample 10. In figure T small secondary calcite crystals grow on the test wall, while in S these secondary crystals are not visible. This demonstrates that the preservation is not always homogeneous over a single test. It is important to mention that the secondary crystals in T were recognized under the binocular microscope due to a local decrease in transparency.

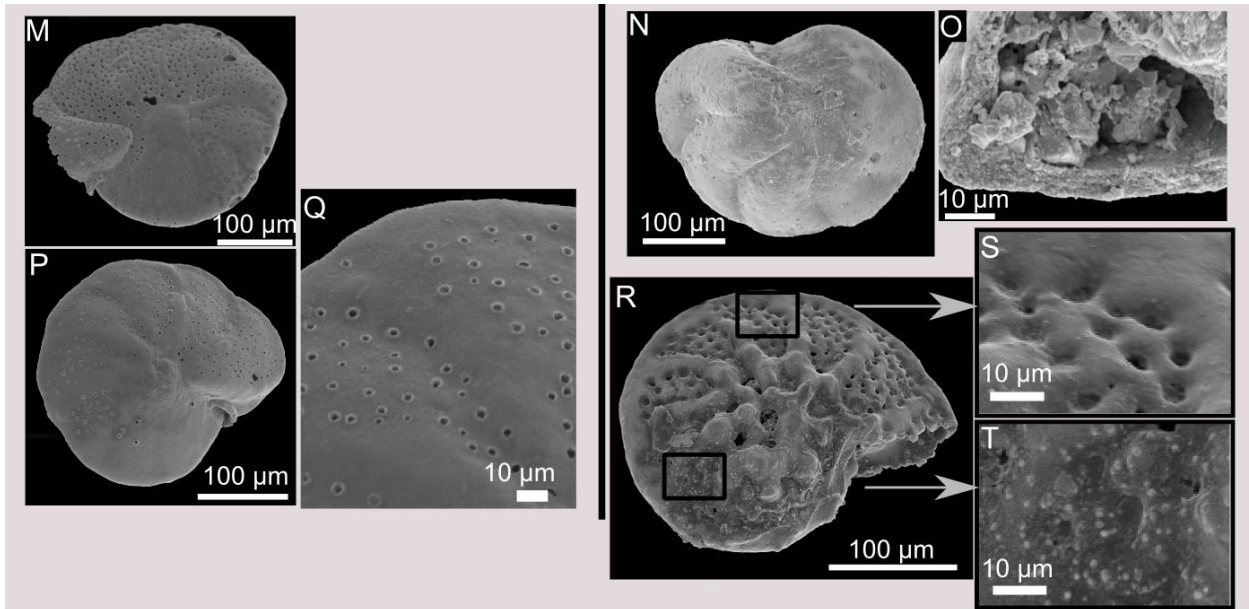


Figure 29 (continued).

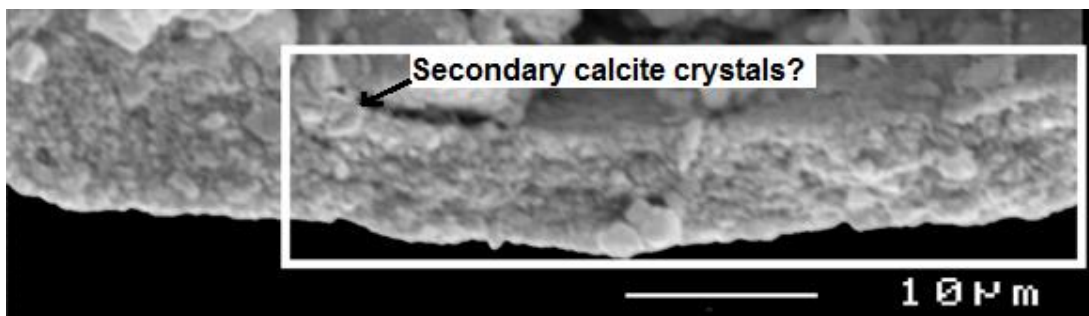


Figure 30. The figure demonstrates the cross section of the test wall of *Cibicidoides decoratus* from Sample 5. The inner test wall appears to consist of secondary crystals formed by the process of recrystallization. It is unclear whether recrystallization was limited to the inner test wall or also occurred in the center of the test.

### 6.2.3 *Anomalinoides acutus*

*Anomalinoides acutus* was measured in several samples of the Aktulagay section. In samples where obvious diagenetic alteration occurred for (almost) all the specimens of *Cibicidoides decoratus*, it was sometimes still possible to find enough *Anomalinoides acutus* specimens for an isotopic measurement with an apparent better preservation. This was the case in samples 3 and 6 and was most likely related to their significant higher abundance. The SEM-images of *Anomalinoides acutus* can be found in Figure 31. It was no longer attempted to intentionally pick specimens with bad preservation for the SEM and thus all specimens photographed in Figure 31 are representative for specimens used for the isotopic measurements. In general the SEM-images of the outer test walls demonstrate rather good preservation. Small secondary calcite crystals similar to the *Cibicidoides decoratus* specimen in Figure 29T were not observed. However, many specimens often had a somewhat rougher texture on their outer test wall (e.g. Figure 31K) and sometimes also on their inner test wall (e.g. Figure 31P). A similar lineation feature as observed for the *Cibicidoides decoratus* specimen of Sample 20 (Figure 29J) is also observed for the

*Anomalinoides acutus* specimen of Sample 8 (Figure 31J). Finally the specimen from Sample 3 (Figure 31F) has some small bulbous accumulations of secondary calcite on its inner test wall.

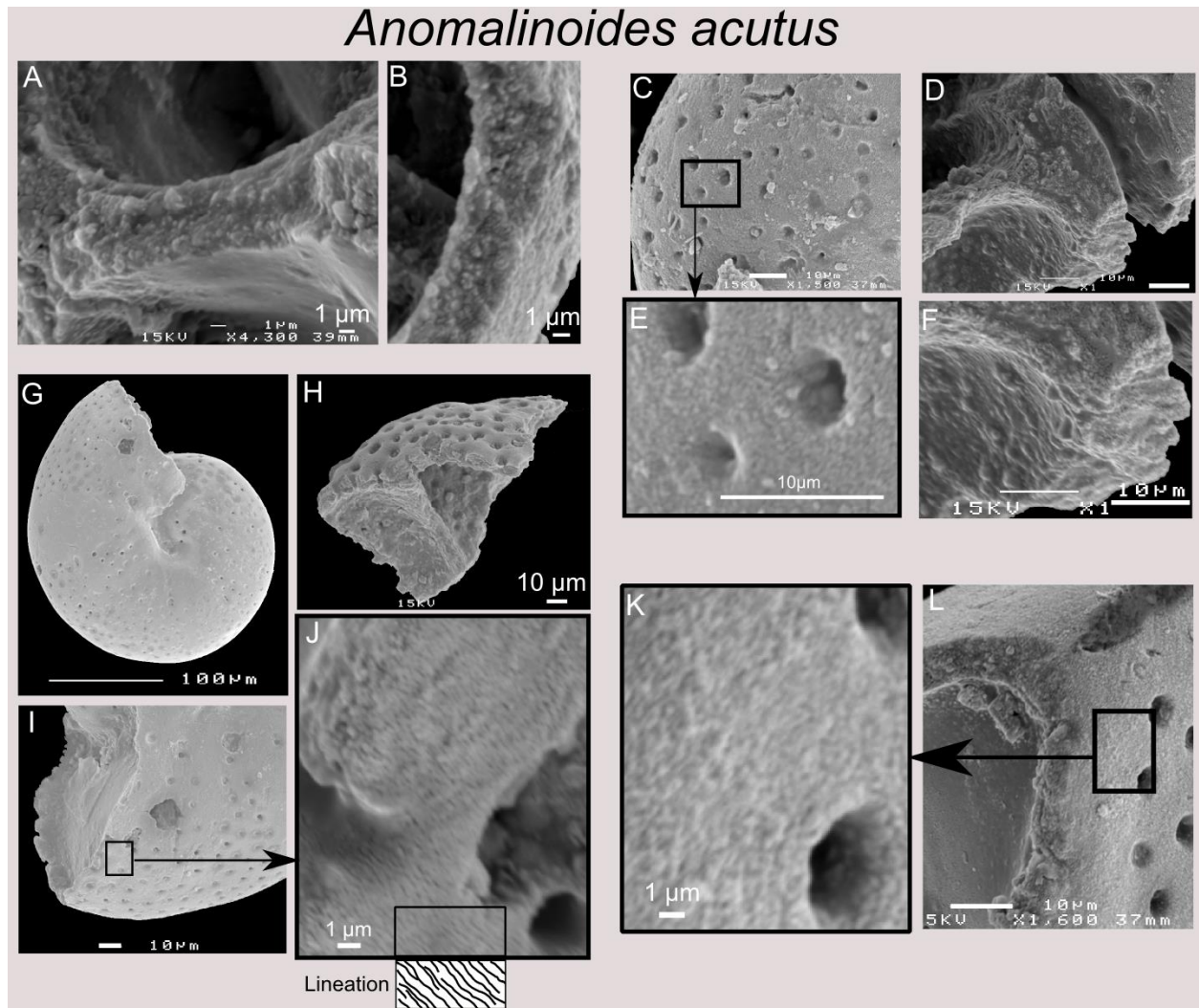


Figure 31. SEM-images of *Anomalinoides acutus* specimens from several samples to discuss the preservation. A and B represent cross sections from a specimen from Sample 2. The cross section in A crosses an internal chamber wall. The rough appearance is likely the result of breaking. Both adjacent chamber walls are very smooth. The cross section of the outer wall in B has a similar appearance, although the outer wall is clearly less smooth and has a more granular appearance, possibly related to dissolution. C, D, E and F are pictures from the test of a specimen from Sample 3. The outer test wall in E has rather a granular appearance. The inner wall in F demonstrates small secondary calcite bulges. G, H, I and J demonstrate a specimen from Sample 8. The test wall appears to be smooth and in J a similar lineation feature is recognized as for the *Cibicidoides decoratus* specimen of Sample 20 (Figure 29J). K and L demonstrate a specimen of Sample 10. The specimen is rather well preserved although the outer wall has again a more granular appearance. M and N are images of a specimen from Sample 6. The inner test wall is smooth and there is no clear sign of secondary calcite. O and P are pictures from a specimen from Sample 24, the inner test wall has a similar rougher appearance than the outer wall although no clear secondary calcite crystals are observed. Q and R demonstrate a specimen from Sample 19, the inner test wall is again somewhat rough. S and T are pictures of a specimen of Sample 25 demonstrating the absence of secondary calcite within the pores.



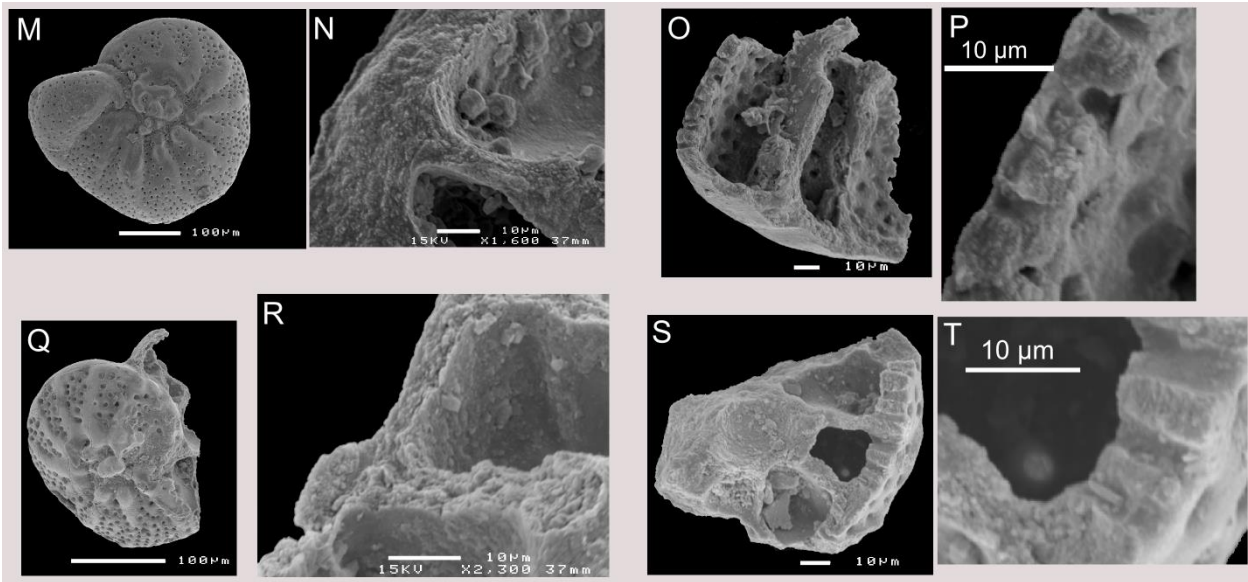


Figure 31 (continued).

#### 6.2.4 Other benthic foraminifera

Figure 32 demonstrates some other specimens from several samples. An *Anomalinoidea zitteli* specimen from Sample 20, a *Bulimina kugleri* specimen from Sample 17 and a *Bulimina aksuatica* specimen from Sample 19 have all smooth tests, open pores and no indications of secondary calcite (Figure 32F;J;K). The *Anomalinoidea zitteli* specimen from Sample 4 has a well preserved inner test wall, but the outer test wall is not so smooth and the cross section demonstrates some loss of the original texture (Figure 32A;B;C). The *Uvigerina elongata* specimen from Sample 24 reveals that secondary calcite can be heterogeneously present within the same specimen (Figure 32D;E;H;I). Secondary calcite filled the pores on one of the test walls. The *Uvigerina elongata* specimen from Sample 25 has secondary calcite precipitated in the pores of all test walls (Figure 32L;M). This secondary calcite was not observed in other specimens like *Pulsiphonina prima* from the sample.

## Benthic foraminifera

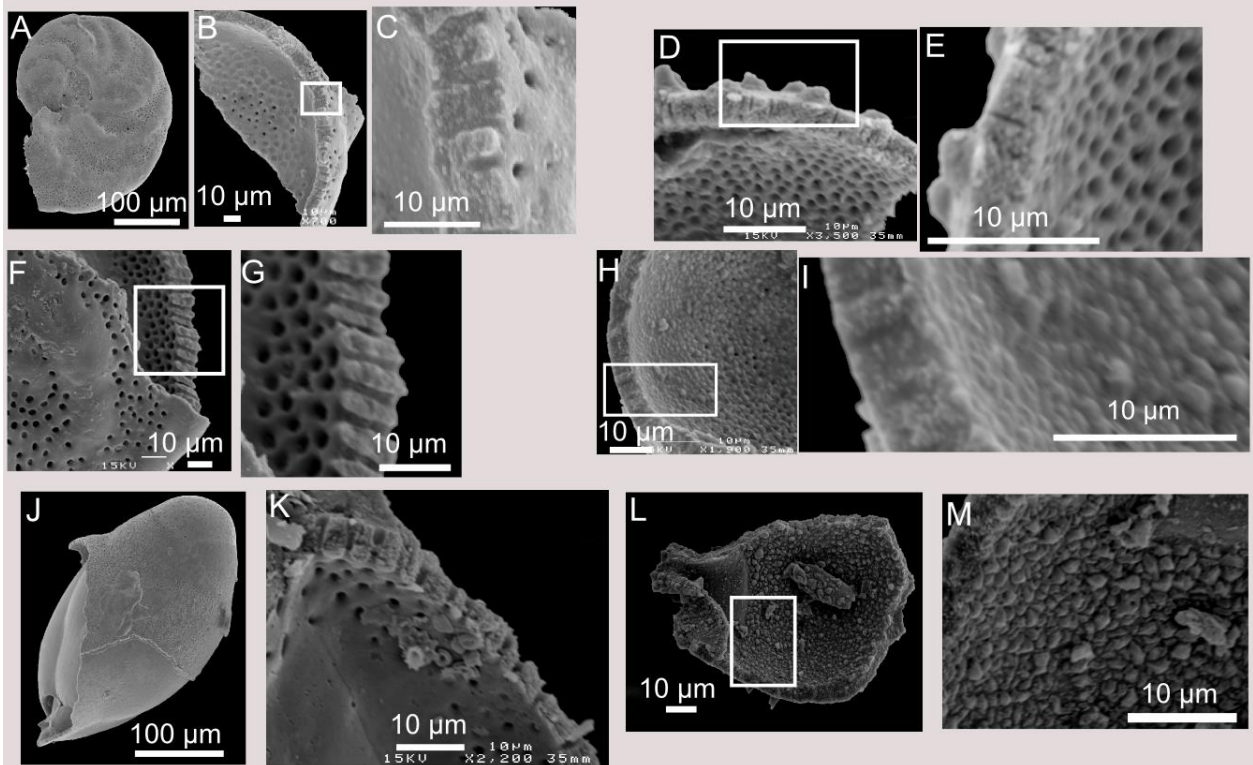


Figure 32. The SEM-images of other benthic specimens than *Anomalinoides acutus* and *Cibicidoides decoratus* from several samples. A, B and C are pictures of an *Anomalinoides zitteli* specimen in Sample 4. The outer test wall in A and C is slightly altered. The pores however are open and the texture of the inner test wall is well preserved. F and G are pictures of a specimen of *Anomalinoides zitteli* from Sample 20. This specimen appears extremely well preserved with smooth surfaces and open pores. D, E, H and I are pictures of the same *Uvigerina elongata* specimen from Sample 24. It is remarkable that the pores in D and E appear open, while the pores in H and I are filled with secondary calcite. This reflects the heterogeneity of the preservation. J is a picture of *Bulimina kugleri* in Sample 17, demonstrating the excellent preservation of a rather fragile test. K is a picture of *Bulimina aksuatica* from Sample 19, the smooth test wall and open pores indicate excellent preservation in this sample. L and M are pictures from a specimen of *Uvigerina elongata* in Sample 25. The pores are clearly filled with secondary calcite but the aperture remained open, the foraminifer does not appear to be recrystallized.

## 6.2.5 Discussion

### 6.2.5.1 Recrystallization & secondary calcite precipitation

Figure 33 demonstrates several specimens that are considered good or at least moderately well preserved specimens by Sexton and Wilson (2009). In comparison with the SEM-images of benthic foraminifers made by Sexton and Wilson (2009), it is clear that the preservation in the samples from Aktulagay section can in general be considered as good. Furthermore it is clear that the decrease in transparency of foraminifers under the binocular microscope can be considered an effective tool to recognize recrystallization. Because Sexton *et al.* (2006) did not observe a significant difference between the  $\delta^{13}\text{C}$  values of clearly diagenetically altered planktic foraminifers and well preserved planktic foraminifers, it is unlikely that  $\delta^{13}\text{C}$  would deviate much from its true value for the rather well preserved benthic specimens in this study. However  $\delta^{18}\text{O}$  is considered much more vulnerable to diagenesis (Sexton *et al.*, 2006; Sexton and Wilson, 2009) and it cannot be excluded that a limited amount of recrystallization (e.g. Figure 29T) and/or secondary calcite (e.g. Figure 32I) was sometimes undetected. However it is unclear whether the extent of the diagenesis in these cases is sufficient to significantly alter the  $\delta^{18}\text{O}$  signature.

To estimate influence of secondary calcite on the isotopic signature, some of the diagenetically altered *Cibicidoides decoratus* specimens were measured in samples 3, 5 and 6 (e.g. Figure 29G). *Anomalinooides acutus* was also measured in samples 3 and 6 with specimens that were clearly better preserved (Figure 31N;F). Since both species are considered epibenthic species (justified in 7.2.1), a linear correlation should exist between well preserved specimens for both their  $\delta^{13}\text{C}$  and  $\delta^{18}\text{O}$  signatures (Katz *et al.*, 2003). The diagenetically altered species should deviate from the correlation. The data is plotted in Figure 34. Based on data of the better preserved samples, the plot demonstrates a strong correlation between *Cibicidoides decoratus* and *Anomalinooides acutus* for both  $\delta^{13}\text{C}$  and  $\delta^{18}\text{O}$  with the coefficients of determination ( $R^2$ ) being 0.77 and 0.76 respectively. Figure 34 allows some valuable conclusions. First of all it is clear that the diagenetically altered *Cibicidoides decoratus* specimens have  $\delta^{18}\text{O}$  values deviating from the curve towards more negative values ( $\Delta\delta^{18}\text{O} = -0.6\text{‰}$ ). Secondly, the  $\delta^{13}\text{C}$  values of diagenetically altered *Cibicidoides decoratus* do not significantly deviate from the predicted values by *Anomalinooides acutus*. This confirms the assumption that the  $\delta^{13}\text{C}$  value is more robust against diagenetic alteration than  $\delta^{18}\text{O}$  value (e.g. Sexton *et al.*, 2006). Thirdly the confirmation that the predicted correlation exists, demonstrates that the measurements from e.g. samples 8 and 10 do not deviate from the trend for both  $\delta^{13}\text{C}$  and  $\delta^{18}\text{O}$ . This supports the assumption that the possible isotopic deviation caused by (unidentified) minor alteration only has a small or possibly negligible effect on the measurement.

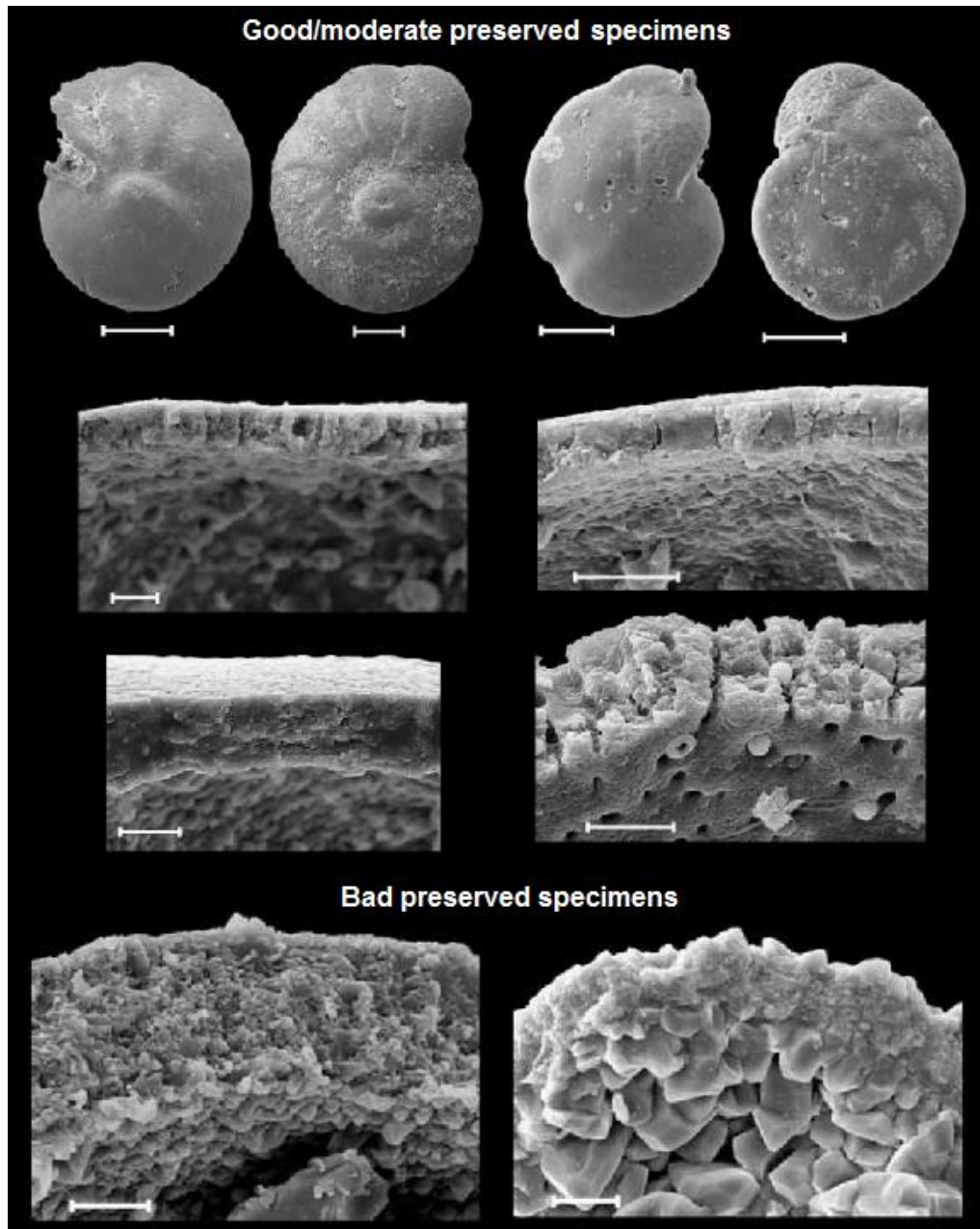


Figure 33. SEM-images of specimens that are considered good or at least moderately preserved by Sexton and Wilson (2009). The scale bar for whole specimens is 100  $\mu\text{m}$ , the scale bar for cross sections is 10  $\mu\text{m}$ . (Modified figure from Sexton and Wilson, 2009)

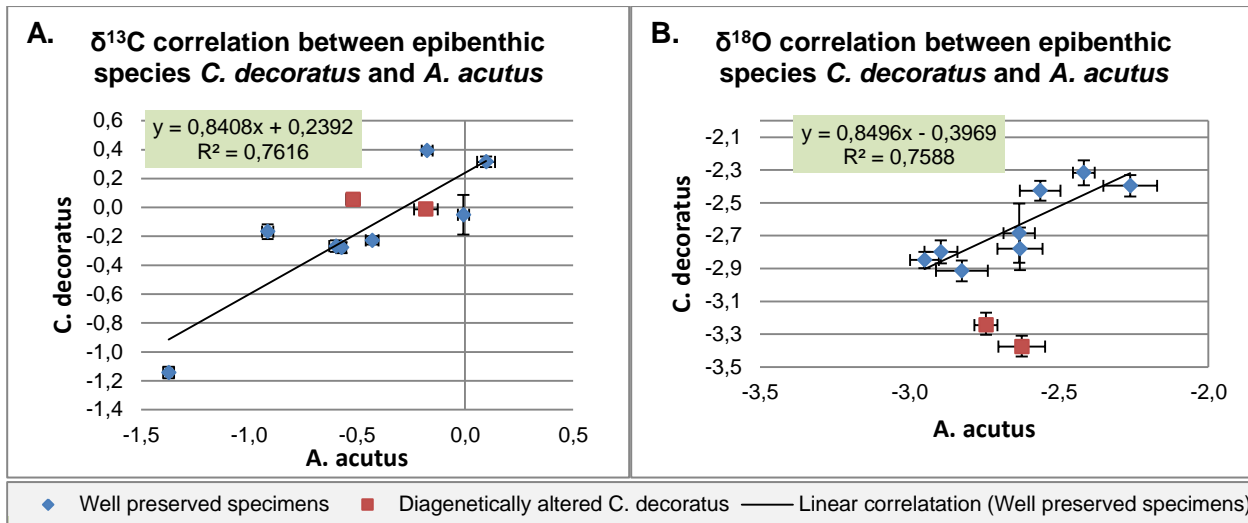


Figure 34. The correlation between epibenthic species *Cibicidoides decoratus* and *Anomalinoidea acutus* for  $\delta^{13}\text{C}$  and  $\delta^{18}\text{O}$ . The well preserved specimens are from Samples 4, 8, 10, 13, 17, 20, 22 and 24. The samples that include diagenetically altered *C. decoratus* are from Sample 3 and Sample 5. For this reason these samples were not included for the calculation of the coefficient of determination ( $R^2$ ). Plot A confirms that  $\delta^{13}\text{C}$  is indeed robust to diagenesis as concluded by Sexton *et al.* (2006). And B clearly demonstrates that  $\delta^{18}\text{O}$  is not and deviates towards more negative values.

### 6.2.5.2 Dissolution

Another feature frequently observed on several specimens in the SEM-pictures was the more “rough” outer test wall (e.g. Figure 31K). Less frequently this was also observed for the inner test wall (Figure 31P). This feature is considered the effect of dissolution. It is assumed that dissolution would only influence the isotopic values of the test if it was more severe.

Finally the lineation feature observed for the *Cibicidoides decoratus* specimen of Sample 20 (Figure 29J) and the *Anomalinoidea acutus* species of Sample 8 (Figure 31J) could be an original test feature. However this remains uncertain because the feature might also be the result of dissolution.

### 6.2.6 Summary

In summary the effect of diagenesis on benthic foraminifers was considered negligible for the benthic  $\delta^{13}\text{C}$  signature over the entire section. However the benthic  $\delta^{18}\text{O}$  signature can become significantly more depleted due the diagenetic alteration. All benthic measurements were indications exist for diagenetic alteration are summarized in Table 2.



Height (m)	Sample Nr.	Foraminifer Species	$\delta^{13}\text{C}(\text{‰})$ Measured	$\delta^{13}\text{C}(\text{‰})$ Standard deviation	$\delta^{18}\text{O}(\text{‰})$ Measured	$\delta^{18}\text{O}(\text{‰})$ Standard deviation	Expected Effect
1.45	3	<i>Cibicoides decoratus</i>	-0.012	0.035	-3.376	0.059	Certain for $\delta^{18}\text{O}\downarrow$
1.45	3	<i>Anomalinoidea acutus</i>	-0.182	0.055	-2.624	0.078	Possible for $\delta^{18}\text{O}\downarrow$
3.40	5	<i>Cibicoides decoratus</i>	-0.267	0.030	-3.431	0.050	Certain for $\delta^{18}\text{O}\downarrow$
3.40	5	<i>Nuttallides truempyi</i>	-0.437	0.039	-3.625	0.073	Certain for $\delta^{18}\text{O}\downarrow$
4.15	6	<i>Anomalinoidea acutus</i>	-0.519	0.031	-2.744	0.039	Possible for $\delta^{18}\text{O}\downarrow$
4.15	6	<i>Cibicoides decoratus</i>	0.055	0.039	-3.034	0.056	Certain for $\delta^{18}\text{O}\downarrow$
5.62	7	<i>Cibicoides decoratus</i>	-0.254	0.030	-3.245	0.058	Certain for $\delta^{18}\text{O}\downarrow$
8.20	10	<i>Cibicoides decoratus</i>	-0.168	0.051	-2.426	0.061	Possible for $\delta^{18}\text{O}\downarrow$
18.95	21	<i>Cibicoides decoratus</i>	0.352	0.031	-3.059	0.068	Certain for $\delta^{18}\text{O}\downarrow$
18.95	21	<i>Cibicoides sp. 1</i>	-0.364	0.060	-3.411	0.115	Certain for $\delta^{18}\text{O}\downarrow$
21.50	24	<i>Uvigerina elongata</i>	-0.774	0.053	-2.311	0.114	Possible for $\delta^{18}\text{O}\downarrow$
23.15	25	<i>Uvigerina elongata</i>	-0.834	0.032	-2.361	0.083	Possible for $\delta^{18}\text{O}\downarrow$

Table 2. Measurements with a possible deviation of their original  $\delta^{18}\text{O}$  signature due diagenesis.

## 6.3 Diagenesis of planktic foraminifers

### 6.3.1 Introduction

Sexton *et al.* (2006) provide several SEM-images to judge the occurrence of diagenetic alteration on planktic foraminifers. They distinguish 2 types of diagenetic alteration. The first type is recrystallization or neomorphism. In this case the replacement of biogenic calcite with inorganic calcite. The second type is calcite cementation, where inorganic calcite overgrowths precipitate over or in the test wall. A third type could be included being dissolution. Sexton *et al.* (2006) use the terms “glassy”, “frosty” and “chalky” to quantify the alteration. Glassy foraminifers have a transparent appearance that is similar to that of modern foraminifers. Frosty material refers to material that has undergone relatively modest alteration and chalky is described as material that has been strongly altered.

In this study all measured planktic foraminifers had a rather transparent test under the binocular microscope. This is an important indication for the absence of major recrystallization. However the preservation is not perfect and an extended subdivision into preservation categories appears to be more appropriate.

### 6.3.2 Results

*Note: in some of the SEM-images extremely smooth surfaces occur on certain parts of the test walls. When these surfaces fill the pores of the test wall and typically contain cracks, they are not part of the foraminifer calcite but are an anomaly related to the gold coating procedure prior to the SEM-photography.*

The SEM-images used to judge the preservation of planktic foraminifers in each sample are displayed in Figure 35 (*Subbotina spp.* and *Parasubbotina spp.*) and Figure 36 (*Acarinina spp.*). The SEM-images of planktic foraminifers used as a reference are displayed in Figure 37 and Figure 38 (Sexton *et al.*, 2006). All sample specific observations regarding preservation of planktic foraminifers are given in Table 3.

First of all the presence of overgrowths and the texture of the outer test surface is examined in Figure 35 and Figure 36. In general most textures are preserved, although sometimes the preservation for an individual specimen can be rather heterogeneous. An excellent example is the specimen *Acarinina medizzai?* from Sample 23 with two well distinguishable cross sections (Figure 36.6c;6d). The upper cross section (Figure 36.6c) demonstrates altered muricae while the lower cross section (Figure 36.6d) demonstrates excellent preservation. Overgrowths of secondary calcite can be recognized by the observation of coarser test surfaces, the observation of rounded crystals that obscure the test texture and/or the observation of rhombohedral crystals on the test wall (Sexton *et al.*, 2006). Indications for overgrowths and the presence of a thin calcite cement coating were sometimes observed on the outer test wall e.g. in Figure 35.1d;2e. Secondly the inner test surface is examined. The images demonstrate that the inner test wall is always well preserved because the surface is smooth and the pores are not filled with secondary calcite. Thirdly the internal structure and the texture are examined in cross section. According

to Sexton *et al.* (2006) well preserved glassy foraminifers display a microgranular texture characteristic of biogenic calcite. In our samples the texture appears to be somewhat coarser possibly indicating minor recrystallization. In some specimens (Figure 37.7b) the site of initial calcification could be distinguished (corresponding to the POM or primary organic membrane). Finally, some specimens are affected by dissolution (e.g. the specimen in Figure 36.6c). This can be deduced from the larger spacing observed between the successive layers from the test. However peeling, which is the mechanical loss of the outer weakened test layer (Sexton *et al.*, 2006), was not observed among the measured specimens.

### 6.3.3 Discussion

A comparison with the frosty foraminifers from Sexton *et al.* (2006) (Figure 38), reveals that our specimens are rather well preserved or at least moderately preserved, although not always as good as the glassy specimens in their study (Figure 37 & Figure 38). There are no real indications for significant recrystallization. First of all the internal test wall surface was always smooth. Secondly most of the internal textures are rather well preserved in cross section although not as good as the pristine specimens from Sexton *et al.* (2006). Thirdly the outer test surface is often slightly altered, but these alteration problems appear rather related to secondary calcite cement than to recrystallization. Nevertheless some specimens have significantly better preservation than the others. For these specimens both the inner and outer test walls appear unaltered and the site of initial calcification can still be distinguished in cross section. These specimens are from samples 15, 16 and 22 (Figure 35.5;6;7 and Figure 36.3;4;7;8). Therefore the specimens were subdivided into moderate (M) and good (G) preservation and positioned on a relative scale in Table 3 and Figure 39. The observation that our specimens had transparent tests under the binocular microscope probably remains one of the main arguments to state that the preservation must have been significantly better than the frosty specimens of Sexton *et al.* (2006).

It appears that the most significant preservation problem for the planktic specimens is not recrystallization but is related to the presence of secondary calcite cement on some of the outer test walls. This is certainly a problem in samples 3 and 4 (Figure 35.1d, Figure 35.2e, Figure 36.1b and Figure 36.2a). The problem possibly also exists to a lesser degree for some of the other moderately preserved specimens because the presence of secondary calcite observed to be heterogeneous. In theory this could also pose a problem for the benthic foraminifers. However due their smooth test wall, irregularities concerning secondary calcite are much easier to detect under the binocular microscope than for planktic foraminifers.

Finally the dissolution observed in e.g. Figure 36.6c is unlikely to have a significant effect on the isotopic measurements. The dissolution was always very limited and never resulted into peeling of the outer test wall.

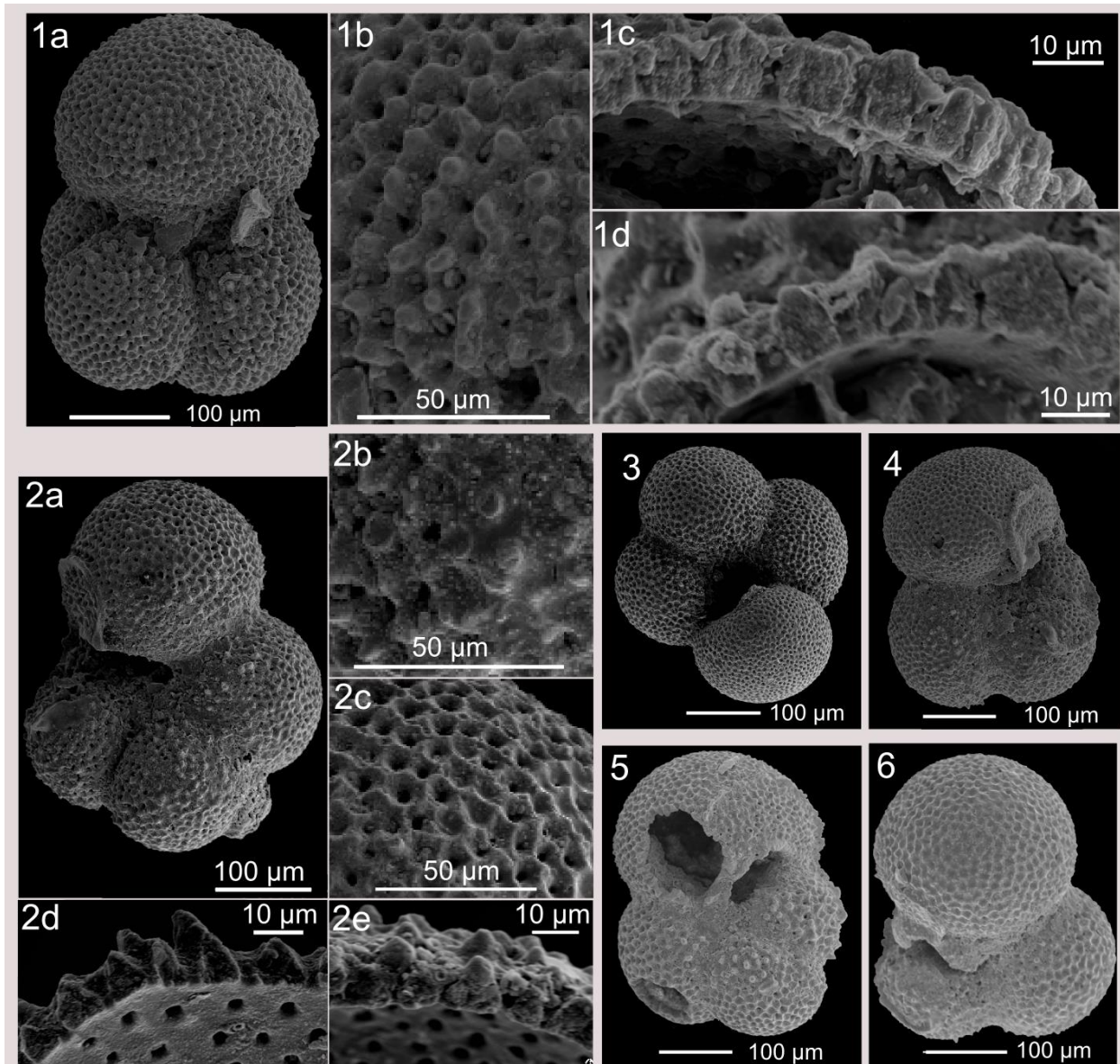


Figure 35. This figure presents a specimen for each isotopic measurement of planktic (sub)thermocline foraminifera that was considered representative for the preservation of the measured specimens (Genera *Subbotina* and *Parasubbotina*). 1a;b;c;d: *Subbotina patagonica*? from Sample 3 (1.45 m). Both cross sections demonstrate rather good preservation however there is clearly a thin layer of secondary calcite present on the outer test wall. 2a;b;c;d present a *Parasubbotina pseudowilsoni*? specimen from Sample 4 (2.35 m). In 2c and 2d the preservation appears fine but in 2b and 2e the outer test wall is clearly affected with secondary calcite. 3: a (*Para*)*Subbotina* sp. 3 specimen from Sample 9 (7.60 m). 4: a *Subbotina patagonica*? specimen from Sample 12 (9.55 m). The preservation of the specimens in 3 and 4 appear moderately preserved. 5: a *Subbotina patagonica*? specimen from Sample 22 (19.45 m). 6: a *Subbotina yegaensis*? specimen from Sample 23 (20.25 m). 7: a *Subbotina yegaensis*? specimen from Sample 16 (13.25 m). The specimens in 5, 6 and 7 appear to have a good to excellent preservation. Certainly because the POM is still well distinguishable in 7b. 8: a (*Para*)*Subbotina* sp. 3 specimen from Sample 12 (9.55 m). The preservation in 8 is rather moderate similar to 3 and 4.

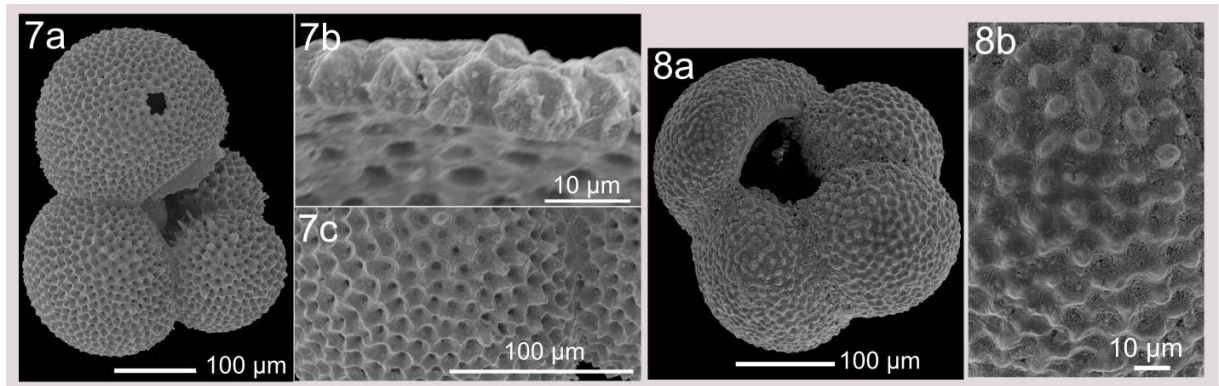


Figure 35 (continued).

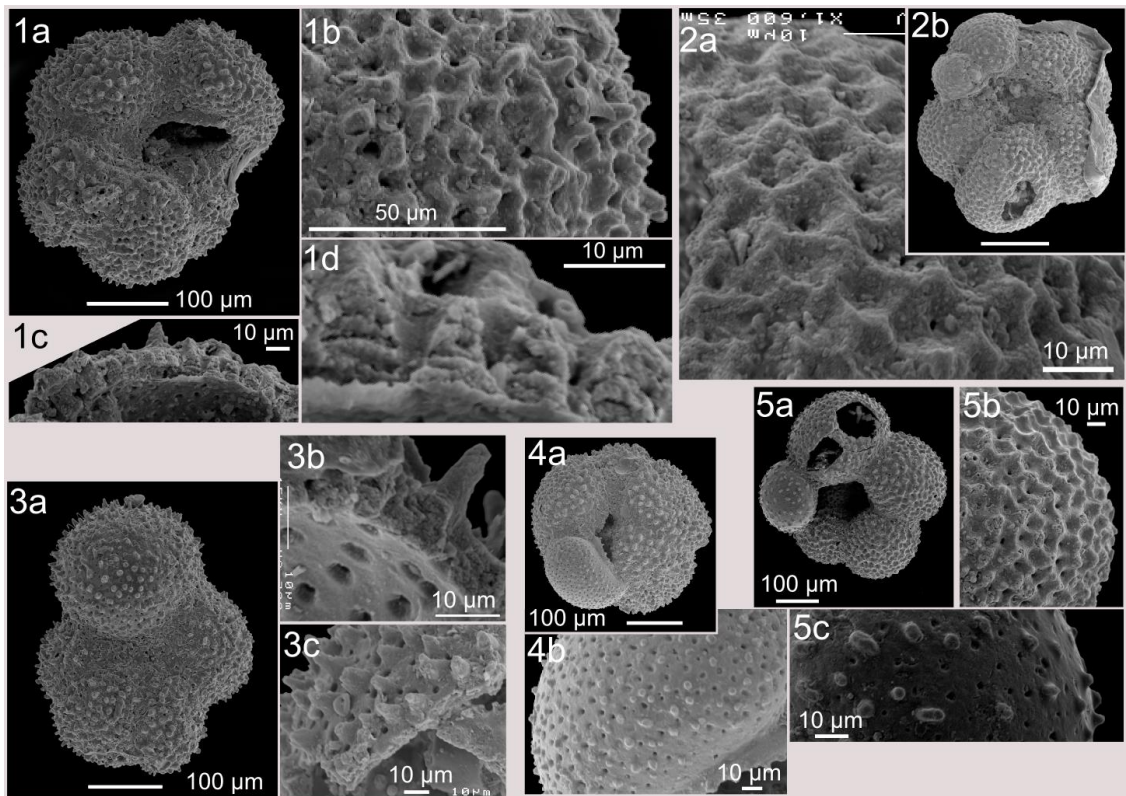


Figure 36. This figure presents a specimen for each isotopic measurement of planktic mixed layer foraminifera that was considered representative for the preservation (Genus *Acarinina*). 1a;b;c;d: *Acarinina cuneicamerata*? specimen from Sample 4 (2.35 m). 2a;b: *Acarinina esnehensis*? specimen from Sample 3 (1.45 m). The specimens in 1 and 2 appear to have altered outer test walls. 3a;b;c: *Acarinina medizai*? specimen from Sample 22 (19.45 m). 4a;b: *Acarinina* sp. 4 specimen from Sample 22 (19.45 m). 5a;b;c: *Acarinina esnehensis*? specimen from Sample 8 (6.75 m). 6a;b;c;d: *Acarinina medizai*? specimen from Sample 23 (20.25 m). 7a;b;c: *Acarinina medizai*? specimen from Sample 15 (12.75 m). 8a;b;c;d: *Acarinina medizai*? specimen from Sample 16 (13.25 m). 9a;b;c;d: *Acarinina* sp. 5 specimen from Sample 25 (23.15 m).



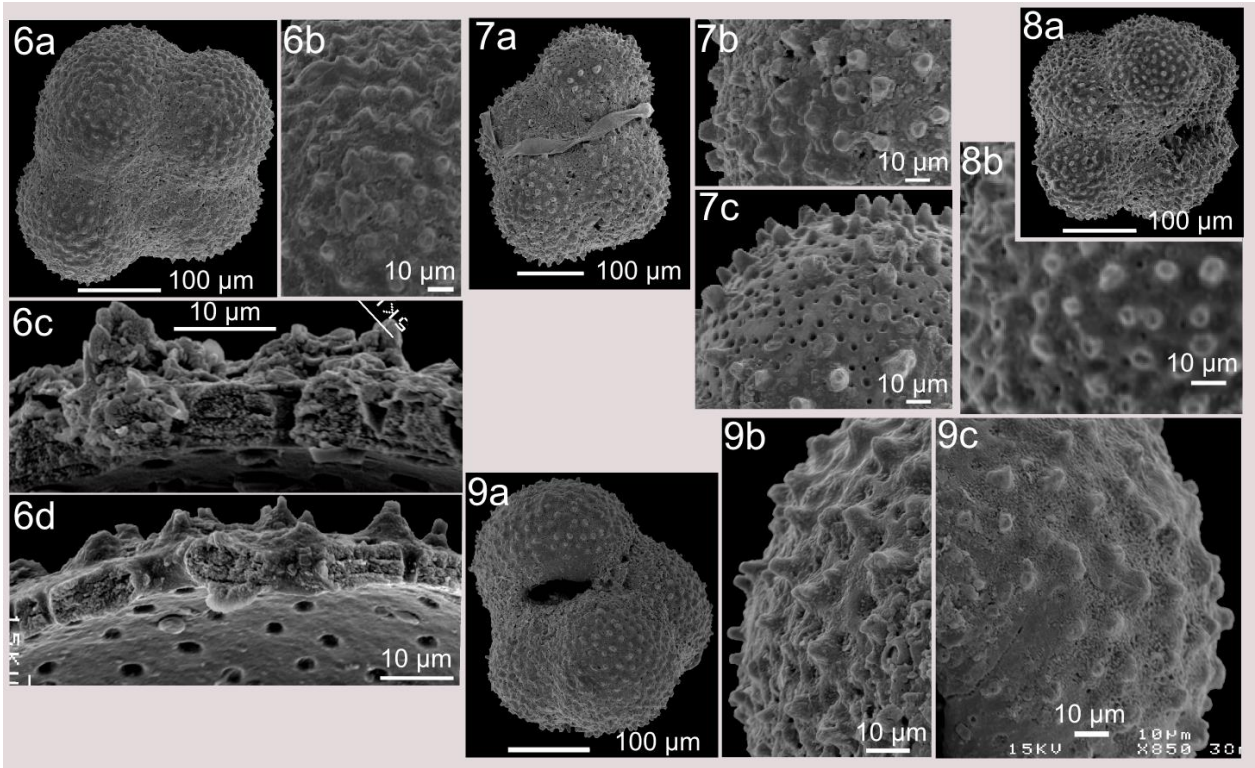


Figure 36 (continued).

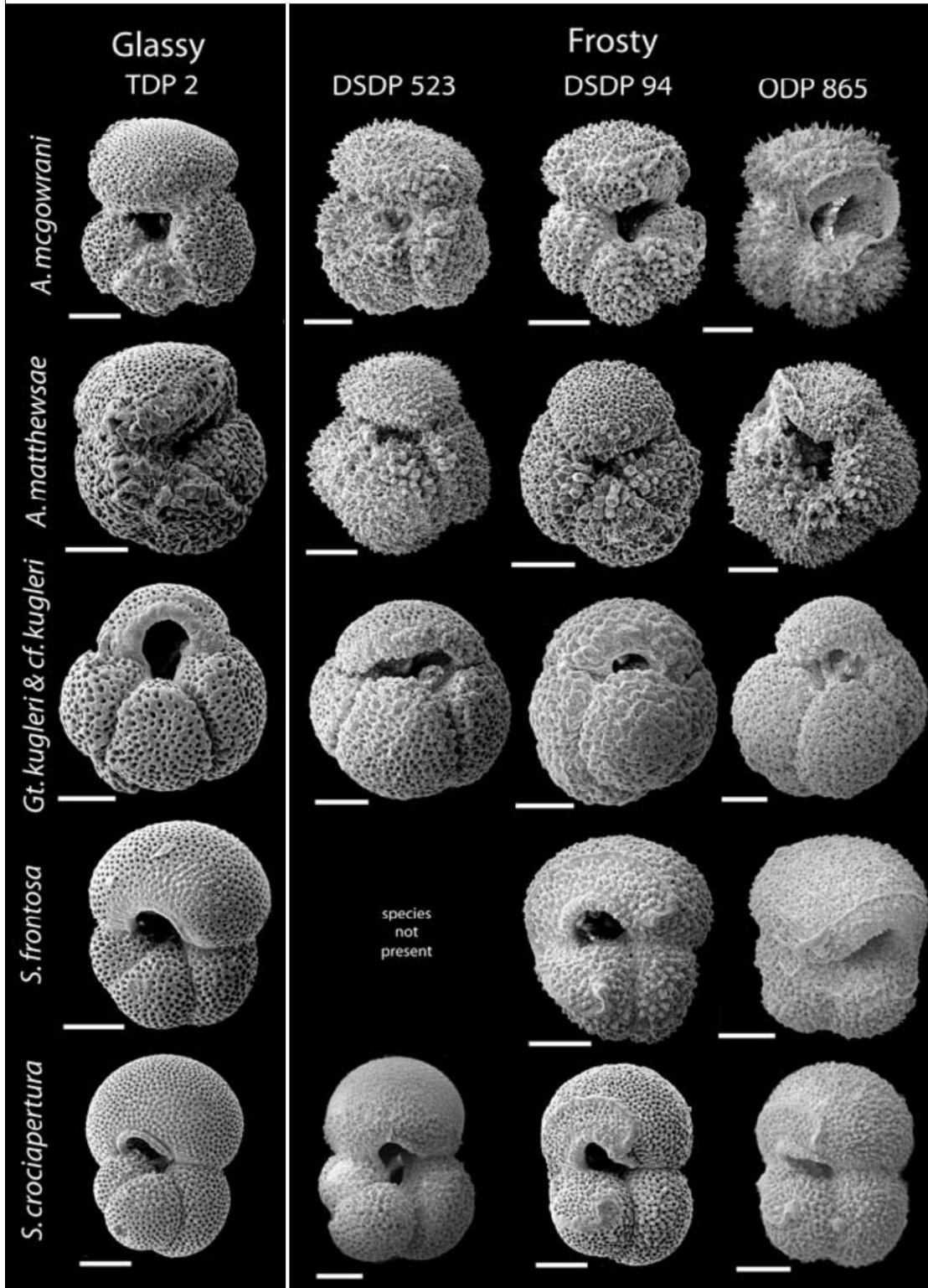


Figure 37. SEM images of well preserved glassy specimens (left) versus a worse preserved frosty specimens (right). The scale bars are 100 µm. The specimens originate from four drill sites (TDP 2, DSDP 94, DSDP 523, and ODP 865). (Edited figure from Sexton *et al.*, 2006)



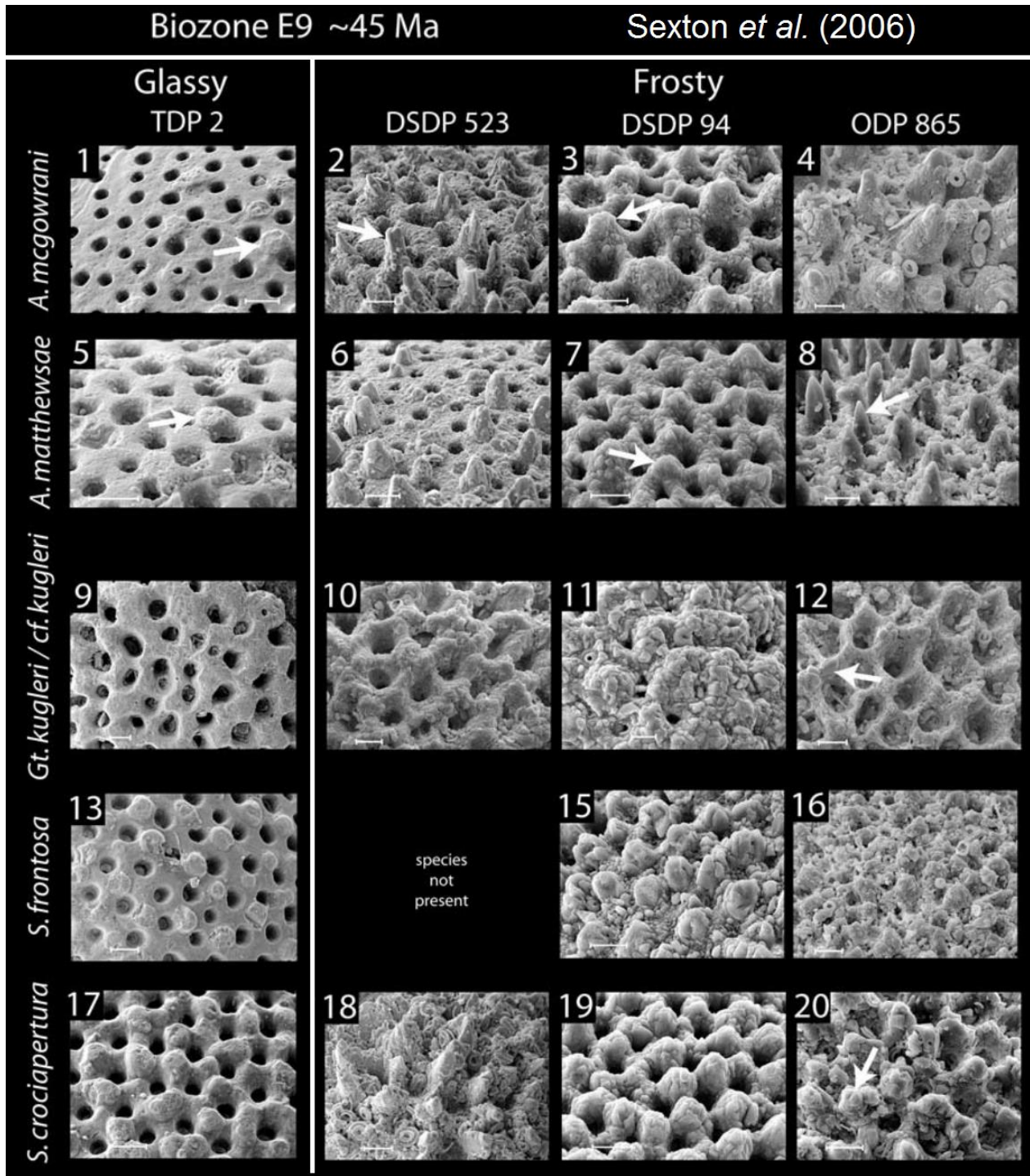


Figure 38. SEM images of well preserved glassy specimens (left) versus a worse preserved frosty specimens (right). The scale bars are 10  $\mu$ m. The specimens originate from four drill sites (TDP 2, DSDP 94, DSDP 523, and ODP 865). (Edited figure from Sexton *et al.*, 2006)



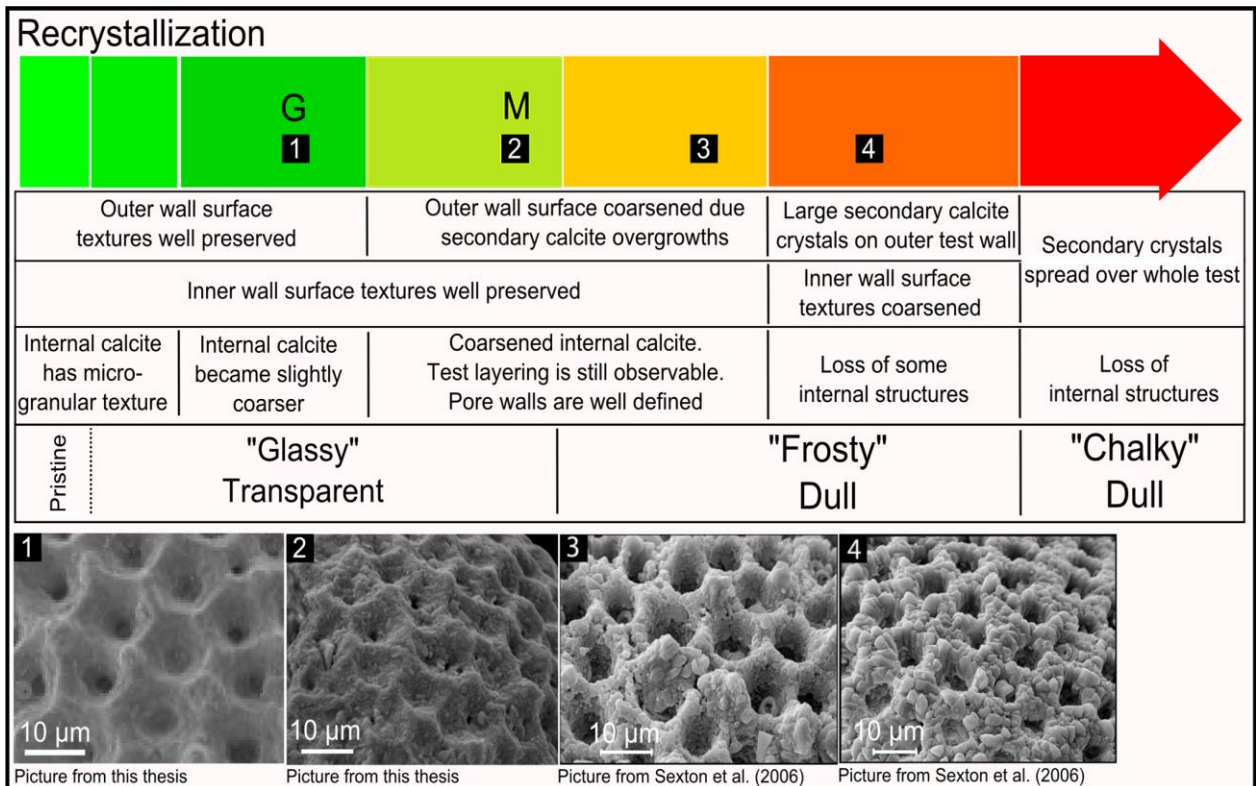


Figure 39. In this figure a relative scale was created to position our specimen categories Good (G) and Moderate (M) from Table 3 on a scale also showing the "glassy", "frosty" and "chalky" subdivision of Sexton *et al.* (2006). Images number 3 and 4 are examples of "frosty" foraminifers taken from Sexton *et al.* (2006).

Sample position	Genus	Observations	Category
Sample 3 (1.45 m)	<i>Acarinina</i>	<ul style="list-style-type: none"> <li>• Presence of small overgrowths on the outer test surface. The test is appears altered</li> </ul>	M/B
	<i>Subbotina</i>	<ul style="list-style-type: none"> <li>• Presence of small overgrowths on the outer test surface.</li> <li>• <b>In cross section a (local) thin coat of secondary calcite is observed.</b></li> <li>• However Pores are not filled and internal shell is often smooth.</li> </ul>	M/B
Sample 4 (2.35 m)	<i>Acarinina</i>	<ul style="list-style-type: none"> <li>• Presence of small overgrowths on the outer test surface.</li> <li>• Cross section contains coarser grains than expected for unaltered biogenic calcite.</li> <li>• The inner test wall around the pores is still smooth</li> <li>• Dissolution in cross section is very limited.</li> </ul>	M/B
	<i>Para-subbotina</i>	<ul style="list-style-type: none"> <li>• Presence of small overgrowths on the outer test surface. The test is appears altered</li> <li>• <b>In cross section a (local) thin coat of secondary calcite is observed.</b></li> </ul>	M/B
Sample 8 (6.75 m)	<i>Acarinina</i>	<ul style="list-style-type: none"> <li>• Presence of tiny overgrowths on the outer test surface.</li> </ul>	M
Sample 9 (7.60 m)	<i>Subbotina</i>	<ul style="list-style-type: none"> <li>• Presence of tiny overgrowths on the outer test surface.</li> </ul>	M
Sample 12 (9.55 m)	<i>Subbotina</i>	<ul style="list-style-type: none"> <li>• Presence of tiny overgrowths on the outer test surface.</li> </ul>	M
Sample 15 (12.75 m)	<i>Acarinina</i>	<ul style="list-style-type: none"> <li>• Some broken muricae, no clear overgrowths.</li> </ul>	G
Sample 16 (13.25 m)	<i>Acarinina</i>	<ul style="list-style-type: none"> <li>• Some broken muricae, no clear overgrowths.</li> </ul>	G
	<i>Subbotina</i>	<ul style="list-style-type: none"> <li>• Excellent preservation of test textures. The original POM (primary organic membrane) structure can be recognized in cross section.</li> <li>• The calcite of the test is more granular than expected for a pristine preservation</li> </ul>	G
Sample 22 (19.45 m)	<i>Acarinina</i>	<ul style="list-style-type: none"> <li>• Good preservation of test textures and structure.</li> <li>• The calcite of the test is more granular than expected a pristine preservation</li> </ul>	G
	<i>Subbotina</i>	<ul style="list-style-type: none"> <li>• No clear indications of overgrowths on test wall.</li> </ul>	G
Sample 23 (20.25 m)	<i>Acarinina</i>	<ul style="list-style-type: none"> <li>• Presence of tiny overgrowths on the outer test surface.</li> <li>• The cross section reveals a clear structure but is affected by dissolution between the successive test layers.</li> </ul>	M
	<i>Subbotina</i>	<ul style="list-style-type: none"> <li>• Good preservation of test textures and structure.</li> </ul>	M/G
Sample 25 (23.15 m)	<i>Acarinina</i>	<ul style="list-style-type: none"> <li>• Presence of small overgrowths on the outer test surface.</li> <li>• Some dissolution features can be recognized on the outer wall.</li> </ul>	M

Table 3. Summary of observations for each sample regarding preservation. Afterwards they were grouped in 3 categories; B (Bad preservation), M (moderate preservation) and G (good preservation).

#### 6.3.4 The effect on $\delta^{13}\text{O}$

The data of Sexton *et al.* (2006) demonstrates that a significant deviation exists for the  $\delta^{18}\text{O}$  values of “frosty” planktic foraminifers due to diagenetic alteration. In all their investigated cores the absolute  $\delta^{18}\text{O}$  values of diagenetically altered planktic foraminifers increased by approximately 1.2‰. This rather consistent offset in Sexton *et al.* (2006) was explained by the incorporation of diagenetic calcite on or within the foraminifer tests at the lower temperatures of the seafloor.

Because it is possible that the secondary calcite in Aktulagay has a meteoric origin instead of a marine origin, the effect of the secondary calcite might be different. According to the data of Bowen and Wilkinson (2002), the current  $\delta^{18}\text{O}$  value of meteoric precipitation in Kazakhstan can be estimated to be about -12‰ VSMOW (Figure 40). Therefore if the secondary calcite would be identified as meteoric calcite instead of marine calcite, the same amount of secondary calcite would have a much more devastating effect on the  $\delta^{18}\text{O}$  original signature.

For the benthic foraminifers, the worst preserved samples with large secondary calcite crystals had  $\delta^{18}\text{O}$  values that were approximately -0.6‰ more depleted than the better preserved benthic foraminifers (6.2.5.1). However this effect does not allow the distinction between early diagenesis and meteoric calcite precipitation. The bulk isotopic measurements of Deprez (2012) present an answer to this problem. Although the bulk material was not observed under the binocular microscope, based on the abundant presence of large secondary crystals in the benthic foraminifers of Samples 3, 5, 6, 7 & 21, it is assumed that the bulk isotopes of these samples are more affected by secondary calcite than other bulk isotopes.

Figure 41 clearly demonstrates that the  $\delta^{18}\text{O}_{\text{BULK}}$  values associated with secondary calcite are up to 1.5‰ more enriched than the other  $\delta^{18}\text{O}_{\text{BULK}}$  values. This enrichment can only be explained if the secondary calcite is of marine origin. Because of the observation that the  $\delta^{18}\text{O}$  measurements of planktic species are similar to or more depleted than the  $\delta^{18}\text{O}_{\text{BULK}}$  values, it is likely that the effect of secondary calcite overgrowths or cement found on planktic foraminifers will cause enrichment of the  $\delta^{18}\text{O}$  signature. This is in line with Sexton *et al.* (2006), who associated a 1.2‰ enrichment of  $\delta^{18}\text{O}$  with diagenetic alteration.

Because *Acarinina spp.* measurements are in general more depleted than the *(Para)Subbotina spp.* due to their mixed layer habitat,  $\delta^{18}\text{O}$  signatures of *Acarinina spp.* will relatively be more vulnerable to the presence of secondary calcite.

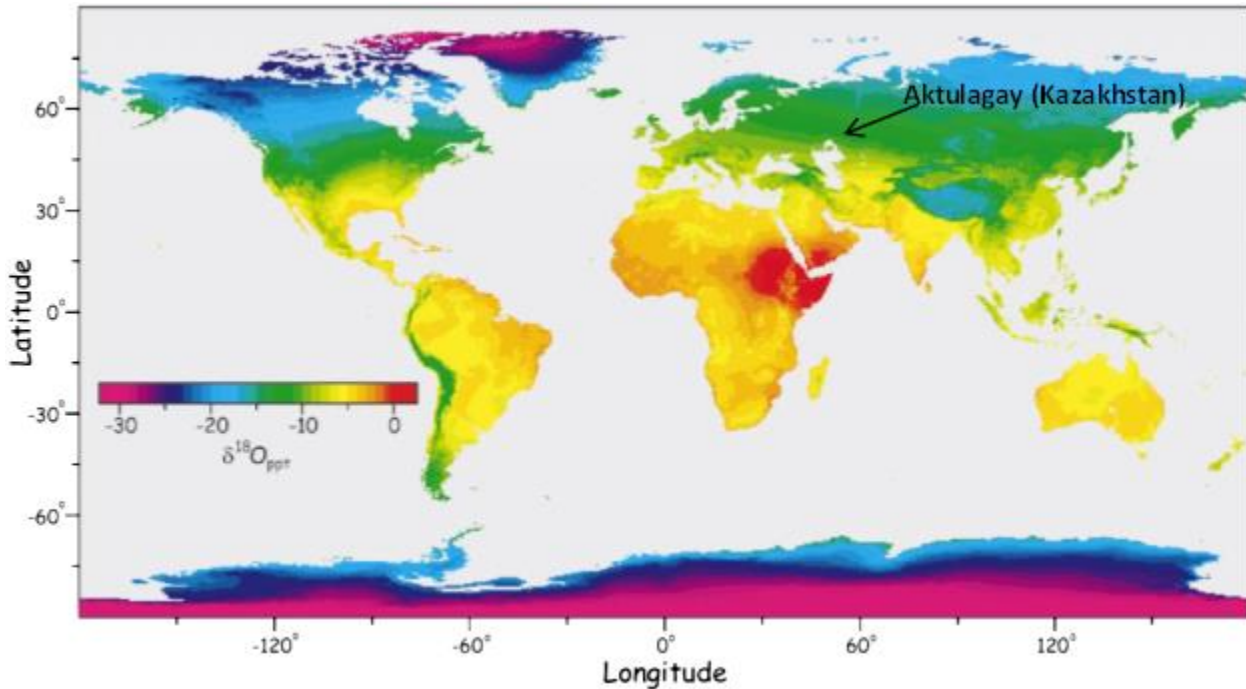
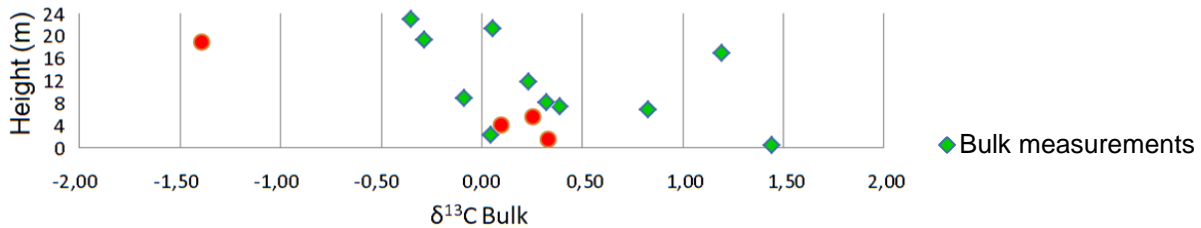


Figure 40. The map displays the modeled spatial distribution of  $\delta^{18}\text{O}$  (VSMOW) in meteoric precipitation over the world (Bowen and Wilkinson, 2002). The model of Bowen and Wilkinson (2002) is based on data of 232 Global Network for Isotopes in Precipitation (GNIP) stations in the third release of the International Atomic Energy Agency (IAEA) and the World Meteorological Organization (WMO) in 1998 (IAEA & WMO, 1998).

**$\delta^{13}\text{C}_{\text{Bulk}}$  over the Aktulagay section  
Data from Deprez (2012)**



**$\delta^{18}\text{O}_{\text{Bulk}}$  over the Aktulagay section  
Data from Deprez (2012)**

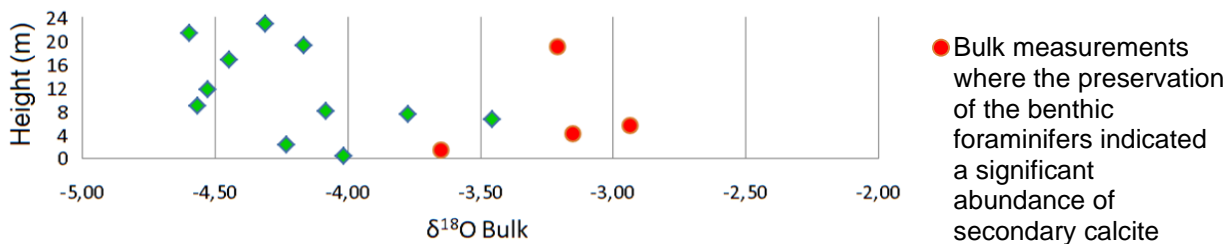


Figure 41. This figure shows a plot of  $\delta^{18}\text{O}_{\text{Bulk}}$  and  $\delta^{13}\text{C}_{\text{Bulk}}$  over the Aktulagay section with data from Deprez (2012). The bulk material was not observed under the binocular microscope. Based on the abundant presence of large secondary crystals in the benthic foraminifers of Samples 3, 5, 6, 7 & 21, it is assumed that the bulk isotopes of these samples are more affected by secondary calcite than other bulk isotopes.

### 6.3.5 The effect on $\delta^{13}\text{C}$

As demonstrated by the results of Sexton *et al.* (2006), the  $\delta^{13}\text{C}$  values of “frosty” foraminifers are still very representative for the  $\delta^{13}\text{C}$  values of the glassy foraminifers. The  $\delta^{13}\text{C}$  values were concluded to be far more robust to diagenesis than  $\delta^{18}\text{O}$  values. Since the preservation of all our specimens can be considered better than the “frosty” specimens of Sexton *et al.* (2006), it is unlikely that the measured  $\delta^{13}\text{C}$  values of the planktic foraminifers with a “Moderate” preservation deviate much from their original  $\delta^{13}\text{C}$  signatures. This is further confirmed by the absence of deviating  $\delta^{13}\text{C}$  values for the benthic foraminifers (6.2.5.1) and the observation that the  $\delta^{13}\text{C}_{\text{BULK}}$  values of samples affected by secondary calcite demonstrate no consequent deviation (Figure 41).

### 6.3.6 Summary

In summary the main preservation problems are related to the presence of secondary calcite cement and secondary calcite overgrowths that occur on the outer test wall. The origin of the secondary calcite is not related to meteoric water and therefore the effect of limited amounts of secondary calcite on the  $\delta^{18}\text{O}$  values should be small. However for the specimens with moderate preservation a possible effect cannot be excluded, especially not for the specimens from samples 3 and 4 at 1.45 m and 2.35 m respectively. The effect of diagenesis on  $\delta^{13}\text{C}$  is expected to be negligible in general.

## 6.4 Contamination

### 6.4.1 Introduction

Remains of bulk material are sometimes found on or within the foraminifer tests and are therefore considered a risk for contamination of the isotopic signature. The bulk material mainly consist of nanoplankton (Figure 42.C&D). The bulk material is often found concentrated within the aperture (Figure 42.A&D), the umbilicus or between depressed sutures. The occurrence of bulk material within benthic foraminifers was rather uncommon and contamination in those cases was usually limited to the outer chamber of the foraminifer. For planktic foraminifers bulk material was more frequently found within the outer chamber and was especially a problem for the genus *Acarinina* where the muricae on the outer wall tend to anchor the bulk material.

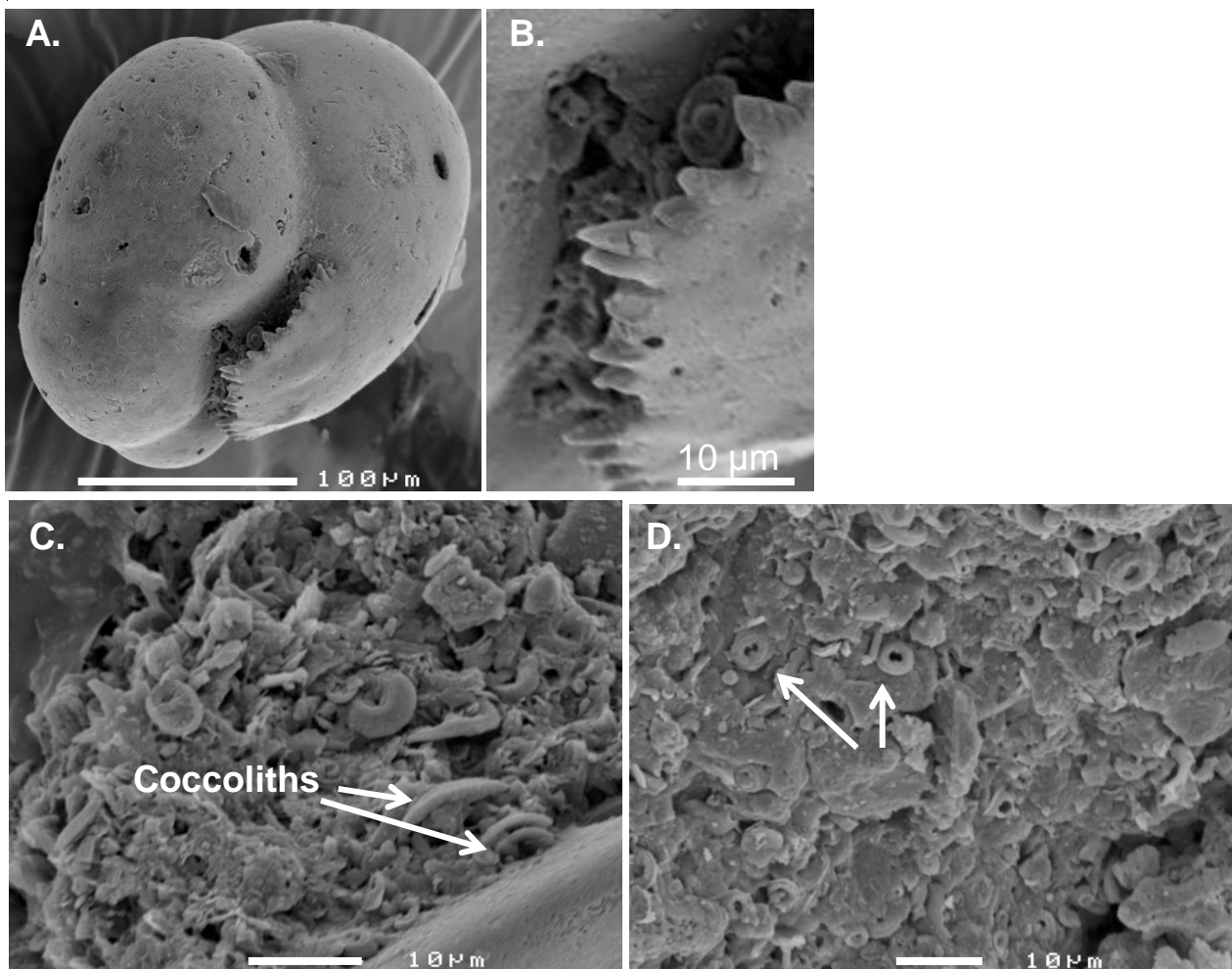


Figure 42. A. SEM-image of bulk material stuck in the aperture of *Allomorphina sp.1* in Sample 13. B. Close up near the aperture. C. & D. SEM-images of bulk material found in Sample 13

### 6.4.2 Prevention of contamination

In general the bulk material was easy to spot due to local decreased test transparency of the foraminifers under the binocular microscope. When the foraminifers remained dull after wetting, they were broken to

verify the absence of filling. Fortunately in the case of bulk filling, the removal of the bulk material with a pencil from the foraminifer test fragments was very effective due the tendency of the bulk material to clump together and not to stick on the smooth inner wall. However when the fossil was also affected by secondary calcite the removal was significantly harder.

As precaution to limit contamination of the isotopic signal by (un)detected bulk material, the foraminifers were always cleaned in an ultrasonic bath for several seconds. The time in the ultrasonic bath was sometimes increased for stronger specimens. Although in those samples where bulk material was a frequent issue it was preferred to clean more fossils than required and select the best specimens rather than increasing the time in the ultrasonic bath. However two problems remained. The first problem was the immediate destruction of small, weak specimen within the ultrasonic bath. Therefore these specimens could not be cleaned, certainly not when they were rare species. This was the case for 20 of the 140 measurements. The second problem was the limited efficiency of the ultrasonic bath for species with a lot of test irregularities that anchored the bulk material. The tests of most benthic foraminifers are rather smooth and therefore possible bulk contamination is limited to the aperture. For benthic foraminifers with less smooth tests like *Uvigerina spp.* (Figure 43), the ultrasonic bath was in general able to remove the problem. Planktic specimens were more vulnerable to bulk contamination than the benthic specimens. The genera *Subbotina* and *Parasubbotina* often had some bulk material within their outer chambers. Therefore these specimens were frequently fragmented to manually remove the bulk material. This method was quite successful but time-consuming. The genus *Acarinina* was less often filled with bulk material but the bulk material was frequently found stuck between the spines on the test mainly within the suture depressions, the aperture and the umbilicus (Figure 44). The ultrasonic bath was often not sufficient to completely remove all traces of bulk material and therefore in some contamination of bulk material on the *Acarinina* measurements can be expected.

### **6.4.3 Direction of the error**

In order to accurately predict the direction of the error due to bulk contamination, the isotopic value of the bulk material from the <10µm fraction would be required for each sample. Although Deprez (2012) did bulk measurements on some of the samples, these bulk values cannot be used since these values are dominated by the foraminifer signature and not by the nannoplankton signature. It is assumed that the bulk material from the <10 µm fraction is determined by the nannoplankton. Therefore the isotopic signal should be similar to the mixed layer planktic genus *Acarinina*. In Table 4 the effect of bulk contamination is evaluated.

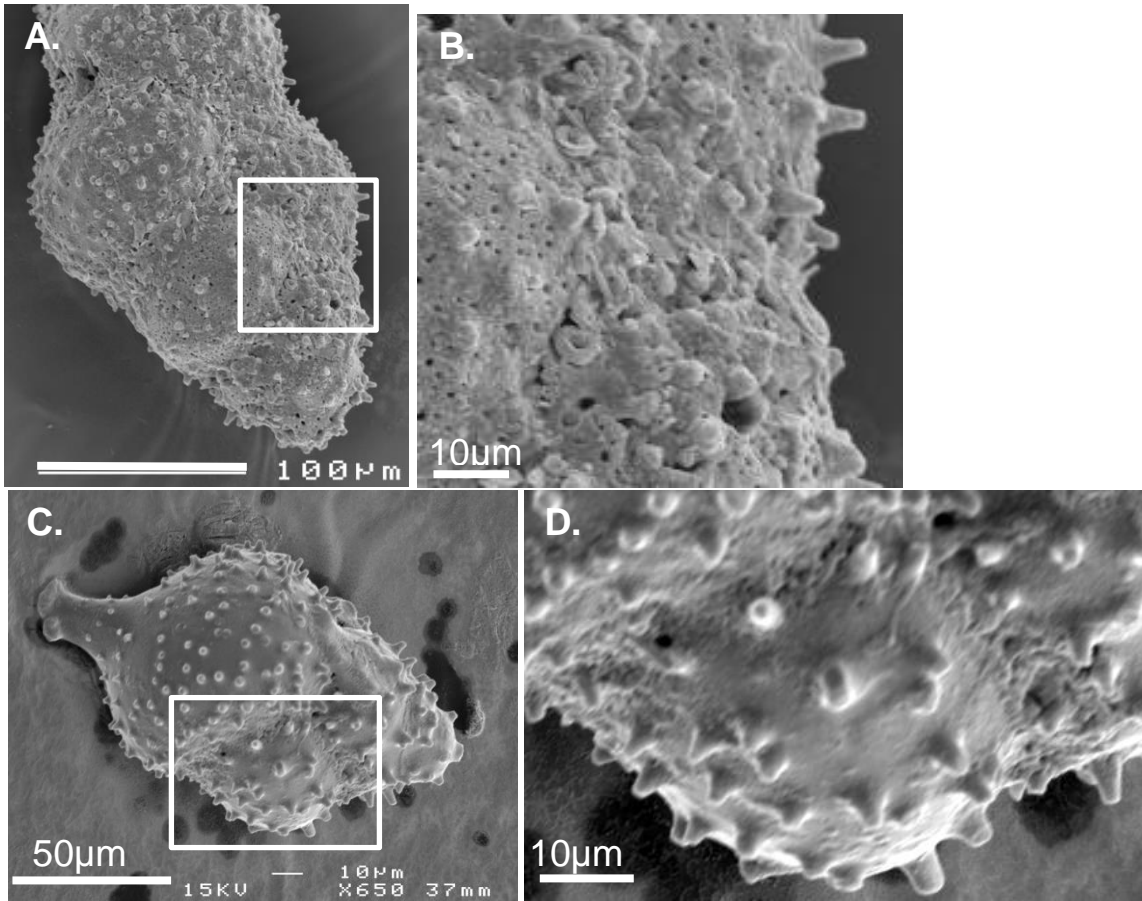


Figure 43. A. SEM-image of a non-cleaned *Uvigerina elongata* from Sample 25 where bulk material is observable in the depressed sutures. B. Close up. C. SEM-image of non-cleaned *Uvigerina elongata* from Sample 8 where bulk material is rare.



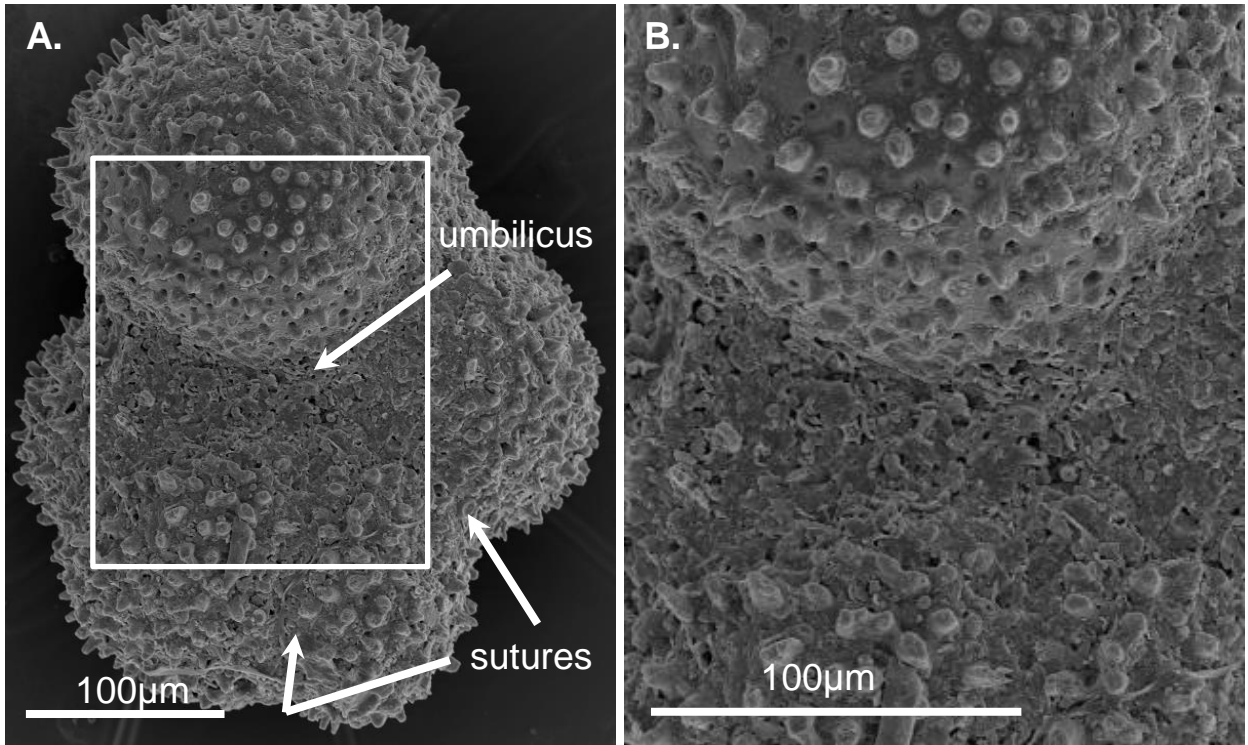


Figure 44. A. SEM-image of a cleaned *Acarinina medizai*(?). The images shows bulk material, possibly not only nannoplankton, stuck in the umbilicus and to a lesser degree between the suture depressions. Other zones on the test are successfully cleaned in the ultrasonic bath.  
B. Close up.

Bulk contamination	Effect on the $\delta^{18}\text{O}$ signal	Effect on the $\delta^{13}\text{C}$ signal	Risk for the occurrence of bulk material on the test	Estimated effect
Deep endobenthic genera	Decrease $\Delta\delta^{18}\text{O} = 1-3\text{‰}$	Increase $\Delta\delta^{13}\text{C} = 4-8\text{‰}$	Very low risk due to very smooth tests of e.g. <i>Lenticulina spp.</i> and <i>Nodosaria spp.</i>	Very low due to extremely massive test of all measured deep endobenthic specimens.
Shallow endobenthic & epibenthic genera	Decrease $\Delta\delta^{18}\text{O} = 1-4\text{‰}$	Increase $\Delta\delta^{13}\text{C} = 3-4\text{‰}$	Only a moderate risk for small foraminifers with irregular tests.	Might be a significant effect for small foraminifers. The tests are often <2 $\mu\text{m}$ thick in the 63-125 $\mu\text{m}$ fraction.
Planktic genus <i>Subbotina spp.</i>	Decrease $\Delta\delta^{18}\text{O} = 0.5-2\text{‰}$	Increase $\Delta\delta^{13}\text{C} = 1-2\text{‰}$	Moderate risk due to frequent occurrence of bulk material inside the outer chamber and the occurrence of bulk material between suture depressions.	Low. Most of the effect of contamination should be buffered by the thick test. All measured specimens were from the 250-300 $\mu\text{m}$ size fraction, the test was approximately 10 $\mu\text{m}$ thick.
Planktic genus <i>Acarinina spp.</i>	Decrease or increase? $\Delta\delta^{18}\text{O} = 0-2\text{‰}$	Decrease or increase? $\Delta\delta^{13}\text{C} = 0-2\text{‰}$	High risk of contamination due to the spines on the test that sometimes anchor the bulk material.	Low. On the one hand the absolute mass of bulk on a single specimen is larger than for all the previous but on the other hand the mass of the test should strongly buffer the effect. The test without spines is approximately 10 $\mu\text{m}$ thick since all measured species are from the 250 $\mu\text{m}$ -300 $\mu\text{m}$ fraction.

Table 4. Evaluation of bulk contamination for all types of genera. The relative effect of on the  $\delta^{18}\text{O}$  signal and  $\delta^{13}\text{C}$  signal was estimated based on the assumption that the isotopic values of the bulk material have a surface water isotopic signal.  $\Delta\delta^{18}\text{O}$  &  $\Delta\delta^{13}\text{C}$  are rough estimates of the difference between the estimated bulk signature and the specimen signal. Larger  $\Delta$ -values will cause larger isotopic deviations for smaller mass percentages of bulk.

#### 6.4.4 The experiment

A small experiment was carried out to estimate the size of the effect of bulk contamination on the measured isotopic values. The experiment consists of 2 measurements. One measurement is performed on specimens from a species that is clearly affected by the presence of a thin layer of bulk material and the other measurement is performed on specimens from the same species that were cleaned in the ultrasonic bath and a carefully selected. The experiment was performed in Sample 22 on the benthic foraminifer *Aragonia aragonensis*. The specimens belonged to the 125-180  $\mu\text{m}$  size fraction. Due the low mass of an individual specimen, 25 to 30 specimens were required for a successful measurement. This large number of specimens should average out the effect of biological and temporal variation on the isotopic signature within the sample. Furthermore the thin tests and the large surface/volume ratio of *Aragonia aragonensis* should maximize the possible effect of bulk material on the measurements.

#### 6.4.5 The results of the experiment

$$\delta^{13}\text{C}_{\text{clean}} = -0.975 \pm 0.014$$

$$\delta^{18}\text{O}_{\text{clean}} = -2.417 \pm 0.050$$

$$\delta^{13}\text{C}_{\text{dirty}} = -0.970 \pm 0.034$$

$$\delta^{18}\text{O}_{\text{dirty}} = -2.612 \pm 0.062$$

$$\delta^{13}\text{C}_{\text{Acarinina}} = 2.535 \pm 0.036 \text{ \& } 2.215 \pm 0.031$$

$$\delta^{18}\text{O}_{\text{Acarinina}} = -3.971 \pm 0.086 \text{ \& } -4.851 \pm 0.078$$

The *Acarinina* measurement in the sample is considered a prediction of the  $\delta^{18}\text{O}$  nanoplankton value. The experiment demonstrates that for this experiment the effect of the bulk material on the measurement is very small to non-existing. For  $\delta^{13}\text{C}$  the precision of the mass spectrometer does not allow to distinguish the dirty and the clean values. For  $\delta^{18}\text{O}$  there is a statistically significant difference between the measurements but it might be too small to ascribe it to the bulk material. Even if the error on the  $\delta^{18}\text{O}$  values is considered a result of the bulk material, the deviation remains very small despite the fact that the bulk contaminated specimens were chosen deliberately.

#### 6.4.6 Summary

In conclusion it is assumable that the effect of bulk material on benthic and planktic foraminifers is very limited and negligible, even for those measurements where the specimens could not be cleaned in the ultrasonic bath.



## 7 Isotope paleoecology

### 7.1 Results

#### 7.1.1 The $\delta^{13}\text{C}$ values

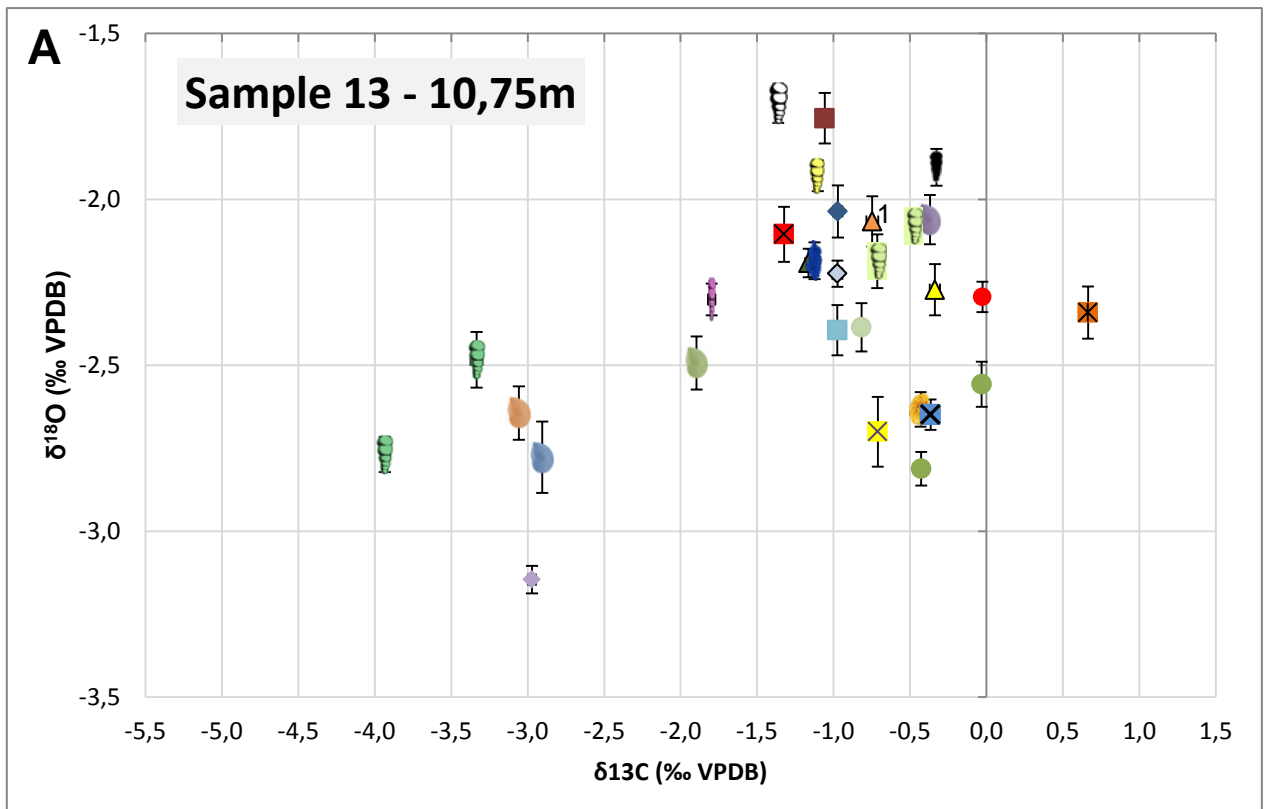
Figure 46 allows comparison of the measured  $\delta^{13}\text{C}$  values of samples 13, 17 and 22. All samples demonstrate a large range for  $\delta^{13}\text{C}$ . The measurements in samples 13, 17 and 22 range over an interval of 4.6‰, 5.7‰ and 5.8‰ respectively. The  $\delta^{13}\text{C}$  signature of *Spiroloculina spp.* is the most enriched of all benthic measurements and is approximately the same in the 3 samples (0.665‰, 0.658‰ and 0.694‰ in sample 13, 17 and 22). Next to *Spiroloculina spp.*, the most positive  $\delta^{13}\text{C}$  values are measured for *Anomalinoidea zitteli*, *Cibicidoides decoratus*, *Cibicidoides cf. rigidus* and *Cibicidoides rigidus*). In Sample 22 these  $\delta^{13}\text{C}$  values are at least 0.4‰ more enriched than the other species measurements. Many species are measured within the range -1.0‰ and 0.0‰; *Alabamina midwayensis*, *Anomalinoidea acutus*, *Anomalinoidea cf. praeacutus*, *Anomalinoidea rubiginosis*, *Anomalinoidea rigidus*, *Aragonia aragonensis*, *Bulimina (aff.) midwayensis*, *Bulimina kugleri*, *Cibicidoides decoratus*, *Cibicidoides cf. decoratus*, *Lenticulina sp. 4*, *Marginulinopsis sp. 1*, *Nuttallides truempyi*, *Percultazonaria sp. 1*, *Pulsiphonina prima*, *Pyramidulina sp. 1*, *Stainforthia sp. 1*, *Turrilina brevispira*, *Uvigerina elongata* and *Valvulineria scrobiculata*. Some of these species were measured in multiple samples were they had similar  $\delta^{13}\text{C}$  values ( $\Delta\delta^{13}\text{C}$  between samples  $\leq 0.2\text{‰}$ ); *Alabamina midwayensis*, *Aragonia aragonensis*, *Pyramidulina sp. 1* *Uvigerina elongata* and *Valvulineria scrobiculata*. For other species this is not the case and they demonstrate more significant isotopic variability between the samples; *Anomalinoidea acutus*, *Anomalinoidea cf. praeacutus*, *Cibicidoides decoratus*, *Lenticulina sp. 4*, *Pulsiphonina prima*. Most of the remaining species have  $\delta^{13}\text{C}$  values between -2‰ and -1‰. These species include; *Allomorphina sp. 1*, *Bulimina aksuatica*, *Bulimina cf. thanetensis*, *Coryphostoma spp.*, *Dentalina sp. 1*, *Lenticulina sp. 2*, *Lenticulina sp. 3*, *Lenticulina sp. 4*, *Loxostomoides applinae*, *Oridorsalis plummerae*, *Ramulina sp. 1* and *Stilostomella sp. 1*. Finally a couple of species have extremely depleted  $\delta^{13}\text{C}$  values, ranging from -6‰ to -2‰. These species are *Percultazonaria sp. 1*, *Marginulinopsis sp. 2*, *Nodosaria sp. 1*, *Lenticulina sp. 1* and *Lenticulina sp. 3*. *Nodosaria sp. 1* is consequently the most depleted measurement in all 3 samples. The *Lenticulina spp.* and the *Percultazonaria sp. 1* are the only species that are measured over the entire range of -4‰ to 0‰ within the 3 samples.

### 7.1.2 The $\delta^{18}\text{O}$ values

The  $\delta^{18}\text{O}$  measurements in samples 13, 17 and 22 range over an interval of 1.4‰, 1.1‰ and 1.2‰ respectively (Figure 45). These ranges are 3 to 5 times smaller than the  $\delta^{13}\text{C}$  ranges. Since the average standard deviation for  $\delta^{18}\text{O}$  is also larger (0.065‰ for  $\delta^{18}\text{O}$  versus 0.034‰ for  $\delta^{13}\text{C}$ ), the variation between the species is much less significant. The most positive  $\delta^{18}\text{O}$  ( $\delta^{18}\text{O} \geq -2.0\text{‰}$ ) values in samples 13 and 17 were measured for; *Allomorphina* sp. 1, *Bulimina* aff. *midwayensis*, *Bulimina* *kugleri*, *Loxostomoides* *applinae*, *Oridorsalis* *plummerae*, *Stilostomella* sp. 1, *Turrilina* *brevispira*, *Uvigerina* *elongata* and *Valvulineria* *scrobiculata*. The most negative  $\delta^{18}\text{O}$  ( $\delta^{18}\text{O} \leq -2.5\text{‰}$ ) values in samples 13 and 17 belong to the genera *Cibicidoides* and *Anomalinoidea* (*Anomalinoidea* *acutus*, *Anomalinoidea* cf. *praeacutus*, *Anomalinoidea* *rubiginosis* and *Cibicidoides* *decoratus*) on the one hand ( $\delta^{13}\text{C} > -1.5\text{‰}$ ) and *Lenticulina* spp., *Marginulinopsis* sp. 2, *Nodosaria* sp. 1 and *Percultazonaria* sp. 1 on the other hand ( $\delta^{13}\text{C} < -1.5\text{‰}$ ). All the other measured species have values in between. In Sample 22 all the species appear to be approximately 0.5‰ more depleted in  $\delta^{18}\text{O}$  than in Samples 13 and 17. In this sample the most enriched  $\delta^{18}\text{O}$  values (-2.5‰ to -2.0‰) were measured for *Alabamina* *midwayensis*, *Aragonia* *aragonensis*, *Bulimina* (aff.) *midwayensis*, *Bulimina* cf. *thanetensis*, *Coryphostoma* spp., *Percultazonaria* sp. 1 and *Uvigerina* *elongata*. The most depleted  $\delta^{18}\text{O}$  values were measured for *Nodosaria* sp. 1 (-3.3‰). All the other  $\delta^{18}\text{O}$  measurements range between -3.0‰ and -2.5‰.

### 7.1.3 The isotopic values of genera

Finally for some genera multiple species were measured within a single sample. These genera are *Anomalinoidea*, *Bulimina*, *Cibicidoides* and *Lenticulina*. Figure 47 demonstrates that the different species of the genera *Anomalinoidea*, *Bulimina* and *Cibicidoides* cluster together for both  $\delta^{13}\text{C}$  and  $\delta^{18}\text{O}$ , while the measurements of *Lenticulina* are spread over larger  $\delta^{13}\text{C}$  and  $\delta^{18}\text{O}$  ranges.



- |                                       |                                    |  |
|---------------------------------------|------------------------------------|--|
| ◆ <i>Alabamina midwayensis</i>        | ■ <i>Allomorphina species 1</i>    | ● <i>Anomalinoidea acutus</i>              |
| ✕ <i>Anomalinoidea cf. praeacutus</i> | ⊠ <i>Anomalinoidea rubiginosis</i> | ● <i>Anomalinoidea zitteli</i>             |
| ■ <i>Aragonia aragonensis</i>         | ■ <i>Aragonia aragonensis (D)</i>  | 🌀 <i>Bulimina (aff.) midwayensis</i>       |
| 🌀 <i>Bulimina aksuatica</i>           | 🌀 <i>Bulimina cf. thanetensis</i>  | ▲ <i>Bulimina kugleri</i>                  |
| ⊗ <i>Cibicidoides cf. decoratus</i>   | ● <i>Cibicidoides cf. rigidus</i>  | ● <i>Cibicidoides decoratus</i>            |
| ● <i>Cibicidoides rigidus</i>         | 🌀 <i>Coryphostoma spp.</i>         | 🌀 <i>Dentalina species1</i>                |
| ● <i>Lenticulina species 1</i>        | ● <i>Lenticulina species 2</i>     | ● <i>Lenticulina species 3</i>             |
| ● <i>Lenticulina species 4</i>        | 🌀 <i>Loxostomoides applinae</i>    | ▲ <i>Marginulinopsis species 1 &amp; 2</i> |
| 🌀 <i>Nodosaria species 1</i>          | ▲ <i>Nuttallides truempyi</i>      | ▲ <i>Oridorsalis plummerae</i>             |
| ◆ <i>Percultazonaria species 1</i>    | ■ <i>Pulsiphonina prima</i>        | 🌀 <i>Pyramidulina species 1</i>            |
| ■ <i>Ramulina species 1</i>           | ✕ <i>Spiroloculina spp.</i>        | ● <i>Stainforthia species 1</i>            |
| 🌀 <i>Stilostomella species 1</i>      | 🌀 <i>Turrilina brevispira</i>      | ● <i>Uvigerina elongata</i>                |
| ◆ <i>Valvulineria scrobiculata</i>    |                                    |  |

Figure 45. All benthic  $\delta^{18}\text{O}$  &  $\delta^{13}\text{C}$  measurements from Sample 13 (A), Sample 17 (B) and Sample 22 (C).

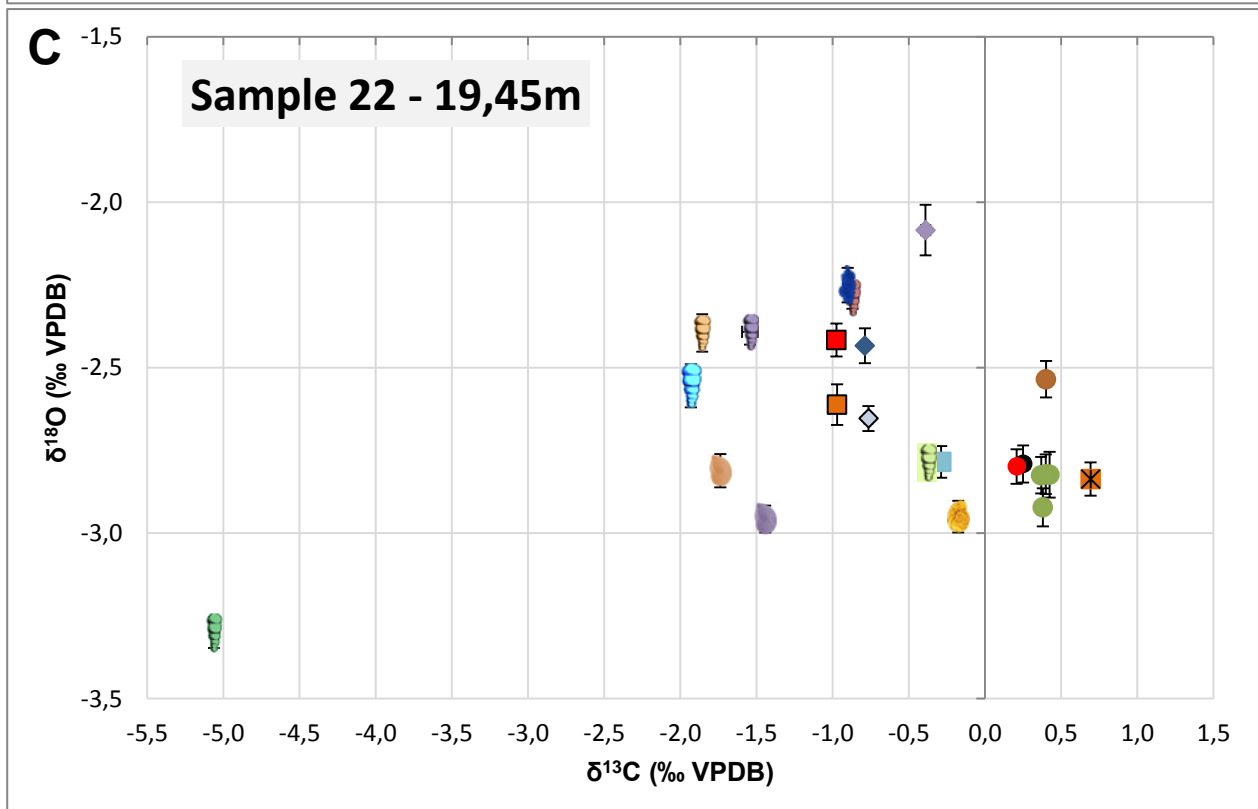
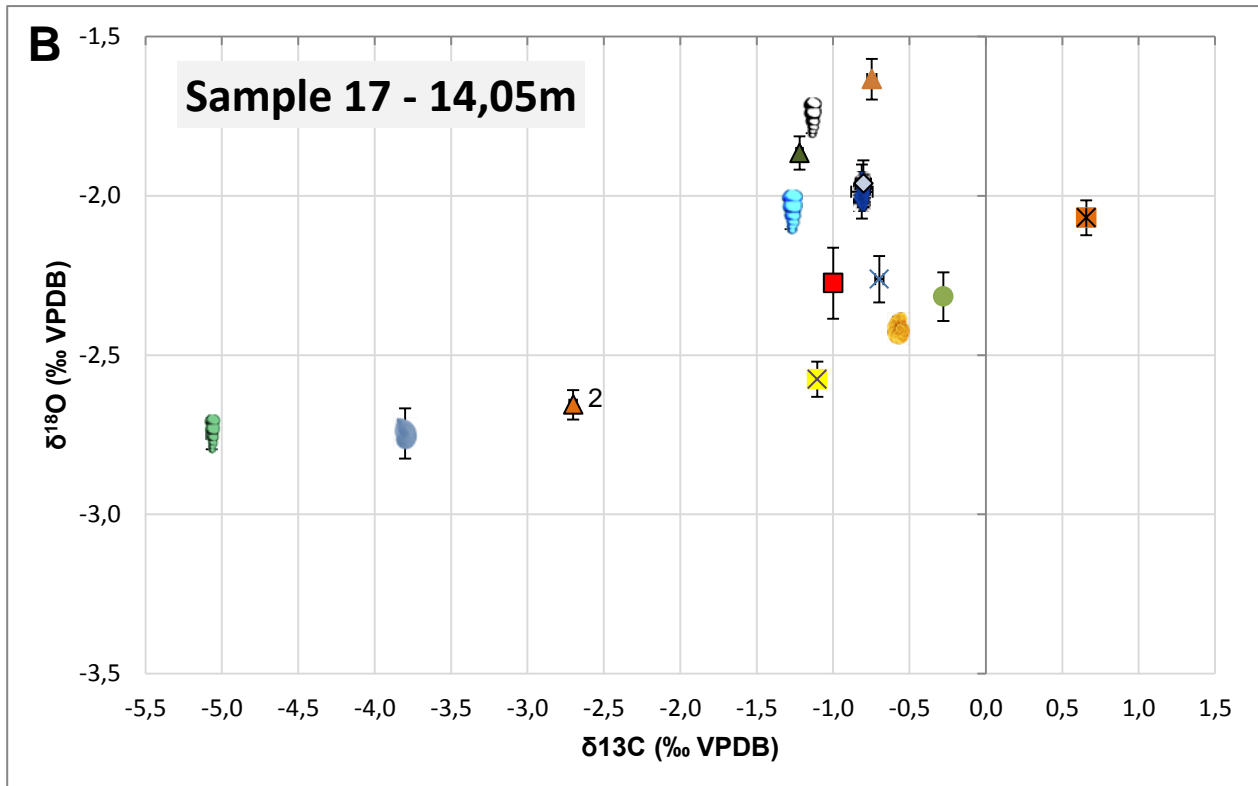


Figure 45 (continued).



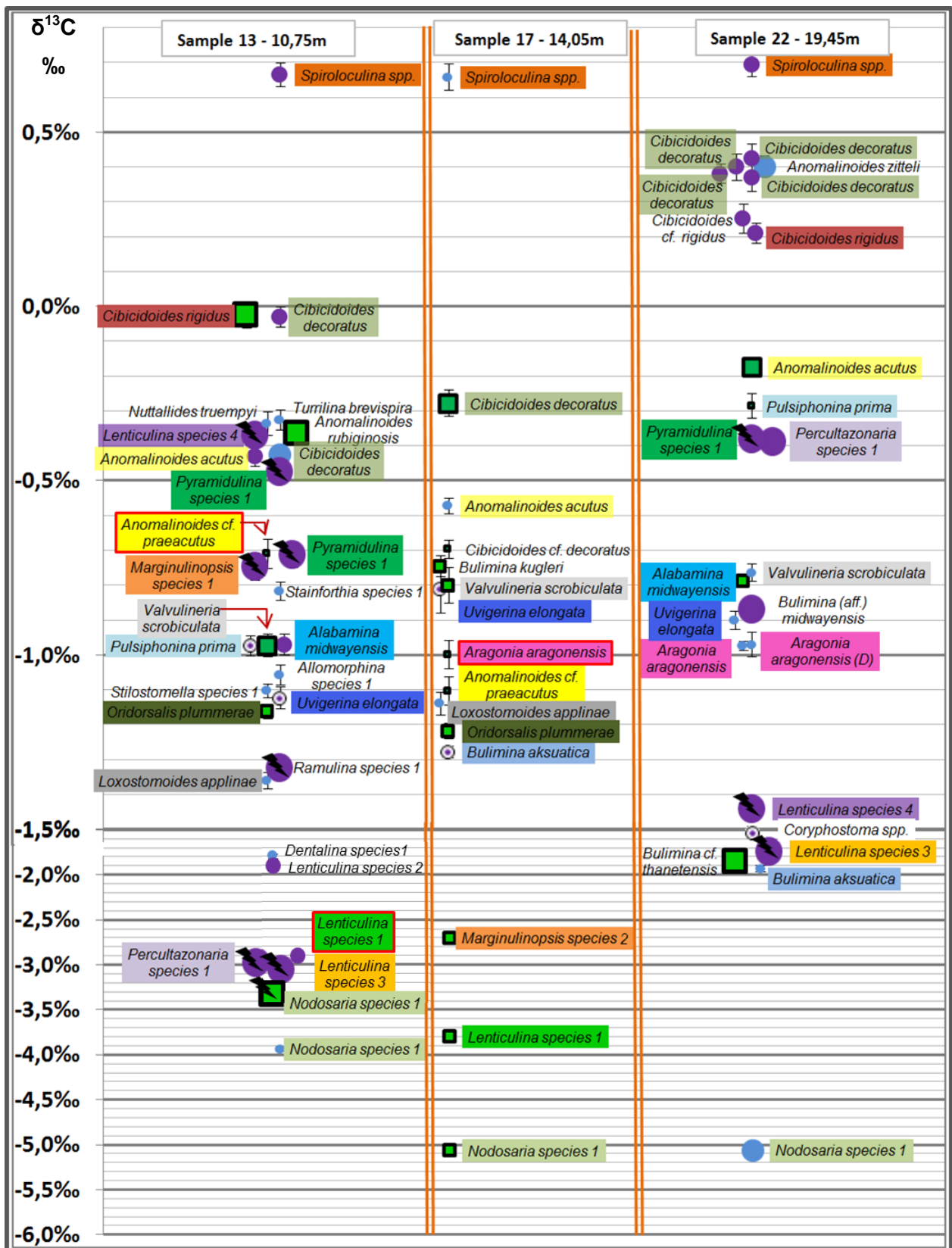


Figure 46. The figure allows comparison of the  $\delta^{13}\text{C}$  values among samples 13, 17 and 22. All species with multiple measurements were marked with a unique color (The legend is on the next page.)












	Size fraction ( $\mu\text{m}$ )	Corresponding Number of specimens
	300+	1 to 2
	250-300+	2 to 6
	250-300	2 to 3
	180-300	3 to 5
	180-250	3 to 9
	125-250	5 to 15
	125-180	5 to 30
	63-180	13 to 40
	63-125	47 to 110
	Fragments were measured, not complete specimens	
	Lower accuracy. There was insufficient CO <sub>2</sub> during dissolution of the specimens in the mass spectrometer	

Figure 46 (continued). Legend. The high variability in the number of specimens within a single size fraction reflects the variability in test thickness and/or shape (elongated versus round specimens)

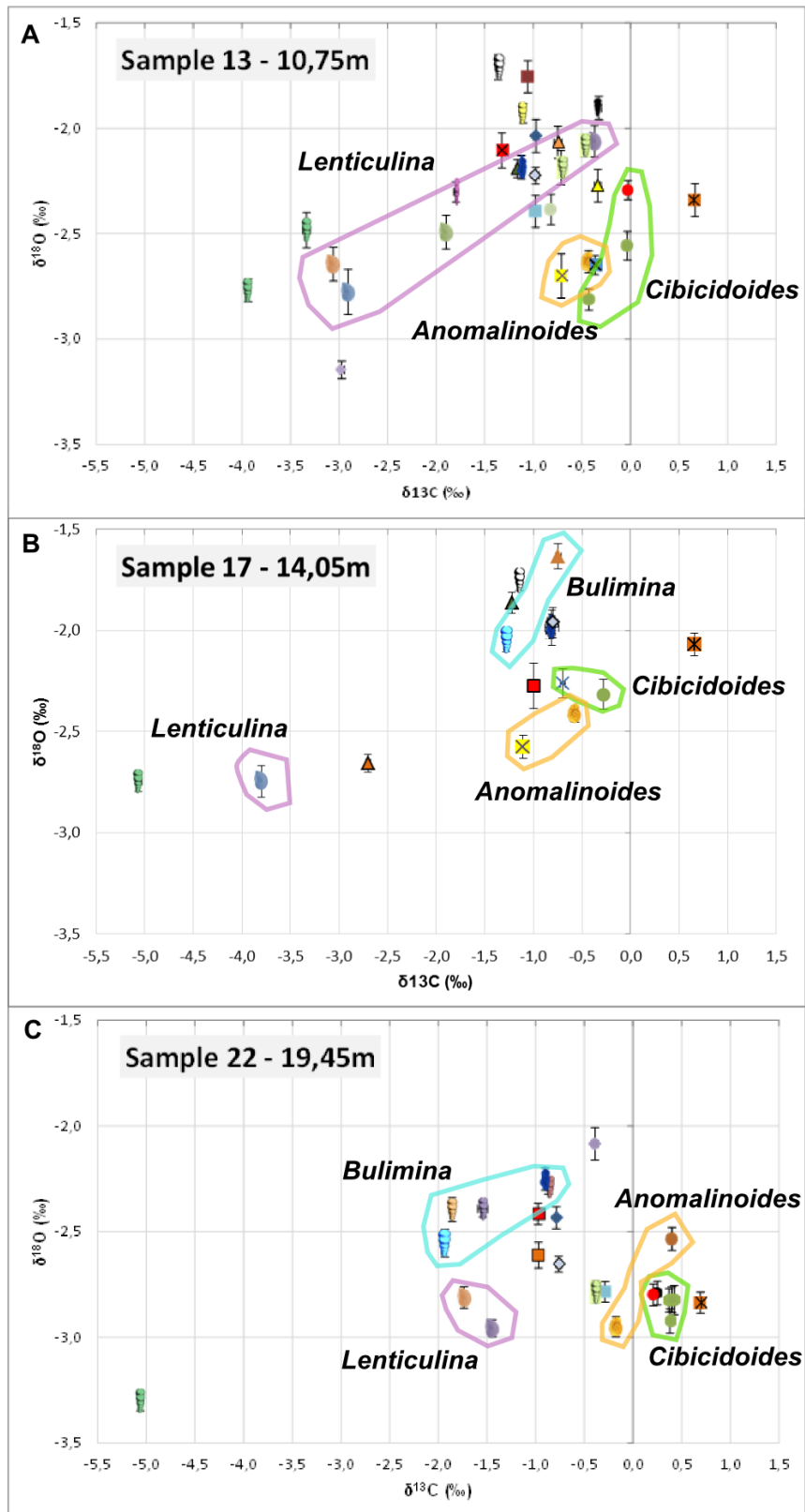


Figure 47. Species of the genera *Anomalinoides*, *Bulimina*, *Cibicidoides* and *Lenticulina* were grouped. The legend of the figure can be found in Figure 45. Many species of the same genus have similar isotopic values. All  $\delta^{13}\text{C}$  and  $\delta^{18}\text{O}$  values are expressed in VPDB (‰)

## 7.2 Discussion

### 7.2.1 Microhabitat identification

#### 7.2.1.1 The $\delta^{13}\text{C}$ values

Benthic foraminifers can either be identified as epibenthic (living on the sediment or within the first centimeter of sediment) or endobenthic species (living within the sediment, Corliss and Emerson, 1990). The data of Rathburn *et al.* (1996), McCorkle *et al.* (1997) and Fontanier *et al.* (2008) of modern foraminifer isotopic values demonstrate that the  $\delta^{13}\text{C}$  values of epibenthic species are 0‰ to 1.5‰ higher than the highest endobenthic  $\delta^{13}\text{C}$  values (Figure 48, Figure 49 and Figure 50). This is mainly considered the result of a  $\delta^{13}\text{C}_{\text{DIC}}$  gradient within the sediment. Exceptions were the measurements of species with aragonite tests or species with a unique granular test wall texture (Rathburn *et al.*, 1996). In this study *Anomalinoidea zitteli*, *Cibicidoides decoratus*, *Cibicidoides cf. rigidus* and *Cibicidoides rigidus* have consistently higher  $\delta^{13}\text{C}$  values than the other benthic species in samples 13, 17 and 22 (Figure 46). Especially in Sample 22 they can be separated from the other measured species with a minimum 0.4‰  $\Delta\delta^{13}\text{C}$  offset (Figure 46). Therefore these species will be classified as epibenthic. *Spiroloculina spp.* has significantly higher  $\delta^{13}\text{C}$  values than the previously mentioned epibenthic species. However due its milioline test wall texture, the interpretation of the isotopic values of this species is more complex and discussed in 7.2.2.3. According to the data of Rathburn *et al.* (1996), McCorkle *et al.* (1997) and Fontanier *et al.* (2008), the majority of the epibenthic specimens are measured in a  $\Delta\delta^{13}\text{C}$  range of 1.0‰. However this range can include several shallow endobenthic species. Nevertheless it is assumable that the species with  $\delta^{13}\text{C}$  values more than 1.0‰ lower than the most  $\delta^{13}\text{C}$  enriched epibenthic species are endobenthic species. In Sample 13, the most enriched  $\delta^{13}\text{C}$  measurement of epibenthic species are -0.026‰ and -0.031‰ of *Cibicidoides rigidus* and *Cibicidoides decoratus*. Therefore all species with values <-1.026‰ are most likely endobenthic species. This includes *Allomorpha sp. 1*, *Dentalina sp. 1*, *Lenticulina sp. 1*, 2 and 3, *Loxostomoides applinae*, *Nodosaria sp. 1*, *Oridorsalis plummerae*, *Percultazonaria sp. 1*, *Ramulina sp. 1*, *Stilostomella sp. 1* and *Uvigerina elongata*. In Sample 17, the most enriched  $\delta^{13}\text{C}$  measurement of epibenthic species is -0.278‰ (*Cibicidoides decoratus*), therefore the species with  $\delta^{13}\text{C}$  <-1.278‰ will be considered endobenthic. This only includes *Bulimina aksuatica*, *Marginulinopsis sp. 1*, *Lenticulina sp. 1* and *Nodosaria sp. 1*. Finally in Sample 22 the most enriched  $\delta^{13}\text{C}$  measurement of epibenthic species is 0.424‰ (*Cibicidoides decoratus*) and therefore all species with  $\delta^{13}\text{C}$  <-0.576‰ will be considered endobenthic. This includes *Alabamina midwayensis*, *Aragonia aragonensis*, *Bulimina aksuatica*, *Bulimina (aff.) midwayensis*, *Coryphostoma spp.*, *Bulimina cf. thanetensis*, *Nodosaria sp. 1*, *Lenticulina sp. 3*, *Lenticulina sp. 4*, *Uvigerina elongata* and *Valvulineria scrobiculata*. For the remaining species the microhabitat is harder to identify solely based on  $\delta^{13}\text{C}$ , therefore it should be evaluated whether  $\delta^{18}\text{O}$  can provide additional information about the foraminifer microhabitat.

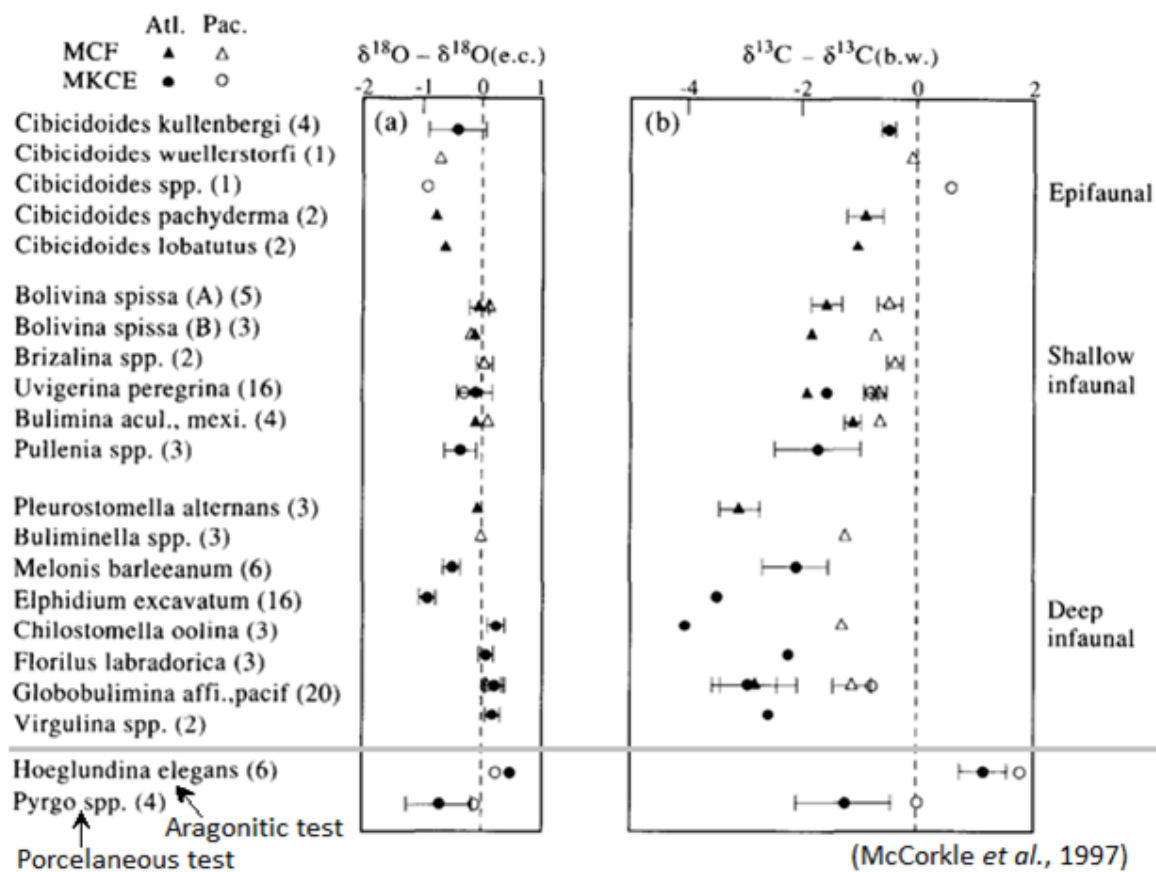


Figure 48. This figure was made by McCorkle *et al.* (1997). It presents modern foraminifer data of the Atlantic Ocean (triangles) and the Pacific Ocean (circles). It is a combination of data from McCorkle *et al.* (1990) and McCorkle *et al.* (1997). McCorkle *et al.* (1997) attempted to order the species according to their preferential microhabitat depth. Epifaunal = epibenthic, infaunal = endobenthic &  $\delta^{18}\text{O}(\text{e.c.}) = \delta^{18}\text{O}_{\text{equilibrium calcite}}$  &  $\delta^{13}\text{C}(\text{b.w.}) = \delta^{13}\text{C}_{\text{bottom water}}$ .

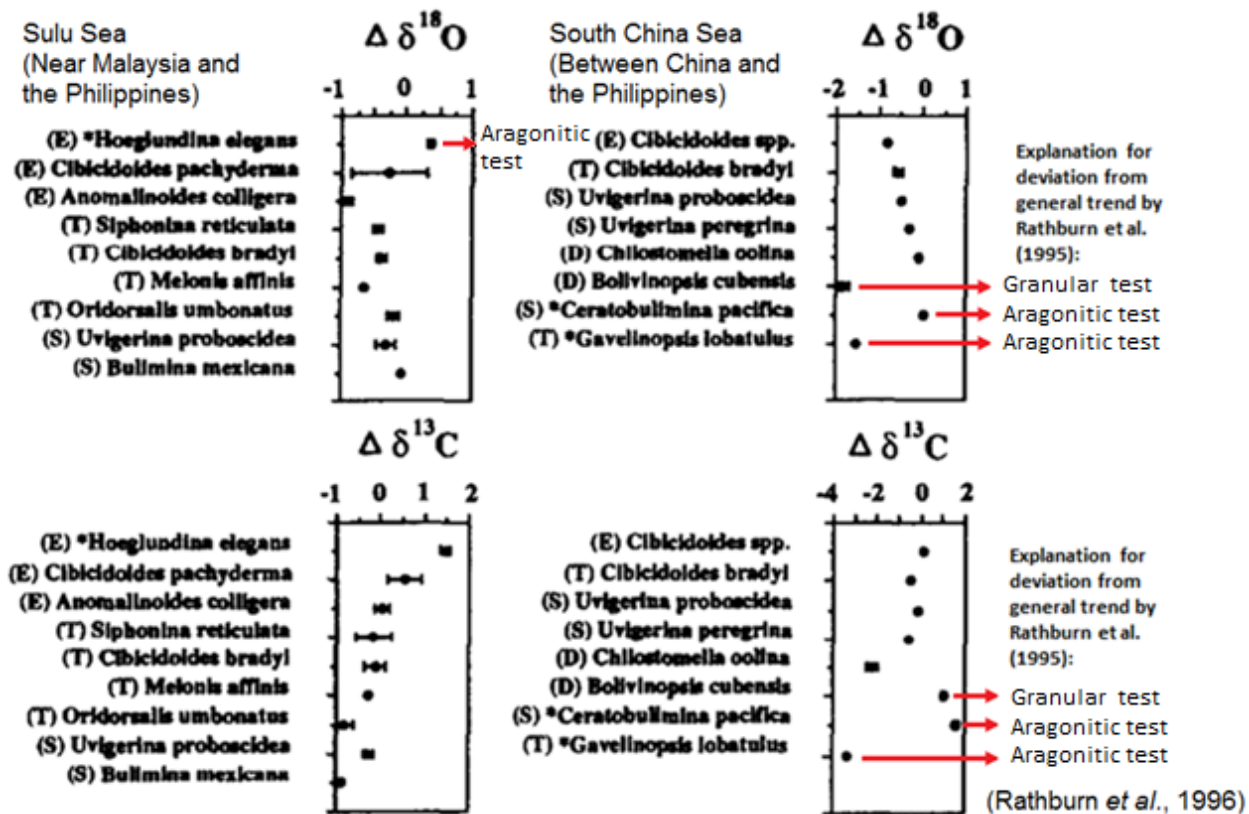


Figure 49. The data from Rathburn *et al.* (1996) demonstrates  $\Delta\delta^{18}\text{O}$  and  $\Delta\delta^{13}\text{C}$  of different species.  $\Delta\delta^{18}\text{O}$  represents the difference between  $\delta^{18}\text{O}_{\text{foraminifer test}}$  and  $\delta^{18}\text{O}_{\text{equilibrium calcite}}$  and  $\Delta\delta^{13}\text{C}$  represents the difference between  $\delta^{13}\text{C}_{\text{foraminifers test}}$  and  $\delta^{13}\text{C}_{\text{bottom water (estimate)}}$ . All taxa shown in the figure are represented by multiple isotopic analyses. Microhabitat preferences are delineated by the following symbols: E = epibenthic, T = transitional, S = shallow endobenthic and D = deep endobenthic. The data origins from the South China Sea and the Sulu Sea (Rathburn *et al.*, 1996).

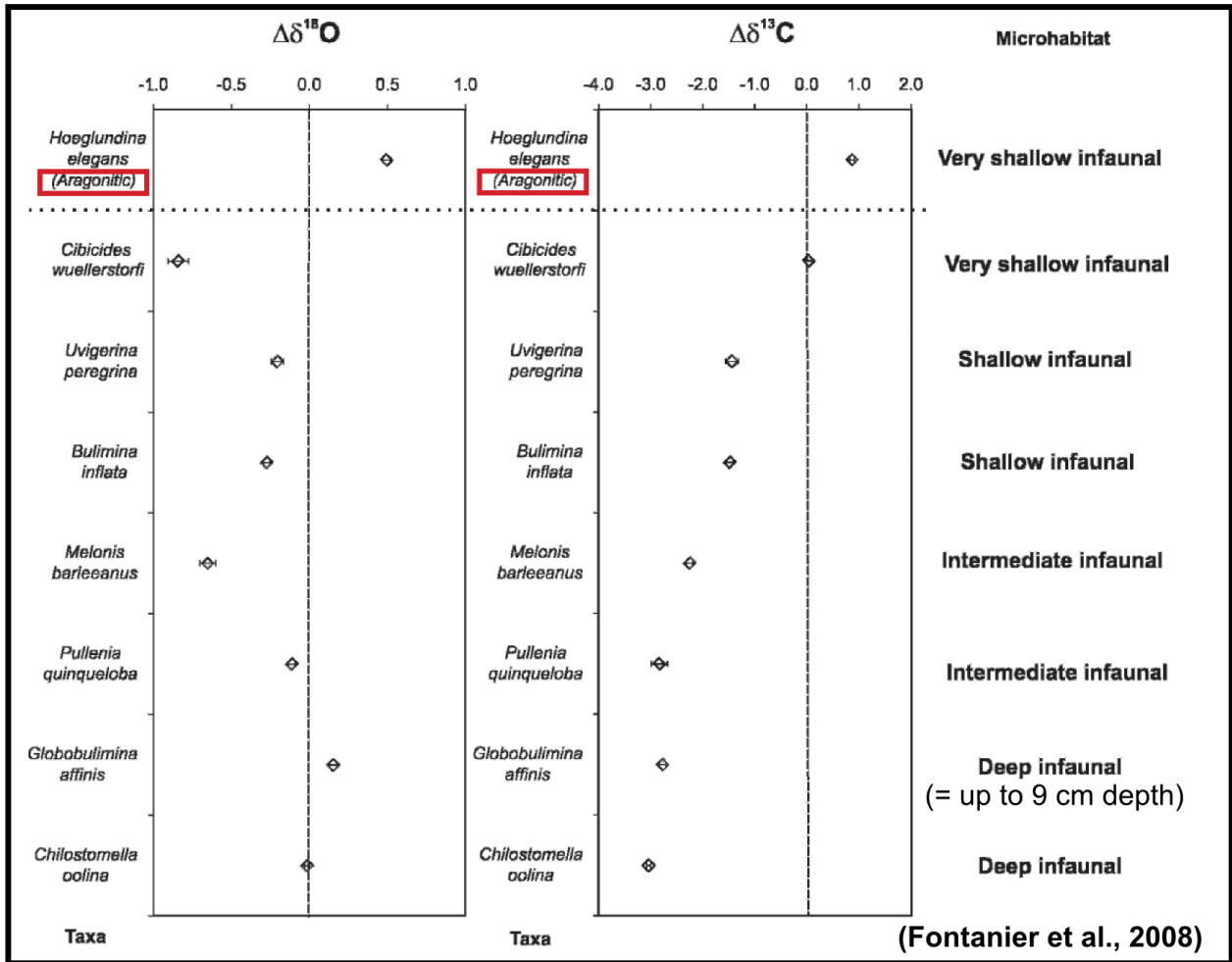


Figure 50. Isotopic data provided by Fontanier *et al.* (2008) of modern foraminifera in the Bay of Biscay (North of Spain) at 2800 m depth.  $\Delta\delta^{18}\text{O}_{\text{species}} = \delta^{18}\text{O}_{\text{species}} - \delta^{18}\text{O}_{\text{equilibrium calcite}}$  &  $\Delta\delta^{13}\text{C}_{\text{species}} = \delta^{13}\text{C}_{\text{species}} - \delta^{13}\text{C}_{\text{DIC}}$  at the sediment surface. Note that *Hoeglundina elegans* have aragonitic tests.

### 7.2.1.2 The $\delta^{18}\text{O}$ values

Isotopic data of McCorkle *et al.* (1997), Rathburn *et al.* (1996) and Fontanier *et al.* (2008) of modern foraminifera suggest a gradual  $\delta^{18}\text{O}$  trend from more negative  $\delta^{18}\text{O}$  values for epibenthic species to more positive  $\delta^{18}\text{O}$  values for deep endobenthic species over a range of approximately 1‰. However several measurements do not respect this  $\delta^{18}\text{O}$  trend. McCorkle *et al.* (1997) consider  $\delta^{18}\text{O}$  inappropriate to identify microhabitats. They suggest that the depleted  $\delta^{18}\text{O}$  of the measured epibenthic species are a consequence of vital effects and not of their microhabitat. Fontanier *et al.* (2008) also deny a  $\delta^{18}\text{O}$  trend in their data, referring to the relatively negative measurement of *Melonis barleeanus* (Figure 50). Rathburn *et al.* (1996) recognize a possible  $\delta^{18}\text{O}$  - microhabitat relation for the South China Sea data but do not recognize a trend for the Sulu Sea data (Figure 49). Other authors do consider  $\delta^{18}\text{O}$  related to the microhabitat of benthic foraminifera. Bemis *et al.* (1998) considered the  $\delta^{18}\text{O}$  paleotemperature predictions based on *Cibicidoides spp.* more in agreement with planktic temperature predictions than *Uvigerina spp.* temperature predictions. They suggested that the  $\delta^{18}\text{O}$  signature of *Uvigerina spp.* is influenced by the



pore water pH ( $\text{CO}_3^{2-}$  concentration). The pH influence on the  $\delta^{18}\text{O}$  signature would be a consequence of an enrichment of  $^{18}\text{O}$  in  $\text{HCO}_3^-$  relative to  $\text{CO}_3^{2-}$ . The influence of pH has indeed been demonstrated for planktic foraminifers by Spero *et al.* (1997) but not yet for benthic foraminifers. Friedrich *et al.* (2006) support the hypothesis that  $\delta^{18}\text{O}$  can be used to distinguish endobenthic from epibenthic species based on their isotopic analysis of Cretaceous species (Figure 51). They suggest that the pore water pH gradient might have been stronger in the Cretaceous compared to the modern oceans causing a more significant  $\delta^{18}\text{O}$  difference between the microhabitats. In conclusion there is still a debate whether  $\delta^{18}\text{O}$  can be used to identify the microhabitat of species. It is clear that relatively negative  $\delta^{18}\text{O}$  values are often associated with the epibenthic species but that these values are not restricted to the epibenthic species. Therefore the  $\delta^{18}\text{O}$  signature should only be considered an indication and should not be consulted as a primary argument for the identification of the microhabitats.

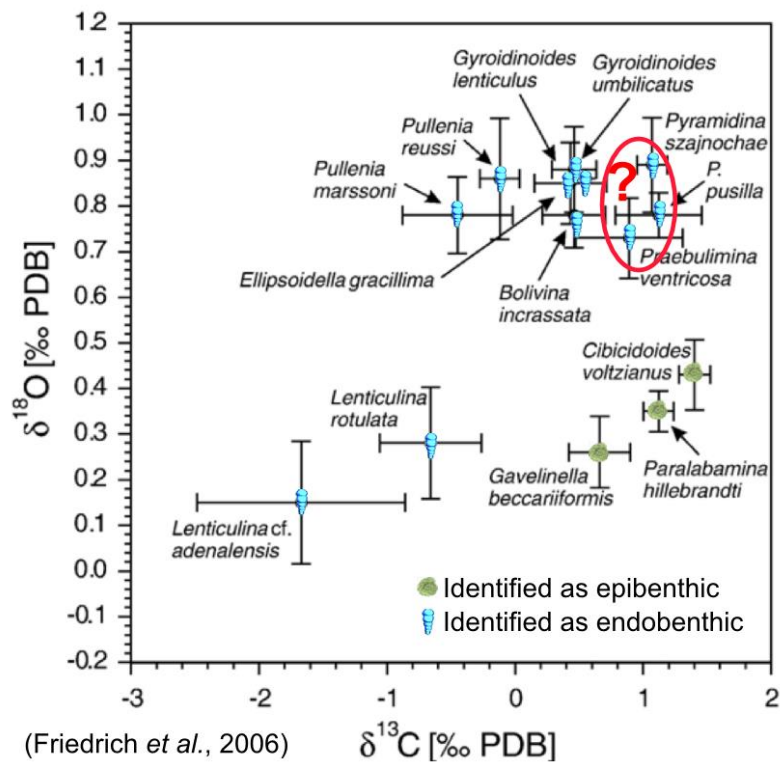


Figure 51. Modified figure of Friedrich *et al.* (2006). Their microhabitat interpretation based on isotopic values and morphology was added to their isotope plot. Friedrich *et al.* (2006) suggested that the 3 circled species could have been either epibenthic or endobenthic with vital effects causing the relatively high  $\delta^{13}\text{C}$ .

### 7.2.1.3 The remaining species

All the species identified as endobenthic in 7.2.1.1 were marked in Figure 52. In Sample 13 (Figure 52A), the  $\delta^{13}\text{C}$  value of *Lenticulina sp. 4* is approximately equal to the  $\delta^{13}\text{C}$  value of the epibenthic species *Cibicidoides decoratus*. However this species was at first considered endobenthic because of the extremely negative  $\delta^{13}\text{C}$  and  $\delta^{18}\text{O}$  values measured in Sample 22 (Figure 52C). It appears that *Lenticulina spp.* encompass an extremely large isotopic range of approximately 2.5‰ for  $\delta^{13}\text{C}$  and 0.8‰ for  $\delta^{18}\text{O}$ .



Their extremely depleted isotopic values and their anomalously large isotopic range are likely related to other parameters than their microhabitat preference. A similar conclusion can be drawn for *Marginulinopsis* spp., *Nodosaria* sp. 1 and *Percultazonaria* sp. 1 because they can have extremely negative both  $\delta^{13}\text{C}$  and  $\delta^{18}\text{O}$  values and were measured over large isotopic ranges. Therefore these species will be discussed separately in 7.2.2.2.

According to the  $\delta^{13}\text{C}$  values in Sample 13 (Figure 52A), *Pulsiphonina prima*, *Stainforthia* sp. 1 are likely endobenthic, while *Anomalinoides acutus*, *Anomalinoides rubiginosis*, *Nuttallides truempyi* and *Turrilina brevispira* are rather epibenthic. The relatively depleted  $\delta^{18}\text{O}$  values of *Anomalinoides acutus*, *Anomalinoides rubiginosis* support their microhabitat interpretation. The  $\delta^{13}\text{C}$  values of *Anomalinoides cf. praeacutus* and *Pyramidulina* sp. 1 are positioned in between both microhabitats in the plot. In Sample 17 (Figure 52B), *Anomalinoides cf. praeacutus* has more depleted  $\delta^{13}\text{C}$  values than endobenthic species *Aragonia aragonensis*, *Uvigerina elongata* and *Valvulineria Scrobiculata*, therefore the species will be identified as endobenthic despite their depleted  $\delta^{18}\text{O}$  values. The  $\delta^{13}\text{C}$  values of *Bulimina kugleri*, *Cibicidoides cf. decoratus* and *Anomalinoides acutus* are positioned in between both microhabitats in the plot. Although *Bulimina kugleri* is likely endobenthic because the  $\delta^{13}\text{C}$  value is approximately equal to the values of *Valvulineria Scrobiculata* and *Uvigerina elongata* and because the  $\delta^{18}\text{O}$  are strongly enriched. In Sample 22 (Figure 52C) the measurements of *Anomalinoides acutus*, *Pulsiphonina prima* and *Pyramidulina* sp. 1 also are positioned in between both microhabitats in the plot. The species that have intermediate  $\delta^{13}\text{C}$  values between epibenthic and endobenthic species will further be referred to as transitional species. This is a result of the theoretical strict boundary between epibenthic and endobenthic species at 1 cm depth that in reality does not exist.

Finally the species identified as endobenthic can be subdivided into shallow endobenthic and deep endobenthic species. *Coryphostoma* spp., *Bulimina cf. thanetensis*, *Bulimina aksuatica* and *Dentalina* sp. 1 can be considered deep endobenthic species based on their strongly depleted  $\delta^{13}\text{C}$  signatures in at least one of the samples ( $< -1.5\text{‰}$ ). A summary of the species microhabitat interpretations based on isotopic values is given in Table 5.

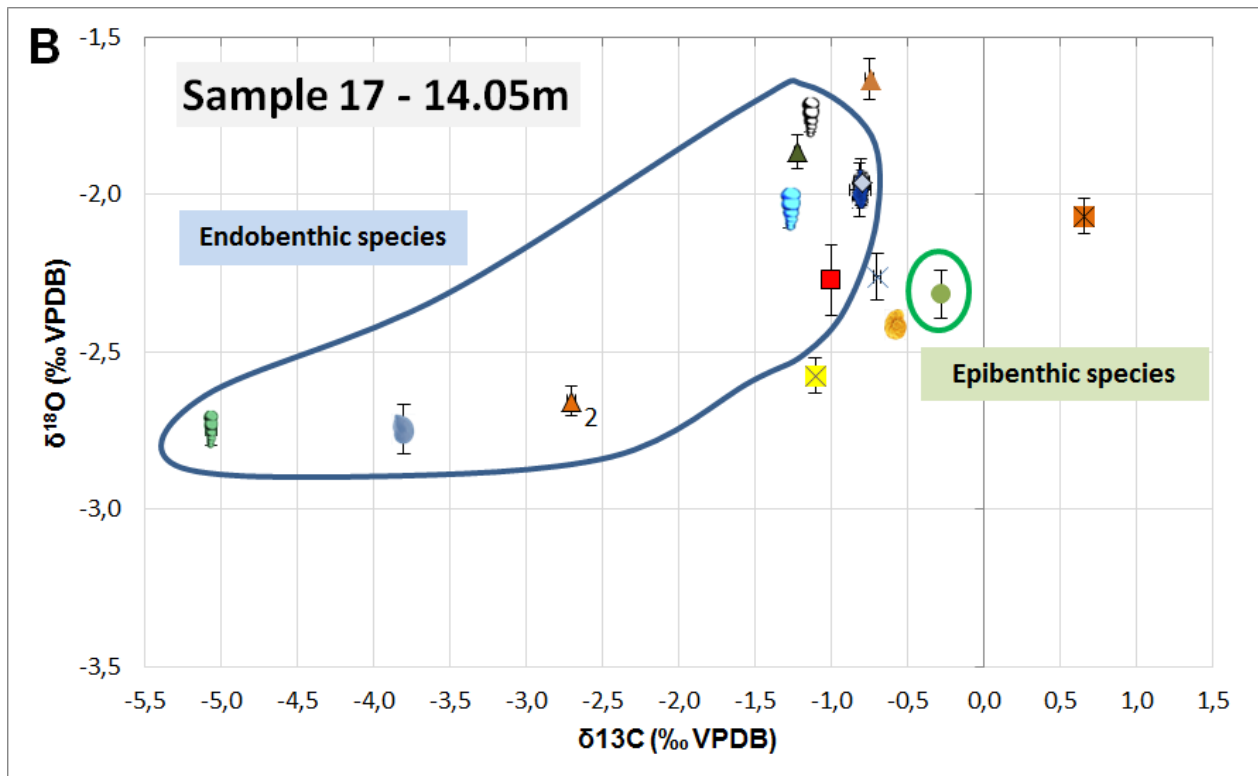
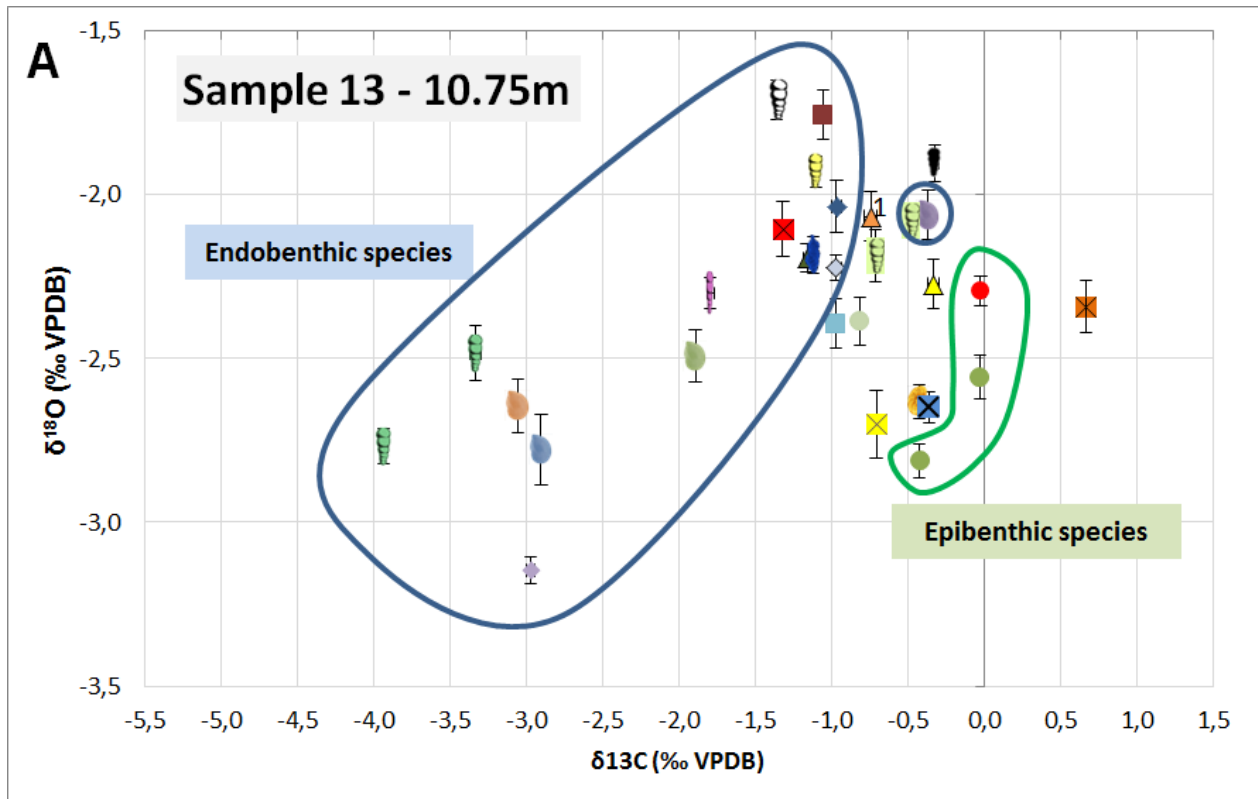
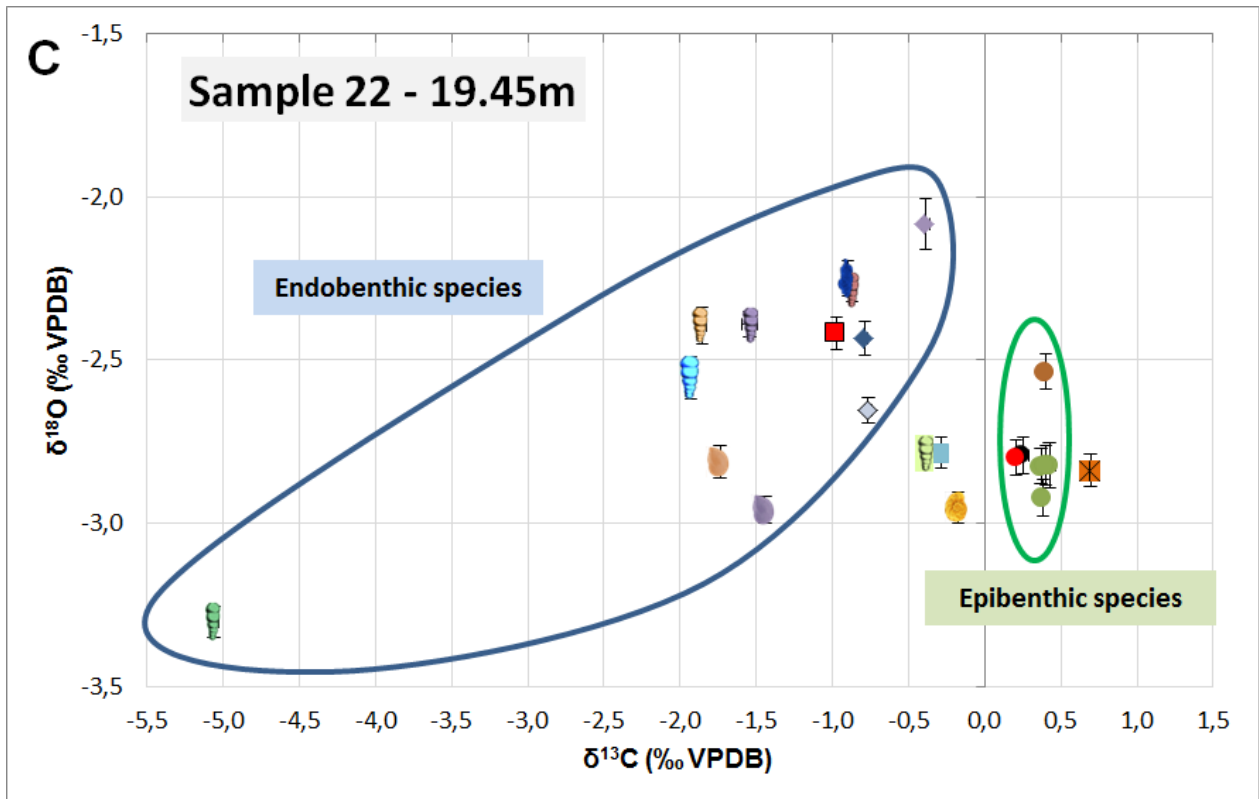


Figure 52. The isotopic data of sample 13 (A), sample 17 (B) and sample 22 (C). The species microhabitats that were identified solely based on their  $\delta^{13}\text{C}$  value in 7.1.1 were marked. The position of the remaining species in the plot can aid in their microhabitat identification.



- |                                       |                                    |                                      |
|---------------------------------------|------------------------------------|--------------------------------------|
| ◆ <i>Alabamina midwayensis</i>        | ■ <i>Allomorpha species 1</i>      | ● <i>Anomalinoidea acutus</i>        |
| ✕ <i>Anomalinoidea cf. praeacutus</i> | ✕ <i>Anomalinoidea rubiginosis</i> | ● <i>Anomalinoidea zitteli</i>       |
| ■ <i>Aragonia aragonensis</i>         | ■ <i>Aragonia aragonensis (D)</i>  | 🍷 <i>Bulimina (aff.) midwayensis</i> |
| 🍷 <i>Bulimina aksuatica</i>           | 🍷 <i>Bulimina cf. thanetensis</i>  | ▲ <i>Bulimina kugleri</i>            |
| ✕ <i>Cibicidoides cf. decoratus</i>   | ● <i>Cibicidoides cf. rigidus</i>  | ● <i>Cibicidoides decoratus</i>      |
| ● <i>Cibicidoides rigidus</i>         | 🍷 <i>Coryphostoma spp.</i>         | 🍷 <i>Dentalina species1</i>          |
| 🍷 <i>Lenticulina species 1</i>        | 🍷 <i>Lenticulina species 2</i>     | 🍷 <i>Lenticulina species 3</i>       |
| 🍷 <i>Lenticulina species 4</i>        | 🍷 <i>Loxostomoides applinae</i>    | ▲ <i>Marginulinopsis species 1?</i>  |
| 🍷 <i>Nodosaria species 1</i>          | ▲ <i>Nuttallides truempyi</i>      | ▲ <i>Oridorsalis plummerae</i>       |
| ◆ <i>Percultazonaria species 1</i>    | ■ <i>Pulsiphonina prima</i>        | 🍷 <i>Pyramidulina species 1</i>      |
| ■ <i>Ramulina species 1</i>           | ✕ <i>Spiroloculina spp.</i>        | ● <i>Stainforthia species 1</i>      |
| 🍷 <i>Stilostomella species 1</i>      | 🍷 <i>Turrilina brevispira</i>      | 🍷 <i>Uvigerina elongata</i>          |
| ◆ <i>Valvulineria scrobiculata</i>    |                                    |                                      |

Figure 52 (continued).

The microhabitat of benthic species in Aktulagay under normal oxygen and food conditions			
Epibenthic species	Transitional species (Epibenthic to shallow endobenthic)	Shallow endobenthic species	Deep endobenthic species
<i>Anomalinoides acutus</i>	<i>Cibicidoides cf. decoratus</i>	<i>Alabamina midwayensis</i>	<i>Bulimina aksuatica</i>
<i>Anomalinoides rubiginosis</i>	<i>Cibicidoides sp. 1**</i>	<i>Allomorphina sp. 1</i>	<i>Bulimina cf. thanetensis</i>
<i>Anomalinoides zitteli</i>	<i>Lenticulina spp.*</i> (rather epibenthic)	<i>Anomalinoides cf. praeacutus</i>	<i>Coryphostoma spp.</i>
<i>Cibicidoides cf. rigidus</i>	<i>Marginulinopsis spp.*</i>	<i>Aragonia aragonensis</i>	<i>Dentalina sp. 1</i>
<i>Cibicidoides decoratus</i>	<i>Nuttallides truempyi</i> (rather epibenthic)	<i>Bulimina (aff.) midwayensis</i>	<i>Nodosaria sp. 1*</i>
<i>Cibicidoides rigidus</i>	<i>Percultazonaria sp. 1*</i>	<i>Bulimina Kugleri</i>	
	<i>Pyramidulina sp. 1</i> (rather endobenthic)	<i>Loxostomoides applinae</i>	
	<i>Pulsiphonina prima</i> (epibenthic to shallow endobenthic, migrating?) **	<i>Oridorsalis plummerae</i>	
	<i>Spiroloculina sp. 1*</i> (rather epibenthic)	<i>Ramulina sp. 1</i>	
	<i>Stainforthia sp. 1</i> (rather endobenthic)	<i>Stilostomella sp. 1</i>	
	<i>Turrilina brevispira</i> (rather epibenthic)**	<i>Uvigerina elongata</i> (Shallow to deep endobenthic, migrating?) **	
		<i>Valvulineria scrobiculata</i>	

Table 5. Summary of the final interpretation of species microhabitats.

\* Discussed in 7.2.2.

\*\* Discussed in 9.2.2, 9.2.3 and 9.2.5 (based on additional results)

The species that could be either epibenthic or shallow endobenthic species were called transitional species.

## 7.2.2 Complications

### 7.2.2.1 Comparison with other datasets

The microhabitat interpretation of species *Lenticulina spp.*, *Marginulinopsis spp.*, *Nodosaria sp. 1* and *Percultazonaria sp. 1* is more complex. To discuss these species, it is illustrative to combine the data of the 3 samples into 1 isotopic plot (Figure 53) and to compare with other datasets (Figure 51, Figure 54 & Figure 55). In Figure 53 the isotopic data of samples 17 and 22 was corrected to the isotopic data of Sample 13. The correction was based on the foraminifer *Anomalinoides acutus*. It is assumed that differences in their epibenthic  $\delta^{18}\text{O}$  signal only reflect temperature changes between the samples and that the differences in their  $\delta^{18}\text{O}$  signature reflect  $\delta^{13}\text{C}_{\text{DIC}}$  changes at the water sediment interface. Figure 55 is a comparison between the data of Friedrich *et al.* (2006), Wendler *et al.* (2013) and the data of this study. Both authors provide additional *Lenticulina spp.* data from the Cretaceous. The comparison reveals that the relative  $\delta^{18}\text{O}$  and  $\delta^{13}\text{C}$  values of *Lenticulina spp.* are very similar in the 3 studies. The most depleted

$\delta^{13}\text{C}$  measurements of *Lenticulina* spp. are approximately 3‰ more depleted than the epibenthic species, while the most positive  $\delta^{13}\text{C}$  values reach similar values as epibenthic species in both this study and the study of Wendler *et al.* (2013). In all 3 studies the most negative  $\delta^{13}\text{C}$  values are associated with the most negative  $\delta^{18}\text{O}$  values that can be up to 0.2‰ more depleted than the most negative epibenthic  $\delta^{18}\text{O}$  values in the 3 studies. Similar the most positive  $\delta^{13}\text{C}$  values are associated with the most positive  $\delta^{18}\text{O}$  values in the 3 studies. The total range of the  $\delta^{18}\text{O}$  values of *Lenticulina* spp. in this study and the study of Wendler *et al.* (2013) reaches 1‰.

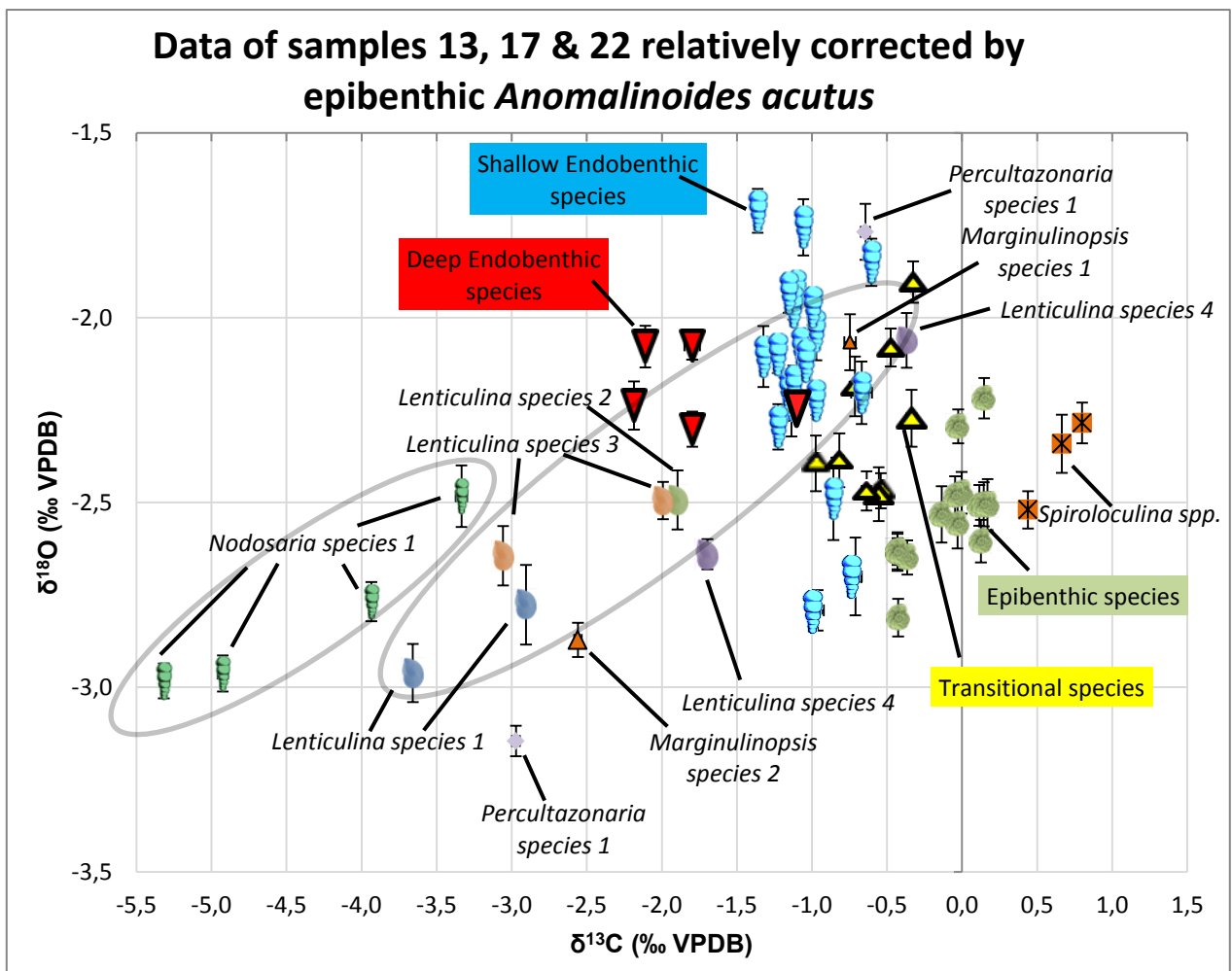


Figure 53. This figure plots the data from samples 13, 17 and 22. The data of samples 17 and 22 was corrected to the data of Sample 13. The correction is based on epibenthic species *Anomalinoidea acutus*. Most species were assigned to a specific microhabitat as discussed in 7.2.1 (Summarized in Table 3). Note that the symbols are often larger than the standard deviations.

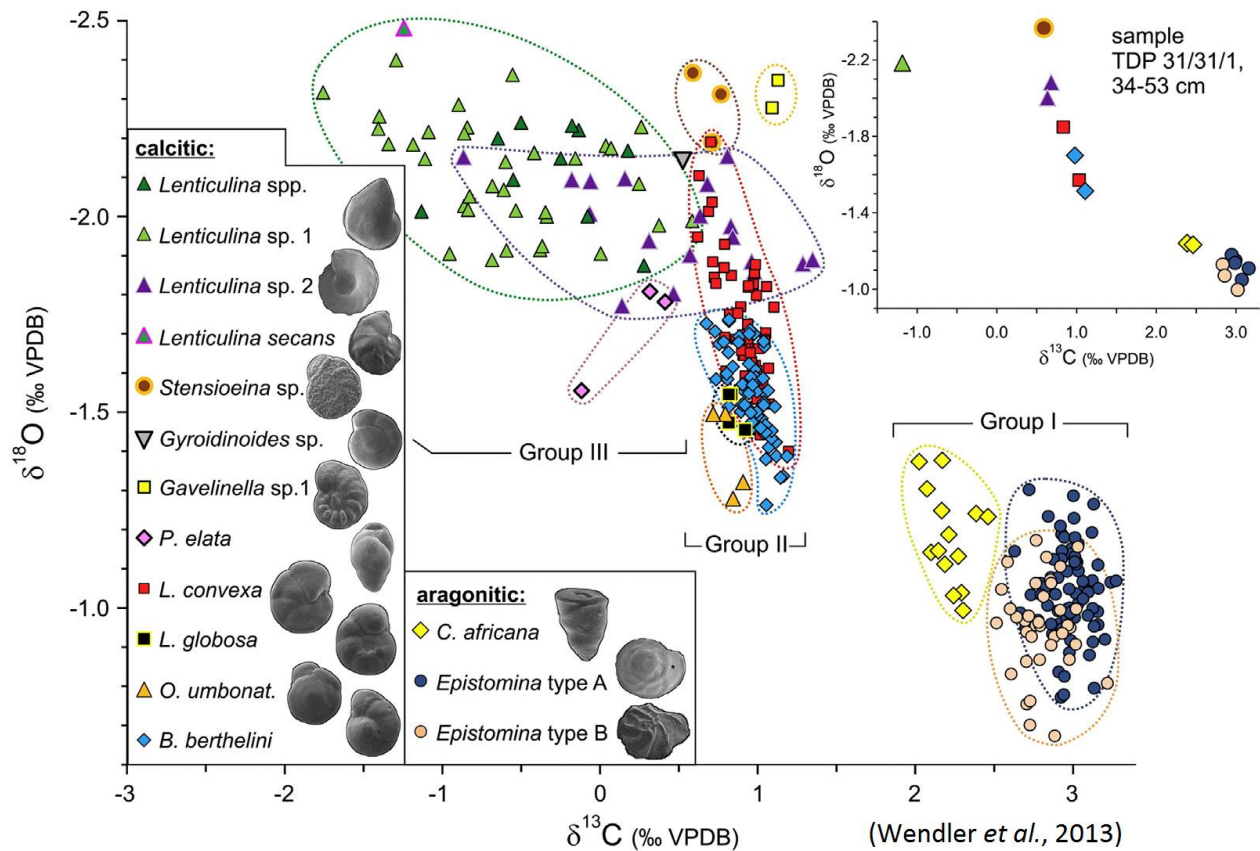


Figure 54. Figure from Wendler et al. (2013). Note that their  $\delta^{18}\text{O}$  axis is reversed compared to the  $\delta^{18}\text{O}$  axis in Figure 53. They divide their species into 3 groups. Group 1 is composed of species with aragonitic tests; *Colomia africana* and *Epistomina* type A & B. Group 2 is composed of species with calcite tests with intermediate  $\delta^{13}\text{C}$  and  $\delta^{18}\text{O}$  values. Group 3 is composed of species with the lowest  $\delta^{13}\text{C}$  and  $\delta^{18}\text{O}$  values; *Lenticulina* species. For Group 2 they made microhabitat interpretations based on the isotopic values, morphology and a comparison with other publications. *Berthelina berthelini*, *Lingulogavelinella globosa*, *Gavelinella* sp. 1, *Lingulogavelinella convexa*, *Oridorsalis umbonatus*, *Stensioeina* species were interpreted as epibenthic to shallow endobenthic. *Praebulimina elata* and *Gyroidinoides* spp. were considered shallow to moderately deep endobenthic.

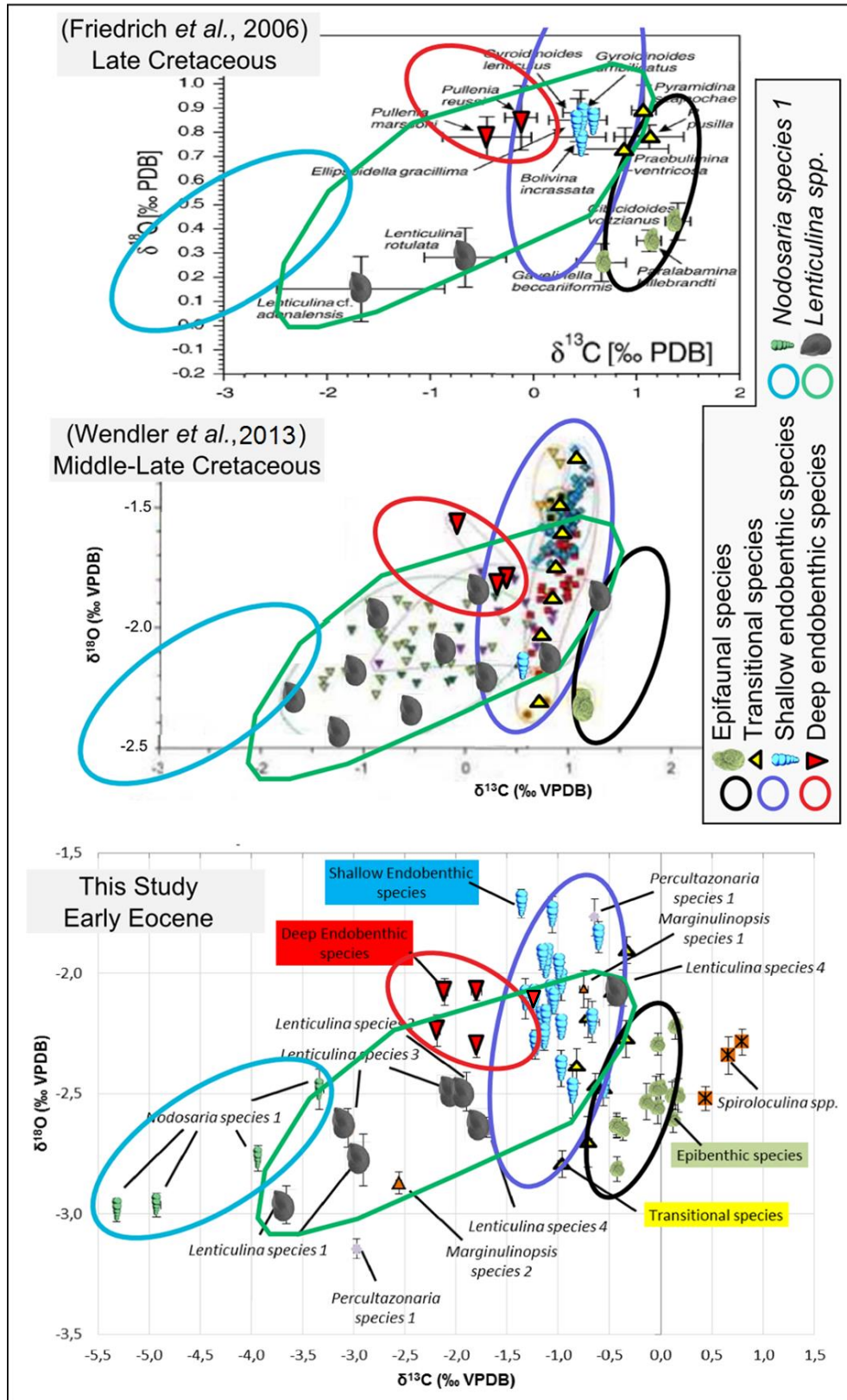


Figure 55. Comparison of the data of Friedrich *et al.* (2006), Wendler *et al.* (2013) and this study. A detailed figure of the datasets can be found in Figure 51, Figure 54 & Figure 53 respectively. Note that the axes ( $\delta^{13}\text{C}$  and  $\delta^{18}\text{O}$ ) have the same scale to allow direct comparison.



### 7.2.2.2 Kinetic disequilibrium calcite precipitation

*Lenticulina spp.*, *Nodosaria sp. 1*, *Marginulinopsis spp.* and *Percultazonaria sp. 1* are odd species because at least 1 of the measurements of these species had extremely depleted  $\delta^{18}\text{O}$  ( $\leq -2.5\text{‰}$ ) and  $\delta^{13}\text{C}$  ( $\leq -1.5\text{‰}$ ) values (Figure 53). Nevertheless some measurements with more enriched  $\delta^{18}\text{O}$  and  $\delta^{13}\text{C}$  values were also made for *Lenticulina spp.*, *Marginulinopsis spp.* and *Percultazonaria sp. 1*. Figure 53 demonstrates the large isotopic range of these species and indicates a positive correlation between  $\delta^{18}\text{O}$  and  $\delta^{13}\text{C}$ . Friedrich *et al.* (2006) suggests that a deep endobenthic microhabitat, different feeding strategies and/or specific vital effects could explain the depleted signature of *Lenticulina spp.* They excluded kinetic disequilibrium fractionation due to the absence of a  $\delta^{18}\text{O}$  and  $\delta^{13}\text{C}$  correlation in their dataset (Figure 51 & Figure 55). Our data on the other hand clearly suggests a correlation. Kinetic disequilibrium fractionation is the effect of isotopic disequilibrium (compared to equilibrium calcite) due to rapid precipitation of biogenic calcite (McConnaughey, 1989). Kinetic disequilibrium fractionation causes depletion of  $\delta^{18}\text{O}$  and  $\delta^{13}\text{C}$  and could thus be a plausible explanation for these species. However the amount of data in this study remains limited to support this hypothesis. Fortunately Wendler *et al.* (2013) recently presented a large dataset with 60 measurements of *Lenticulina spp.* from SE Tanzania, dated middle to late Cretaceous (Figure 54 & Figure 55). Wendler *et al.* (2013) also observed the correlation between  $\delta^{18}\text{O}$  and  $\delta^{13}\text{C}$  for *Lenticulina* species. They considered the kinetic effect to be a plausible explanation because *Lenticulina spp.* are often considered opportunistic species (e.g. Stassen *et al.*, 2012; Deprez *et al.*, submitted). Opportunistic species are species that can quickly reproduce and react rapidly to organic matter fluxes. Wendler *et al.* (2013) further suggested that the species could be interpreted as either deep endobenthic with vital effects or as shallow to epibenthic species with strong vital effects. Based on our data in Figure 53 and the data of Wendler *et al.* (2013) in Figure 54, a deep endobenthic microhabitat seems less plausible because a clear  $\delta^{13}\text{C}$  overlap with the transitional and shallow endobenthic species exists in both datasets. However it remains possible that the microhabitat variability between the different *Lenticulina* species exists. McConnaughey (1989) provides data on the effect of disequilibrium precipitation for the non-photosynthetic coral *Tubastrea sp.* For this species the disequilibrium precipitation resulted in the following relation between  $\delta^{18}\text{O}$  and  $\delta^{13}\text{C}$ :  $\delta^{18}\text{O} = 3.31 * \delta^{13}\text{C} + 2.34$  (Figure 56; McConnaughey, 1989). Although it is unknown whether this relation is applicable to foraminifers, a similar relation would be expected because in both cases it is biologic calcite precipitation in sea water. Figure 57 demonstrates that the slope of the equation of McConnaughey (1989) strongly agrees with the data of both *Lenticulina spp.* and *Nodosaria sp. 1*. The observation that *Nodosaria sp. 1* consistently has more depleted  $\delta^{13}\text{C}$  values than *Lenticulina spp.* suggests that *Nodosaria sp. 1* are related to the deep or possibly shallow endobenthic species while *Lenticulina spp.* would rather be related to the epibenthic species or the transitional species. The strongly depleted  $\delta^{18}\text{O}$  and  $\delta^{13}\text{C}$  of *Marginulinopsis sp. 2* and *Percultazonaria sp. 1* suggest that these species are also affected by the kinetic disequilibrium precipitation effect. It should be noted that the *Percultazonaria sp. 1* isotopic values are not within the wide isotopic range of *Lenticulina spp.* This might be related to additional ontogenetic effects for this species. Additional measurements would be required to confirm this. Finally it



is possible that the species identified as deep endobenthic are actually shallow endobenthic species moderately affected by the kinetic effect. However *Lenticulina spp.*, *Nodosaria sp. 1*, *Marginulinopsis spp.* and *Percultazonaria sp. 1* are all characterized by extremely thick tests compared to other species in the same size fraction. It is possible that their thick tests are related to their lifestyle of rapid precipitation. The species identified as deep endobenthic (*Bulimina cf. thanetensis*, *Bulimina aksuatica*, *Coryphostoma spp.* and *Dentalina sp. 1*) are not characterized by a thick test. Therefore there are no indications to assume that the kinetic effect is important for these species. Multiple measurements of these species are required to verify this assumption. Additional measurements of *Bulimina aksuatica* in Figure 26 support that no important kinetic effect exists for this species.

Because *Lenticulina spp.*, *Nodosaria sp. 1*, *Marginulinopsis spp.* and *Percultazonaria sp. 1* have a large scatter on their isotopic  $\delta^{13}\text{C}$  signatures (interpret as a result of the kinetic disequilibrium calcite precipitation effect), these species cannot be used for paleoenvironmental studies.

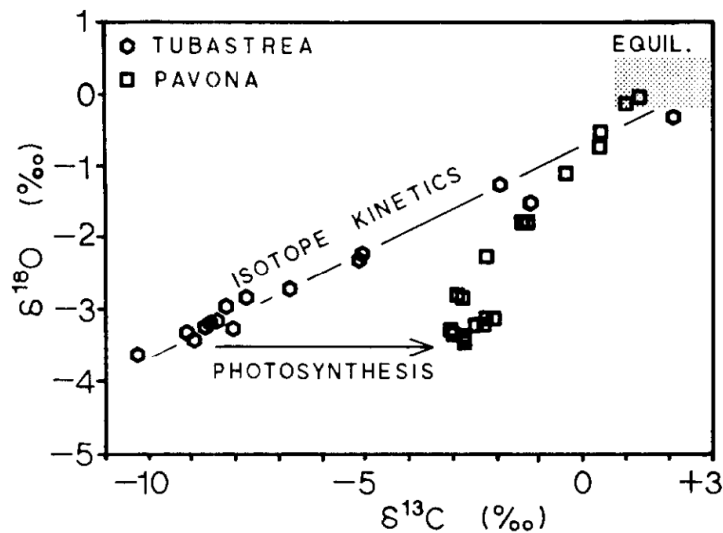


Figure 56. Data from McConnaughey (1989). The effect of disequilibrium calcite precipitation on the non-photosynthetic coral *Tubastrea sp.* An equation that demonstrates the relation between  $\delta^{18}\text{O}$  and  $\delta^{13}\text{C}$  due to kinetic disequilibrium for this species can be derived from the figure:  

$$\delta^{18}\text{O} = 3,31 * \delta^{13}\text{C} + 2,34$$

**Data of samples 13, 17 & 22 relatively corrected by  
epibenthic *Anomalinoides acutus***

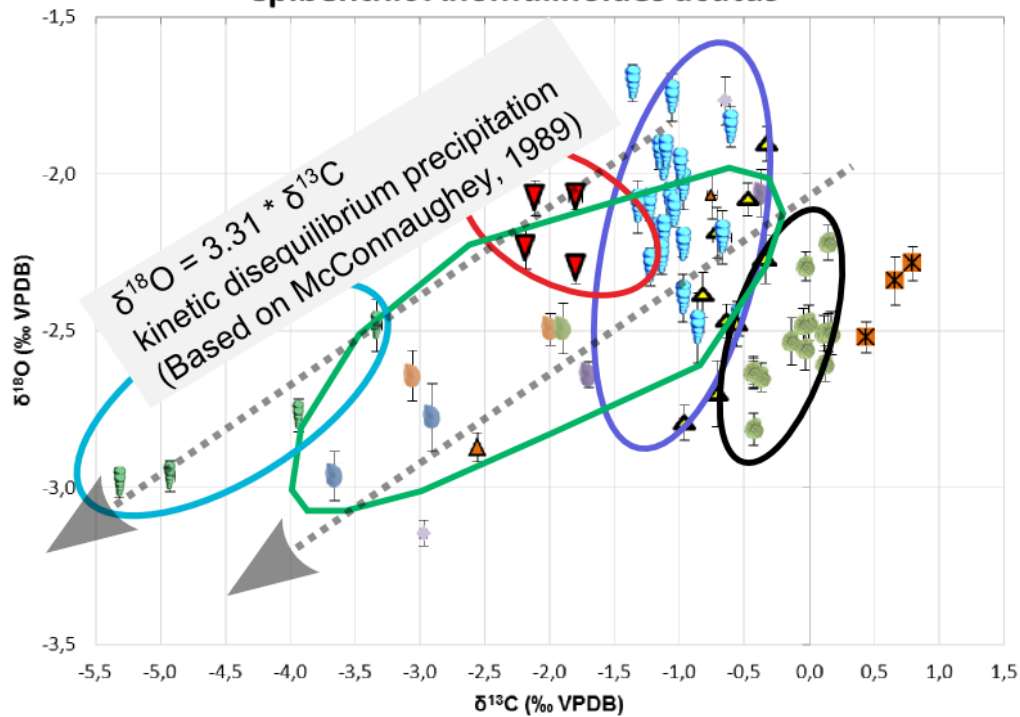


Figure 57. The figure demonstrates that the slope of the equation of kinetic disequilibrium precipitation ( $\delta^{18}\text{O} = 3,31 * \delta^{13}\text{C} + \text{cst}$ ) based on data of McConnaughey (1989), strongly agrees with our data for both *Nodosaria sp. 1* and *Lenticulina spp.* The legend of the figure can be found in Figure 53.

### 7.2.2.3 Miliolid test wall texture

*Spiroloculina spp.* was measured in samples 13, 17 and 22 and is associated with uniquely high  $\delta^{13}\text{C}$  values (Figure 45; Figure 46). The variation of the  $\delta^{13}\text{C}$  signature,  $0,665 \pm 0,033\text{‰}$ ,  $0,658 \pm 0,036\text{‰}$  and  $0,694 \pm 0,037\text{‰}$  in sample 13, 17 and 22 can be considered statistically insignificant. The  $\delta^{18}\text{O}$  signal on the other hand does vary significantly and demonstrates the similar  $\Delta\delta^{18}\text{O}$  shifts between the species as other species like e.g. *Valvulineria Scrobiculata*. A hypothesis to explain the unique  $\delta^{13}\text{C}$  signature would be the Miliolid test wall texture of the species. It is the only measured species in this study that belongs to the order Miliolida. This hypothesis is based on the data of McCorkle *et al.* (1990) and Rathburn *et al.* (1996). They measured  $\delta^{13}\text{C}$  values for the modern species *Bolivinospis cubensis* and *Pyrgo spp.* that were not related to the species microhabitat but considered associated to their different test wall texture. Therefore the high  $\delta^{13}\text{C}$  signature of *Spiroloculina spp.* could be a consequence of a Miliolid test wall texture and is not necessarily related to an epibenthic microhabitat.

### 7.2.3 Morphologic microhabitat interpretation

In Figure 47 the species of the same genera were marked in sample 13, 17 and 22. The observation that *Anomalinoides*, *Cibicidoides* and *Bulimina* species are restricted to relatively small isotopic ranges suggests that their morphological resemblance indeed reflected a similar microhabitat and life style.

Rosoff and Corliss (1992) provide information of modern deep sea benthic foraminifers to predict the species microhabitat based on the morphology of the species. They demonstrated that rounded trochospiral, planoconvex, biconvex and milioline species are in general related to an epibenthic microhabitat while rounded planispiral, flat ovoid, cylindrical/conical, spherical and flat tapered species are related to an endobenthic microhabitat (Figure 58). Based on their observations, a morphologic interpretation was proposed for the species in this study (Table 6). Seven contradictions exist between the isotopic interpretations and the morphologic interpretations; *Alabamina midwayensis* (planoconvex), *Allomorphina sp. 1* (rounded trochospiral), *Anomalinoidea cf. praeacutus* (planoconvex), *Oridorsalis plummerae* (biconvex), *Pulsiphonina prima* (biconvex), *Turrilina brevispira* (tapered cylindrical) and *Valvulineria scrobiculata* (biconvex). Twenty six species did not contradict. Therefore the morphological interpretations had an estimated 81% accuracy based on the isotopic results. This is in line with the result of Buzas *et al.* (1993). They concluded that a microhabitat interpretation based on morphology has a 75% accuracy based on a statistical evaluation of the microhabitats of living (stained) foraminifers.

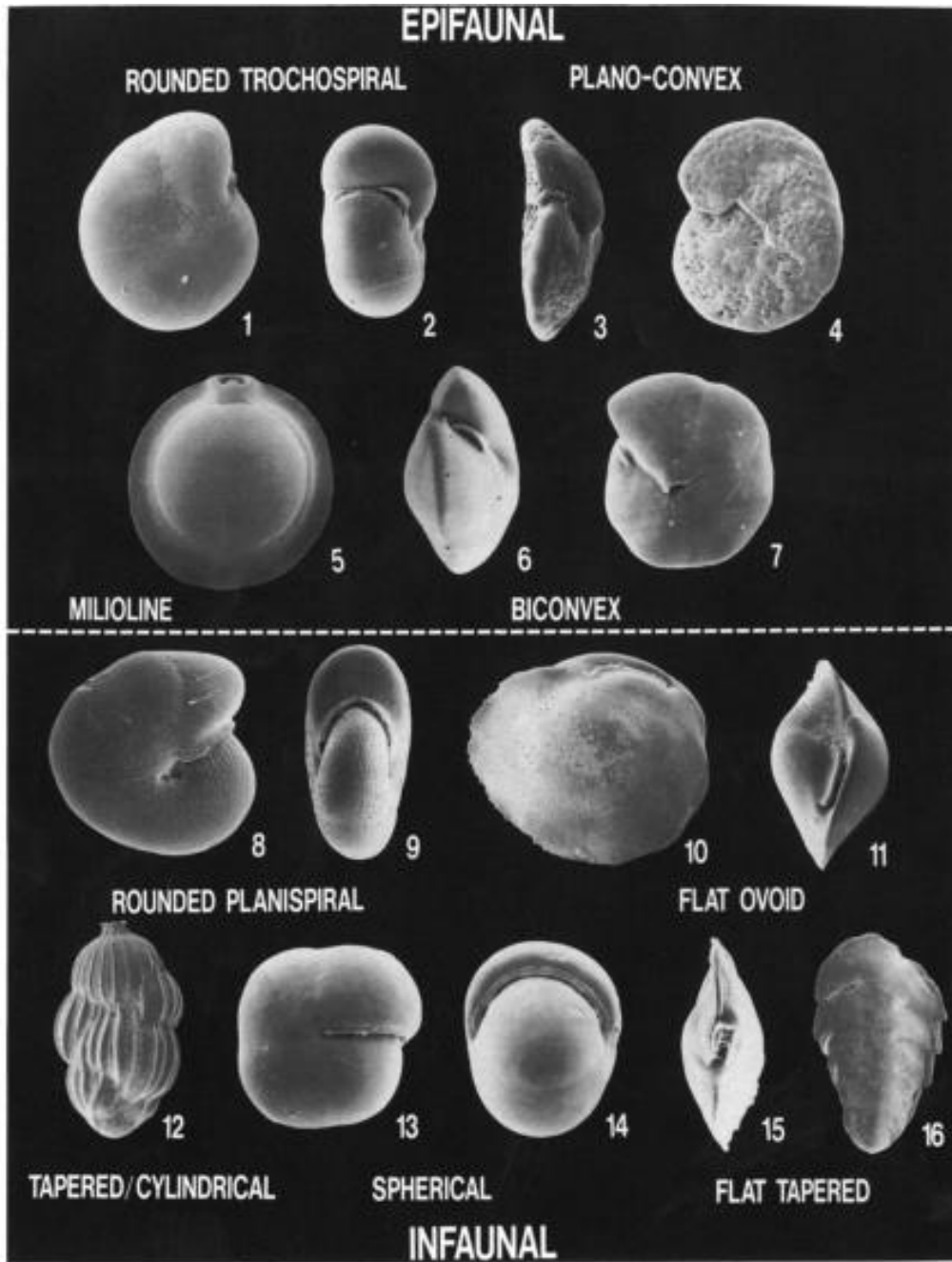


Figure 58. A figure made by Rosoff and Corliss (1992) that allows microhabitat interpretation based on morphology. Their study is based on recent deep-sea benthic foraminifers from the Norwegian and Greenland seas.

		Microhabitat	
		Isotopic interpretation	Morphologic interpretation
<b>Species</b>	<i>Alabamina midwayensis</i>	Shallow endobenthic	Epibenthic
	<i>Allomorphina sp. 1</i>	Shallow endobenthic	Epibenthic
	<i>Anomalinoides acutus</i>	Epibenthic	Epibenthic
	<i>Anomalinoides cf. praeacutus</i>	Shallow endobenthic	Epibenthic
	<i>Anomalinoides rubiginosis</i>	Epibenthic	Epibenthic
	<i>Anomalinoides zitteli</i>	Epibenthic	Epibenthic
	<i>Aragonia aragonensis</i>	Shallow endobenthic	Endobenthic
	<i>Bulimina (aff.) midwayensis</i>	Shallow endobenthic	Endobenthic
	<i>Bulimina aksuatica</i>	Deep endobenthic	Endobenthic
	<i>Bulimina cf. thanetensis</i>	Deep endobenthic	Endobenthic
	<i>Bulimina kugleri</i>	Shallow endobenthic	Endobenthic
	<i>Cibicidoides cf. rigidus</i>	Epibenthic	Epibenthic
	<i>Cibicidoides cf. decoratus</i>	Transitional	Epibenthic
	<i>Cibicidoides decoratus</i>	Epibenthic	Epibenthic
	<i>Cibicidoides rigidus</i>	Epibenthic	Epibenthic
	<i>Cibicidoides sp. 1</i>	Transitional	Epibenthic
	<i>Coryphostoma spp.</i>	Deep endobenthic	Endobenthic
	<i>Dentalina species1</i>	Deep endobenthic	Endobenthic
	<i>Lenticulina sp. 1</i>	Transitional (epibenthic?)	?
	<i>Loxostomoides applinae</i>	Shallow endobenthic	Endobenthic
	<i>Marginulinopsis spp.</i>	Transitional	Endobenthic
	<i>Nodosaria sp. 1</i>	Deep endobenthic	Endobenthic
	<i>Nuttallides truempyi</i>	Transitional (epibenthic?)	Epibenthic
	<i>Oridorsalis plummerae</i>	Shallow endobenthic	Epibenthic
	<i>Percultazonaria sp. 1</i>	Transitional	Endobenthic
	<i>Pulsiphonina prima</i>	Transitional (migrating?)	Epibenthic
	<i>Pyramidulina sp. 1</i>	Transitional (endobenthic?)	Endobenthic
	<i>Ramulina sp. 1</i>	Shallow endobenthic	Endobenthic
	<i>Spiroloculina spp.</i>	Transitional (epibenthic?)	Epibenthic
	<i>Stainforthia sp. 1</i>	Transitional (endobenthic?)	Endobenthic
<i>Stilostomella sp. 1</i>	Shallow endobenthic	Endobenthic	
<i>Turrilina brevispira</i>	Transitional (epibenthic?)	Endobenthic	
<i>Uvigerina elongata</i>	Endobenthic (migrating?)	Endobenthic	
<i>Valvulineria scrobiculata</i>	Shallow endobenthic	Epibenthic	

Table 6. Comparison of the microhabitat interpretation based on the isotopic signatures with a microhabitat interpretation based on the morphology. The contradictions were marked. The species that could be either epibenthic or shallow endobenthic species were called transitional species.

### 7.3 Summary

First of all the preferential microhabitat of several species was identified based on our isotopic results. *Anomalinoidea acutus*, *Anomalinoidea rubiginosis*, *Anomalinoidea zitteli*, *Cibicidoides cf. rigidus*, *Cibicidoides decoratus* and *Cibicidoides rigidus* were identified as epibenthic species. *Cibicidoides cf. decoratus*, *Cibicidoides sp. 1*, *Lenticulina spp.*, *Marginulinopsis spp.*, *Nuttallides truempyi*, *Percultazonaria sp. 1*, *Pyramidulina sp. 1*, *Spiroloculina sp. 1*, *Stainforthia sp. 1* and *Turrilina brevispira* were referred to as transitional species and could be either epibenthic or shallow endobenthic species. *Alabamina midwayensis*, *Allomorpha sp. 1*, *Anomalinoidea cf. praeacutus*, *Aragonia aragonensis*, *Bulimina (aff.) midwayensis*, *Bulimina kugleri*, *Loxostomoides applinae*, *Oridorsalis plummerae*, *Pulsiphonina prima*, *Ramulina sp. 1*, *Stilostomella sp. 1*, *Uvigerina elongata* and *Valvulineria scrobiculata* were identified as shallow endobenthic species. Finally *Bulimina aksuatica*, *Bulimina cf. thanetensis*, *Coryphostoma spp.*, *Dentalina sp. 1* and *Nodosaria sp. 1* were identified as deep endobenthic species. Secondly the  $\delta^{13}\text{C}$  values of most species were considered representative for the  $\delta^{13}\text{C}_{\text{DIC}}$  gradient within the sediment and thus related to their relative depth. However the  $\delta^{13}\text{C}$  values of *Lenticulina spp.*, *Marginulinopsis spp.*, *Nodosaria sp. 1* and *Percultazonaria sp. 1* and *Spiroloculina spp.* were considered exceptions. The  $\delta^{18}\text{O}$  and the  $\delta^{13}\text{C}$  values of *Lenticulina spp.*, *Marginulinopsis spp.*, *Nodosaria sp. 1* and *Percultazonaria sp. 1* were considered strongly affected kinetic disequilibrium calcite precipitation. This interpretation was also suggested by Wendler *et al.* (2013) for *Lenticulina spp.* and could be further supported by the disequilibrium calcite precipitation equation of McConnaughey (1989) based on modern non-photosynthetic coral *Tubastrea sp.* The interpretation indicates that the use of the isotopic values of these species should be avoided for paleoenvironmental studies. The  $\delta^{13}\text{C}$  values of *Spiroloculina spp.* were assumed to be related to their miliolid test wall texture and not necessarily to an epibenthic microhabitat. Finally the microhabitat results were compared with the microhabitat interpretation based on the morphology. Seven contradictions were found; *Alabamina midwayensis*, *Allomorpha sp. 1*, *Anomalinoidea cf. praeacutus*, *Oridorsalis plummerae*, *Pulsiphonina prima*, *Turrilina brevispira* and *Valvulineria scrobiculata*. For 26 measurements there was no contradiction between the morphologic interpretation and the isotopic interpretation, therefore 19% of the morphologic interpretations are considered incorrect in this study.

## 8 The epibenthic isotopic record

### 8.1 Introduction

The  $\delta^{18}\text{O}$  and the  $\delta^{13}\text{C}$  signatures of epibenthic species are considered to mainly reflect the  $\delta^{18}\text{O}$  and  $\delta^{13}\text{C}$  signatures of seawater at the sediment water interface (e.g. Jorissen, 1999). Therefore a correlation exists between the isotopic signature of the seawater and the signatures of different epibenthic species. In this study *Cibicidoides decoratus* was chosen to create the epibenthic record for several reasons. First of all the results from the ecological study clearly demonstrated that the species has an epibenthic microhabitat. Secondly the species occurred over most of the section according to the relative abundance data of Deprez (2012). Finally *Cibicidoides spp.* are frequently used in other paleoclimatic studies and are used to generate the Cenozoic long term isotope record of Zachos *et al.* (2001). However the species was insufficiently available in samples 1, 2, 19, 23 and 25 for isotopic measurements. Since no other *Cibicidoides* species were available in sufficient numbers over a significant part of the section, *Anomalinoides acutus* was chosen to complete the epibenthic record. *Anomalinoides acutus* has already been applied to supplement *Cibicidoides* records in other studies, e.g. Cramer *et al.* (1999) and Stassen *et al.* (2012). Furthermore 5 measurements were performed on *Anomalinoides zitteli* to further calibrate the epibenthic isotope record.

### 8.2 Isotopic variability within a sample

Figure 59 and Figure 60 demonstrate the correlation between *Cibicidoides decoratus* and *Anomalinoides acutus* for  $\delta^{13}\text{C}$  and  $\delta^{18}\text{O}$  respectively. For both species a positive correlation can be proven with  $R^2$  values of 0.76. The difference between the predicted  $\delta^{18}\text{O}$  values (based on *Anomalinoides acutus*) and the measured  $\delta^{18}\text{O}$  values of *Cibicidoides decoratus* only differ  $\leq 0.15\text{‰}$ . This deviation can be considered acceptable given the average measurement standard deviation of 0.062‰. For  $\delta^{13}\text{C}$  much larger deviations exist up to 0.4‰ despite the average measurement standard deviation of only 0.037‰. The strongest deviations of the correlation are reported in Sample 4, 10, 20 and 22.

The intrasample variation of  $\delta^{13}\text{C}$  and  $\delta^{18}\text{O}$  of *Cibicidoides decoratus* has been studied within Sample 22 (Figure 61). Sample 22 was chosen because the species had a relatively high abundance in this sample and because there were no preservation issues observed. Four measurements were made in the sample; each measurement represented an average of 5 to 7 specimens. The measurements resulted into relatively small  $\Delta\delta^{18}\text{O}$  and  $\Delta\delta^{13}\text{C}$  ranges of 0.10‰ and 0.06‰ respectively. However, because of suspicious values of the original *Cibicidoides decoratus* measurements in samples 13 and 20 (based on the assumed isotopic correlation with *Anomalinoides acutus*), *Cibicidoides decoratus* was remeasured in these samples (Figure 62). The new measurements revealed significantly larger isotopic ranges than observed in Sample 22. The  $\Delta\delta^{18}\text{O}$  ranges were 0.35‰ and 0.20‰ and the  $\Delta\delta^{13}\text{C}$  ranges were 0.40‰ and 0.20‰ in samples 13 and 20 respectively. The fact that these ranges are only based on 2

measurements suggests that the real isotopic ranges between individual specimens are even larger. The interspecies range observed in Sample 22 can thus not be considered representative for all the samples. In conclusion the results demonstrated that the deviations between the predicted *Cibicoides decoratus* measurements based on *Anomalinoidea acutus* and the actual *Cibicoides decoratus* measurements are of the same magnitude as the deviations between *Cibicoides decoratus* measurements of an individual sample. The range of the  $\delta^{18}\text{O}$  measurements are in general relatively small ( $\leq 0.15\text{‰}$ ) except for Sample 13 where it reached  $0.25\text{‰}$ . The ranges of  $\delta^{13}\text{C}$  were sometimes larger (up to  $0.40\text{‰}$  in samples 10 and 13).

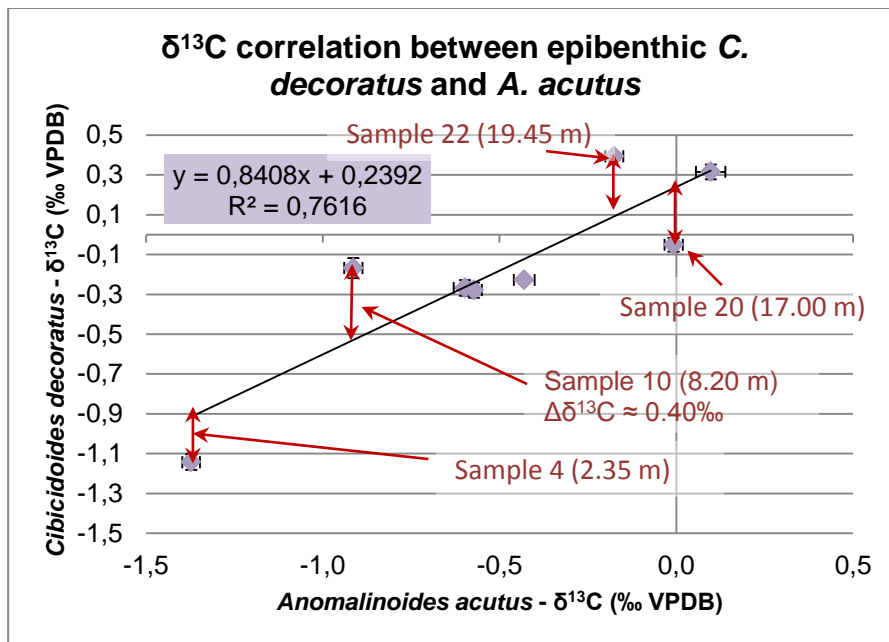


Figure 59. The correlation between *Anomalinoidea acutus* and *Cibicoides decoratus* for  $\delta^{13}\text{C}$ . Although the expected correlation clearly exists, errors between the predicted and the real *Cibicoides decoratus* signature are up to  $0.40\text{‰}$ . These errors cannot be considered insignificant.



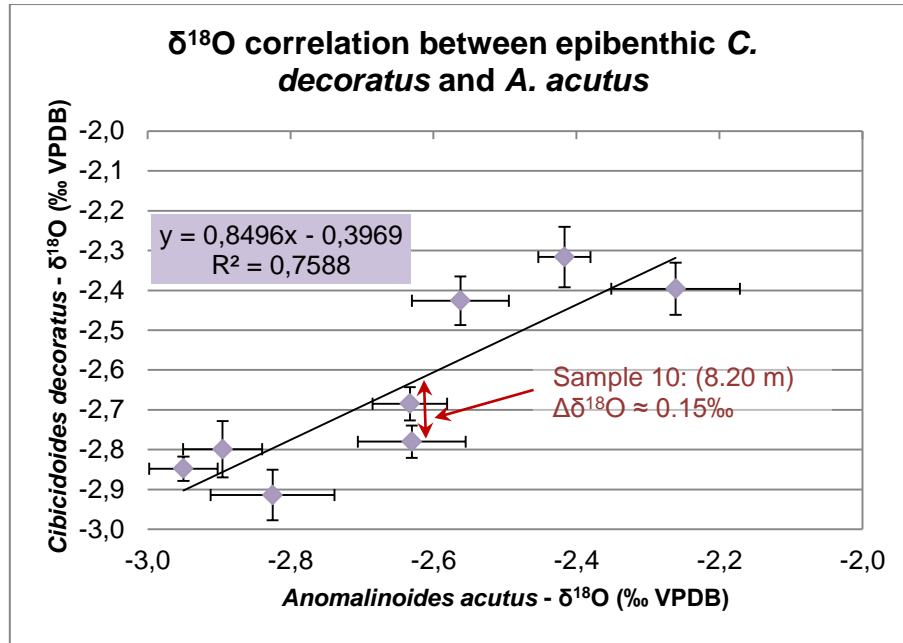


Figure 60. The correlation between *Anomalinoideus acutus* and *Cibicoides decoratus* for  $\delta^{18}\text{O}$ . Based on the  $R^2$  values, the strength of the correlation is comparable to the correlation for  $\delta^{13}\text{C}$ . However the errors between the predicted and the real *Cibicoides decoratus* signature are rather small (in the order of 0.15‰). These errors can be considered acceptable, certainly given the measurement imprecision.

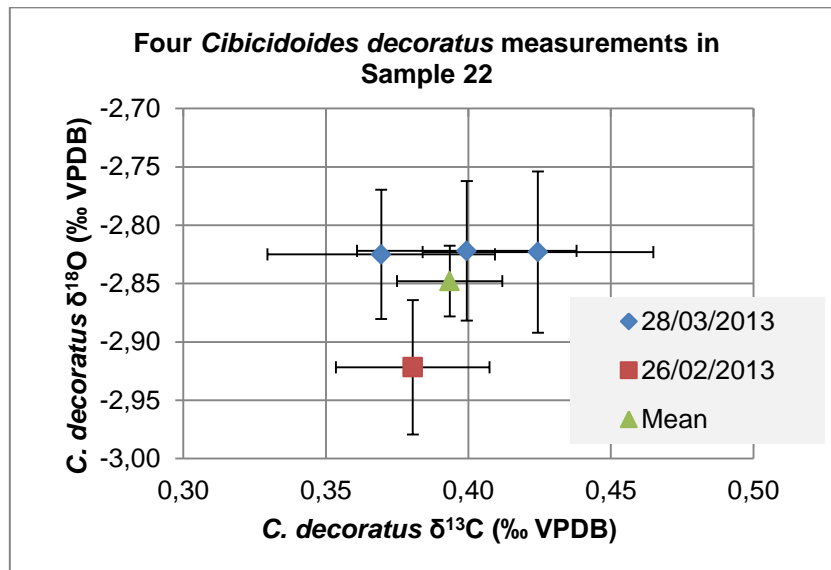


Figure 61. This plot contains multiple *Cibicoides decoratus* measurements within Sample 22. The data reveals a rather low isotopic variability in the sample (0.06‰ for  $\Delta\delta^{13}\text{C}$  and 0.10‰ for  $\Delta\delta^{18}\text{O}$ ). The measurements suggest that a range of 0.10‰ for  $\Delta\delta^{18}\text{O}$  could be the result of imperfect calibration of the measurements performed on different days. Nevertheless, the error bars ( $1\sigma$ ) of all measurements do overlap a common interval.

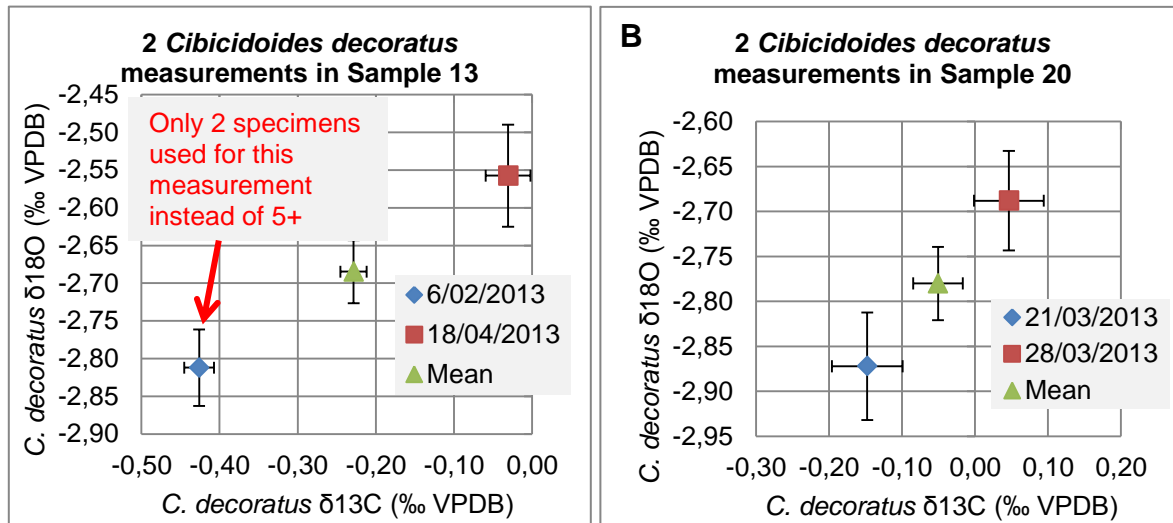


Figure 62. *Cibicoides decoratus* was remeasured in Sample 13 (A) and Sample 20 (B) due to suspicious values based on the correlation with *Anomalinoides acutus*. The results of the new *Cibicoides decoratus* measurements revealed in both samples that the isotopic ranges were indeed significantly higher than observed in Sample 22 (Figure 61). The ranges are 0.35‰ and 0.20‰ for  $\Delta\delta^{18}\text{O}$  and 0.40‰ and 0.20‰ for  $\Delta\delta^{13}\text{C}$  in samples 13 and 20 respectively.

The data revealed significant isotopic variability within a sample that cannot be explained by measurement precision. Several hypotheses can be proposed to explain the variability.

A first explanation would be related to preservation or contamination problems within these samples. In Sample 10 ( $\Delta\delta^{13}\text{C}\approx 0.40\text{‰}$ ) possible bulk contamination is reported for *Anomalinoides acutus*. However this cannot explain the range because significant contamination would have caused *Anomalinoides acutus* to deviate towards more positive  $\delta^{13}\text{C}$  values and not towards more negative values. In sample 20 ( $\Delta\delta^{13}\text{C}\approx 0.20\text{‰}$ ) the effect of recrystallization could not be 100% excluded for *Anomalinoides acutus* and could therefore possibly explain the  $\delta^{13}\text{C}$  deviation. Nevertheless this hypothesis can easily be rejected because no such deviation was observed for  $\delta^{18}\text{O}$  which is highly more vulnerable to recrystallization (Sexton *et al.*, 2006).

A second explanation would be that the variation is related to the natural isotopic variability within the population of both species (related to vital effects). Natural variation in isotopic values has been reported for modern species. For example the isotopic natural variability of epibenthic modern (thus sampled over a negligible time interval) *Cibicoides wuellerstorfi* has been studied by Franco-Franguas *et al.* (2011). Their measurements were performed on single specimens, resulting in a maximum range for  $\Delta\delta^{13}\text{C}$  and  $\Delta\delta^{18}\text{O}$  of about 0.40‰ (almost independent of size fraction). A similar natural variation could be assumed for *Cibicoides decoratus* and *Anomalinoides acutus*. However given the fact that our measurements represent averages of multiple specimens (mostly 5 to 6), the standard deviation by natural variability on our measurements can be calculated to be only 0.04‰ for  $\delta^{13}\text{C}$  based on the data of Franco-Franguas *et al.* (2011) (Appendix IV). Even if the natural variability of these species would have been twice the natural

variability of *Cibicidoides wuellerstorfi*, it would still be insufficient to explain the observed isotopic variability within several samples.

The third hypothesis is that the sampled time interval encompasses a significant variation in the seawater  $\delta^{13}\text{C}$  values. King *et al.* (submitted) reported bioturbation in most parts of the Aktulagay section which could significantly increase the sampled time interval. Furthermore reworking and the presence of nearby omission surfaces could also have had a significant impact on the sampled time interval of several samples. Samples 7, 8, 13, 15 and 19 were sampled only 3 to 5 cm below interburrowed omission surfaces (King *et al.*, submitted). Finally the variation in the relative abundance of species with time could also have amplified the isotopic measurement variability within a sample (Figure 63). Because several CIEs were identified in the Early Eocene by Cramer *et al.* (2003), strong isotopic variability within a sample could also be related to nearby CIEs.

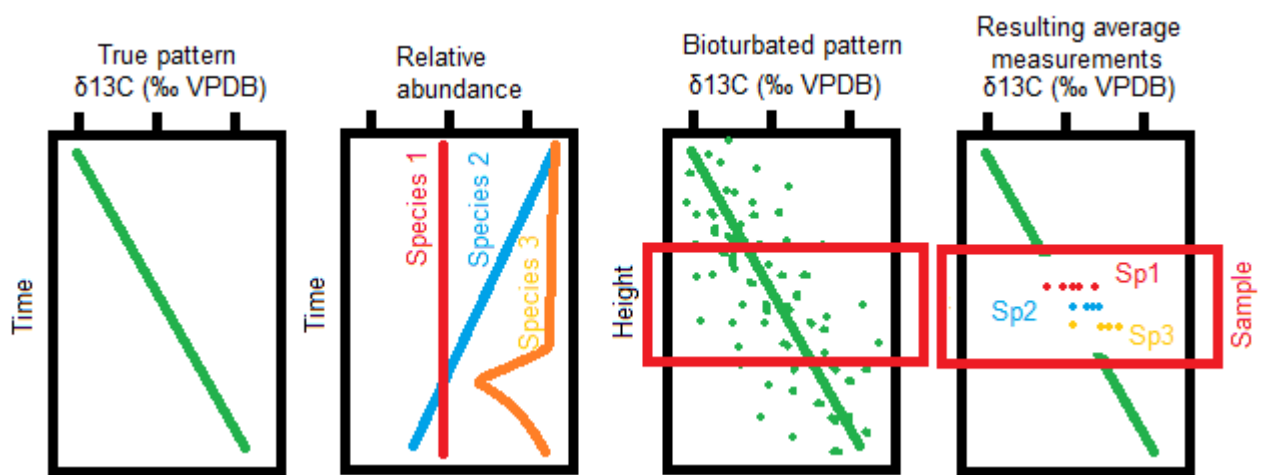


Figure 63. This figure illustrates how bioturbation & reworking, the size of sampled interval and the relative abundance of different species all can have influence on the resulting isotopic measurements.

### 8.3 Equilibrium calcite and correction factors

Epibenthic species have an isotopic offset between their isotopic signature and the isotopic signature of equilibrium calcite. This has been demonstrated by the modern species isotopic data of McCorkle *et al.* (1997), Rathburn *et al.* (1996) and Fontanier *et al.* (2008) (Figure 48, Figure 49 & Figure 50). Their datasets consistently demonstrated that the epibenthic species have 0.8 to 1.0‰ more depleted  $\delta^{18}\text{O}$  values than the  $\delta^{18}\text{O}$  signature of equilibrium calcite ( $\delta^{18}\text{O}_{\text{e.c.}}$ ). Furthermore the isotopic signature of deep endobenthic species often represented the  $\delta^{18}\text{O}$  signature of equilibrium calcite. The  $\delta^{13}\text{C}$  signature of epibenthic species precipitates either in equilibrium with seawater or with up to 1‰ offset towards more depleted or enriched values. The determination of  $\delta^{18}\text{O}_{\text{e.c.}}$  is essential for the seafloor paleotemperature estimates. The determination of  $\delta^{13}\text{C}_{\text{e.c.}}$  is less important but could be used for comparisons.

#### 8.3.1 *Cibicidoides decoratus*

Based on the difference between the  $\delta^{18}\text{O}$  signature of *Cibicidoides decoratus* and the  $\delta^{18}\text{O}$  signature of deep endobenthic species (Figure 45), the  $\delta^{18}\text{O}_{\text{e.c.}}$  can be estimated to be 0.3‰ to 0.6‰ higher than the  $\delta^{18}\text{O}$  signature of *Cibicidoides decoratus*. Zachos *et al.* (2001) and Cramer *et al.* (1999) corrected the  $\delta^{18}\text{O}$  signature of *Cibicidoides* species with 0.64‰. Katz *et al.* (2003) suggested that 0.28‰ is a more appropriate correction based on the  $\delta^{18}\text{O}$  values of *Oridorsalis spp.* In their study they assumed that *Oridorsalis spp.* precipitated in equilibrium with seawater. In this study 2 measurements of *Oridorsalis plummerae* are available in samples 13 and 17, suggesting an offset of 0.4‰ with *Cibicidoides decoratus*. In conclusion the proposed range of 0.3‰ to 0.6‰ is supported by the literature and a correction of 0.45‰ ( $\pm 0.15\%$ ) will be applied to the data (Eq. 1).

$$\delta^{18}\text{O}_{\text{e.c.}} = \delta^{18}\text{O}_{(\text{Cibicidoides decoratus})} + 0.450\text{‰} (\pm 0.150\text{‰})$$

Eq. 1. The correction of  $\delta^{18}\text{O}_{(\text{Cibicidoides decoratus})}$  to  $\delta^{18}\text{O}_{\text{e.c.}}$  (‰ VPDB).

Based on the data of Rathburn *et al.* (1996), McCorkle *et al.* (1997) and Fontanier *et al.* (2008) (Figure 48, Figure 49 & Figure 50), the  $\delta^{13}\text{C}$  of epibenthic species precipitates either in equilibrium with seawater or with a shift of up to 1‰ towards more positive or a negative values. Based on the relative position of *Cibicidoides decoratus* in samples 13, 17 and 22,  $\delta^{13}\text{C}_{(\text{C. decoratus})}$  can be estimated to be 0.0‰ to 0.5‰ more depleted than  $\delta^{13}\text{C}_{\text{e.c.}}$  (Eq. 2). Zachos *et al.* (2001) assumed equilibrium calcite precipitation for  $\delta^{13}\text{C}$  of *Cibicidoides spp.* Unlike  $\delta^{18}\text{O}_{\text{e.c.}}$ , the absolute value of  $\delta^{13}\text{C}_{\text{e.c.}}$  is not important for this study, therefore epibenthic species will be corrected to *Cibicidoides decoratus* and not to equilibrium calcite.

$$\delta^{13}\text{C}_{\text{e.c.}} = \delta^{13}\text{C}_{(\text{Cibicidoides decoratus})} + 0.250\text{‰} (\pm 0.250\text{‰})$$

Eq. 2. The correction of  $\delta^{13}\text{C}_{(\text{Cibicidoides decoratus})}$  to  $\delta^{13}\text{C}_{\text{e.c.}}$  (‰ VPDB).

#### 8.3.2 *Anomalinoides acutus*

As demonstrated in Figure 64, our data suggests that the strongest correlation between *Anomalinoides acutus* and *Cibicidoides decoratus* for  $\delta^{13}\text{C}$  is given by Eq. 3:

$$\delta^{13}\text{C}_{(Cibicidoides\ decoratus)} (\text{‰}) = 0.841 * \delta^{13}\text{C}_{(Anomalinoides\ acutus)} (\text{‰}) + 0,239\text{‰}$$

Eq. 3. Strongest correlation between  $\delta^{13}\text{C}_{(Cibicidoides\ decoratus)}$  and  $\delta^{13}\text{C}_{(Anomalinoides\ acutus)}$  (‰ VPDB).

However if this equation would be applied to predict *Cibicidoides decoratus*, it would affect the  $\Delta\delta^{13}\text{C}$  between measurements of *Anomalinoides acutus*. It is questionable whether this can be justified. The slope of the equation is affected by the lack of data and outliers. Furthermore the statistical results of Katz *et al.* (2003) demonstrated that most correlations between epibenthic species can be represented by linear equations with a slope of one. In Appendix V it is demonstrated that the difference between the predicted  $\delta^{13}\text{C}_{(C.\ decoratus)}$  and the measured  $\delta^{13}\text{C}_{(C.\ decoratus)}$  based on the above equation result in a standard deviation of 0.230. While a simplified equation with slope 1 results in a standard deviation of 0.242. Therefore the simplified equation will be applied to predict  $\delta^{13}\text{C}_{(C.\ decoratus)}$  (Figure 64A & Eq. 4).

$$\delta^{13}\text{C}_{(C.\ decoratus)} = \delta^{13}\text{C}_{(A.\ acutus)} + 0,318\text{‰}$$

Eq. 4. The prediction of  $\delta^{13}\text{C}_{(Cibicidoides\ decoratus)}$  based on  $\delta^{13}\text{C}_{(Anomalinoides\ acutus)}$  (‰ VPDB).

The same reasoning can be applied for  $\delta^{18}\text{O}$  (Appendix VI). The standard deviation based on the predicted values and the measured values is 0.114 for the strongest correlation (Eq. 5), while the simplified equation with slope 1 has a standard deviation of 0.119 (Figure 64B, Eq. 6). Based on Eq. 1 and Eq. 6, the equation to predict  $\delta^{18}\text{O}_{\text{e.c.}}$  based on  $\delta^{18}\text{O}_{(Anomalinoides\ acutus)}$  can be derived (Eq. 7).

$$\delta^{18}\text{O}_{(C.\ decoratus)} = 0,850 * \delta^{18}\text{O}_{(A.\ acutus)} + 0,397\text{‰}$$

Eq. 5. Strongest correlation between  $\delta^{18}\text{O}_{(Cibicidoides\ decoratus)}$  and  $\delta^{18}\text{O}_{(Anomalinoides\ acutus)}$  (‰ VPDB).

$$\delta^{18}\text{O}_{(C.\ decoratus)} = \delta^{18}\text{O}_{(A.\ acutus)} + 0,001\text{‰}$$

Eq. 6. The prediction of  $\delta^{18}\text{O}_{(Cibicidoides\ decoratus)}$  based on  $\delta^{18}\text{O}_{(Anomalinoides\ acutus)}$  (‰ VPDB).

$$\delta^{18}\text{O}_{\text{e.c.}} = \delta^{18}\text{O}_{(A.\ acutus)} + 0.451\text{‰} (\pm 0.150\text{‰})$$

Eq. 7. The prediction of  $\delta^{18}\text{O}_{\text{equilibrium calcite}}$  based on  $\delta^{18}\text{O}_{(Anomalinoides\ acutus)}$  (‰ VPDB).

### 8.3.3 *Anomalinoides zitteli*

Five measurements of *Anomalinoides zitteli* are available. Since only 3 measurements can directly be correlated with *Cibicidoides decoratus*, the correlation will be calculated based on *Anomalinoides acutus* were all 5 measurements can be correlated. The calculations can be found in the Appendices VII, VIII, IX & X. For  $\delta^{13}\text{C}$  the correlation is very strong with  $R^2 \approx 0.96$  between *Anomalinoides acutus* and *Anomalinoides zitteli* (Figure 65A). The simplified equation (slope = 1) for correcting *Anomalinoides zitteli* to *Anomalinoides acutus* is given by Eq. 8. This equation can be applied to estimate the correction factor

between *Anomalinoides zitteli* and *Cibicidoides decoratus* (Eq. 9). The equation does not contradict with the *Cibicidoides decoratus* data (Figure 65B).

$$\delta^{13}\text{C}_{(A. acutus)} = \delta^{13}\text{C}_{(A. zitteli)} - 0.360\text{‰}$$

Eq. 8. The prediction of  $\delta^{13}\text{C}_{(Anomalinoides acutus)}$  based on  $\delta^{18}\text{O}_{(Anomalinoides zitteli)}$  (‰ VPDB).

$$\delta^{13}\text{C}_{(C. decoratus)} = \delta^{13}\text{C}_{(A. zitteli)} - 0.042\text{‰}$$

Eq. 9. The prediction of  $\delta^{13}\text{C}_{(Cibicidoides decoratus)}$  based on  $\delta^{18}\text{O}_{(Anomalinoides zitteli)}$  (‰ VPDB).

The  $\delta^{18}\text{O}$  correlation between *Anomalinoides acutus* and *Anomalinoides zitteli* is rather poor ( $R^2 \approx 0.41$ ). It does not allow an accurate determination of the correction factor (Figure 66A & B) and the additional uncertainty on the  $\delta^{18}\text{O}$  correction factor can be roughly estimated to be 0.20‰. The measurement of Sample 4 might be responsible for the weak correlation. Nevertheless insufficient data is available to accurately determine this correction factor (Eq. 10 & Eq. 11).

$$\delta^{18}\text{O}_{(C. decoratus)} = \delta^{18}\text{O}_{(A. zitteli)} - 0,134\text{‰} (\pm 0.20\text{‰})$$

Eq. 10. The prediction of  $\delta^{18}\text{O}_{(Cibicidoides decoratus)}$  based on  $\delta^{18}\text{O}_{(Anomalinoides zitteli)}$  (‰ VPDB).

$$\delta^{18}\text{O}_{e.c.} = \delta^{18}\text{O}_{(A. zitteli)} + 0.316\text{‰} (\pm 0.35\text{‰})$$

Eq. 11. The prediction of  $\delta^{18}\text{O}_{e.c.}$  based on  $\delta^{18}\text{O}_{(Anomalinoides zitteli)}$  (‰ VPDB).

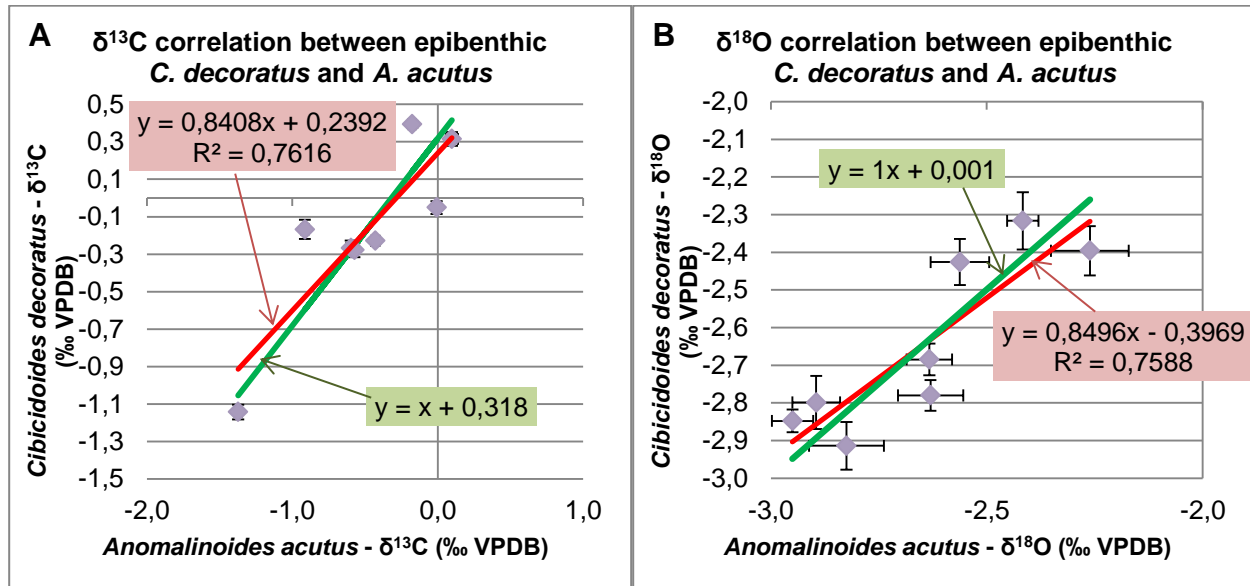


Figure 64. The  $\delta^{13}\text{C}$  correlation and the  $\delta^{18}\text{O}$  correlation between epibenthic *C. decoratus* and *A. acutus* are shown in A and B respectively. The red line represents the best fit equation while the green line represents the best fit in the assumption of a slope = 1. The main reason for the simplification is to respect the original  $\Delta\delta^{13}\text{C}$  between the data.

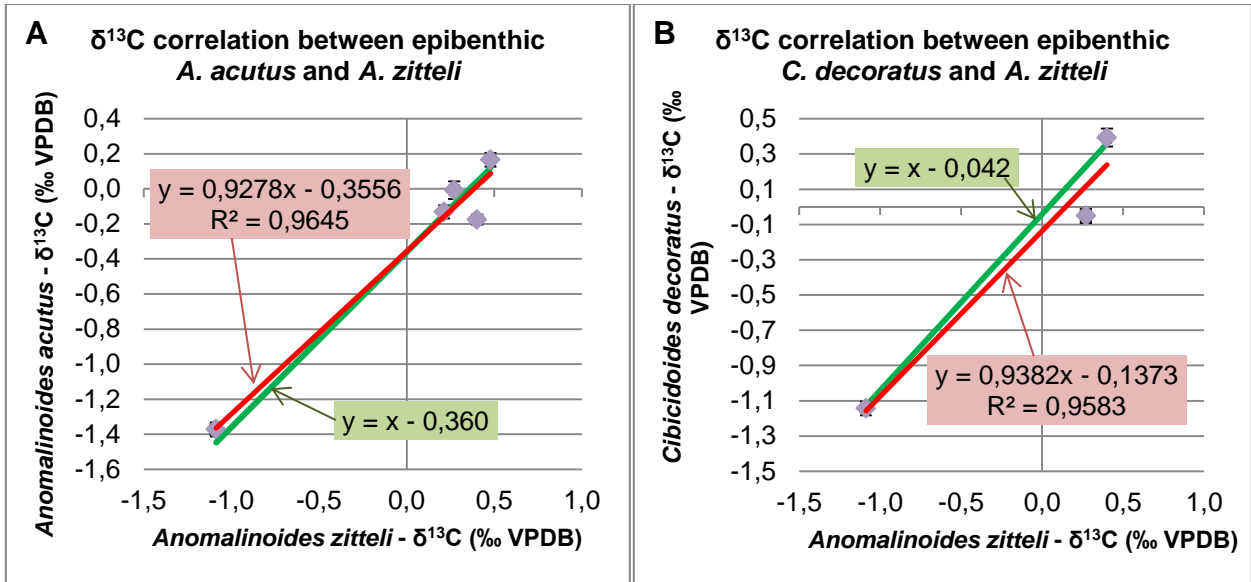


Figure 65. The  $\delta^{13}\text{C}$  correlation between epibenthic *A. acutus* and *A. zitteli* (A) and between *C. decoratus* and *A. zitteli* (B). The red line represents the best fit equation while the green line represents the best fit in the assumption of a slope = 1. The main reason for the simplification is to respect the original  $\Delta\delta^{13}\text{C}$  between the data.

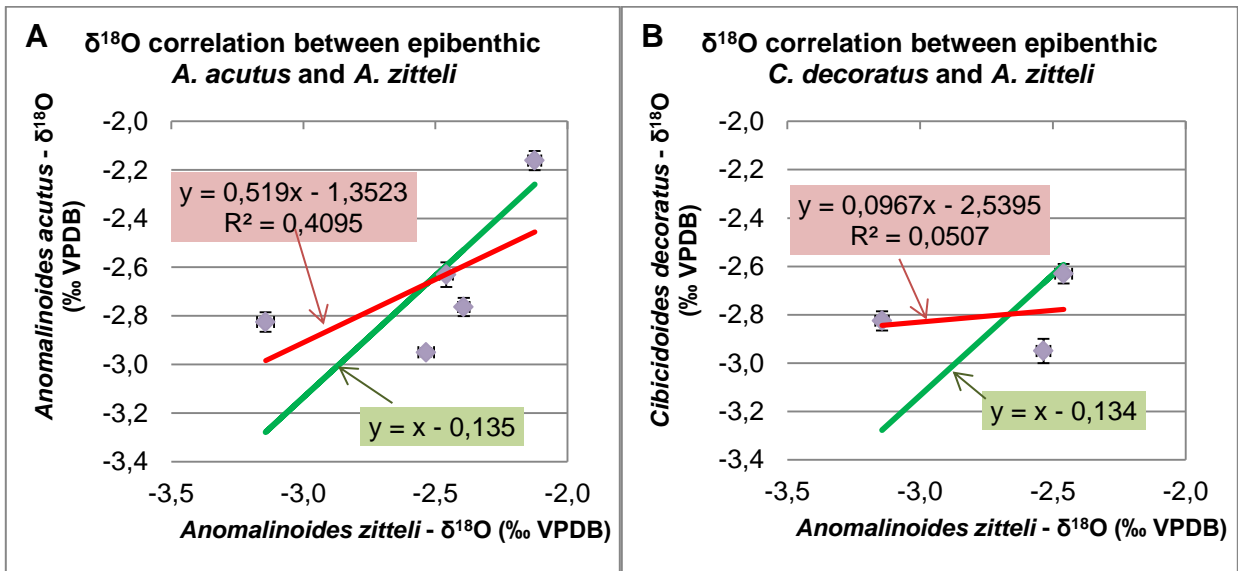


Figure 66. The  $\delta^{18}\text{O}$  correlation between epibenthic *A. acutus* and *A. zitteli* (A) and between *C. decoratus* and *A. zitteli* (B). The red line represents the best fit equation while the green line represents the best fit in the assumption of a slope = 1. The prediction of the correction factor is inaccurate due the lack of data and possible outliers.

## 8.4 The seafloor temperature predictions

The  $\delta^{18}\text{O}$  signature of benthic foraminifers can be used to predict seafloor temperatures. To eliminate vital effects and to predict the signature of equilibrium calcite, several corrections were proposed;

$$\delta^{18}\text{O}_{(\text{Cibicoides decoratus})} + 0.450\text{‰} = \delta^{18}\text{O}_{\text{e.c.}} (\pm 0.150\text{‰}) \quad (\text{Eq. 1})$$

$$\delta^{18}\text{O}_{(\text{Anomalinoidea acutus})} + 0.451\text{‰} = \delta^{18}\text{O}_{\text{e.c.}} (\pm 0.150\text{‰}) \quad (\text{Eq. 7})$$

$$\delta^{18}\text{O}_{(\text{Anomalinoidea zitteli})} + 0.316\text{‰} = \delta^{18}\text{O}_{\text{e.c.}} (\pm 0.350\text{‰}) \quad (\text{Eq. 11})$$

The errors are rough estimates of the true range of  $\delta^{18}\text{O}_{\text{e.c.}}$ , they cannot be calculated based on the strength of the correlations between the species because the isotopic variation within a sample is considered partially a result of the  $\delta^{18}\text{O}$  seawater variation within the sampled time interval (8.2). The resulting  $\delta^{18}\text{O}_{\text{e.c.}}$  predictions are plotted in Figure 67A.

Another uncertainty is related to salinity. This parameter is directly related to the isotopic composition of seawater. Most authors assume one  $\delta^{18}\text{O}_{\text{seawater}}$  value for the entire thermocline/deep water zone based on estimates of the global ice volume (e.g. Zachos *et al.*, 1994 & Pearson *et al.*, 2007). Fortunately during the Early Eocene the global ice volume is considered either non-existing or negligible (Wise *et al.*, 1991, Zachos *et al.*, 1994, Pearson *et al.*, 2007 & Roberts *et al.* 2011). This assumption is based on the absence of ice rafting debris records (Wise *et al.*, 1991 & Zachos *et al.*, 1994) and on proxies that indicate high temperatures at higher latitudes (e.g. Keating-Bitonti *et al.*, 2011). For the Aktulagay section however the problem might be more complex due to the limited depth (175 to 200 m according to Deprez *et al.*, submitted) and the proximity of the continent. Nevertheless the thermocline planktic  $\delta^{18}\text{O}$  and  $\delta^{13}\text{C}$  values are strictly separated from the benthic  $\delta^{18}\text{O}$  and  $\delta^{13}\text{C}$  values (Figure 26), indicating a distinct water column stratification in temperature and/or salinity. If this was not the case it could have indicated a shallower water depth and/or water mixing. A rather constant salinity will be assumed that does not deviate much from the global  $\delta^{18}\text{O}$  seawater signature. Different mean ice free world seawater  $\delta^{18}\text{O}$  signatures have been proposed by several authors for the Early Eocene (Table 7). Based on these values a prediction of  $-1.00\text{‰}$  ( $\pm 0.25\text{‰}$ ) will be applied in this study (Eq. 12).

Authors	Estimated $\delta^{18}\text{O}_{\text{sw-mean}}$ (VSMOW)
Pearson <i>et al.</i> , 2007	-0.75‰
Roberts <i>et al.</i> , 2011	-0.81‰
Zachos <i>et al.</i> , 1994	-0.96‰
Tindall <i>et al.</i> , 2010	-1.00‰
Cramer <i>et al.</i> , 1999	-1.20‰

Table 7. Overview of different  $\delta^{18}\text{O}_{\text{sw-mean}}$  estimates for the Early Eocene.

$$\delta^{18}\text{O}_{\text{sw-mean}} = -1.00\text{‰} \pm 0.25\text{‰}$$

Eq. 12. The  $\delta^{18}\text{O}_{\text{sw-mean}}$  estimate applied in this study based on Table 7 (‰ VSMOW).



Finally with  $\delta^{18}\text{O}_{\text{e.c.}}$  and  $\delta^{18}\text{O}_{\text{sw-mean}}$  estimated, the paleotemperature can be calculated. According to Grossman (2012) there are several equations available to make this calculation and they might give significantly different results. In this study the equation of Erez and Luz (1983) (Eq. 13) is applied because of three reasons. First of all the temperature equation of Erez and Luz (1983) is calculated based of foraminifer calcite instead of synthetic calcite. Secondly the equation of Erez and Luz (1983) was calculated for temperatures ranging from 14 °C to 30 °C, which is approximately the range of temperatures that are expected in Aktulagay. Finally the equation of Erez and Luz (1983) is also applied in several other paleoclimatic studies (e.g. Zachos *et al.*, 1994 & Pearson *et al.*, 2007). The resulting temperature predictions are plotted in Figure 67B.

$$T (\text{°C}) = 17.0 - 4.52 (\delta^{18}\text{O}_{\text{calcite}} - \delta^{18}\text{O}_{\text{sw}} + 0.22) + 0.03 (\delta^{18}\text{O}_{\text{calcite}} - \delta^{18}\text{O}_{\text{sw}} + 0.22)^2$$

Eq. 13. The temperature equation from Erez and Luz (1983). The  $\delta^{18}\text{O}_{\text{calcite}}$  is expressed in VPDB (‰) and  $\delta^{18}\text{O}_{\text{seawater}}$  is expressed in VSMOW (‰). Note that the equation has been edited by Grossman (2012) to correct PDB to VPDB.

The resulting temperature record demonstrates strong temperature variation with time. The sea floor temperatures vary between 19 °C and 24 °C ( $\pm 1.8$  °C). Three colder intervals (0 to 1 m, 5 to 10 m and 12 to 15 m) and three warmer intervals (1 to 5 m, 10 to 12 m and 15 to 23 m) can be identified in the section.

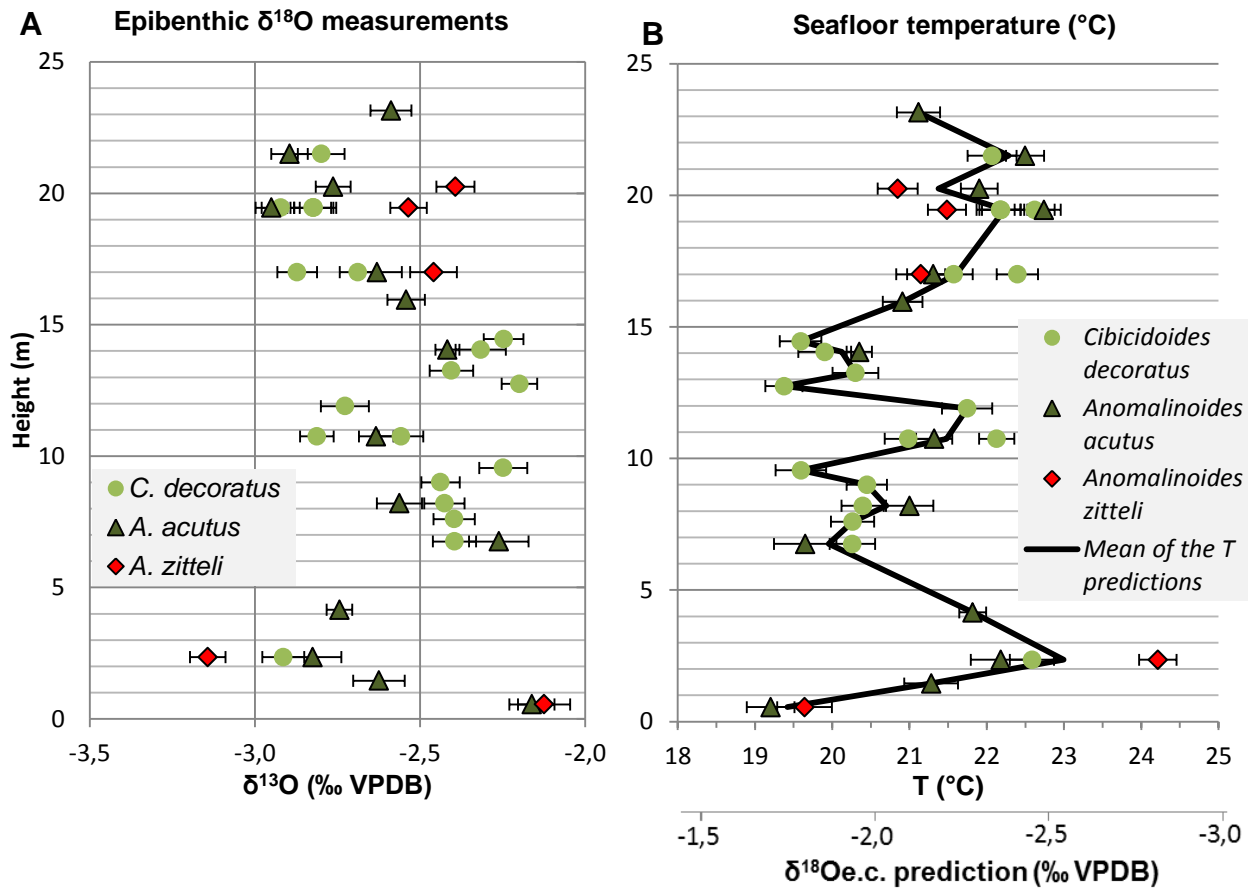


Figure 67. The plot in (A) demonstrates the original  $\delta^{18}\text{O}$  values. The plot in (B) plots the predicted equilibrium calcite isotopic values and the resulting seafloor paleotemperature predictions. The error bars of 1 standard deviation are related to the mass spectrometer imprecision. The inaccuracy of the equilibrium calcite prediction and  $\delta^{18}\text{O}_{\text{seawater}}$  predictions cause **an additional uncertainty of 1.8  $^{\circ}\text{C}$  on the absolute temperature values** (Not the relative values). Small errors due to preservation might exist in the lower 5 m of the section. Finally  $\delta^{18}\text{O}_{\text{e.c.}}$  predictions based on *Anomalinoidea zitteli* are considered less accurate and could deviate up to 0.2‰.

## 8.5 The epibenthic $\delta^{13}\text{C}$ record

As stated before, the absolute values of  $\delta^{13}\text{C}_{\text{DIC}}$  are not important for this study. If the values are required they can be estimated by Eq. 2. In this study the epibenthic  $\delta^{13}\text{C}$  record will be based on *Cibicoides decoratus*. The  $\delta^{13}\text{C}$  of *Anomalinoides acutus* and *Anomalinoides zitteli* can be corrected based on Eq. 4 and Eq. 9. The resulting predictions are plotted in Figure 68.

The resulting  $\delta^{13}\text{C}$  record reveals a strong negative isotopic gradient in the lower 3 m, from 0.5‰ at 0.55 m to -1.1‰ at 2.35 m. From 3 m onwards the  $\delta^{13}\text{C}_{\text{DIC}}$  gradually increases to a final value of 0.9‰ at 23.15 m.

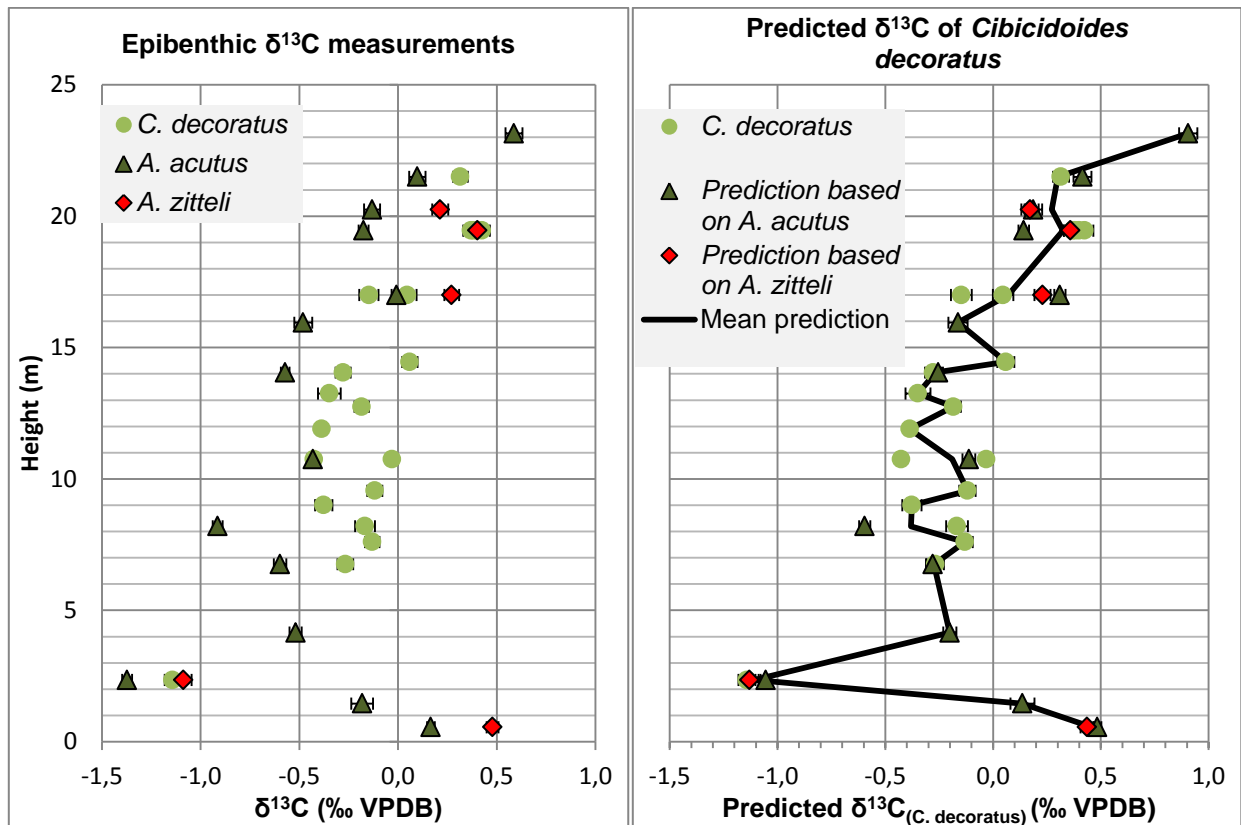


Figure 68. The plots demonstrate the conversion from the original  $\delta^{13}\text{C}_{A. acutus}$  and the  $\delta^{13}\text{C}_{A. zitteli}$  values (A) to the predicted  $\delta^{13}\text{C}_{(C. decoratus)}$  values (B) based on Eq. 4 and Eq. 9.

## 8.6 Discussion

### 8.6.1 Identification of CIEs and hyperthermals

The resulting  $\delta^{13}\text{C}$  and  $\delta^{18}\text{O}$  records reveal strong isotopic variation with time. The co-occurrence of depleted  $\delta^{13}\text{C}$  and  $\delta^{18}\text{O}$  values might reveal the presence of hyperthermals. To identify the hyperthermals the results are compared with the bulk  $\delta^{13}\text{C}$  record of Cramer *et al.* (2003) (Figure 69). Their record encompasses bulk isotope data from multiple Deep Sea Drilling Project Sites (1051 and 690) and Ocean Drilling program sites (550 and 577) (Figure 69). The records were correlated based on the nannofossil zones. Comparison of the  $\delta^{13}\text{C}$  records indicates that several CIEs might influence the data in the Aktulagay record below the hiatus at the boundary of subunits B1 and B2. The strongest indication for a nearby CIE is the  $\delta^{13}\text{C}$  measurement at 2.35 m. Three epibenthic measurements confirmed the anomalously low  $\delta^{13}\text{C}$  values. The  $\Delta\delta^{13}\text{C}_{\text{DIC}}$  anomaly is approximately 1.0‰ to 1.6‰ relative to the  $\delta^{13}\text{C}$  data from the samples at 0.15 m and 4.15 m. According to the  $\delta^{18}\text{O}$  record, the sample is also associated with a temperature rise of up to 4 °C and thus demonstrates the hyperthermal character of the CIE. Although the biostratigraphic position of the CIE compared with the record of Cramer *et al.* (2003) would suggest the H2-event is responsible for the anomaly, there are several arguments that the  $\delta^{13}\text{C}$  anomaly at 2.35 m could also be a consequence of the H1-event/ETM2. The first argument is the magnitude of the CIE and the temperature rise. The data of e.g. Cramer *et al.* (2003) and Galeotti *et al.* (2010) suggest that the H2-event would be smaller, furthermore the low sampling interval in Aktulagay could cause the total  $\Delta\delta^{13}\text{C}_{\text{DIC}}$  to be underestimated because the exact position of the hyperthermal is uncertain. A second argument is the imperfection of the biostratigraphy combined with possible variation in sedimentation rate with time. King *et al.* (submitted) identified a large amount of interburrowed lithological contacts (especially between 5 m and 7 m, Figure 69) that they interpreted as omission surfaces. If their interpretation is correct these omission surfaces could significantly alter the relative position of the CIEs within the NP11 time interval. Furthermore Galeotti *et al.* (2010) identified ETM2 at a relatively later position within NP11 than Cramer *et al.* (2003) did. Further CIEs cannot be identified based on our limited dataset but several indications exist that they are be present. First of all the depleted  $\delta^{13}\text{C}$  value (-0.6‰) at 8.20 m based on *Anomalinooides acutus*, might be related to the influence of the J-event. Nevertheless the *Cibicidoides decoratus* measurement within the same sample did not support the higher  $\delta^{13}\text{C}$  values. Both measurements could be the result of rapid changing  $\delta^{13}\text{C}$  within the sampled time interval as discussed in 8.2, but it could also be the result of statistical coincidence and higher isotopic variability within the sample. Secondly the influence of the hyperthermal ETM3 (K-event) is possibly responsible for the more depleted  $\delta^{13}\text{C}$  and  $\delta^{18}\text{O}$  between 10.75 and 11.90 m. These indications might help future research if the Aktulagay section would be resampled.

### 8.6.2 The global $\delta^{18}\text{O}$ trend

The samples in between the samples that are possibly influenced by hyperthermals reveal maximum  $\delta^{18}\text{O}$  values of approximately -1.8‰ for the lower part of the section (0 to 15 m), while above 15 m the highest

$\delta^{18}\text{O}$  values are approximately  $-2.2\text{‰}$  (Figure 67). This  $\Delta\delta^{18}\text{O}$  shift between the lower and the higher part of the section suggests a temperature rise of approximately  $1.9\text{ °C}$  in Aktulagay (from  $19.6\text{ °C}$  to  $21.5\text{ °C}$ ). Whether this is a local trend or a global trend can be revealed by comparing with the long term record of Cramer *et al.* (2009). The data of Cramer *et al.* (2009) in Vandenberghe *et al.* (2012) demonstrates the isotopic signature of the deep ocean during the entire Ypresian. In Figure 70 the Aktulagay record is correlated with Cramer *et al.* (2009) by the nannofossil biostratigraphic zones. Their record reveals a gradual global  $\delta^{18}\text{O}$  trend during NP11 and NP12 towards more depleted values. The  $\Delta\delta^{18}\text{O}$  shift is approximately  $0.3\text{‰}$  from  $-0.5\text{‰}$  to  $-0.8\text{‰}$ . If converted to temperatures, this would correspond to a  $1.3\text{ °C}$  temperature rise from  $13.8\text{ °C}$  to  $15.1\text{ °C}$ . These temperatures are lower than the temperatures in Aktulagay because the data of Cramer *et al.* (2009) represents deep ocean temperatures and not outer shelf temperatures. However the temperature trend is similar in both records and indicates that the gradual temperature rise in Aktulagay is rather not a local phenomenon but could reflect the global warming trend towards the EECO (Early Eocene Climatic Optimum, Figure 70).

### 8.6.3 The global $\delta^{13}\text{C}$ trend

Our data in Figure 68 clearly suggests a gradual rising  $\delta^{13}\text{C}$  trend from the measurement at 4.15 m ( $-0.2\text{‰}$ ) to the measurement at 23.15 m ( $0.9\text{‰}$ ). Whether this is a local trend or a global trend can be investigated based on a comparison with the  $\delta^{13}\text{C}$  record based on data of the Ypresian oceans (Cramer *et al.*, 2009) in Figure 70. The  $\delta^{13}\text{C}$  patterns in both studies are remarkably similar. The  $\delta^{13}\text{C}$  values of Cramer *et al.* (2009) demonstrate a strong decrease during NP10 till the occurrence of ETM2 in NP11. Our few isotopic measurements support this trend since the values at 0.55 m ( $0.4\text{‰}$ ) are the 2<sup>nd</sup> highest  $\delta^{13}\text{C}$  values measured over the section. Given the uncertainty of the position of the NP10-NP11 boundary in Vandenberghe *et al.* (2012), the biostratigraphy of King *et al.* (submitted) in combination with our isotopic measurements suggests that the boundary of NP10-NP11 should be positioned slightly lower in their record. From ETM2 to ETM3 the maximal  $\delta^{13}\text{C}$  values between the CIEs remain rather constant in both records ( $\delta^{13}\text{C}$  of  $-0.3\text{‰}$  to  $0.0\text{‰}$  in Aktulagay compared to  $0.2$  to  $0.4\text{‰}$  in the oceans). The difference in absolute  $\delta^{13}\text{C}$  between both records could be a real difference in  $\delta^{13}\text{C}_{\text{DIC}}$ . However this is highly uncertain given that a difference of  $\leq 1\text{‰}$  can perfectly be related to vital effects between different *Cibicidoides* species as demonstrated by the modern *Cibicidoides* data of McCorkle *et al.* (1997) (Figure 48). Furthermore the prediction of  $\delta^{13}\text{C}_{\text{e.c.}}$  in this study predicts a deviation of  $0.25\text{‰}$  towards more negative values for *Cibicidoides decoratus* (Eq. 2). After ETM3 the  $\delta^{13}\text{C}$  values gradually rise till middle NP13 in both records ( $\Delta\delta^{13}\text{C} = 0.5\text{‰}$  to  $1.0\text{‰}$ ). The observation that NP12 is significantly longer in the record of Cramer *et al.* (2009) than in the Aktulagay record could reflect the importance of the hiatus. However a comparison with the absolute and relative dates of Luterbacher *et al.* (2004) demonstrated the huge uncertainty on the absolute and relative dates reflected by the NP-zones, therefore a conclusion concerning sedimentation rates of the lithologic units is strongly discouraged (2.5.3). In conclusion the  $\delta^{13}\text{C}$  trend in Aktulagay is considered a reflection of the global  $\delta^{13}\text{C}$  trend in the oceans.

#### 8.6.4 Comparison with the isotopic data from the Kheu River Section

The Kheu River Section is located in southern Russia, approximately 200 km east of the Black Sea. The section has been studied by Oberhänsli & Beniamovskii (2000) and partially encompasses nanofossil zones NP12 and NP13. Their study provides an epibenthic foraminifer isotopic record. They focused their measurements on the sapropelic layers within the Kheu section but also provided isotopic data from the intervals between the sapropels. In general these sapropels have been observed in a large area between the Black Sea and Aktulagay. It has been suggested that they can be correlated (e.g. King *et al.*, submitted). Based on the position of the sapropels and the identified NP12-NP13 boundary, an attempt was made to correlate the Kheu River section with the Aktulagay section (Figure 71). The isotopic measurements of Oberhänsli & Beniamovskii (2000) demonstrate that the sapropels are characterized by depleted  $\delta^{13}\text{C}$  values and enriched  $\delta^{18}\text{O}$  values. The positive  $\Delta\delta^{18}\text{O}$  shifts are related to an increased salinity and/or a decreased temperature. The significant  $\Delta\delta^{13}\text{C}$  and  $\Delta\delta^{18}\text{O}$  shifts near and within sapropels in the record of Oberhänsli & Beniamovskii (2000) could explain that the large variation in  $\delta^{13}\text{C}$  values at 17.00 m in the Aktulagay section because of the nearby sapropel (16.80 m) and brown fissile layer (17.13 m). Since both layers were described as highly bioturbated by King *et al.* (submitted).

The absolute  $\delta^{13}\text{C}$  values from the intervals between the sapropels are approximately 0.0‰ to 0.4‰ in both the Kheu River and the Aktulagay section. This difference is insignificant as would be expected in the same sea. The absolute  $\delta^{18}\text{O}$  values of both sections however do strongly differ. The  $\delta^{18}\text{O}$  values in Aktulagay are approximately -2.2‰, while the  $\delta^{18}\text{O}$  values in the Kheu River are approximately -3.0‰. It is unlikely that a 0.8‰ difference can be solely explained because of vital effects of the epibenthic foraminifers. If the isotopic difference only represents a temperature difference, the seafloor temperature of the Kheu River section would be 3.6 °C higher than the seafloor temperature of the Aktulagay Section. This is certainly unexpected since the position of the Kheu River section on the map of Steurbaut (2011) suggests a more central (deeper?) position in the Peri-Tethys (Figure 71). Three explanations are possible for the  $\delta^{18}\text{O}$  difference. The first explanation would be that the Kheu River section is at much shallower depth than expected, although this is the least plausible explanation. The second explanation suggests that the lower  $\delta^{18}\text{O}$  values in Aktulagay reflect colder, more saline waters at the seafloor in Aktulagay. This could be the result of the nearby Turgai Strait that is connected to the West Siberian Sea. The third explanation would be that the foraminifers of Oberhänsli & Beniamovskii (2000) have been diagenetically altered. It is therefore most unfortunate that Oberhänsli & Beniamovskii (2000) did not provide evidence about the preservation of their foraminifers.

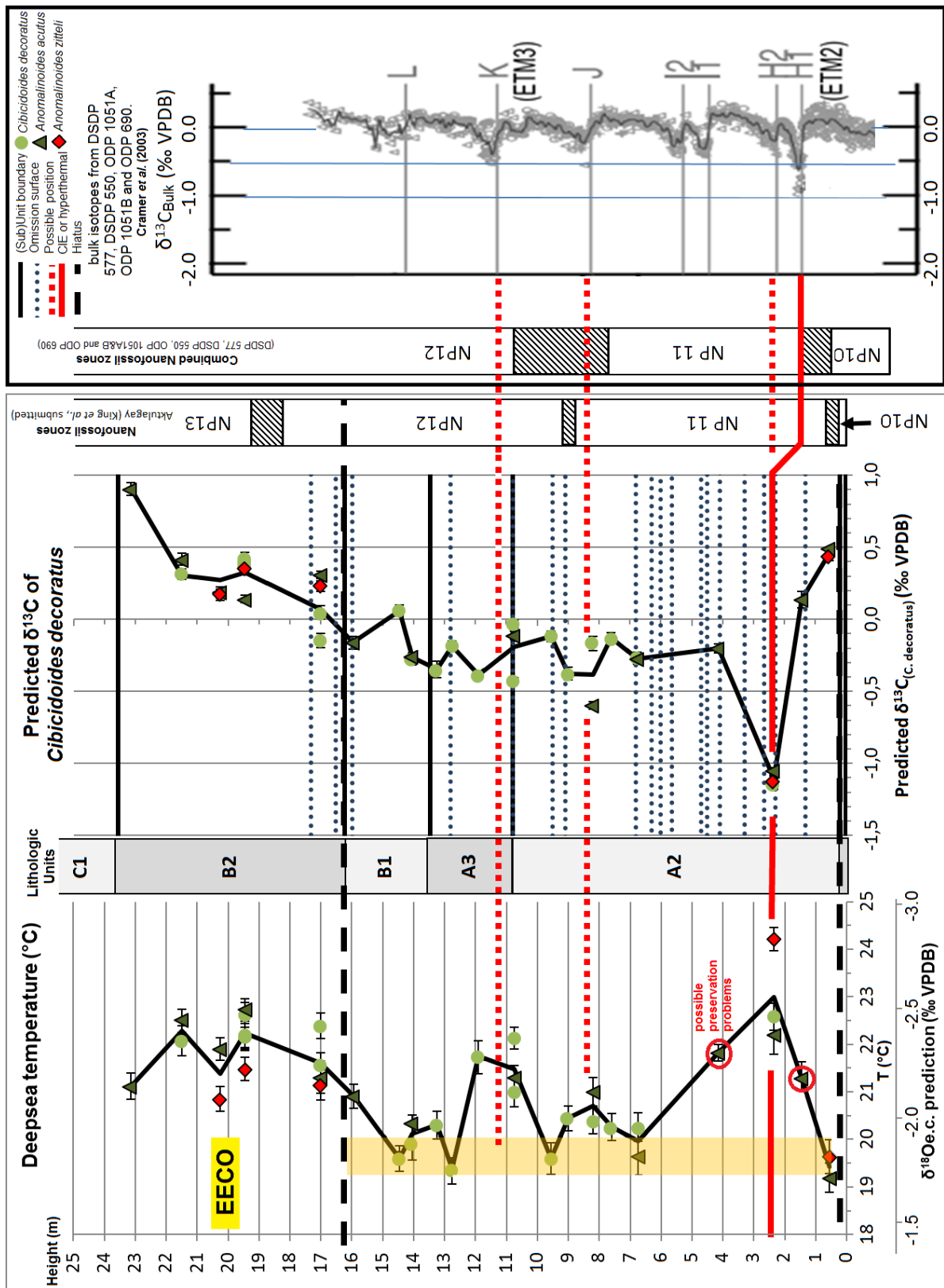


Figure 69. Comparison of the isotopic record with Cramer *et al.* (2003). The comparison demonstrates that the influence of certain CIEs on our data cannot be excluded.

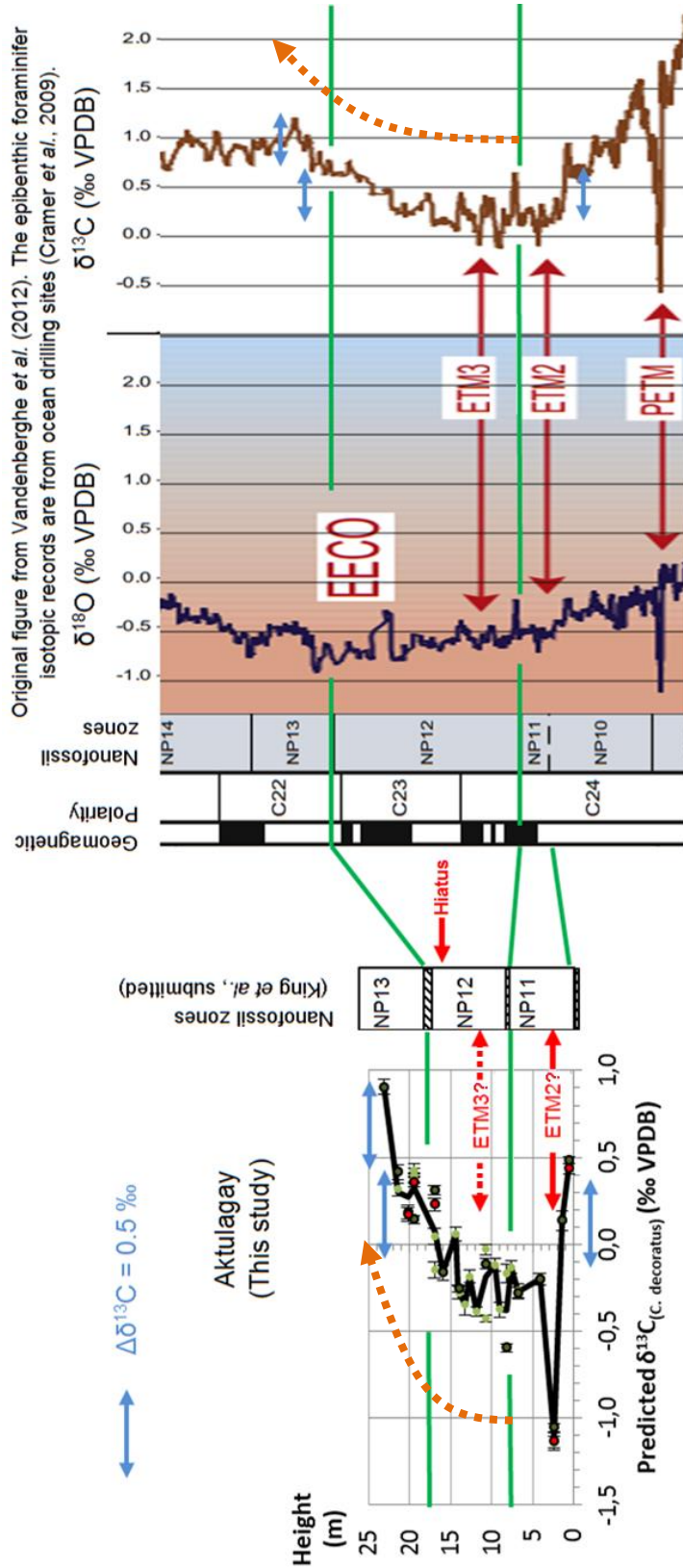


Figure 70. Comparison with the Ypresian record from Cramer *et al.* (2009) in Vandenberghe *et al.* (2012). The record is composed of epibenthic foraminifer isotopic values of several ocean drilling sites. The recognized trend was drawn in both records with the dotted orange arrow.



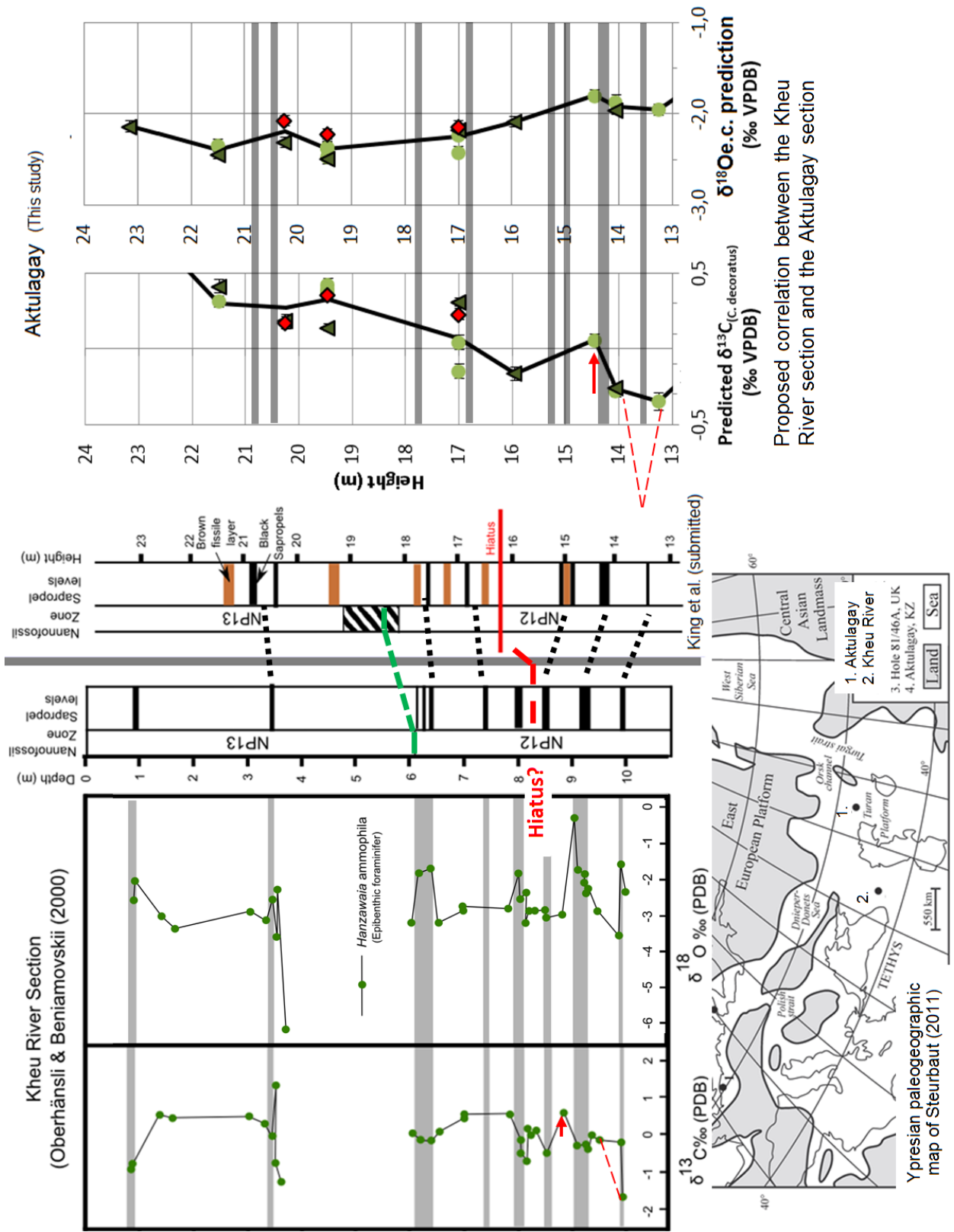


Figure 71. Comparison of the isotopic record of the Kheu River Section (Oberhänsli & Beniamovskii, 2000) with the isotopic record of Aktulagay. The locations were marked on the map of Steurbaut (2011).

## 8.7 Summary

The predicted *C. decoratus*  $\delta^{13}\text{C}$  record revealed strong isotopic variation in the Aktulagay section during NP11, NP12 and NP13. The  $\delta^{13}\text{C}$  record is likely influenced by the occurrence of nearby CIEs. Strong indications exist for a hyperthermal event near 2.35 m. Based on Cramer *et al.* (2009) this hyperthermal event can most likely be identified as the H1-event/ETM2. Nevertheless the H2-event could also be responsible for the isotopic excursion. The influence of the J-event and the K-event (ETM3) might also have affected the isotopic record but this cannot be proven by our data. The  $\delta^{13}\text{C}$  record further revealed a  $\delta^{13}\text{C}$  decreasing trend in the lower 4 m, from 0.5‰ at 0.55 m to -0.2‰ at 4.15 m, that was followed by an gradual increasing  $\delta^{13}\text{C}$  trend from 4 m (-0.2‰) onwards to a final value of 0.9‰ at 23.15 m. This trend was considered to reflect the global ocean  $\delta^{13}\text{C}_{\text{DIC}}$  trend during the Early Eocene based on the isotopic record of Cramer *et al.* (2009). The  $\delta^{18}\text{O}$  record revealed high paleotemperatures varying from 19 °C to 24 °C ( $\pm 1.8$  °C) at the sea floor in Aktulagay. A temperature rise of approximately 3 °C to 4 °C was predicted at 2.35 m and was considered related to the nearby hyperthermal ETM2/H1 event or the H2 event. A temperature rise of 2 °C between 10 m and 12 m could possibly be related to ETM3. Finally the 1.9 °C higher temperatures in the interval between 15 m and 22 m were associated with the EECO. The temperature variation in Aktulagay was considered mainly a consequence of global temperature variation based on Cramer *et al.* (2009). Based on the data of Oberhänsli & Beniamovskii (2000) it was concluded that nearby sapropels could have influenced the isotopic values of some measurements e.g. at 17.00 m. The  $\delta^{13}\text{C}$  values measured in the Kheu River Section did not significantly differ from the values in Aktulagay as would be expected for the same time interval and the same sea. The  $\delta^{18}\text{O}$  values in the Kheu River Section were 0.8‰ more depleted than in Aktulagay. These higher  $\delta^{18}\text{O}$  values could indicate colder and more saline waters in Aktulagay or could be related to preservation problems for the isotopic data of the Kheu River Section.

## 9 The endobenthic record

*Bulimina aksuatica* and *Uvigerina elongata* were measured in several samples. These 2 species were chosen because *Bulimina aksuatica* was identified as a deep endobenthic species and *Uvigerina elongata* was identified as a shallow endobenthic species in the ecological study. However *Bulimina aksuatica* is not present in most samples of Unit A. Additional measurements were made for *Alabamina midwayensis*, *Pulsiphonina prima* and *Bulimina (aff.) midwayensis*. The behavior of the endobenthic species will be studied in this section. Their  $\delta^{13}\text{C}$  signature can reveal migration events and changes in the  $\delta^{13}\text{C}_{\text{DIC}}$  gradient within the sediment which can be related to changes in the availability of organic matter or changes in the oxygen level at the seafloor (Jorissen *et al.*, 1999).

### 9.1 Results

#### 9.1.1 $\Delta\delta^{13}\text{C}$ values

The  $\delta^{13}\text{C}$  values of endobenthic species are compared with the predicted *Cibicidoides decoratus*  $\delta^{13}\text{C}$  values in Figure 72. The epibenthic  $\delta^{13}\text{C}$  record is assumed to be equal or at constant offset with the  $\delta^{13}\text{C}_{\text{DIC}}$  signature at the sediment-water interface (Eq. 2). On the other hand the  $\delta^{13}\text{C}$  signature of endobenthic species is mainly determined by the  $\delta^{13}\text{C}_{\text{DIC}}$  of the pore water. The  $\Delta\delta^{13}\text{C}$  values of endobenthic species relative to the predicted  $\delta^{13}\text{C}$  *Cibicidoides decoratus* values are given in Figure 73. The  $\Delta\delta^{13}\text{C}$  values of *Uvigerina elongata* in lithologic Subunit A2 and in Subunit B2 are similar (1.1‰ to 1.3‰), except for the increased  $\Delta\delta^{13}\text{C}$  value at 23.57 m (1.7‰). In subunit B1 the absolute  $\delta^{13}\text{C}$  values of *Uvigerina elongata* are remarkably higher causing the  $\Delta\delta^{13}\text{C}$  values to decrease. At 15.95 m the  $\Delta\delta^{13}\text{C}$  becomes zero. *Bulimina aksuatica* has consistently more depleted  $\delta^{13}\text{C}$  values than *Uvigerina elongata* and is thus associated with larger  $\Delta\delta^{13}\text{C}$  values. An exception was measured at 9.00 m where both values are equal. The lowest  $\Delta\delta^{13}\text{C}$  values of *Bulimina aksuatica* are also measured within B1 and  $\Delta\delta^{13}\text{C}$  approaches zero at 15.95 m just like *Uvigerina elongata*. The  $\Delta\delta^{13}\text{C}$  values of *Alabamina midwayensis* at 2.35 m and at 10.75 m are approximately equal despite the anomalously low  $\delta^{13}\text{C}$  values at 2.35 m. *Pulsiphonina prima* demonstrates a unique  $\Delta\delta^{13}\text{C}$  shift between Sample 13 and 22. The  $\Delta\delta^{13}\text{C}$  shift between 22 and 25 is similar to *Uvigerina elongata*.

#### 9.1.2 $\Delta\delta^{18}\text{O}$ values

The  $\delta^{18}\text{O}$  values of endobenthic species are compared with the predicted equilibrium calcite  $\delta^{18}\text{O}$  values at the sediment-water interface in Figure 74. The  $\Delta\delta^{18}\text{O}$  values of endobenthic species relative to the predicted equilibrium calcite values at the sediment-water interface are given in Figure 75. It would be expected that  $\Delta\delta^{18}\text{O}$  shifts between samples are consistent for all species because they would be mainly determined by the temperature. Due to the lower precision of the measurements and the relatively large variation in the equilibrium calcite  $\delta^{18}\text{O}$  predictions (certainly at 19.45 m), most of the variation observed in Figure 75 cannot be considered significant. However some exceptions exist. The first exception is the *Pulsiphonina prima* measurement at 23.15 m, but this might be related to the occurrence of secondary

calcite within the specimens and the higher vulnerability of smaller specimens. The second exception is the occurrence of significantly more depleted  $\delta^{18}\text{O}$  values at 6.75 m and at 10.00 m of *Uvigerina elongata* relative to the  $\delta^{18}\text{O}$  of equilibrium calcite (Figure 79). Finally *Uvigerina elongata* and *Bulimina aksuatica* are characterized by relatively enriched  $\delta^{18}\text{O}$  values at 15.95 m (Sample 19).

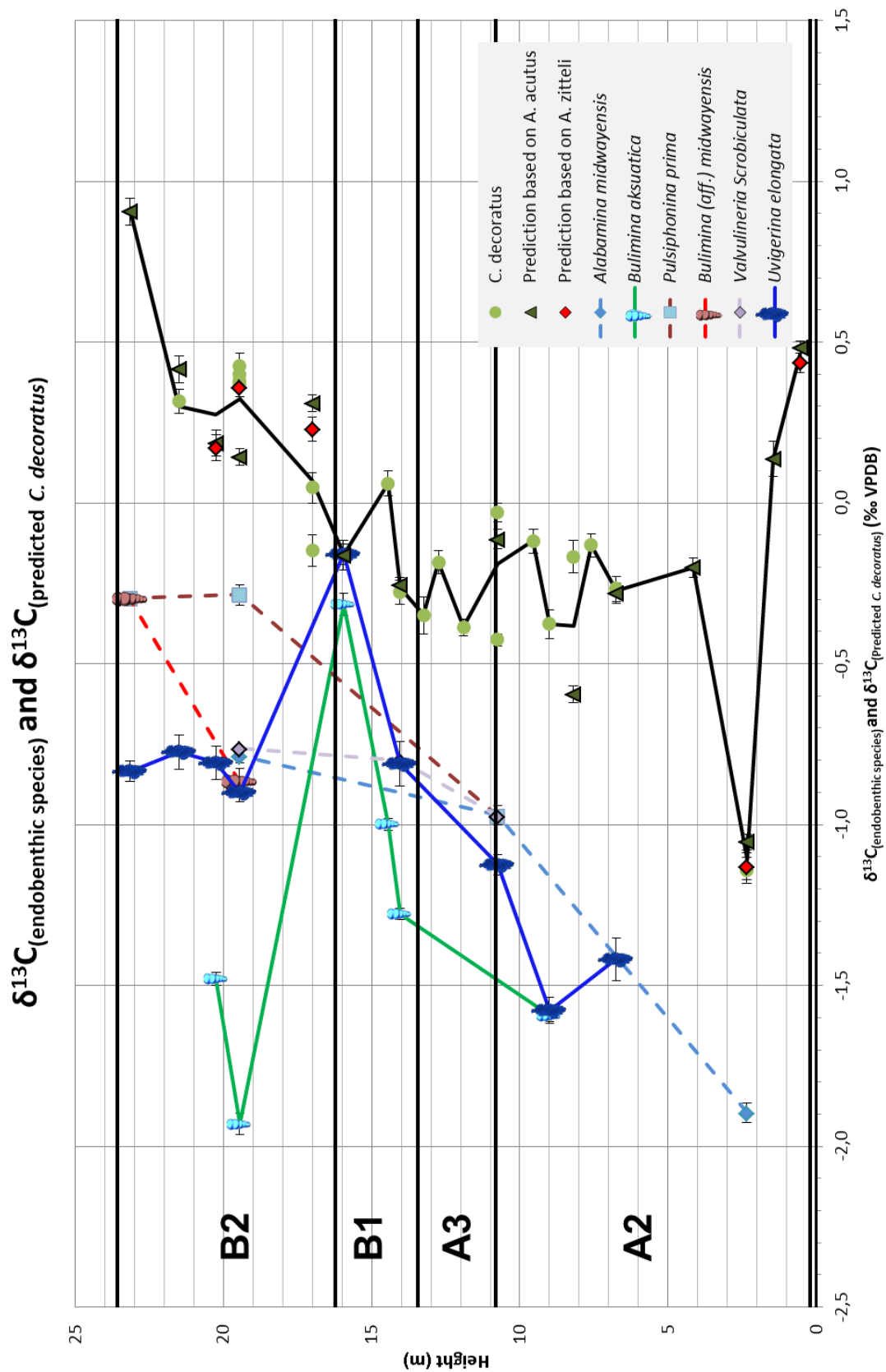


Figure 72. The absolute  $\delta^{13}\text{C}$  values of the endobenthic species and the predicted  $\delta^{13}\text{C}$  values of *Cibicidoides decoratus*.

# $\Delta\delta^{13}\text{C}$ : Epibenthic $\delta^{13}\text{C}$ - Endobenthic $\delta^{13}\text{C}$

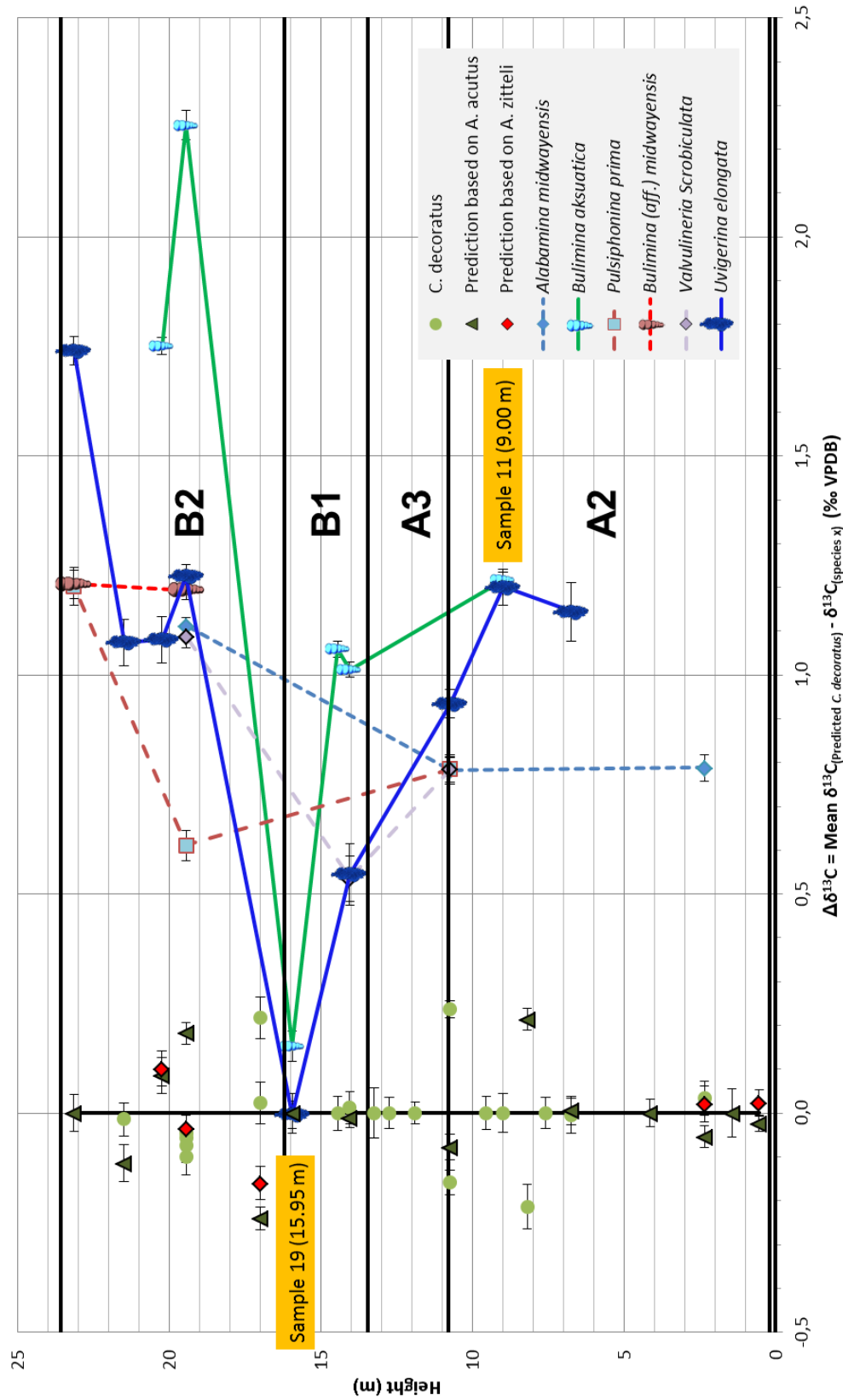


Figure 73. The  $\delta^{13}\text{C}$  values of endobenthic species relative to the predicted *Cibicidoides decoratus*  $\delta^{13}\text{C}$  values.

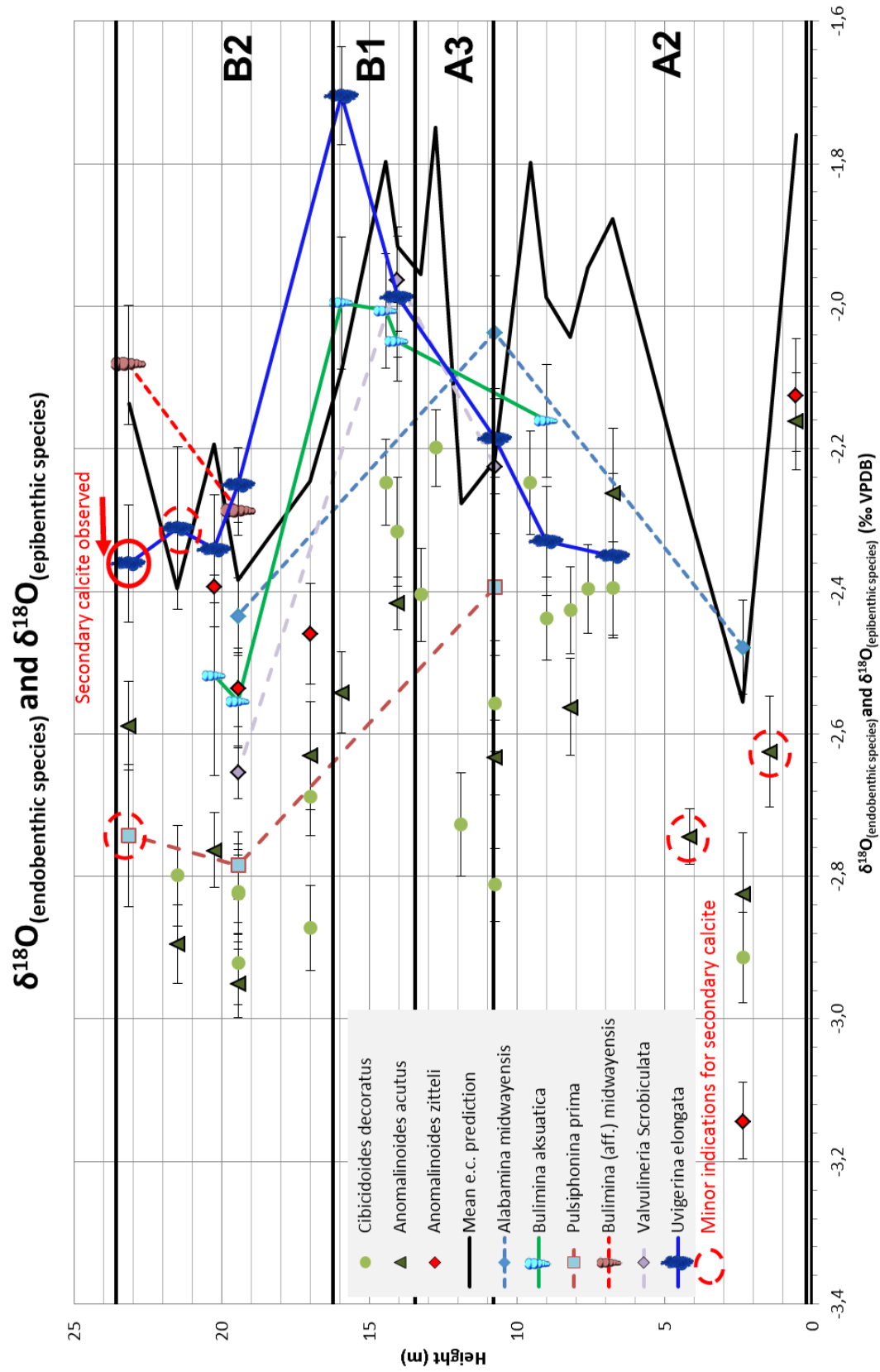


Figure 74. The absolute  $\delta^{18}\text{O}$  signature of epibenthic and endobenthic species and the predicted equilibrium calcite  $\delta^{18}\text{O}$  values at the sediment water interface.

# $\Delta\delta^{18}\text{O}$ : Epibenthic $\delta^{18}\text{O}$ - Endobenthic $\delta^{18}\text{O}$

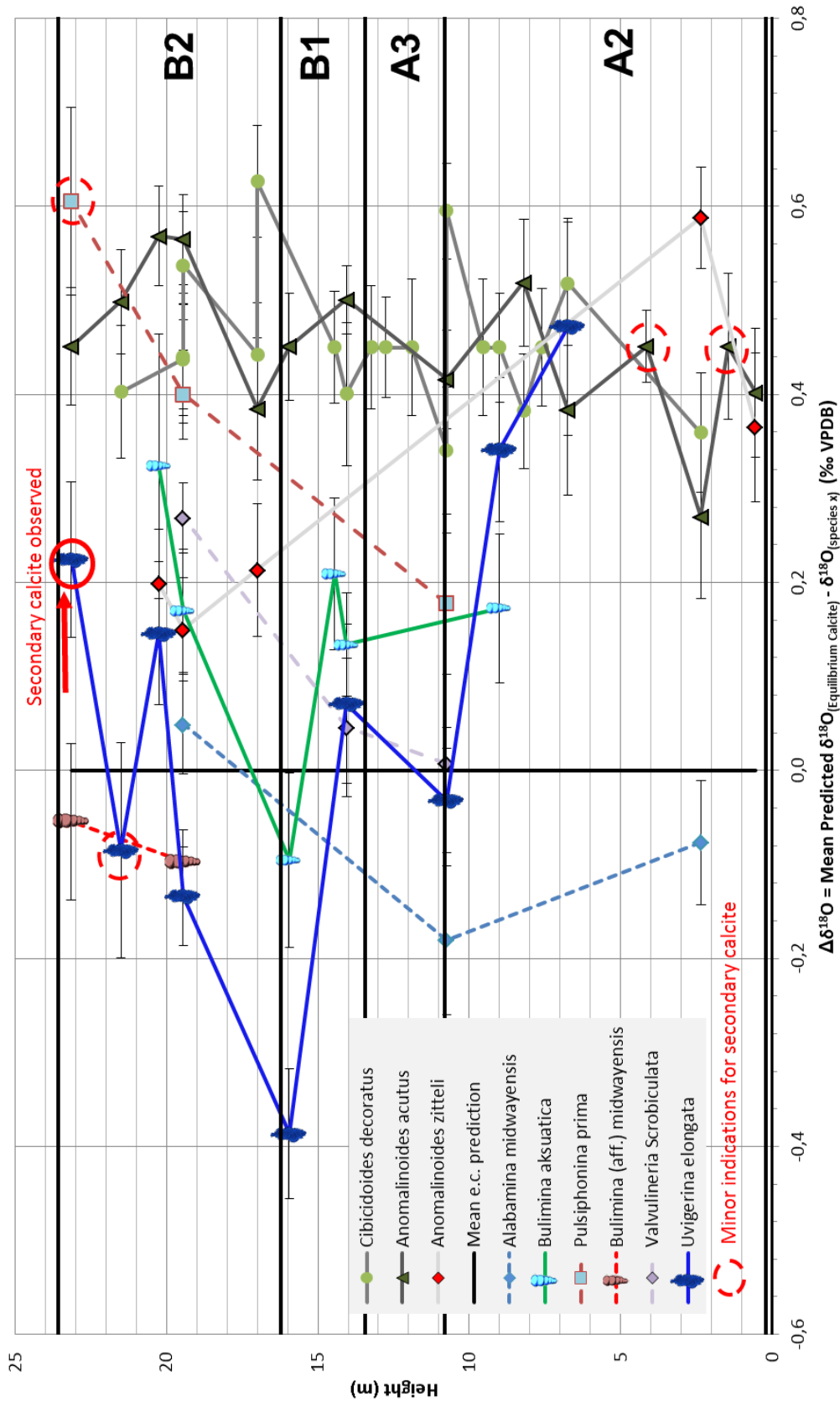


Figure 75. The  $\delta^{18}\text{O}$  values of epibenthic and endobenthic species relative to the predicted  $\delta^{18}\text{O}$  equilibrium calcite values at the sediment water interface.



## 9.2 Discussion

As discussed in Chapter 7, foraminifer species can be assigned to a microhabitat based on their  $\delta^{13}\text{C}$  values. Their  $\delta^{13}\text{C}$  value is considered mainly determined by the  $\delta^{13}\text{C}_{\text{DIC}}$  gradient within the sediment. This gradient exists due to the microbial oxidation of particulate organic matter (POM) rich in  $^{12}\text{C}$  (McCorkle *et al.*, 1985; Papadimitriou *et al.*, 2004). Due to the  $\delta^{13}\text{C}_{\text{DIC}}$  gradient, there is a general relation between the preferential living depth (microhabitat) of the foraminifers and their  $\delta^{13}\text{C}$  signature. Based on the measured  $\delta^{13}\text{C}$  values, *Cibicidoides decoratus*, *Anomalinoidea acutus*, *Anomalinoidea zitteli* were identified as epibenthic, while *Uvigerina elongata* and *Bulimina (aff.) midwayensis* were identified as shallow endobenthic and *Bulimina aksuatica* was as a deep endobenthic species (Table 6). However the  $\delta^{13}\text{C}_{\text{DIC}}$  gradient can change with time, changing the  $\Delta\delta^{13}\text{C}$  between species. Furthermore under different environmental circumstances, some species might migrate towards a different microhabitat.

### 9.2.1 Suboxic conditions at 15.95 m

The most remarkable result of the endobenthic measurements are the  $\Delta\delta^{13}\text{C}$  values approaching zero for both *Bulimina aksuatica* and *Uvigerina elongata* at 15.95 m. The absolute  $\delta^{13}\text{C}$  values demonstrate a clear enrichment of the endobenthic  $\delta^{13}\text{C}$  values at 15.95 m (Figure 72). It is therefore assumed that the endobenthic species are responsible for the deviating  $\Delta\delta^{13}\text{C}$  values and not the epibenthic species. These extreme  $\Delta\delta^{13}\text{C}$  values cannot be explained with a changing  $\delta^{13}\text{C}_{\text{DIC}}$  gradient in the sediment since it would require a  $\delta^{13}\text{C}_{\text{DIC}}$  gradient of zero. It is thus more plausible to assume that the species migrated upwards in the sediment and adapted an epibenthic microhabitat due to different environmental circumstances. Jorissen *et al.* (1999) proposed four parameters determining the vertical distribution of endobenthic species; bottom water oxygenation, food availability, competition & predation and bioturbation. Because of the high organic matter content in Subunit B1 (13.45 m – 16.22 m) (Deprez, 2012; King *et al.*, submitted) it is implausible that insufficient food caused the specimens to migrate upwards in the sediment. Suboxic conditions are on the other hand a plausible explanation because not all organic matter in the samples was oxidized. This upward migration was not observed at 14.05 m or 14.45 m and therefore a certain oxygen threshold must have been exceeded at 15.95 m. Nevertheless no sapropel was recognized at or near 15.95 m according to King *et al.* (submitted). Additional information about the sample is provided by the relative abundance data of Deprez *et al.* (submitted) (Figure 24). According to their data, the relative abundance of *Bulimina aksuatica* is extremely high at 14.05 m and 14.45 m (respectively 20.00% and 19.58%) but dropped in relative abundance at 15.95 m to 1.74%. On the other hand *Uvigerina elongata* had relatively low abundances at 14.05 m and 14.45 m (1.21% and 0.60% respectively) but became very abundant at 15.95 m (13.19%) (Deprez *et al.*, submitted). To explain these observations it is suggested that the relative abundance of *Bulimina aksuatica* was higher at 14.05 m and 14.45 m due the high food supply and the sufficient (although limited) oxygen at greater depths. However due to the lower oxygen levels at 15.95 m, *Bulimina aksuatica* was forced to migrate upwards where it was rather unsuccessful competing with the other species. Therefore it is suggested that *Bulimina aksuatica* is tolerant to low oxygen levels but not to the extent that it can survive in anoxic environment. The rise in relative

abundance of *Uvigerina elongata* can be explained if the species had less trouble surviving under the suboxic circumstances than other shallow endobenthic and epibenthic species, facilitating competition. Because the isotopic data revealed the difference in oxygen circumstances between samples 14.05 m, 14.45 m and 15.95 m, characteristics of other species can also be interpreted based on the relative abundance data of Deprez *et al.* (submitted) (Figure 24).

#### **9.2.1.1 Species that benefit from the suboxic conditions**

*Turrilina brevispira* has relative abundances of 0.0%, 0.3% and 8.86% at 14.05 m, 14.45 m and 15.95 m respectively. *Coryphostoma spp.* has relative abundances of 0.91%, 0.90% and 5.56% at 14.05 m, 14.45 m and 15.95 m respectively (Deprez *et al.*, submitted). The rise in relative abundance above 14.05 m for these species can thus be related to their oxygen tolerance. This allowed them to compete with other species that suffered under the suboxic circumstances. *Anomalinoidea acutus* is somewhat unique and has relative abundances of 4.55%, 18.07% and 18.75% at 14.05 m, 14.45 m and 15.95 m respectively (Deprez *et al.*, submitted). The high relative abundance at 14.45 m might be related to the opportunistic behavior of the species just after a sapropelic interval. Nevertheless the high abundance at 15.95 m reveals that the species benefits from the suboxic conditions. This supports the results of Stassen *et al.* (2012) who studied 2 cores of the New Jersey Coastal Plain over the biostratigraphic interval NP9 to NP10. They also considered *Anomalinoidea acutus* as an opportunistic species that is tolerant to dysoxic conditions.

#### **9.2.1.2 Species that suffer under the suboxic conditions**

*Loxostomoides applinae* has relative abundances of 2.12%, 3.61% and 0.35% at 14.05 m, 14.45 m and 15.95 m respectively. *Cibicidoides cf. decoratus* has relative abundances of 5.76%, 2.41% and 0.00% at 14.05 m, 14.45 m and 15.95 m respectively (Deprez *et al.*, submitted). Although the relative abundances are smaller, these species still demonstrate significant decreases at 15.95 m and are thus unsuccessful competing with the other species under decreasing oxygen conditions.

#### **9.2.1.3 Species that appear indifferent to the suboxic conditions**

Species that do not appear to suffer or benefit from the suboxic conditions based on their relative abundances are *Anomalinoidea cf. praeacutus*, *Epistominella minuta*, *Gyroidinoidea octocameratus*, *Lenticulina spp.*, *Oridorsalis plummerae*, *Paralabamina lunata*, *Spiroloculina spp.*, *Spiroplectinella esnaensis*, *Valvalabamina depressa*, *Valvulineria scrobiculata* (Data from Deprez *et al.*, submitted). However a rather constant relative abundance is not necessarily related to a constant absolute abundance.

### **9.2.2 Rejection of the pH-microhabitat relation hypothesis**

The  $\delta^{18}\text{O}$  signatures of *Bulimina aksuatica* and *Uvigerina elongata* are relatively enriched at 15.95 m (Figure 74), resulting in a  $\Delta\delta^{18}\text{O}$  increase relative to the epibenthic foraminifers (Figure 75). The  $\Delta\delta^{18}\text{O}$  increase is associated with a  $\Delta\delta^{13}\text{C}$  decrease at this level. The  $\Delta\delta^{13}\text{C}$  decrease was explained by the

hypothesis of migration of endobenthic species towards an epibenthic microhabitat. It is thus plausible that the changing  $\delta^{18}\text{O}$  values are also related to the migration within the sediment. As explained in 7.2.1.2, a debate exists whether there is a relation between  $\delta^{18}\text{O}$  and the depth microhabitat of foraminifers. Some authors suggest that a  $\delta^{18}\text{O}$  gradient exists within the sediment as a consequence of a pH gradient (e.g. Bemis *et al.*, 1998; Schmiiedl *et al.*, 2004; Friedrich *et al.*, 2006; Wendler *et al.*, 2013). They refer to Spero *et al.* (1997) that was able to demonstrate the effect of pH for planktic foraminifers. Friedrich *et al.* (2006) further suggested that the strong difference in  $\delta^{18}\text{O}$  between epibenthic and endobenthic species measured in their study (Figure 51) might reflect a stronger pH gradient during the Cretaceous. Assuming that the more depleted  $\delta^{18}\text{O}$  values of epibenthic species are indeed (partially) a consequence of a pH gradient in the sediment, it would be expected that upwards migrating species gain more depleted  $\delta^{18}\text{O}$  values. In Figure 76 it is demonstrated that this is not the case. Therefore either the hypothesis of migration is incorrect or a dominant pH control on the  $\delta^{18}\text{O}$  signature does not exist. If the hypothesis of migration was incorrect, another explanation would be required to explain the  $\delta^{13}\text{C}$  increase that only affects the endobenthic species. A possibility would be a significant decrease in calcite precipitation rate and thus a kinetic disequilibrium effect as proposed for *Lenticulina* spp. (Figure 57). This hypothesis is rejected because:

- The approximately equal  $\delta^{13}\text{C}$  values at 15.95 m of the epibenthic species and endobenthic species are then considered a coincidence
- This would suggest that kinetic disequilibrium calcite precipitation is not exceptional. This is not conform with the modern isotopic foraminifer data of McCorkle *et al.* (1997), Rathburn *et al.* (1996) and Fontanier *et al.* (2008)
- The data of *Uvigerina elongata* and *Bulimina aksuatica* suggest that the disequilibrium calcite precipitation equation of McConnaughey (1989) is not be respected (The effect on  $\delta^{13}\text{C}$  would be either too large or the effect on  $\delta^{18}\text{O}$  too small).

Since no other alternative hypothesis was found, the isotopic data strongly supports the hypothesis of McCorkle *et al.* (1997) and Fontanier *et al.* (2008) that  $\delta^{18}\text{O}$  is not microhabitat related and that a significant pH influence on the  $\delta^{18}\text{O}$  values does not exist. The observation that most epibenthic species are associated with more depleted  $\delta^{18}\text{O}$  values than endobenthic species should be related to their life style and not to their microhabitat; e.g. food preference, different metabolisms, respiration rate and/or growth rate (e.g. Schmiiedl. *et al.*, 2004; Basak *et al.*, 2009; Wendler *et al.*, 2013). This would still explain the indirect relation with the species microhabitat.

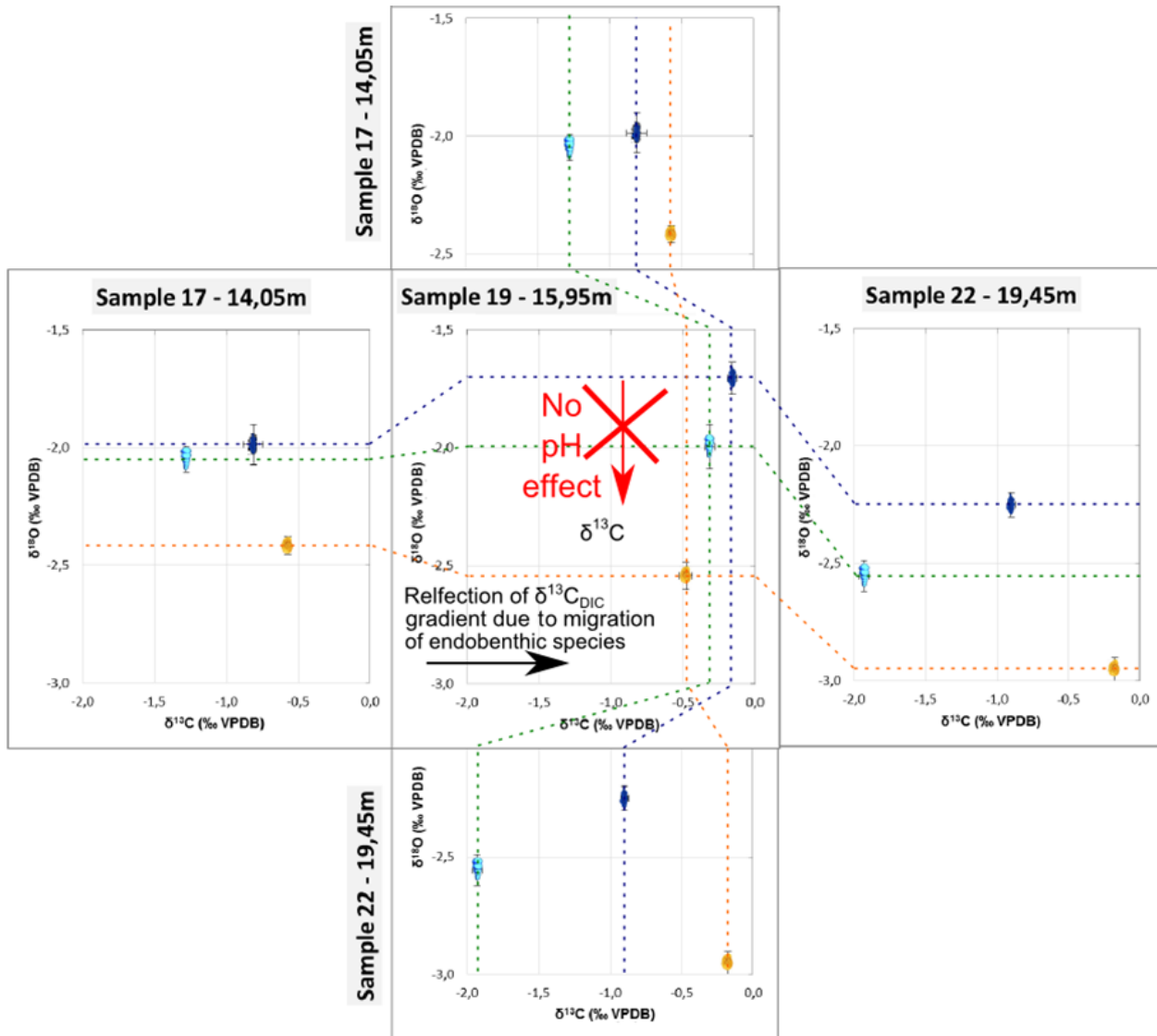


Figure 76. A comparison between the isotopic values of species *Anomalinoides acutus*, *Uvigerina elongata* and *Bulimina aksuatica* at 14.05 m, 15.95 m and 19.45 m. The decrease of  $\Delta\delta^{13}\text{C}$  between epibenthic and endobenthic species at 15.95 m reveals the migration of the endobenthic species to an epibenthic microhabitat. For  $\Delta\delta^{18}\text{O}$  such decrease is not observed, to the contrary  $\Delta\delta^{18}\text{O}$  even rises between 14.05 m and 15.95 m. If  $\Delta\delta^{18}\text{O}$  was mainly a consequence of a pH gradient within the sediment, this observation would not be possible. (Note: in this figure *Anomalinoides acutus* was not corrected to *Cibicidoides decoratus*).

### 9.2.3 The microhabitat of *Uvigerina elongata* and *Bulimina aksuatica* in subunit A2

At 9.00 m the  $\delta^{13}\text{C}$  (-1.58‰) signature of *Uvigerina elongata* is equal to the  $\delta^{13}\text{C}$  signature of *Bulimina aksuatica* (-1.59‰) (Figure 72). To the contrary at 14.05 m, 19.45 m and 20.25 m *Uvigerina elongata* consistently has a more enriched  $\delta^{13}\text{C}$  signature, although the difference in  $\delta^{13}\text{C}$  between both species is variable. Several explanations are possible. It could be the result isotopic variability, ontogenetic effects and/or migration of the species to a common depth. First of all, unlike the epibenthic measurements, the isotopic results of *Uvigerina elongata* and *Bulimina aksuatica* are extremely averaged out. The measurements at 9.00 m are averages of 25 specimens for *Bulimina aksuatica* and 51 specimens for *Uvigerina elongata*. It is therefore unlikely that the isotopic variation within the sample could be responsible for the deviating  $\delta^{13}\text{C}$  values. Secondly ontogenetic effects might have contributed to the  $\delta^{13}\text{C}$  deviation, although the modern foraminifer data of Schumacher *et al.* (2010) suggests that a deviation in the order of 0.1‰ is more realistic than a deviation of 0.5‰. Therefore it is assumed that the deviating  $\delta^{13}\text{C}$  values are a result of the migration of both species to a common depth. However it is unclear which of both species migrated. If the  $\delta^{13}\text{C}$  values between Subunit A2 and Subunit B2 are compared, it appears that the *Bulimina aksuatica* migrated to a shallower depth. However this might also be the result of different  $\delta^{13}\text{C}_{\text{DIC}}$  gradients within the sediment at the time of deposition. When observing the  $\delta^{18}\text{O}$  record, the  $\delta^{18}\text{O}$  signature of *Uvigerina elongata* deviates and becomes relatively more depleted at 6.75 m and 9.00 m. In theory the additional depletion of these specimens could be the effect of secondary calcite, but no secondary calcite was observed with the SEM. Therefore the change in  $\delta^{18}\text{O}$  values could be the reflection of different behavior of *Uvigerina elongata*. In conclusion it is uncertain which of the species migrated, the best way to find out is to measure other shallow endobenthic specimens in the Sample at 9.00 m. An explanation for the migration might be related to the different lithology (Unit A versus Unit B, King *et al.*, submitted) and thus the different paleoenvironment and foraminifer assemblage (Deprez *et al.*, submitted).

### 9.2.4 The influence of hyperthermals on the foraminifer assemblage

The most prominent indication for a nearby hyperthermal was measured at 2.35 m (Identified as either the H1-event/ETM2 or the H2-event). The isotopic measurements at 10.75 m and 19.45 m strongly suggested that the endobenthic species *Alabamina midwayensis* behaves similar as *Valvulineria scrobiculata* and *Uvigerina elongata* because of the constant (relatively small)  $\delta^{13}\text{C}$  offset between the species (Table 5). *Alabamina midwayensis* has been measured at 2.35 m. The observation that the extreme absolute  $\delta^{13}\text{C}$  values at 2.35 m do not result in extreme  $\Delta\delta^{13}\text{C}$  values relative to the epibenthic species, demonstrates that the microhabitat of this species is not strongly affected by the occurrence of the hyperthermal. This is not surprising given that the relative abundance data of Deprez *et al.* (submitted) demonstrated no significant changes in the foraminifer assemblage at 2.35 m. Furthermore King *et al.* (submitted) did not describe any lithologic changes at or near 2.35 m. In conclusion it appears that the occurrence of the hyperthermal near 2.35 m had remarkably low impact on the foraminifer assemblage in Aktulagay.

### 9.2.5 *Pulsiphonina prima*

The  $\Delta\delta^{13}\text{C}$  shift of *Pulsiphonina prima* between Sample 13 (10.75 m) and Sample 22 (19.45 m) is 0.4‰ greater than expected when comparing with most other species in Figure 46. In contrast to many other species it is extremely unlikely that the deviations can be related to isotopic variation within the sample because the measurements represent averages of 40+ specimens. Furthermore ontogenetic effects appear insufficient to explain the  $\Delta\delta^{13}\text{C}$  shift based on the data of Schumacher *et al.* (2010). Therefore the  $\Delta\delta^{13}\text{C}$  shift is possibly related to migration for unknown reasons. The measurements at 23.15 m propose a similar  $\Delta\delta^{13}\text{C}$  shift between 19.45 m and 23.15 m for *Pulsiphonina prima* and *Uvigerina elongata*. This  $\Delta\delta^{13}\text{C}$  shift is not observed for endobenthic species *Bulimina (aff.) midwayensis* and the epibenthic species. These  $\Delta\delta^{13}\text{C}$  shifts can again be a consequence of migration of *Uvigerina elongata* and *Pulsiphonina prima*.

### 9.2.6 The consequence of migration

The interpretation that *Pulsiphonina prima* and *Uvigerina elongata* frequently migrate has large consequences for the ecological study. It demonstrates that the detailed microhabitat interpretation in Table 5 is only representative for a snapshot in time. An ecological study based on 3 samples does not allow to distinguish species that frequently migrate like *Pulsiphonina prima* and *Uvigerina elongata* from other species. Finally if the species that were identified as epibenthic would sometimes adapt an endobenthic microhabitat, it would have major consequences for the interpretation of the epibenthic record. However there were no indications that *Anomalinoidea acutus*, *Anomalinoidea zitteli* and *Cibicidoides decoratus* would have adapted an endobenthic microhabitat in some parts of the section.

## 9.3 Summary

First of all the endobenthic  $\delta^{13}\text{C}$  record revealed an upward migration event at 15.95 m for endobenthic species *Bulimina aksuatica* and *Uvigerina elongata*. The migration could be explained by the occurrence of suboxic conditions at 15.95 m that were considered more severe than at 14.05 m and 14.45 m. The identified low oxygen conditions at 15.95 m were combined with the relative abundance data of Deprez *et al.* (submitted) to study the behavior of several species under these low oxygen conditions. *Anomalinoidea acutus*, *Coryphostoma spp.*, *Turrilina brevispira* and *Uvigerina elongata* significantly increased in relative abundance at 15.95 m. It is proposed that these species are very tolerant to low oxygen conditions which enabled them to better compete with the species that suffered under the suboxic conditions. Other species like *Bulimina aksuatica*, *Cibicidoides cf. decoratus* and *Loxostomoides applinae* decreased significantly in relative abundance at 15.95 m. Their decrease in relative abundance was considered a consequence of being unsuccessful under low oxygen conditions. The  $\delta^{18}\text{O}$  values of the migrating species *Bulimina aksuatica* and *Uvigerina elongata* became relatively more enriched in  $\delta^{18}\text{O}$  at 15.95 m. This was not conform to the proposed pH-microhabitat relation by e.g. Bemis *et al.* (1998), Schmiedl *et al.*, (2004), Friedrich *et al.* (2006) and Wendler *et al.* (2013). Therefore the hypothesis that a pH gradient is responsible for a  $\delta^{18}\text{O}$  gradient within the sediment was rejected, which is support in support of McCorkle

*et al.* (1997) and Fontanier *et al.* (2008). The observation that most epibenthic species are associated with more depleted  $\delta^{18}\text{O}$  values than endobenthic species was related to their life style; e.g. food preference, different metabolisms, respiration rate and/or growth rate (e.g. Schmiedl. *et al.*, 2004; Basak *et al.*, 2009; Wendler *et al.*, 2013). Secondly in Subunit A2 the  $\delta^{13}\text{C}$  values of *Bulimina aksuatica* and *Uvigerina elongata* became equal. This was interpreted as a consequence of migration towards a common depth, although it is uncertain which species migrated. The migration was proposed to be related to the different paleoenvironment circumstances and different foraminifer assemblage during the deposition of lithological Units A and B. Thirdly the  $\delta^{13}\text{C}$  isotopes of *Alabamina midwayensis* at 2.35 m indicated that no migration event occurs at 2.35 m despite the nearby presence of the hyperthermal ETM2/the H1-event or the H2-event. Finally it was concluded that *Pulsiphonina prima* can migrate within the sediment for unknown reasons that do not cause other species to migrate. Furthermore both *Pulsiphonina prima* and *Uvigerina elongata* migrate towards a deeper microhabitat at 23.15 m. It should therefore be realized that the detailed microhabitat interpretation in Table 5 is only representative for a snapshot in time and that some species like *Pulsiphonina prima* and *Uvigerina elongata* can migrate frequently.





## 10 The planktic isotopic record

### 10.1 Ontogenetic effects and the $\delta^{18}\text{O}_{\text{e.c}}$ derived from planktic foraminifers

Ontogenetic effects are known to influence the  $\delta^{13}\text{C}$  and  $\delta^{18}\text{O}$  signatures of the foraminifer tests. Spero and Lea (1996) demonstrated strong ontogenetic effects for modern non-symbiotic planktic foraminifer *Globigerina bulloides* for specimens that grew under controlled temperature conditions (Figure 77). The data of D'Hondt *et al.* (1994) demonstrates that this effect also existed during the Late Paleocene (Figure 78). In order to restrict the influence of the ontogenetic effect, the specimens of *Acarinina spp.* were sampled in the 250-300  $\mu\text{m}$  size fraction. The data of Spero and Lea (1996) demonstrated that planktic foraminifers can precipitate their test in strong disequilibrium with seawater  $\delta^{13}\text{C}$  and  $\delta^{18}\text{O}$ . Since it is unknown how large the effect is for *Subbotina* and *Acarinina* species, the uncertainties to predict equilibrium calcite isotopic values become very large. The effect is roughly predicted in Eq. 14 based on the data of Spero and Lea (1996) (Figure 77), assuming that the disequilibrium precipitation of modern *Globigerina bulloides* is representative for the extinct *Subbotina* and *Acarinina* species.

$$\delta^{18}\text{O}_{\text{e.c.}} = \delta^{18}\text{O} + 1\text{‰} (\pm 0.5\text{‰})$$

$$\delta^{13}\text{C}_{\text{DIC}} = \delta^{13}\text{C} + 3\text{‰} (\pm 1.5\text{‰})$$

Eq. 14. The prediction of  $\delta^{18}\text{O}_{\text{e.c.}}$  and  $\delta^{13}\text{C}_{\text{e.c.}}$  based on the isotopic values of non-symbiotic planktic foraminifer species.

Since other parameters still have to be considered, no further attempt will be made to predict  $\delta^{13}\text{C}_{\text{DIC}}$  and only relative  $\Delta\delta^{13}\text{C}_{\text{DIC}}$  will be studied.

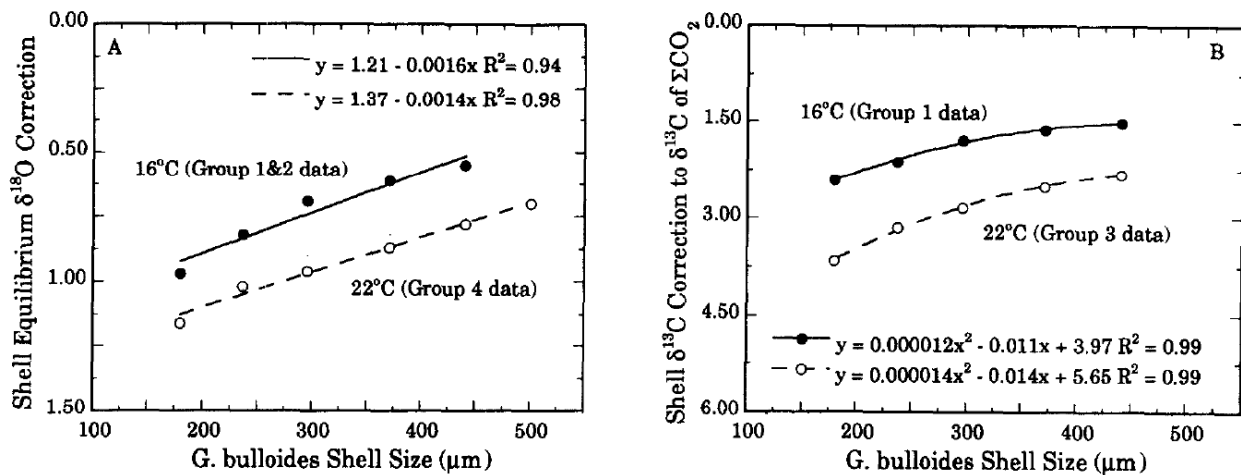


Figure 77. Figures from Spero and Lea (1996). Their experiments on the modern non-symbiotic planktic foraminifer *Globigerina bulloides* demonstrated a significant ontogenetic effect for both  $\delta^{13}\text{C}$  and  $\delta^{18}\text{O}$ . Their experiments were performed at constant temperature; an experiment at 16 °C and at 22 °C. For all specimens the  $\delta^{13}\text{C}$  and  $\delta^{18}\text{O}$  signatures were significantly more depleted than the equilibrium calcite values. The disequilibrium is consistently larger for smaller/juvenile specimens and is also determined by temperature.

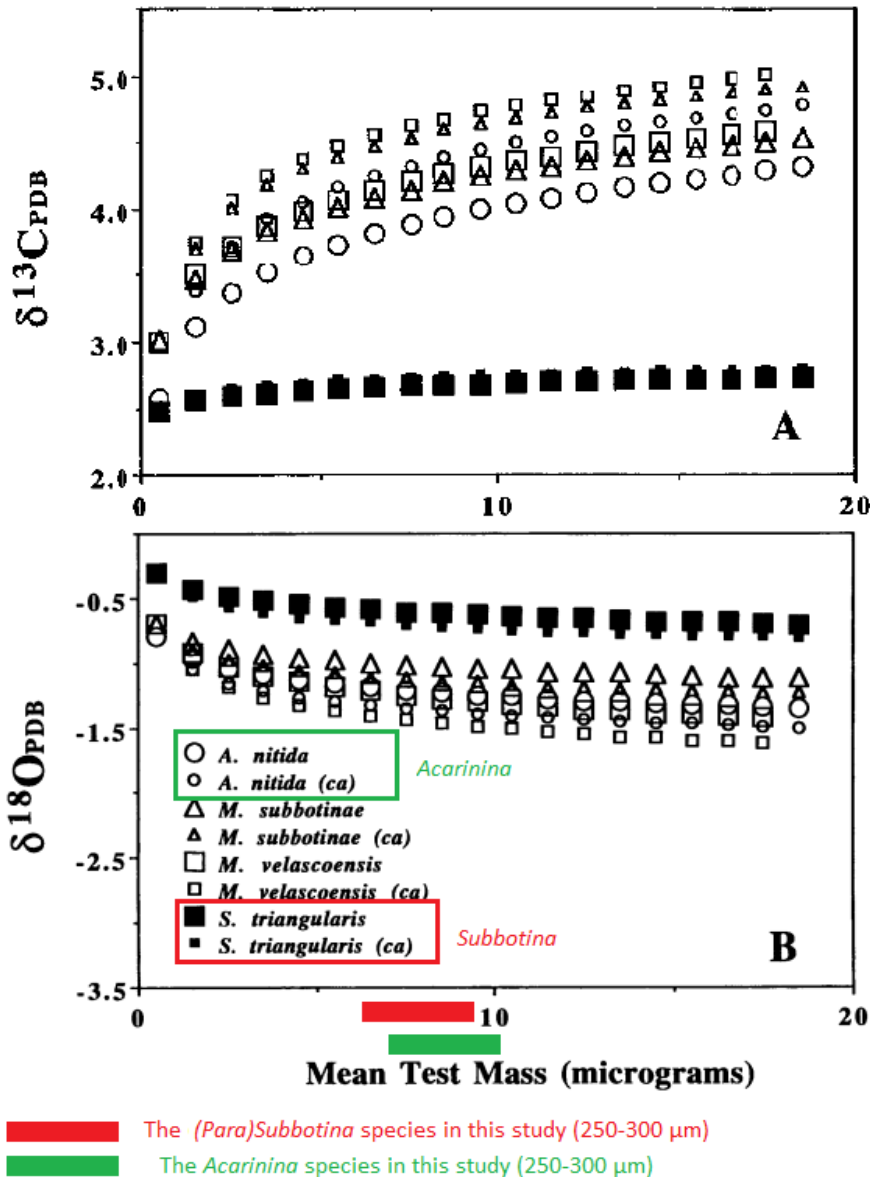


Figure 78. The measurements from D'Hondt *et al.* (1994) demonstrate the ontogenetic effect for *Acarinina* and *Subbotina* species of the Late Paleocene. For this reason, the planktic specimens in this study were strictly picked from the 250-300  $\mu\text{m}$  size fraction. Based on their data, the ontogenetic effects in this study will be considered negligible. Although a small effect of 0.2‰ can still exist for the  $\delta^{13}\text{C}$  signature of *Acarinina* species. (from D'Hondt *et al.*, 1994)

## 10.2 The $\delta^{18}\text{O}_{\text{sw}}$ prediction and the salinity of the mixed layer

The  $\delta^{18}\text{O}_{\text{sw}}$  estimate is required to predict the paleotemperatures with the equation of Erez and Luz (1983). Unlike the seafloor, the uncertainty on the salinity of the mixed layer waters is very high due to variable precipitation and evaporation. Additional uncertainty exists because of the proximity of the continent and possible fluvial water input. The salinity of the surface water can be estimated in several ways.

### 10.2.1 Prediction based on Zachos *et al.* (1994)

Zachos *et al.* (1994) calculated a formula to estimate the  $\delta^{18}\text{O}_{\text{sw}}$  of the shallow mixed layer by latitude based on modern  $\delta^{18}\text{O}_{\text{sw}}$  values. According to Zachos *et al.* (1994), the latitudinal variability is caused by evaporation, precipitation, Rayleigh distillation and atmospheric vapor transport. After using the formula, Zachos *et al.* (1994) corrected the present day value with the mean  $\delta^{18}\text{O}_{\text{sw}}$  of the Early Eocene (Eq. 15).

$$\begin{aligned} \delta^{18}\text{O}_{\text{sw}} (\text{present day value}) &= 0.576 + 0.041 * \text{Latitude} - 0.0017 * \text{Latitude}^2 + 1.35*10^{-5} * \text{Latitude}^3 \\ \delta^{18}\text{O}_{\text{sw}} (\text{Early Eocene}) &= \delta^{18}\text{O}_{\text{sw-mean}} + 0.576 + 0.041 * \text{Latitude} - 0.0017 * \text{Latitude}^2 + 1.35*10^{-5} * \text{Latitude}^3 \\ \delta^{18}\text{O}_{\text{sw}} (\text{Aktulagay at } 48^\circ\text{N}) &= \delta^{18}\text{O}_{\text{sw-mean}} + 0.120\text{‰} \end{aligned}$$

Eq. 15. The  $\delta^{18}\text{O}_{\text{seawater}}$  values are expressed in ‰ VSMOW' and the latitudes are expressed in degrees. (Zachos *et al.*, 1994) The equations predict  $\delta^{18}\text{O}_{\text{seawater}}$  of the mixed layer.

According to Zachos *et al.* (1994), the latitudinal correction should be made for mixed layer dwelling planktic foraminifers but not for deeper thermocline planktic foraminifers or benthic foraminifers. When the formula of Zachos *et al.* (1994) is applied on Aktulagay (~48°N), the present day  $\delta^{18}\text{O}_{\text{sw}}$  is estimated to be 0.120‰ (VSMOW). Based on the variation in  $\delta^{18}\text{O}_{\text{sw-mean}}$  predictions (Table 7), the surface  $\delta^{18}\text{O}_{\text{sw}}$  can be estimated to be -0.880‰ ( $\pm 0.25\text{‰}$ ). However the equation of Zachos *et al.* (1994) is made for the open ocean waters and additional uncertainty exist for outer shelf settings.

#### 10.2.1.1 Prediction based on Tindall *et al.* (2010)

A more recent attempt to accurately estimate  $\delta^{18}\text{O}_{\text{sw}}$  of surface waters was made by Tindall *et al.* (2010). They argue that the longitudinal variation of  $\delta^{18}\text{O}_{\text{sw}}$  in the modern ocean can vary significantly by 2‰ and that the hydrological cycle during the Early Eocene differs from today. Therefore they claim that the method of Zachos *et al.* (1994) bears significant uncertainties that cause temperature estimate errors of several degrees. Tindall *et al.* (2010) used a General Circulation Model (HadCM3) to simulate the distribution of  $\delta^{18}\text{O}_{\text{sw}}$  during the Early Eocene (Figure 79). Important is that Tindall *et al.* (2010), like Zachos *et al.* (1994), only apply their model for estimates of the mixed layer and not for the thermocline or sub-thermocline zones of the ocean. Tindall *et al.* (2010) reveals additional problems estimating sea surface  $\delta^{18}\text{O}_{\text{sw}}$  in Aktulagay. The location of Aktulagay is characterized by highly variable  $\delta^{18}\text{O}_{\text{sw}}$  values ranging from  $\delta^{18}\text{O}_{\text{sw-mean}} - 2.0\text{‰}$  to  $\delta^{18}\text{O}_{\text{sw-mean}} + 0.5\text{‰}$  (VSMOW). This results in Eq. 16.

$$\delta^{18}\text{O}_{\text{sw-mixed layer}} = \delta^{18}\text{O}_{\text{sw-mean}} - 0.75 \pm 1.25\text{‰ VSMOW}$$

Eq. 16. The prediction of the  $\delta^{18}\text{O}_{\text{sw-mixed layer}}$  values based on Tindall *et al.* (2010).

However two important problems exist with the prediction based on Tindall *et al.* (2010). First the paleogeographic map used in the model lacks a connection between the North Sea Basin and the Peri-Tethys in contrast to the maps of Dercourt *et al.* (2000) and Steurbaut (2011). Secondly most of their data to generate the model is from the Southern Hemisphere, which decreases the accuracy of the estimates in the Northern Hemisphere. Therefore their results remain highly uncertain in the Peri-Tethys.

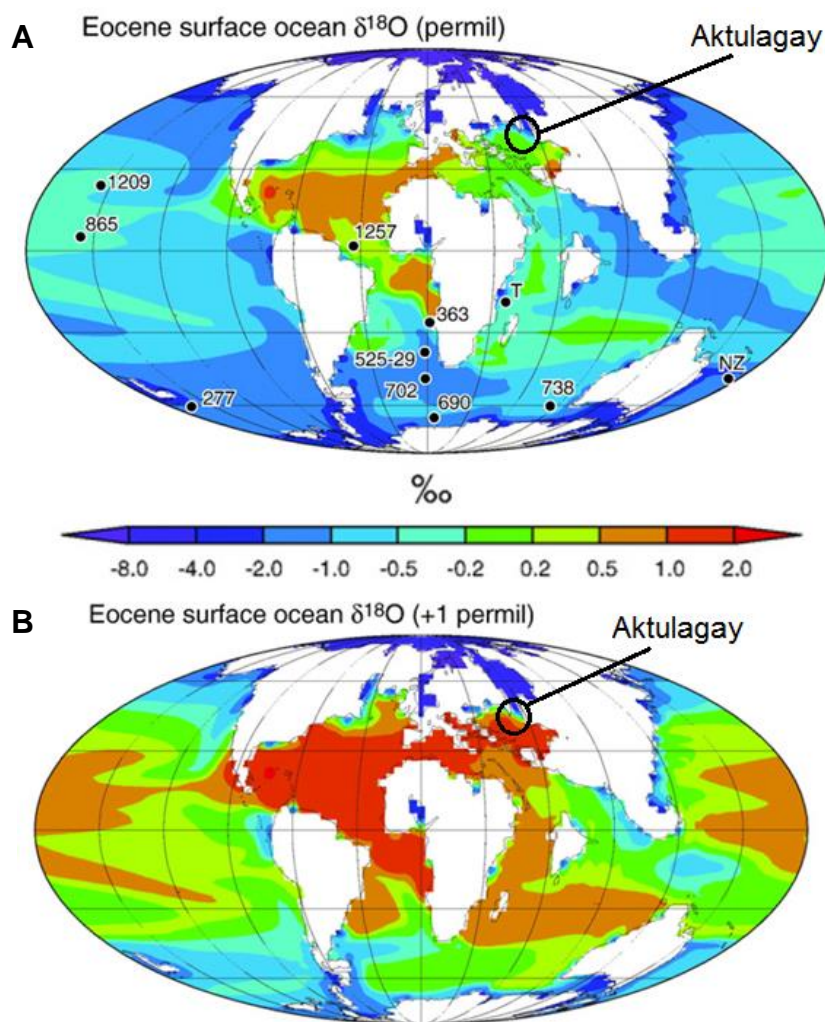


Figure 79. Figure A demonstrates the simulated distribution of  $\delta^{18}\text{O}_{\text{sw}}$  (mixed layer) by Tindall *et al.* (2010) during the Early Eocene. The black dots are the data locations. Aktulagay is marked on the map based on the map of Steurbaut (2011). Tindall *et al.* (2010) used an estimate of mean ocean  $\delta^{18}\text{O} = -1\text{‰}$ . Figure 4B allows to correct  $\delta^{18}\text{O}_{\text{sw}}$  (mixed layer) with other mean ocean  $\delta^{18}\text{O}$ -values.

#### 10.2.1.2 Prediction based on Roberts *et al.* (2011)

Another simulation model of  $\delta^{18}\text{O}_{\text{sw}}$  was made by Roberts *et al.* (2011). They applied another general circulation model (GISS ModelE-R) and other boundary conditions than Tindall *et al.* (2010). Important is that their paleogeographic map differs from Tindall *et al.* (2010) and that their map contains a connection between the Tethys ocean and the North Sea, which is in agreement with the map of Steurbaut (2011). The relative predicted values of  $\delta^{18}\text{O}_{\text{sw}}$  by Roberts *et al.* (2011) are shown in Figure 80, these values are not yet corrected for the  $\delta^{18}\text{O}_{\text{sw-mean}}$  value. Based on the paleogeographic location of Aktulagay the  $\delta^{18}\text{O}_{\text{sw-mixed layer}}$  ranges between  $\delta^{18}\text{O}_{\text{sw-mean}} - 0.75\text{‰}$  to  $\delta^{18}\text{O}_{\text{sw-mean}} - 2.00\text{‰}$  (VSMOW). This would result in Eq. 17.

$$\delta^{18}\text{O}_{\text{sw-mixed layer}} = \delta^{18}\text{O}_{\text{sw-mean}} - 1.375 \pm 0.625\text{‰ VSMOW}$$

Eq. 17. The prediction of the  $\delta^{18}\text{O}_{\text{sw-mixed layer}}$  values based on Roberts *et al.* (2010).

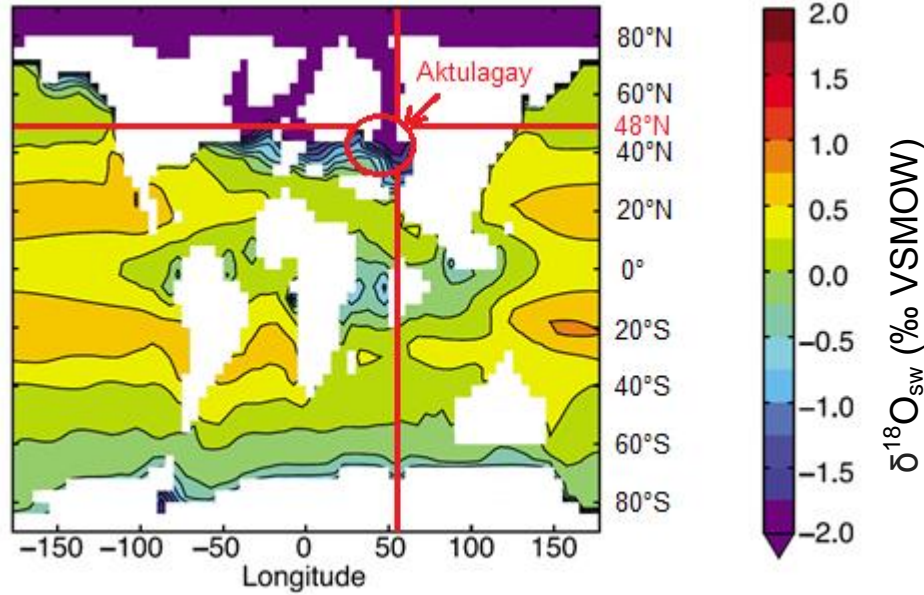


Figure 80. Map of surface ocean  $\delta^{18}\text{O}_{\text{sw}}$  (‰ VSMOW) distribution during the Early Paleogene (Roberts *et al.*, 2011). The Paleogene values are adjusted to a  $\delta^{18}\text{O}_{\text{sw-mean}}$  value of **zero** and therefore must be corrected with an assumption of the mean Early Eocene mean values. Roberts *et al.* (2011) used  $-0.81\text{‰}$  as mean ocean  $\delta^{18}\text{O}$ . The red circle marks an estimated position of the Aktulagay Section based on the map of Steurbaut (2011) (Figure 7).

### 10.2.1.3 Summary

In summary the salinity predictions of the mixed layer seawater are:

- $\delta^{18}\text{O}_{\text{sw-mixed layer}} = \delta^{18}\text{O}_{\text{sw-mean}} + 0.120\text{‰ VSMOW}$  (Eq. 15, Zachos *et al.*, 1994)
- $\delta^{18}\text{O}_{\text{sw-mixed layer}} = \delta^{18}\text{O}_{\text{sw-mean}} - 0.750 \pm 1.25\text{‰ VSMOW}$  (Eq. 16, Tindall *et al.*, 2010)
- $\delta^{18}\text{O}_{\text{sw-mixed layer}} = \delta^{18}\text{O}_{\text{sw-mean}} - 1.375 \pm 0.625\text{‰ VSMOW}$  (Eq. 17, Roberts *et al.*, 2011)

Even though the model of Roberts *et al.* (2010) is likely the most accurate, it is hard to criticize their boundary conditions and the applied circulation model. Therefore the most objective prediction of the  $\delta^{18}\text{O}_{\text{sw-mixed layer}}$  encompasses the predictions all 3 authors. Since the range determined by the model of Tindall *et al.*, 2010 encompasses the predictions of both Zachos *et al.* (1994) and Roberts *et al.* (2011), the uncertainty on the prediction of  $\delta^{18}\text{O}_{\text{sw-mixed layer}}$  in this study will be based on their results (Eq. 18).

$$\delta^{18}\text{O}_{\text{sw-mixed layer}} = \delta^{18}\text{O}_{\text{sw-mean}} - 0.75\text{‰} \pm 1.25\text{‰ (VSMOW)}$$

Eq. 18. Based on the results of Zachos *et al.* (1994), Tindall *et al.* (2010) and Roberts *et al.* (2011), this equation predicts the  $\delta^{18}\text{O}_{\text{sw-mixed layer}}$  value based on the  $\delta^{18}\text{O}_{\text{sw-mean}}$  prediction of entire the ocean (Table 7).

### 10.3 The $\delta^{18}\text{O}_{\text{sw}}$ prediction and the salinity at the thermocline

According to Zachos *et al.* (1994), thermocline species are considered sufficiently deep in the open ocean to assume the  $\delta^{18}\text{O}$  signature of the seawater to be homogeneous. However it is uncertain whether this assumption is still valid in outer shelf setting of Aktulagay. It is likely that the thermocline species lived at shallower depths in this setting. Nevertheless the range of the measured  $\delta^{18}\text{O}$  values of the thermocline species is significantly smaller ( $\Delta\delta^{18}\text{O} = 0.69\text{‰}$ ) than the range measured for the mixed layer species ( $\Delta\delta^{18}\text{O} = 2.98\text{‰}$ ) indicating that seasonality was not significant at their living depth. Because of the large range in  $\delta^{18}\text{O}_{\text{mixed layer}}$  predictions based on Tindall *et al.* (2010) and Roberts *et al.* (2011) an additional possible error should be considered;  $\delta^{18}\text{O}_{\text{sw-mean}} - 1\text{‰ VSMOW} \leq \delta^{18}\text{O}_{\text{sw-thermocline}} \leq \delta^{18}\text{O}_{\text{sw-mean}} + 0\text{‰ VSMOW}$

This resulting equation is presented in Eq. 19.

$$\delta^{18}\text{O}_{\text{sw-thermocline}} = \delta^{18}\text{O}_{\text{sw-mean}} - 0.5 \pm 0.5\text{‰ VSMOW}$$

Eq. 19. Based on the results of Zachos *et al.* (1994), Tindall *et al.* (2010) and Roberts *et al.* (2011), this equation predicts the  $\delta^{18}\text{O}_{\text{sw-thermocline}}$  value in Aktulagay based on the  $\delta^{18}\text{O}_{\text{sw-mean}}$  prediction of entire the ocean (Table 7).

## 10.4 Results

### 10.4.1 $\delta^{13}\text{C}$

The  $\delta^{13}\text{C}$  values of *(Para)Subbotina spp.* reflect  $\delta^{13}\text{C}_{\text{DIC}}$  at the thermocline. They are within the range of 0.6‰ to 1.5‰, except for the measurement at 2.35 m which is -0.26‰ (Figure 81A). The isotope excursion at 2.35 m is equal in size ( $\pm 1.5\text{‰}$ ) as the isotope excursion recorded in the epibenthic record. Most of the  $\delta^{13}\text{C}$  measurements are in agreement with the epibenthic record with a constant positive offset of approximately 1.0‰. This is remarkable certainly given that the record is based on several *(Para)Subbotina* species. Only the measurement at 7.60 m (1.46‰) and one of the measurements at 13.25 m (1.37‰) are relatively more enriched compared to the epibenthic record.

The 9 *Acarinina spp.* measurements are spread over a significant range ( $\Delta\delta^{13}\text{C} = 3\text{‰}$ ). The  $\delta^{13}\text{C}$  values should represent the  $\delta^{13}\text{C}_{\text{DIC}}$  of the mixed layer water, but they are also influenced by the photosynthesis of their symbionts. Based on the measurements at 13.25 m a significant  $\delta^{13}\text{C}$  range of at least 1‰ exists within a single sample.

### 10.4.2 $\delta^{18}\text{O}$ and temperature

The uncorrected  $\delta^{18}\text{O}$  results are presented in Figure 81B. The  $\delta^{18}\text{O}$  values of *(Para)Subbotina spp.* range between -4.1‰ and -3.5‰. The three *(Para)Subbotina spp.* measurements at 9.55 m demonstrate that a  $\Delta\delta^{18}\text{O}$  range of 0.3‰ can exist within a single sample. The *(Para)Subbotina spp.*  $\delta^{18}\text{O}$  record does not respect the observed trends in the epibenthic  $\delta^{18}\text{O}$  record. In contrast to the  $\delta^{18}\text{O}$  values of *(Para)Subbotina spp.*, the  $\delta^{18}\text{O}$  values of *Acarinina spp.* vary over a much larger range (-7.0‰ to -4.0‰). At 19.45 m a large isotopic range of 0.9‰ is demonstrated within a single sample based on only 2

measurements. The most depleted  $\delta^{18}\text{O}$  values were measured at 1.45 m, 2.35 m and 20.25 m, ranging from -7.0‰ to -6.0‰. Moderate  $\delta^{18}\text{O}$  values were measured at 6.75 m and 13.25 m ranging from -6.0‰ to -5.0‰. The most enriched  $\delta^{18}\text{O}$  values were measured at 12.75 m, 19.45 m and 23.15 m ranging from -5.0‰ to -4.0‰.

Based on the equation of Erez and Luz (1983) (Eq. 13) and the following assumptions the temperature of the mixed layer and the thermocline can be estimated in (Figure 82):

- Negligible fluvial input
- No deviations due preservation
- $\delta^{18}\text{O}_{\text{sw-mean}} = -1\text{‰} \pm 0.25\text{‰}$  VSMOW (Eq. 12)
- $\delta^{18}\text{O}_{\text{e.c.}} = \delta^{18}\text{O} + 1\text{‰} \pm 1\text{‰}$  VPDB (Eq. 14)
- $\delta^{18}\text{O}_{\text{sw-mixed layer}} = \delta^{18}\text{O}_{\text{sw-mean}} - 0.75 \pm 1.25\text{‰}$  VSMOW (Eq. 18)
- $\delta^{18}\text{O}_{\text{sw-thermocline}} = \delta^{18}\text{O}_{\text{sw-mean}} - 0.5 \pm 0.5\text{‰}$  VSMOW (Eq. 19)

Some of these assumptions will turn out to be invalid as will be discussed in 10.5.

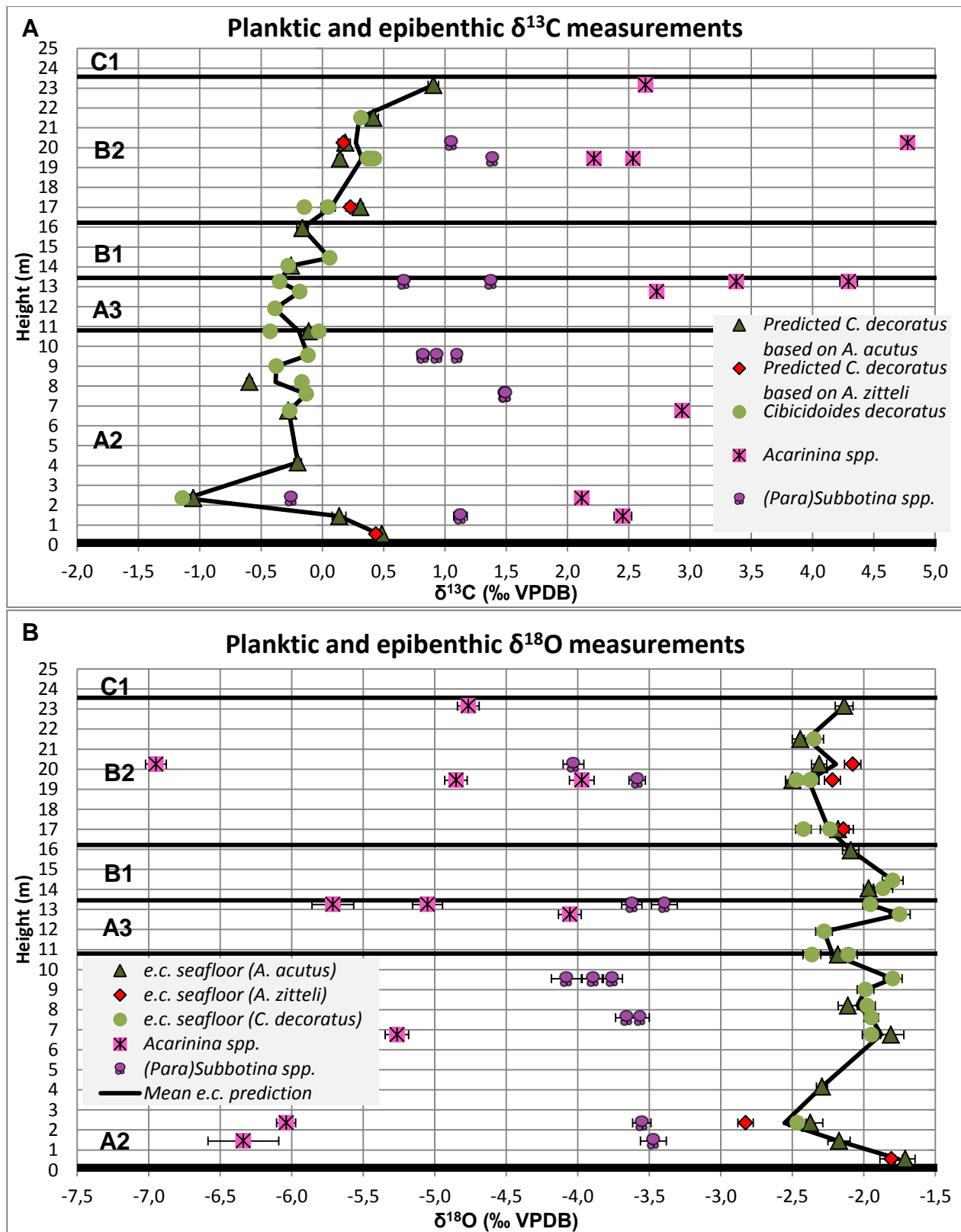


Figure 81. These plots allow to compare  $\delta^{13}\text{C}$  and  $\delta^{18}\text{O}$  of planktic foraminifers with the predicted *Cibicoides decoratus*  $\delta^{13}\text{C}$  values (A) and the predicted equilibrium calcite  $\delta^{18}\text{O}$  values at the seafloor (B).



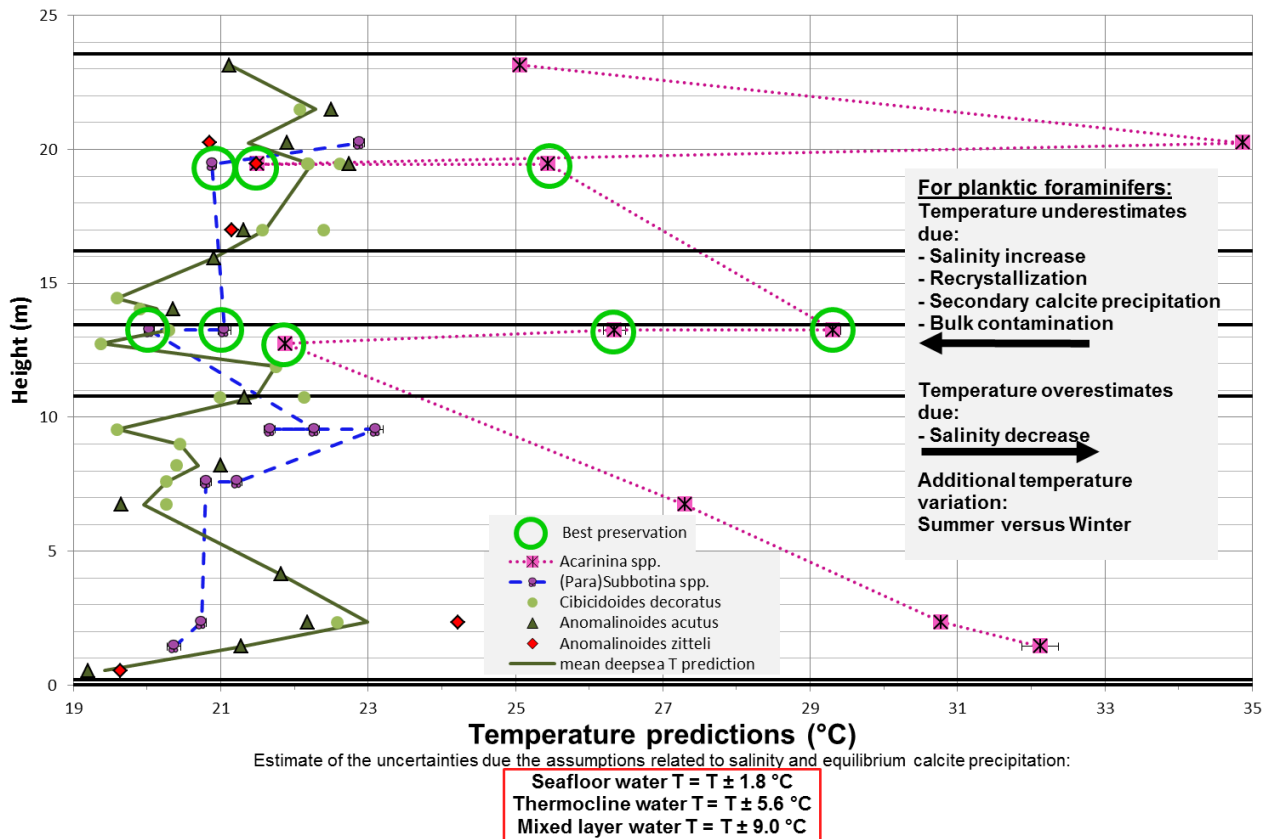


Figure 82. Temperature predictions for seafloor, thermocline and mixed layer water are calculated in the assumption of no extreme salinity deviations e.g. due monsoons or fluvial waters. This assumption will turn out to be invalid (10.5.2). Note that the thermocline water is sometimes predicted to be colder than the seafloor water. This is can be explained on the basis of the larger uncertainties on the thermocline temperature predictions.

## 10.5 Discussion planktic foraminifer isotopic values

### 10.5.1 Seasonality

According to Bemis *et al.* (2000) several reports have been made of  $\delta^{13}\text{C}$  variability exceeding 2‰ among mixed layer planktic foraminifers, despite similar water temperature and  $\delta^{13}\text{C}_{\text{DIC}}$ . One of the mean reasons for the  $\delta^{13}\text{C}$  variability is symbiont photosynthesis. The  $\delta^{13}\text{C}$  signature of the planktic mixed layer *Acarinina* species is considered to be influenced by their symbionts (D'Hondt *et al.*, 1994). According to Bemis *et al.* (2000) symbionts preferentially remove  $^{12}\text{C}$  from their microenvironment for photosynthesis and therefore cause the foraminifers to have enriched  $\delta^{13}\text{C}$  test values. The magnitude of the enrichment is related to the solar irradiance levels. Bemis *et al.* (2000) compared  $\delta^{13}\text{C}$  signatures of foraminifers that lived under solar irradiance levels of 20 to 30  $\mu\text{mol photons}\cdot\text{m}^{-2}$  with foraminifers that lived under solar irradiance levels exceeding 386  $\mu\text{mol photons}\cdot\text{m}^{-2}$  (386  $\mu\text{mol photons}\cdot\text{m}^{-2}$  corresponds to the maximum symbiont photosynthesis rate). For symbiotic foraminifer *Orbulina universa*, they observed 1‰ enrichment in the mean  $\delta^{13}\text{C}$  signature due to the higher irradiance levels. In order to predict the variation in  $\delta^{13}\text{C}$  due to the presence of symbionts in Aktulagay, the variability in irradiance should be evaluated. The magnitude of

the interannual variation in solar irradiance at the top of the atmosphere at 48°N (The position of Aktulagay in the Early Eocene based on the map of Steurbaut (2011)) varies between 100 and 480 Wm<sup>-2</sup> (Figure 83, Wisconsin State Climatology Office, 2010). Since the magnitude of the variation is of the same order as in the experiments of Bemis *et al.* (2000), a 1‰ difference between the mean δ<sup>13</sup>C signature of species that bloom during the summer and winter can be expected. This effect, combined with other vital effects can explain why a strong δ<sup>13</sup>C excursion due to ETM2 is not measured at 2.35 m and can explain the significant δ<sup>13</sup>C range within the sample at 19.45 m (Figure 81A). The effect can however not explain the relative enrichment at 20.25 m and 13.25 m compared with the other measurements. Since the irradiance variations should be related to summer and winter, the effect should also be visible in δ<sup>18</sup>O, where the winter temperatures are lower and thus result in more depleted δ<sup>18</sup>O values. At 13.25 m the more enriched δ<sup>13</sup>C measurements corresponds to the more depleted 18O measurements, indicating that it might reflect the difference between summer and winter. However at 19.45 m this is not the case and no general correlation between δ<sup>13</sup>C and δ<sup>18</sup>O exists. Therefore the variation in δ<sup>13</sup>C and δ<sup>18</sup>O values cannot be exclusively linked to seasonal temperature variation. This can inter alia be explained due to salinity variation.

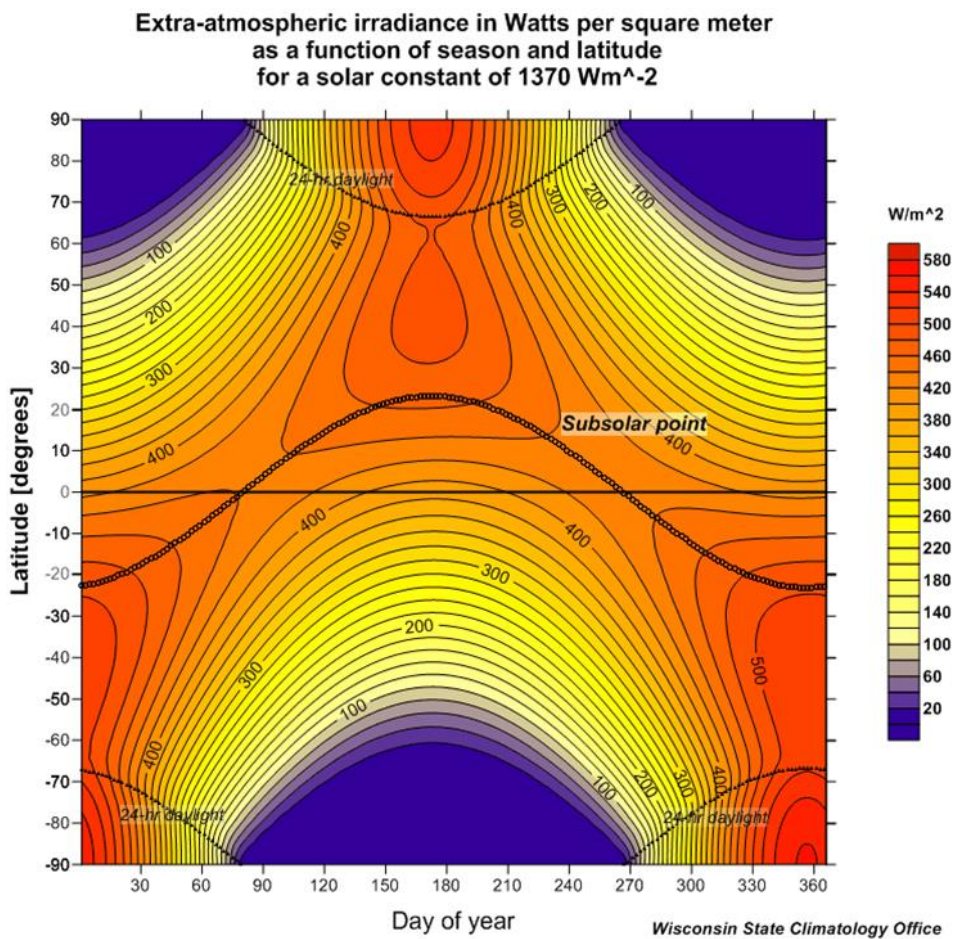


Figure 83. A plot of the theoretical average irradiance as a function of the season and latitude in W/m<sup>2</sup> for a solar constant of 1370 Wm<sup>-2</sup> (Wisconsin State Climatology Office, 2010). At 48°N the average irradiance varies between 100 and 480 Wm<sup>-2</sup>.

### 10.5.2 Productivity variation and fluvial water influence

The most enriched  $\delta^{13}\text{C}$  measurements of *Acarinina* spp. are 4.29‰ and 4.77‰ at 13.25 m and 20.25 m respectively. These  $\delta^{13}\text{C}$  values are 1.5‰ to 2.5‰ more enriched than the *Acarinina* spp. measurements in the other samples. It is unlikely that these  $\delta^{13}\text{C}$  outliers can be explained solely due large vital effects and seasonal variability. Furthermore both measurements are averages of 5 specimens. It is important to note that the  $\delta^{13}\text{C}$  outliers are not measured in the corresponding epibenthic and thermocline  $\delta^{13}\text{C}$  records. Therefore these outliers correspond to a significant  $\Delta\delta^{13}\text{C}_{\text{DIC}}$  gradient increase in the water column. A possible explanation for the significant increase in the  $\delta^{13}\text{C}_{\text{DIC}}$  gradient is a significant increase in productivity. The 'productivity' refers to the production of organic matter and thus the abundance of phytoplankton in the surface waters. Phytoplankton preferentially takes up  $^{12}\text{C}$  during photosynthesis, causing enrichment in  $\delta^{13}\text{C}_{\text{DIC}}$  of the surrounding surface water (Katz *et al.*, 2010). Thereby the tests of mixed layer planktic foraminifers will become more enriched. If the water masses mix sufficiently this productivity increase in the surface waters should also significantly increase the  $\delta^{13}\text{C}_{\text{DIC}}$  of the thermocline waters, the observation that this is not the case indicates that the water column is well stratified by temperature and/or salinity. Figure 81 demonstrates that the outliers in  $\delta^{13}\text{C}$  correspond to rather depleted  $\delta^{18}\text{O}$  values. At 20.25 m the most depleted  $\delta^{18}\text{O}$  (-6.95‰) was measured. The rise in productivity, the strong water stratification and the depleted  $\delta^{18}\text{O}$  values can be explained by the influence of brackish (fluvial/estuarine?) waters that decrease the salinity (and  $\delta^{18}\text{O}$ ) and deliver nutrients from the continent raising the productivity in the surface waters. It would also support the hypothesis that the water was well stratified due salinity. In conclusion the isotopic values indicate brackish water influence at 13.25 m and 20.25 m. The observation that the  $\delta^{18}\text{O}$  values of the thermocline species also tend to decrease at 20.25 m could thus also be related to a salinity decrease. Comparing with the data of King *et al.* (submitted) or Deprez *et al.* (submitted) does not reveal a correlation with the relative abundance of planktic foraminifers or the relative abundance of *Subbotina* spp. at 13.25 m and 20.25 m. Therefore it appears that the species were relatively tolerant to lower salinities and that the salinity decrease did not pass a certain threshold. The density of the planktic isotopic record does not allow to judge the frequency of these episodes of more brackish nutrient rich water. However the observation that the samples at 13.25 m and 20.25 m were both 20 cm below a sapropel suggests that a relation with the sapropels is possible, this is supported by the assumption that sapropels are characterized by an increase in productivity. Finally the episodes of brackish nutrient rich water could be related to the flooding events in the transgression-regression cycles.

### 10.5.3 Secondary Calcite

The preservation of the *Subbotina* spp. and *Acarinina* spp. was discussed in 6.3. A significant effect of secondary calcite on the  $\delta^{13}\text{C}$  isotopic value was considered unlikely but the effect on  $\delta^{18}\text{O}$  could not be excluded. Only the planktic specimens at 12.75 m, 13.25 m and 19.45 m did not have indications of preservation problems. The observation that most planktic measurements had more enriched  $\delta^{18}\text{O}$  values than the  $\delta^{18}\text{O}$  values of the well preserved specimens at 13.25 m and the similarity of the *Subbotina* spp.

record with the benthic record was to some extent supporting the hypothesis that the secondary calcite was not significantly influencing the  $\delta^{18}\text{O}$  values. However, even though the  $\delta^{13}\text{C}$  values of *Subbotina spp.* at 1.45 m and 2.35 m are certainly in agreement with the benthic record, the  $\delta^{18}\text{O}$  values are not. An attempt to explain these  $\delta^{18}\text{O}$  values due to significantly higher salinities at the thermocline seems implausible. Since for the specimens at 1.45 m and 2.35 m were considered the worst preserved planktic specimens and a thin coat of secondary calcite was locally observed on their tests (SEM-pictures Figure 35.1d; Figure 35.2e), it must be concluded that this thin coating was not insignificant and probably responsible for a relative 0.5+‰ increase. Although the presence of such coat was not proven for the other measurements, it becomes less unlikely that these measurements could also be influenced by some secondary calcite. It is therefore dangerous to interpret smaller variations in  $\delta^{18}\text{O}$  in the planktic records.

#### 10.5.4 The temperature predictions

The absolute temperature prediction at the thermocline has an estimated uncertainty of 5.6 °C (Figure 82). However the uncertainty on the prediction of the thermocline temperature relative to the seafloor temperature is smaller because the value cannot be lower than the temperatures at the seafloor (Figure 82) and because the uncertainty is mainly based on salinity. Thus if the salinity at the seafloor is underestimated, it is assumable that the salinity at the thermocline is also underestimated. Therefore it is concluded that the temperatures at the thermocline must have been 0 to 2.5 °C higher than the seafloor temperatures based on the measurements of well-preserved specimens at 19.45 m. This is in line with the assumed outer shelf setting of Aktulagay.

The same reasoning cannot be made for temperature estimates of the mixed layer. The large uncertainty concerning the salinity of the mixed layer based on the models of Tindall *et al.* (2010) and Roberts *et al.* (2011), combined with the large measured  $\delta^{18}\text{O}$  variation do not allow an accurate temperature prediction.

### 10.6 Summary

First of all *Acarinina spp.* were considered mixed layer symbiont bearing planktic foraminifers. The up to 0.9‰ intrasample variation in  $\delta^{13}\text{C}$  was considered mainly a reflection of the seasonal variation in the activity of their photo symbionts. In addition vital effects might have caused  $\delta^{13}\text{C}$  differences between different species. However both effects were considered insufficient to explain the highly enriched  $\delta^{13}\text{C}$  values at 20.25 m and at 13.25 m. These high  $\delta^{13}\text{C}$  values corresponded to extremely depleted  $\delta^{18}\text{O}$  values. It was proposed that these extreme  $\delta^{13}\text{C}$  values corresponded to periods of increased paleoproductivity and that the depleted  $\delta^{18}\text{O}$  values corresponded to salinity decreases. Therefore it was assumed that these periods were characterized by the influence of fluvial/estuarine nutrient rich water. It was further speculated that these periods of increased productivity were possibly related to the nearby sapropels. The observation that these strong isotopic variations were not observed for thermocline *Subbotina spp.* was suggested to be a reflection of the strong water column stratification mainly as a consequence of salinity. The smaller variations in  $\delta^{18}\text{O}$  measured for planktic species were not interpreted because the influence of secondary calcite could not be excluded, certainly not in the lower 5 m of the

section. Due to the high uncertainty concerning salinity, the mixed layer temperatures could not be predicted. The thermocline temperatures on the other hand could be estimated to be 0 to 2.5 °C warmer than the seafloor temperatures based on the well preserved specimens at 19.45 m. Although this temperature difference might not be representative for the entire section and information about the salinity would be desired to confirm this temperature estimate.



## 11 Conclusion

In conclusion this study provides valuable information concerning the paleoenvironment and paleoecology in Aktulagay during the Early Eocene.

First of all the microhabitats of several benthic species were identified. *Anomalinoidea acutus*, *Anomalinoidea rubiginosis*, *Anomalinoidea zitteli*, *Cibicidoides cf. rigidus*, *Cibicidoides decoratus* and *Cibicidoides rigidus* were identified as epibenthic species. *Cibicidoides cf. decoratus*, *Cibicidoides sp. 1*, *Lenticulina spp.*, *Marginulinopsis spp.*, *Nuttallides truempyi*, *Percultazonaria sp. 1*, *Pyramidulina sp. 1*, *Spiroloculina sp. 1*, *Stainforthia sp. 1* and *Turrilina brevispira* were identified as either epibenthic or shallow endobenthic species. *Alabamina midwayensis*, *Allomorphina sp. 1*, *Anomalinoidea cf. praeacutus*, *Aragonia aragonensis*, *Bulimina (aff.) midwayensis*, *Bulimina kugleri*, *Loxostomoides applinae*, *Oridorsalis plummerae*, *Pulsiphonina prima*, *Ramulina sp. 1*, *Stilostomella sp. 1*, *Uvigerina elongata* and *Valvulineria scrobiculata* were identified as shallow endobenthic species and *Bulimina aksuatica*, *Bulimina cf. thanetensis*, *Coryphostoma spp.*, *Dentalina sp. 1* and *Nodosaria sp. 1* were identified as deep endobenthic species.

Secondly the effect of kinetic disequilibrium calcite precipitation proposed by Wendler *et al.* (2013) for *Lenticulina spp.* during the Cretaceous could be verified for the *Lenticulina* species of the Early Eocene. In addition *Marginulinopsis spp.*, *Nodosaria sp. 1* and *Percultazonaria sp. 1* were also considered affected by the kinetic disequilibrium calcite precipitation effect. It is therefore discouraged to apply isotopic measurements of these species for paleoenvironmental reconstructions.

Thirdly the isotopes indicated a migration event of endobenthic species through sediment that could be associated with low oxygen conditions at the seafloor. By comparing with the relative abundance data of Deprez *et al.* (submitted), the tolerance of these species for low oxygen conditions could be estimated. *Anomalinoidea acutus*, *Coryphostoma spp.*, *Turrilina brevispira* and *Uvigerina elongata* were considered tolerant to low oxygen conditions while *Bulimina aksuatica*, *Cibicidoides cf. decoratus* and *Loxostomoides applinae* were considered unsuccessful under low oxygen conditions. *Anomalinoidea cf. praeacutus*, *Epistominella minuta*, *Gyroidinoidea octocameratus*, *Lenticulina spp.*, *Oridorsalis plummerae*, *Paralabamina lunata*, *Spiroloculina spp.*, *Spiroplectinella esnaensis*, *Valvalabamina depressa*, *Valvulineria scrobiculata* did not significantly change in relative abundance during these circumstances.

Fourthly the hypothesis that a pH gradient within the sediment has a dominant effect on the  $\delta^{18}\text{O}$  values of foraminifers was rejected (proposed by e.g. Bemis *et al.*, 1998; Schmiedl *et al.*, 2004; Friedrich *et al.*, 2006; Wendler *et al.*, 2013), this is in support of e.g. McCorkle *et al.* (1997) and Fontanier *et al.* (2008). It was concluded that  $\delta^{18}\text{O}$  is mainly a reflection of the food preference and the vital effects of foraminifers instead of their microhabitat.

Fifthly the paleotemperature at the sea floor during the studied time interval was estimated to vary between 19 °C and 24 °C ( $\pm 1.8$  °C), the thermocline temperatures were estimated to be 0 °C to 2.5 °C higher. The mixed layer temperature could not be estimated due to the high ( $\pm 9$  °C) uncertainty on temperature predictions that is mainly a consequence of the unknown salinity. The highest seafloor

temperatures were associated with the nearby presence of a hyperthermal (likely ETM2) and with the EECO.

Sixthly the seafloor  $\delta^{13}\text{C}$  record revealed a gradual increasing  $\delta^{13}\text{C}$  trend from middle NP11 to middle NP 13 ( $\Delta\delta^{13}\text{C} = 1\text{‰}$ ) in Aktulagay. This trend was considered a reflection of the global deep sea  $\delta^{13}\text{C}$  trend after comparison with Cramer *et al.* (2009).

Seventhly enriched  $\delta^{13}\text{C}$  values associated with depleted  $\delta^{18}\text{O}$  values of mixed layer planktic foraminifers indicated the occurrence of periods with increased influx of nutrient rich fluvial waters in Aktulagay.

Given our interesting results, additional research in Aktulagay is certainly encouraged.

A first suggestion would be to carry out Mg/Ca ratio measurements on the foraminifers in Aktulagay. Jorissen *et al.* (2007) and Katz *et al.* (2010) consider Mg/Ca ratio measurements required next to the  $\delta^{18}\text{O}$  measurements to successfully reconstruct the paleotemperature and the salinity of the seawater. Since salinity remains a major problem in this study, Mg/Ca measurements would significantly decrease the uncertainties on the temperature predictions and would allow a temperature prediction for the mixed layer. A second suggestion is to sample the sapropels and to perform isotopic measurements on the foraminifers within these layers.

A third suggestion is to continue the isotopic record into the Tolagaysor formation (Lithological Unit C, above the Aktulagay Formation), although it is possible that the preservation of the foraminifers in these coarser sediments will not allow it.



## 12 References

- Basak, C., Rathburn, A.E., Pérez, M.E., Martin, J.B., Kluesner, J.W., Levin, L.A., De Deckker, P., Gieskes, J.M. and Abriani, M. (2009). Carbon and oxygen isotope geochemistry of live (stained) benthic foraminifera from the Aleutian Margin and the Southern Australian Margin. *Marine Micropaleontology* 70, p. 89-101.
- Bemis, B.E., Spero, H.J., Bijma, J. and Lea, D.W. (1998). Reevaluation of the oxygen isotopic composition of planktonic foraminifera: Experimental results and revised paleotemperature equations. *Paleoceanography* 13, p. 150-160.
- Bemis, B.E., Spero, H.J., Lea, D.W. and Bijma, J. (2000). Temperature influence on the carbon isotopic composition of *Globigerina bulloides* and *Orbulina universa* (planktonic foraminifera). *Marine Micropaleontology* 38, p. 213-228.
- Bijl, P.K., Schouten, S., Sluijs, A., Reichert, G.-J., Zachos, J.C. and Brinkhuis, H. (2009). Early Palaeogene temperature evolution of the southwest Pacific Ocean. *Nature* 461, p. 776-779.
- Bowen, G.J. and Wilkinson, B. (2002). Spatial distribution of  $\delta^{18}\text{O}$  in meteoric precipitation. *Geology* 30, p. 315-318.
- Buzas, M.A., Culver, S.J., and Jorissen, F.J. (1993). A statistical evaluation of the microhabitats of living (stained) infaunal benthic foraminifera. *Mar. Micropaleontol.* 20, p. 311–320.
- Carney, R.S. (1989). Examining Relationships Between Organic Carbon Flux and Deep-Sea Deposit Feeding. *In Ecology of Marine Deposit Feeders*, G. Lopez, G. Taghon, and J. Levinton (eds.), Springer New York, p. 24-58.
- Cooke, S. and Rohling, E.J. (2001). Stable Isotopes in Foraminiferal Carbonate. Southampton Oceanography Centre Internal Document 72, 55 p.
- Corliss, B.H. and Emerson, S. (1990). Distribution of rose bengal stained deep-sea benthic foraminifera from the Nova Scotian continental margin and Gulf of Maine. *Deep Sea Res. Part Ocean. Res. Pap.* 37, p. 381-400.
- Cramer, B.S., Aubry, M.-P., Miller, K.G., Olsson, R.K., Wright, J.D. and Kent, D.V. (1999). An exceptional chronologic, isotopic, and clay mineralogic record of the latest Paleocene thermal maximum, Bass River, NJ, ODP 174AX. *Bull. Soc. Geol. Fr.* 170, p. 883-897.
- Cramer, B.S., Wright, J.D., Kent, D.V. and Aubry, M.-P. (2003). Orbital climate forcing of  $\delta^{13}\text{C}$  excursions in the late Paleocene–early Eocene (chrons C24n–C25n). *Paleoceanography* 18(4), 25 p.
- Cramer, B.S., Toggweiler, J.R., Wright, J.D., Katz, M.E. and Miller, K.G. (2009). Ocean overturning since the Late Cretaceous: Inferences from a new benthic foraminiferal isotope compilation. *Paleoceanography* 24(4), 14 p.
- Creech, J.B., Baker, J.A., Hollis, C.J., Morgans, H.E.G. and Smith, E.G.C. (2010). Eocene sea temperatures for the mid-latitude southwest Pacific from Mg/Ca ratios in planktonic and benthic foraminifera. *Earth and Planetary Science Letters* 299, p. 483-495.

- D'Hondt, S. and Arthur, M.A. (1996). Late Cretaceous Oceans and the Cool Tropic Paradox. *Science* 271, p. 1838-1841.
- D'Hondt, S., Zachos, J.C. and Schultz, G. (1994). Stable isotope signals and photosymbiosis in late Paleocene planktic foraminifera. *Paleobiology* 20, p. 391-406.
- Deprez, A. (2012). Micropaleontologische karakterisering van paleomilieuontwikkelingen in Aktulagay, Kazachstan, tijdens de Vroeg-Eocene broeikasaarde. Promotor: Speijer, R. P. KULeuven. 145 p.
- Deprez, A., Stassen, P., D'haenens, S., Steurbaut, E., King, C. and Speijer, R.P. (submitted). Early Eocene changes in trophic and redox conditions in the northern Peri-Tethys (Aktulagay, Kazakhstan) based on benthic foraminifera. *Marine Micropaleontology*, 34 p.
- Dercourt, J., Gaetani, M., Vrielynck, B., Barrier, E., Biju-Duval, B., Brunet, M.F., Cadet, J.P., Crasquin, S. and Sandulescu, M. (2000). Atlas peri-Tethys palaeogeographical maps, Commission for the Geological Map of the World, 268 p.
- Edgar, K.M., Bohaty, S.M., Gibbs, S.J., Sexton, P.F., Norris, R.D. and Wilson, P.A. (2012). Symbiotic "bleaching" in planktic foraminifera during the Middle Eocene Climatic Optimum. *Geology* 41, p. 15-18.
- Emrich, K., Ehhalt, D.H. and Vogel, J.C. (1970). Carbon isotope fractionation during the precipitation of calcium carbonate. *Earth and Planetary Science Letters* 8, p. 363-371.
- Erez, J. and Luz, B. (1983). Experimental paleotemperature equation for planktonic foraminifera. *Geochim. Cosmochim. Acta* 47, p. 1025-1031.
- Fontanier, C., Mackensen, A., Jorissen, F.J., Anschutz, P., Licari, L. and Griveaud, C. (2006). Stable oxygen and carbon isotopes of live benthic foraminifera from the Bay of Biscay: Microhabitat impact and seasonal variability. *Mar. Micropaleontol.* 58, p. 159-183.
- Franco-Fraguas, P., Costa, K.B. and Toledo, F.A.D.L. (2011). Stable isotope/test size relationship in *Cibicides wuellerstorfi*. *Braz. J. Ocean.* 59(3), p. 287-291.
- Friedrich, O., Schmiedl, G. and Erlenkeuser, H. (2006). Stable isotope composition of Late Cretaceous benthic foraminifera from the southern South Atlantic: Biological and environmental effects. *Marine Micropaleontology* 58, p. 135-157.
- Geological map of Kazakhstan, original authors unknown. consulted in 2013.  
[http://img-fotki.yandex.ru/get/3415/invngn.10/0\\_37e75\\_ee7b6068\\_orig](http://img-fotki.yandex.ru/get/3415/invngn.10/0_37e75_ee7b6068_orig)
- Gaetani, M., Dercourt, J. and Vrielynck, B. (2003). The Peri-Tethys programme: achievements and results. *Episodes* 26(2), p. 79-93.
- Galeotti, S., Krishnan, S., Pagani, M., Lanci, L., Gaudio, A., Zachos, J.C., Monechi, S., Morelli, G. and Lourens, L. (2010). Orbital chronology of Early Eocene hyperthermals from the Contessa Road section, central Italy. *Earth and Planetary Science Letters* 290, p. 192-200.
- Gradstein, F.M., Ogg, J.G. and Schmitz, M.D. (2012). *The geologic time scale 2012*, Amsterdam; Boston: Elsevier.

- Grossman, E.L. (2012). Applying Oxygen Isotope Paleothermometry in Deep Time. *In* Ivany, L.C. and Huber, B.T. (eds.), *Reconstructing Earth's Deep-Time Climate-The State of the Art in 2012*. The Paleontological Society Papers 18, p. 67.
- Head, J.J., Bloch, J.I., Hastings, A.K., Bourque, J.R., Cadena, E.A., Herrera, F.A., Polly, P.D. and Jaramillo, C.A. (2009). Giant boid snake from the Palaeocene neotropics reveals hotter past equatorial temperatures. *Nature* 457, p. 715-717.
- Hollis, C.J., Handley, L., Crouch, E.M., Morgans, H.E.G., Baker, J.A., Creech, J., Collins, K.S., Gibbs, S.J., Huber, M., Schouten, S., Zachos, J.C. and Pancost R.D. (2009). Tropical sea temperatures in the high-latitude South Pacific during the Eocene. *Geology* 37, p. 99-102.
- Hou, Z., Sket, B., Fišer, C. and Li, S. (2011). Eocene habitat shift from saline to freshwater promoted Tethyan amphipod diversification. *Proceedings of the National Academy of Sciences of the United States of America* 108(35), p. 14533-14538.
- Huber, M. and Caballero, R. (2011). The early Eocene equable climate problem revisited. *Climate of the Past* 7, p. 603–633.
- International Atomic Energy Agency (IAEA) and World Meteorological Organization (WMO) (1998). Global Network for Isotopes in Precipitation (GNIP) database, 3rd release.  
<http://www-naweb.iaea.org/napc/ih/index.html>.
- Jorissen, F.J. (1999). Benthic foraminiferal microhabitats below the sediment-water interface. *In* Sen Gupta, B. K. *Modern Foraminifera*, Dordrecht: Kluwer Academic Publishers, p. 161-179.
- Jorissen, F., Fontanier, C. and Thomas, E. (2007). Paleooceanographical proxies based on deep-sea benthic foraminiferal assemblage characteristics. *In* Hillaire-Marcel C. and de Vernal, A., *Proxies Late Cenozoic Paleooceanogr. Pt. 2: Biological tracers and biomarkers*, p. 263-326.
- Katz, M.E., Katz, D.R., Wright, J.D., Miller, K.G., Pak, D.K., Shackleton, N.J. and Thomas, E. (2003). Early Cenozoic benthic foraminiferal isotopes: Species reliability and interspecies correction factors. *Paleoceanography* 18(2), 12 p.
- Katz, M.E., Cramer, B.S., Franzese, A., Hönisch, B., Miller, K.G., Rosenthal, Y. and Wright, J.D. (2010). Traditional and Emerging Geochemical Proxies in Foraminifera. *Journal of Foraminiferal Research* 40(2), p. 165-192.
- Keating-Bitonti, C.R., Ivany, L.C., Affek, H.P., Douglas, P. and Samson, S.D. (2011). Warm, not super-hot, temperatures in the early Eocene subtropics. *Geology* 39(8), p. 771-774.
- Kennett, J.P. and Stott, L.D. (1990). Proteus and Proto-oceanus: ancestral Paleogene oceans as revealed from Antarctic stable isotopic results: ODP Leg 113. *In* Barjer, P. F., Kennet, J. P., *et al.*, *Proc. Ocean Drill. Program 113*, p. 685-880.
- King, C., Iakovleva, A. I., Steurbaut, E., Heilmann-Clausen, C. and Ward, D. J. (submitted). The Aktulagay section, west Kazakhstan: a key site for Early Eocene northern mid-latitude stratigraphy. *Stratigraphy*, p. 96.

- Lourens, L.J., Sluijs, A., Kroon, D., Zachos, J.C., Thomas, E., Röhl, U., Bowles, J. and Raffi, I. (2005). Astronomical pacing of late Palaeocene to early Eocene global warming events. *Nature* 435, p. 1083-1087.
- Luterbacher, H.P., Ali, J.R., Brinkhuis, H., Gradstein, F.M., Hooker, J.J., Monechi, S., Ogg, J.G., Powell, J., Röhl, U., Sanfilippo, A. and Schmitz B. (2005). The Paleogene Period. *In* Gradstein, F., Ogg, J. and Smith, A. (eds.), *A Geologic Time Scale 2004*, Cambridge University Press, p. 384-408.
- Mackensen, A., Schumacher, S., Radke, J. and Schmidt, D.N. (2000). Microhabitat preferences and stable carbon isotopes of endobenthic foraminifera: clue to quantitative reconstruction of oceanic new production? *Mar. Micropaleontol.* 40, p. 233-258.
- McConnaughey, T. (1989).  $^{13}\text{C}$  and  $^{18}\text{O}$  isotopic disequilibrium in biological carbonates: I. Patterns. *Geochim. Cosmochim. Acta* 53, p. 151-162.
- McCorkle, D.C., Emerson, S.R. and Quay, P.D. (1985). Stable carbon isotopes in marine porewaters. *Earth and Planetary Science Letters* 74, p. 13-26.
- McCorkle, D.C., Keigwin, L.D., Corliss, B.H. and Emerson, S.R. (1990). The influence of microhabitats on the carbon isotopic composition of deep-sea benthic foraminifera. *Paleoceanography* 5, p. 161-185.
- McCorkle, D.C., Corliss, B.H. and Farnham, C.A. (1997). Vertical distributions and stable isotopic compositions of live (stained) benthic foraminifera from the North Carolina and California continental margins. *Deep Sea Res. Part Ocean. Res. Pap.* 44, p. 983-1024.
- Microsoft Corporation and NAVTEQ (2013). World Map, Online Maps, Satellite Maps - National Geographic. From <http://maps.nationalgeographic.com/map-machine>
- Moodley, L., van der Zwaan, G., Rutten, G.M., Boom, R.C., and Kempers, A. (1998). Subsurface activity of benthic foraminifera in relation to porewater oxygen content: laboratory experiments. *Mar. Micropaleontol.* 34, p. 91-106.
- Mulholland, J.W. (1998). The parasequence. *The Leading Edge of Geophysics Exploration*, Society of Exploration Geophysicists, p. 1374-1376.
- Muttoni, G., Gaetani, M., Kent, D.V., Sciunnach, D., Angiolini, L., Berra, F., Garzanti, E., Mattei, M., and Zanchi, A.M. (2009). Opening of the Neo-Tethys Ocean and the Pangea B to Pangea A transformation during the Permian. *Georabia* 14, p. 17-48.
- Nørgaard, J.V., Kipphardt, H., Valkiers, S. and Taylor P.D.P. (1999): IMEP-8: Carbon and oxygen isotope ratios in  $\text{CO}_2$ , Institute for Reference Materials and Measurements, 46 p.
- Oberhänsli, H. and Benjamovski, V. (2000). Dysoxic bottom water events in the peri-Tethys during the late Ypresian: A result of changes in the evaporation/precipitation balance in adjacent continental regions. *GFF* 122:1, p. 121-123.
- Pak, D.K. and Miller, K.G. (1995). Isotopic and faunal record of Paleogene deep-water transition in the North Pacific: Proceedings of the Ocean Drilling Program, *Scientific Results* 145, p. 265-281.

- Papadimitriou, S., Kennedy, H. and Thomas, D.N. (2004). Rates of organic carbon oxidation in deep sea sediments in the eastern North Atlantic from pore water profiles of O<sub>2</sub> and the  $\delta^{13}\text{C}$  of dissolved inorganic carbon. *Mar. Geol.* 212, p. 97-111.
- Pearson, P.N., Ditchfield, P.W., Singano, J., Harcourt-Brown, K.G., Nicholas, C.J., Olsson, R.K., Shackleton, N.J. and Hall, M.A. (2001). Warm tropical sea surface temperatures in the Late Cretaceous and Eocene epochs. *Nature* 413, p. 481-487.
- Pearson, P.N., Van Dongen, B.E., Nicholas, C.J., Pancost, R.D., Schouten, S., Singano, J.M. and Wade, B.S. (2007). Stable warm tropical climate through the Eocene Epoch. *Geology* 35, p. 211-214.
- Rathburn, A.E., Corliss, B.H., Tappa, K.D. and Lohmann, K.C. (1996). Comparisons of the ecology and stable isotopic compositions of living (stained) benthic foraminifera from the Sulu and South China Seas. *Deep Sea Research I* 43(10), p. 1617-1646.
- Risgaard-Petersen, N., Langezaal, A.M., Ingvarsdén, S., Schmid, M.C., Jetten, M.S.M., Op den Camp, H.J.M., Derksen, J.W.M., Piña-Ochoa, E., Eriksson, S.P., Nielsen, P.L., Revsbech, N.P., Cedhagen, T. and Van der Zwaan G.J. (2006). Evidence for complete denitrification in a benthic foraminifer. *Nature* 443, p. 93-96.
- Roberts, C.D., LeGrande, A.N. and Tripathi, A.K. (2011). Sensitivity of seawater oxygen isotopes to climatic and tectonic boundary conditions in an early Paleogene simulation with GISS ModelE-R. *Paleoceanography* 26, 16 p.
- Rosoff, D.B., and Corliss, B.H. (1992). An analysis of recent deep-sea benthic foraminiferal morphotypes from the Norwegian and Greenland seas. *Palaeogeogr. Palaeoclim. Palaeoecol.* 91, p. 13-20.
- Schmiedl, G., Pfeilsticker, M., Hemleben, C. and Mackensen, A. (2004). Environmental and biological effects on the stable isotope composition of recent deep-sea benthic foraminifera from the western Mediterranean Sea. *Mar. Micropaleontol.* 51, p. 129-152.
- Schumacher, S., Jorissen, F.J., Mackensen, A., Gooday, A.J. and Pays, O. (2010). Ontogenetic effects on stable carbon and oxygen isotopes in tests of live (Rose Bengal stained) benthic foraminifera from the Pakistan continental margin. *Mar. Micropaleontol.* 76, p. 92-103.
- Scotese, C. R. (2001). Atlas of Earth History, PALEOMAP Project, *Paleogeography* 1, 52 p.
- Sexton, P.F. and Wilson, P.A. (2009). Preservation of benthic foraminifera and reliability of deep-sea temperature records: Importance of sedimentation rates, lithology, and the need to examine test wall structure. *Paleoceanography* 24, 14 p.
- Sexton, P.F., Wilson, P.A. and Pearson, P.N. (2006). Microstructural and geochemical perspectives on planktic foraminiferal preservation: "Glassy" versus "Frosty." *Geochemistry Geophysics Geosystems* 7(12), 29 p.
- Sluijs, A., Schouten, S., Pagani, M., Woltering, M., Brinkhuis, H., Damsté, J.S.S., Dickens, G.R., Huber, M., Reichert, G.-J., Stein, R., Matthiessen J., Lourens L.J., Pendergast N., Backman J., Moran, K., Clemens S., Cronin T., Eynaud F., Gattacceca J., Jakobsson M., Jordan R., Kaminski M., King J., Koc N., Martinez N. C., McInroy D., Moore T.C., O'Regan M., Onodera J., Pälike H., Rea B., Rio D., Sakamoto T., Smith D.C., St John K. E. K., Suto I., Suzuki N., Takahashi K., Watanabe M.

- and Yamamoto M. (2006). Subtropical Arctic Ocean temperatures during the Palaeocene/Eocene thermal maximum. *Nature* 441, p. 610-613.
- Smith, R.Y., Basinger, J.F. and Greenwood, D.R. (2009). Depositional setting, fossil flora, and paleoenvironment of the Early Eocene Falkland site, Okanagan Highlands, British Columbia. *Canadian Journal of Earth Sciences* 46, p. 811-822.
- Spero, H.J. and Lea, D.W. (1996). Experimental determination of stable isotope variability in *Globigerina bulloides*: implications for paleoceanographic reconstructions. *Mar. Micropaleontol.* 28, p. 231-246.
- Spero, H.J., Bijma, J., Lea, D.W. and Bemis, B.E. (1997). Effect of seawater carbonate concentration on foraminiferal carbon and oxygen isotopes. *Nature* 390, p. 497-500.
- Stassen, P., Thomas, E. and Speijer, R. (2012). The progression of environmental changes during the onset of the Paleocene-Eocene thermal maximum (New Jersey Coastal Plain). *Austrian Journal of Earth Sciences* 105, p. 169-178.
- Steurbaut, E. (2011). New calcareous nannofossil taxa from the Ypresian (Early Eocene) of the North Sea Basin and the Turan Platform in West Kazakhstan. *Bulletin de l'Institut royal des Sciences naturelles de Belgique, Sciences de la Terre* 81, p. 247-277.
- Tindall, J., Flecker, R., Valdes, P., Schmidt, D.N., Markwick, P. and Harris, J. (2010). Modelling the oxygen isotope distribution of ancient seawater using a coupled ocean-atmosphere GCM: Implications for reconstructing early Eocene climate. *Earth and Planetary Science Letters* 292, p. 265-273.
- Ulmishek, Gregory F. (2003). Petroleum Geology and Resources of the West Siberian Basin, Russia, U.S. Geological Survey Bulletin, 49 p.
- Vandenbergh, N., Hilgen, F.J., Speijer, R.P., Ogg, J.G., Gradstein, F.M., Hammer, O., Hollis, C.J. and Hooker, J.J. (2012). Chapter 28 - The Paleogene Period. *In The Geologic Time Scale*, Boston: Elsevier, p. 855-921.
- Wendler, I., Huber, B.T., MacLeod, K.G. and Wendler, J.E. (2013). Stable oxygen and carbon isotope systematics of exquisitely preserved Turonian foraminifera from Tanzania - Understanding isotopic signatures in fossils. *Marine Micropaleontology* 102, p. 1-33.
- Wise, S.W., Jr., Breza, J.R., Harwood, D.M. and Wei, W. (1991). Paleogene glacial history of Antarctica. *In Müller, D.W., McKenzie, J.A., and Weissert, H. (eds.), Controversies in Modern Geology: Evolution of Geological Theories in Sedimentology, Earth History and Tectonics*: Cambridge, Cambridge University Press, p. 133-171.
- Zachos, J., Pagani, M., Sloan, L., Thomas, E. and Billups, K. (2001). Trends, Rhythms, and Aberrations in Global Climate 65 Ma to Present. *Science* 292, p. 686-693.
- Zachos, J.C., Stott, L.D. and Lohmann, K.C. (1994). Evolution of Early Cenozoic marine temperatures. *Paleoceanography* 9, p. 353-387.

- Zachos, J.C., Schouten, S., Bohaty, S., Quattlebaum, T., Sluijs, A., Brinkhuis, H., Gibbs, S.J., and Bralower, T.J. (2006). Extreme warming of mid-latitude coastal ocean during the Paleocene-Eocene Thermal Maximum: Inferences from TEX86 and isotope data. *Geology* 34, p. 737-740.
- Zachos, J.C., Dickens, G.R. and Zeebe, R.E. (2008). An early Cenozoic perspective on greenhouse warming and carbon-cycle dynamics. *Nature* 451, p. 279-283.





Appendix I.: Measurements - Benthic species											
Height (m)	Number of Sample	Species name	Number of fossils (Size fraction, µm)	Corrected δ <sup>13</sup> C Mean	Corrected δ <sup>13</sup> C Standard Deviation	Corrected δ <sup>18</sup> O Mean	Corrected δ <sup>18</sup> O Standard Deviation	measured mass (µg)	Ultrasonic bath (yes/no)	Total CO <sub>2</sub> pressure in mass spectrometer	Number of gas expansions
2.35	4	<i>Alabamina midwayensis</i>	6 (180-250)	-1.897	0.031	-2.478	0.066		y	812	0
10.75	13	<i>Alabamina midwayensis</i>	6 (180-250)	-0.971	0.030	-2.036	0.079		y	658	0
19.45	22	<i>Alabamina midwayensis</i>	13 = 10 (125-180) + 3 (180-250)	-0.788	0.020	-2.434	0.053	45	y	763	0
10.75	13	<i>Allomorpha sp. 1</i>	8(125-180)	-1.057	0.029	-1.755	0.076		y	324	0
0.55	2	<i>Anomalinoideus acutus</i>	6(180-250)	0.166	0.019	-2.161	0.068		y	676	0
1.45	3	<i>Anomalinoideus acutus</i>	6(180-250)	-0.182	0.055	-2.624	0.078		y	410	0
2.35	4	<i>Anomalinoideus acutus</i>	6 (180-250)	-1.372	0.025	-2.825	0.087		y	818	0
4.15	6	<i>Anomalinoideus acutus</i>	5 (180-250)	-0.519	0.031	-2.744	0.039		y	1181	1
6.75	8	<i>Anomalinoideus acutus</i>	6 (180-250)	-0.598	0.032	-2.261	0.090		y	816	0
8.20	10	<i>Anomalinoideus acutus</i>	6 (180-250)	-0.914	0.026	-2.562	0.068		y	649	0
10.75	13	<i>Anomalinoideus acutus</i>	6 (180-250)	-0.430	0.030	-2.633	0.052		y	631	0
14.05	17	<i>Anomalinoideus acutus</i>	12 (125-180)	-0.572	0.022	-2.417	0.036		y	814	0
15.95	19	<i>Anomalinoideus acutus</i>	14 (125-180)	-0.481	0.045	-2.542	0.057		y	707	0
17.00	20	<i>Anomalinoideus acutus</i>	5 (180-250)	-0.008	0.026	-2.630	0.076		y	700	0
19.45	22	<i>Anomalinoideus acutus</i>	3 (180-300)	-0.176	0.025	-2.950	0.048	49	y	745	0
20.25	23	<i>Anomalinoideus acutus</i>	6 (180-250)	-0.132	0.041	-2.763	0.053		y	920	0
21.50	24	<i>Anomalinoideus acutus</i>	5 (180-250)	0.097	0.042	-2.895	0.055	49	y	837	0
23.15	25	<i>Anomalinoideus acutus</i>	6 (180-250)	0.587	0.043	-2.588	0.062		y	767	0
10.75	13	<i>Anomalinoideus cf. praeacutus</i>	18 = 3 (125- 180) and 15 (63-125)	-0.710	0.043	-2.700	0.105		y	769	0
14.05	17	<i>Anomalinoideus cf. praeacutus</i>	24 = 17(125- 180) + 7 (63-125)	-1.103	0.041	-2.576	0.055		y	1070	0
10.75	13	<i>Anomalinoideus rubiginosis</i>	2 = 1 (300+) + 1 (125- 180)	-0.365	0.022	-2.649	0.046	41	y	756	0
0.55	2	<i>Anomalinoideus zitteli</i>	7 = 3 (125- 180) + 4 (180-250)	0.478	0.030	-2.124	0.079		y	491	0
2.35	4	<i>Anomalinoideus zitteli</i>	3 (250-300)	-1.088	0.042	-3.143	0.054		y	800	0
17.00	20	<i>Anomalinoideus zitteli</i>	3 (250-300)	0.271	0.037	-2.459	0.071	53	y	658	0
19.45	22	<i>Anomalinoideus zitteli</i>	2 (250-300)	0.402	0.030	-2.535	0.055	53	y	778	0
20.25	23	<i>Anomalinoideus zitteli</i>	2 (250-300) + 4(180- 250)	0.213	0.040	-2.393	0.057		y	818	0
14.05	17	<i>Aragonia aragonensis</i>	19 = 5 (125- 180) + 14 (63-125)	-0.999	0.041	-2.274	0.112		n	272	0
19.45	22	<i>Aragonia aragonensis</i>	30 (125-180)	-0.975	0.014	-2.417	0.050		y	702	0
19.45	22	<i>Aragonia aragonensis (Bulk contamination)</i>	25 (125-180)	-0.970	0.035	-2.612	0.062	52	y	726	0
19.45	22	<i>Bulimina (aff.) midwayensis</i>	2 (300+)	-0.869	0.021	-2.288	0.034	51	y	639	0
23.15	25	<i>Bulimina (aff.) midwayensis</i>	3 (250-300)	-0.302	0.033	-2.082	0.083		y	657	0
9.00	11	<i>Bulimina aksuatica</i>	25 (125-180)	-1.594	0.018	-2.160	0.079		y	757	0

**Appendix I.: Measurements - Benthic species**

Height (m)	Number of Sample	Species name	Number of fossils (Size fraction, µm)	Corrected δ <sup>13</sup> C Mean	Corrected δ <sup>13</sup> C Standard Deviation	Corrected δ <sup>18</sup> O Mean	Corrected δ <sup>18</sup> O Standard Deviation	measured mass (µg)	Ultrasonic bath (yes/no)	Total CO <sub>2</sub> pressure in mass spectrometer	Number of gas expansions
14.05	17	<i>Bulimina aksuatica</i>	50 (63-125)	-1.279	0.017	-2.050	0.055		n	847	0
14.45	18	<i>Bulimina aksuatica</i>	22 (125-180)	-1.000	0.018	-2.006	0.081		y	590	0
15.95	19	<i>Bulimina aksuatica</i>	26 (125-180)	-0.316	0.034	-1.995	0.093		n	702	0
19.45	22	<i>Bulimina aksuatica</i>	24 (125-180)	-1.931	0.033	-2.555	0.065		y	618	0
20.25	23	<i>Bulimina aksuatica</i>	24 (125-180)	-1.478	0.020	-2.518	0.141		y	415	0
19.45	22	<i>Bulimina cf. thanetensis</i>	3 (300+) and 3 (250-300)	-1.855	0.030	-2.395	0.056	51	y	829	0
1.45	3	<i>Cibicidoides decoratus</i>	4 (180-250)	-0.012	0.035	-3.376	0.059	44	y		
2.35	4	<i>Cibicidoides decoratus</i>	7 (180-250)	-1.143	0.039	-2.914	0.064	53	y	815	0
3.40	5	<i>Cibicidoides decoratus</i>	6 (180-250)	-0.267	0.030	-3.431	0.050		y	688	0
4.15	6	<i>Cibicidoides decoratus</i>	4 (180-250)	0.055	0.039	-3.034	0.056	51	y	949	0
5.62	7	<i>Cibicidoides decoratus</i>	6 (180-250)	-0.254	0.030	-3.245	0.058		y		
6.75	8	<i>Cibicidoides decoratus</i>	4 (180-250)	-0.268	0.040	-2.396	0.066	46	y	869	0
7.60	9	<i>Cibicidoides decoratus</i>	6 (180-250)	-0.131	0.036	-2.397	0.062		y		
8.20	10	<i>Cibicidoides decoratus</i>	5 (180-250)	-0.168	0.051	-2.426	0.061	42	y	715	0
9.00	11	<i>Cibicidoides decoratus</i>	1 (180-250) + 8 (125- 180)	-0.377	0.044	-2.438	0.058	41	y	787	0
9.55	12	<i>Cibicidoides decoratus</i>	5 (180-250)	-0.119	0.038	-2.248	0.073	56	y	549	0
10.75	13	<i>Cibicidoides decoratus</i>	2 (250-300)	-0.426	0.019	-2.812	0.051	39	y	663	0
10.75	13	<i>Cibicidoides decoratus</i>	6 (180-250)	-0.031	0.029	-2.557	0.068		y	860	0
11.90	14	<i>Cibicidoides decoratus</i>	6 (180-250)	-0.387	0.026	-2.727	0.073		y	733	0
12.75	15	<i>Cibicidoides decoratus</i>	6 (180-250)	-0.184	0.036	-2.199	0.054	48	y	629	0
13.25	16	<i>Cibicidoides decoratus</i>	6 = 3 (180- 250) + 3 (125-180)	-0.349	0.058	-2.405	0.066		y	688	0
14.05	17	<i>Cibicidoides decoratus</i>	3 = 2 (180- 250) + 1 (250-300)	-0.278	0.038	-2.316	0.076		y		
14.45	18	<i>Cibicidoides decoratus</i>	6 (180-250)	0.059	0.039	-2.247	0.060	42	y	638	0
17.00	20	<i>Cibicidoides decoratus</i>	5 (180-250)	-0.148	0.048	-2.872	0.060	52	y	638	0
17.00	20	<i>Cibicidoides decoratus</i>	6 (180-250)	0.046	0.048	-2.688	0.055		y	663	0
18.95	21	<i>Cibicidoides decoratus</i>	4 (180-250)	0.352	0.031	-3.059	0.068		y	634	0
19.45	22	<i>Cibicidoides decoratus</i>	5 (180-250)	0.381	0.027	-2.922	0.058	48	y	645	0
19.45	22	<i>Cibicidoides decoratus</i>	6 (180-250)	0.369	0.040	-2.825	0.055		y	722	0
19.45	22	<i>Cibicidoides decoratus</i>	7 (180-250)	0.424	0.040	-2.823	0.069		y	1034	0
19.45	22	<i>Cibicidoides decoratus</i>	6 (180-250)	0.399	0.039	-2.822	0.060		y	780	0
21.50	24	<i>Cibicidoides decoratus</i>	9 = 1 (180- 250) + 8 (125-180)	0.315	0.037	-2.799	0.071		y	620	0
0.55	2	<i>Cibicidoides rigidus</i>	6 (180-250)	0.320	0.027	-2.178	0.075		y	841	0
10.75	13	<i>Cibicidoides rigidus</i>	2 = 1 (250- 300) + 1 (300+)	-0.026	0.035	-2.294	0.046		y	942	0
19.45	22	<i>Cibicidoides rigidus</i>	8 (180-250)	0.209	0.029	-2.799	0.052		y	684	0

Appendix I.: Measurements - Benthic species											
Height (m)	Number of Sample	Species name	Number of fossils (Size fraction, $\mu\text{m}$ )	Corrected $\delta^{13}\text{C}$ Mean	Corrected $\delta^{13}\text{C}$ Standard Deviation	Corrected $\delta^{18}\text{O}$ Mean	Corrected $\delta^{18}\text{O}$ Standard Deviation	measured mass ( $\mu\text{g}$ )	Ultrasonic bath (yes/no)	Total $\text{CO}_2$ pressure in mass spectrometer	Number of gas expansions
18.95	21	<i>Cibicidoides sp. 1</i>	7 (180-250)	-0.364	0.060	-3.411	0.115	44	y	825	0
23.15	25	<i>Cibicidoides sp. 1</i>	13 = 1 (180-250) + 12 (125-180)	0.335	0.075	-2.922	0.212		y	724	0
19.45	22	<i>Coryphostoma spp.</i>	52 (63-125)	-1.543	0.052	-2.392	0.039		y	871	0
10.75	13	<i>Dentalina species 1</i>	5 (125-180)	-1.797	0.024	-2.302	0.048		y	569	0
10.75	13	<i>Lenticulina sp. 1</i>	3 (180-250)	-2.905	0.042	-2.777	0.108		y	268	0
14.05	17	<i>Lenticulina sp. 1</i>	5 = 4 (180-250) + 1 (125-180)	-3.800	0.034	-2.746	0.079	65	y	686	0
10.75	13	<i>Lenticulina sp. 2</i>	3 (180-250)	-1.895	0.039	-2.493	0.080	44	y	506	0
10.75	13	<i>Lenticulina sp. 3</i>	fragment (300+)	-3.057	0.031	-2.644	0.080	41	y	700	0
19.45	22	<i>Lenticulina sp. 3</i>	fragment (300+)	-1.738	0.022	-2.812	0.050	50	y	947	0
10.75	13	<i>Lenticulina sp. 4</i>	fragment (300+)	-0.369	0.032	-2.061	0.074	38	n	334	0
19.45	22	<i>Lenticulina sp. 4</i>	fragment (300+)	-1.442	0.025	-2.957	0.041	54	y	958	0
10.75	13	<i>Loxostomoides applinae</i>	9 (125-180)	-1.361	0.024	-1.711	0.059		y	960	0
14.05	17	<i>Loxostomoides applinae</i>	10 (125-180)	-1.139	0.033	-1.756	0.048		y	837	0
10.75	13	<i>Marginulinopsis sp. 1</i>	fragment (300+)	-0.746	0.039	-2.066	0.076	40	y	460	0
14.05	17	<i>Marginulinopsis sp. 2</i>	12 = 9 (125-180) + 3 (180-250)	-2.701	0.025	-2.656	0.046		y	572	0
10.75	13	<i>Nodosaria sp. 1</i>	fragment (300+)	-3.334	0.038	-2.483	0.084		y	789	0
10.75	13	<i>Nodosaria sp. 1</i>	7 (125-180)	-3.935	0.023	-2.769	0.053	48	y	750	0
14.05	17	<i>Nodosaria sp. 1</i>	4 = 2 (125-180) + 2 (180-250)	-5.066	0.035	-2.747	0.049	50	y	467	0
19.45	22	<i>Nodosaria sp. 1</i>	3 (250-300)	-5.062	0.028	-3.300	0.047	51	y	914	0
3.40	5	<i>Nuttallides truempyi</i>	3 (125-180)	-0.437	0.039	-3.625	0.073	47	y	732	0
10.75	13	<i>Nuttallides truempyi</i>	6 (125-180)	-0.336	0.034	-2.272	0.077		y	988	0
10.75	13	<i>Oridorsalis plummerae</i>	9 = 5 (180-250) + 4 (125-180)	-1.163	0.021	-2.192	0.043		y	851	0
14.05	17	<i>Oridorsalis plummerae</i>	12 = 5 (180-250) + 7 (125-180)	-1.220	0.022	-1.866	0.052		y	870	0
10.75	13	<i>Percultazonaria sp. 1</i>	fragment (300+)	-2.972	0.026	-3.146	0.041	45	y	913	0
19.45	22	<i>Percultazonaria sp. 1</i>	1 (300+)	-0.389	0.030	-2.084	0.076	49	y	721	0
10.75	13	<i>Pulsiphonina prima</i>	110 (63-125)	-0.974	0.029	-2.394	0.076		n	1007	0
19.45	22	<i>Pulsiphonina prima</i>	40 = 21 (125-180) + 19 (63-125)	-0.286	0.035	-2.785	0.048		y	849	0

**Appendix I.: Measurements - Benthic species**

Height (m)	Number of Sample	Species name	Number of fossils (Size fraction, µm)	Corrected δ <sup>13</sup> C Mean	Corrected δ <sup>13</sup> C Standard Deviation	Corrected δ <sup>18</sup> O Mean	Corrected δ <sup>18</sup> O Standard Deviation	measured mass (µg)	Ultrasonic bath (yes/no)	Total CO <sub>2</sub> pressure in mass spectrometer	Number of gas expansions
23.15	25	<i>Pulsiphonina prima</i>	5 (63-125)	-0.297	0.043	-2.742	0.100		n	773	0
10.75	13	<i>Pyramidulina sp. 1</i>	fragment (300+)	-0.713	0.036	-2.186	0.081	52	y	829	0
10.75	13	<i>Pyramidulina sp. 1</i>	fragment (300+)	-0.476	0.023	-2.081	0.051		y	741	0
19.45	22	<i>Pyramidulina sp. 1</i>	fragment (300+)	-0.381	0.032	-2.786	0.053	48	y		
10.75	13	<i>Ramulina sp. 1</i>	fragment (300+)	-1.323	0.036	-2.105	0.083	49	y	804	0
10.75	13	<i>Spiroloculina spp.</i>	9 (180-250)	0.665	0.033	-2.341	0.078		y	483	0
14.05	17	<i>Spiroloculina spp.</i>	16 (125-180)	0.658	0.037	-2.069	0.055		y	170	0
19.45	22	<i>Spiroloculina spp.</i>	9 (180-250)	0.694	0.036	-2.837	0.050	49	y	830	0
10.75	13	<i>Stainforthia sp. 1</i>	8 (125-180)	-0.817	0.026	-2.386	0.073		y	564	0
10.75	13	<i>Stilostomella sp. 1</i>	7 (125-180)	-1.103	0.020	-1.929	0.047		y	762	0
10.75	13	<i>Turrilina brevispira</i>	11 (125-180)	-0.326	0.028	-1.903	0.056		y		
6.75	8	<i>Uvigerina elongata</i>	58 (63-125)	-1.419	0.067	-2.350	0.115		n	401	0
9.00	11	<i>Uvigerina elongata</i>	51 (63-125)	-1.578	0.041	-2.329	0.076		n	359	0
10.75	13	<i>Uvigerina elongata</i>	7 (63-125)	-1.124	0.032	-2.185	0.055		n	543	0
14.05	17	<i>Uvigerina elongata</i>	64 (63-125)	-0.811	0.070	-1.987	0.085		n	823	0
15.95	19	<i>Uvigerina elongata</i>	25 (125-180)	-0.159	0.032	-1.704	0.069		y	947	0
19.45	22	<i>Uvigerina elongata</i>	25 (125-180)	-0.901	0.027	-2.251	0.052	56	y	813	0
20.25	23	<i>Uvigerina elongata</i>	23 (125-180)	-0.808	0.052	-2.340	0.076		y	883	0
21.50	24	<i>Uvigerina elongata</i>	23 (125-180)	-0.774	0.053	-2.311	0.114		n	885	0
23.15	25	<i>Uvigerina elongata</i>	38 = 30 (63-125) + 8 (125-180)	-0.834	0.032	-2.361	0.083		n	722	0
10.75	13	<i>Valvulineria scrobiculata</i>	5 = 2(300+) + 3 (180-250)	-0.974	0.033	-2.224	0.039		y	623	0
14.05	17	<i>Valvulineria scrobiculata</i>	16 = 3 (180-250) + 12 (125-180) + 1 (63-125)	-0.801	0.051	-1.962	0.074		y	729	0
19.45	22	<i>Valvulineria scrobiculata</i>	20 (125-180)	-0.764	0.026	-2.654	0.037	47	y	923	0

Appendix II.: Measurements - Planktic species										
Height (m)	Number of Sample	Species name	Number of fossils (Size fraction, $\mu\text{m}$ )	Corrected $\delta^{13}\text{C}$ Mean	Corrected $\delta^{13}\text{C}$ Standard Deviation	Corrected $\delta^{18}\text{O}$ Mean	Corrected $\delta^{18}\text{O}$ Standard Deviation	Ultrasonic bath\$ (yes/no)	Total CO2 pressure in mass spectrometer	Number of gas expansions in mass spectrometer
1.45	3	<i>Acarinina</i> sp. 1: <i>Acarinina esnehensis?</i>	5 (250-300)	2.452	0.072	-6.339	0.247	y	785	0
2.35	4	<i>Acarinina</i> sp. 2: <i>Acarinina cuneicamerata?</i>	5 (250-300)	2.116	0.036	-6.039	0.066	y	692	0
6.75	8	<i>Acarinina</i> sp. 1: <i>Acarinina esnehensis?</i>	5 (250-300)	2.935	0.035	-5.264	0.082	y	512	0
12.75	15	<i>Acarinina</i> sp. 3: <i>Acarinina medizai?</i>	5 (250-300)	2.728	0.026	-4.055	0.079	y	525	0
13.25	16	<i>Acarinina</i> sp. 3: <i>Acarinina medizai?</i>	4 (250-300)	3.378	0.034	-5.051	0.104	y	719	0
13.25	16	<i>Acarinina</i> sp. 3: <i>Acarinina medizai?</i>	5 (250-300)	4.294	0.072	-5.713	0.145	y	446	0
19.45	22	<i>Acarinina</i> sp. 3: <i>Acarinina medizai?</i>	5 (250-300)	2.215	0.031	-4.851	0.078	y	533	0
19.45	22	<i>Acarinina</i> sp. 4: ?	5 (250-300)	2.535	0.036	-3.971	0.086	y	545	0
20.25	23	<i>Acarinina</i> sp. 3: <i>Acarinina medizai?</i>	6 (250-300)	4.774	0.040	-6.950	0.073	n	510	0
23.15	25	<i>Acarinina</i> species 5: ?	6 (250-300)	2.637	0.044	-4.766	0.076	n	479	0
1.45	3	<i>Subbotina</i> sp. 1: <i>Subbotina patagonica?</i>	6 (250-300)	1.127	0.054	-3.470	0.091	y	828	0
2.35	4	<i>Subbotina</i> sp. 2: <i>Parasubbotina pseudowilsoni?</i>	6 (250-300)	-0.256	0.023	-3.552	0.064	n	921	0
7.60	9	<i>Subbotina</i> sp. 1: <i>Subbotina patagonica?</i>	7 (250-300)	1.483	0.035	-3.566	0.066	y	712	0
7.60	9	<i>Subbotina</i> sp. 3: ?	7 (250-300)	1.494	0.021	-3.660	0.075	y	837	0
9.55	12	<i>Subbotina</i> sp. 3: ?	7 (250-300)	0.819	0.046	-4.079	0.105	y	578	0
9.55	12	<i>Subbotina</i> sp. 3: ?	6 (250-300)	0.933	0.035	-3.759	0.070	y	677	0
9.55	12	<i>Subbotina</i> sp. 1: <i>Subbotina patagonica?</i>	6 (250-300)	1.097	0.039	-3.894	0.074	y	628	0
13.25	16	<i>Subbotina</i> sp. 3: ?	7 (250-300)	0.663	0.032	-3.394	0.090	n	632	0
13.25	16	<i>Subbotina</i> sp. 4: <i>Subbotina yegaensis?</i>	6 (250-300)	1.374	0.018	-3.622	0.071	n	1026	0
19.45	22	<i>Subbotina</i> sp. 1: <i>Subbotina patagonica?</i>	6 (250-300)	1.387	0.025	-3.585	0.058	n	750	0
20.25	23	<i>Subbotina</i> sp. 4: <i>Subbotina yegaensis?</i>	6 (250-300)	1.049	0.021	-4.029	0.073	n	692	0

Appendix III.: Preservation issues observed with binocular microscope			
Height (m)	Number of Sample	Species name	Description of observed contamination/preservation risks
0.55	2	<i>Anomalinoides acutus</i>	Moderate preservation, possible start of recrystallization.
0.55	2	<i>Anomalinoides zitteli</i>	Moderate preservation, possible start of recrystallization.
0.55	2	<i>Cibicidoides rigidus</i>	Moderate preservation, possible start of recrystallization.
1.45	3	<i>Anomalinoides acutus</i>	Moderate preservation, possible start of recrystallization.
1.45	3	<i>Cibicidoides decoratus</i>	Clearly affected by recrystallization, faded textures.
3.40	5	<i>Cibicidoides decoratus</i>	Clearly affected by significant secondary calcite precipitation.
3.40	5	<i>Nuttallides truempyi</i>	Does not appear recrystallized but likely affected by secondary calcite.
4.15	6	<i>Anomalinoides acutus</i>	Moderate preservation, possible secondary calcite? Careful selection to take best specimens.
4.15	6	<i>Cibicidoides decoratus</i>	Affected by recrystallization and secondary calcite precipitation.
5.62	7	<i>Cibicidoides decoratus</i>	Affected by recrystallization and secondary calcite precipitation.
8.20	10	<i>Anomalinoides acutus</i>	Bulk contamination possible.
10.75	13	<i>Cibicidoides decoratus</i>	2 fossils of the 250-300 µm fraction. one contains traces of iron oxide.
13.25	16	<i>Cibicidoides decoratus</i>	1 specimen contains significant amount of iron oxide.
14.05	17	<i>Anomalinoides cf. praeacutus</i>	12 specimens with significant amounts of iron oxide
14.05	17	<i>Aragonia aragonensis</i>	13 specimens with significant amounts of iron oxide
14.05	17	<i>Bulimina kugleri</i>	1 specimen with significant amounts of iron oxide
14.05	17	<i>Cibicidoides cf. decoratus</i>	6 specimens with significant amounts of iron oxide
14.05	17	<i>Lenticulina sp. 1</i>	3 specimens contain significant amounts of iron oxide
14.45	18	<i>Bulimina aksuatica</i>	Some specimens with iron oxides
15.95	19	<i>Anomalinoides acutus</i>	3 specimens with significant amounts of iron oxide
15.95	19	<i>Bulimina aksuatica</i>	15 specimens with significant amounts of iron oxide, moderate preservation
15.95	19	<i>Uvigerina elongata</i>	Moderate preservation, possibly slightly affected by secondary calcite?
17.00	20	<i>Anomalinoides acutus</i>	Moderate preservation, possible start of recrystallization
17.00	20	<i>Cibicidoides decoratus</i>	4 specimens contain significant amounts of iron oxide
18.95	21	<i>Cibicidoides decoratus</i>	Secondary calcite and bulk contamination possible (attempt to clean as much as possible)
18.95	21	<i>Cibicidoides sp. 1</i>	Significant risk of secondary calcite precipitation and recrystallization
23.15	25	<i>Uvigerina elongata</i>	Affected by secondary calcite. (verified by SEM)

**Appendix IV.: Natural isotopic variability of epibenthic specimen**

Estimation of the standard deviation (= an average of n specimens) due to natural isotopic variability for epibenthic specimen based on the data of modern epibenthic *Cibicidoides wuellerstorfi* (Franco-Fraguas *et al.*, 2011). Their study provides 16 measurements of *Cibicidoides wuellerstorfi*:

number	$\delta^{18}\text{O}$ (‰ VPDB)	(Mean-measurement) <sup>2</sup>	number	$\delta^{13}\text{C}$ (‰ VPDB)	(Mean-measurement) <sup>2</sup>
1	2.85	0.007987891	1	1.25	0.002082
2	2.94	0.032175391	2	1.43	0.018057
3	2.79	0.000862891	3	1.28	0.000244
4	2.79	0.000862891	4	1.36	0.004144
5	2.86	0.009875391	5	1.34	0.001969
6	2.72	0.001650391	6	1.25	0.002082
7	2.77	8.78906E-05	7	1.37	0.005532
8	2.79	0.000862891	8	1.21	0.007332
9	2.64	0.014550391	9	1.16	0.018394
10	2.63	0.017062891	10	1.21	0.007332
11	2.85	0.007987891	11	1.39	0.008907
12	2.62	0.019775391	12	1.15	0.021207
13	2.91	0.022312891	13	1.44	0.020844
14	2.82	0.003525391	14	1.28	0.000244
15	2.61	0.022687891	15	1.38	0.007119
16	2.58	0.032625391	16	1.23	0.004307
MEAN	2.76		MEAN	1.30	
STD	0.11		STD	0.09	
VAR	0.0130		VAR	0.0087	

	Variance $\delta^{18}\text{O}$	STD $\delta^{18}\text{O}$	Variance $\delta^{13}\text{C}$	STD $\delta^{13}\text{C}$
If 1 specimen is used for 1 measurement:	0.0130	0.11	0.0087	0.09
If 2 specimens are used for 1 measurement:	0.0065	0.08	0.0043	0.07
If 3 specimens are used for 1 measurement:	0.0043	0.07	0.0029	0.05
If 4 specimens are used for 1 measurement:	0.0032	0.06	0.0022	0.05
If 5 specimens are used for 1 measurement:	0.0026	0.05	0.0017	0.04
If 6 specimens are used for 1 measurement:	0.0022	0.05	0.0014	0.04
If 7 specimens are used for 1 measurement:	0.0019	0.04	0.0012	0.04
If 8 specimens are used for 1 measurement:	0.0016	0.04	0.0011	0.03

**Appendix V.:  $\delta^{13}\text{C}$  correlation of *Cibicoides decoratus* and *Anomalinoidea acutus***

Sample	$\delta^{13}\text{C}$ <i>C. decoratus</i> (‰ VPDB)	$\delta^{13}\text{C}$ <i>A. acutus</i> (‰ VPDB)	Best fit correlation	Best fit correlation with slope = 0
			$\delta^{13}\text{C}_{(C. decoratus)} = 0.849 * \delta^{13}\text{C}_{(A. acutus)} + 0.268\text{‰}$	$\delta^{13}\text{C}_{(C. decoratus)} = \delta^{13}\text{C}_{(A. acutus)} + 0.318\text{‰}$
			Predicted $\delta^{13}\text{C}$ <i>C. decoratus</i> (‰ VPDB)	Predicted $\delta^{13}\text{C}$ <i>C. decoratus</i> (‰ VPDB)
4	-1.143	-1.372	-0.897	-1.054
8	-0.268	-0.598	-0.239	-0.280
10	-0.168	-0.914	-0.508	-0.596
13	-0.228	-0.430	-0.097	-0.112
17	-0.278	-0.572	-0.218	-0.254
20	-0.051	-0.008	0.261	0.310
22	0.393	-0.176	0.119	0.143
24	0.315	0.097	0.350	0.415
Mean:	-0.178	-0.496	-0.154	-0.178
Mean <sub>(C. decoratus)</sub> - Mean <sub>(A. acutus)</sub> =		0.318‰		
Measured versus predicted <i>C. decoratus</i> , Standard deviation (1 $\sigma$ )			0.230	0.242

**Appendix VI.:  $\delta^{18}\text{O}$  correlation of *Cibicoides decoratus* and *Anomalinoidea acutus***

Sample	$\delta^{18}\text{O}$ <i>C. decoratus</i> (‰ VPDB)	$\delta^{18}\text{O}$ <i>A. acutus</i> (‰ VPDB)	Best fit correlation	Best fit correlation with slope = 0
			$\delta^{18}\text{O}_{(C. decoratus)} = 0.850 * \delta^{18}\text{O}_{(A. acutus)} + 0.397\text{‰}$	$\delta^{18}\text{O}_{(C. decoratus)} = \delta^{18}\text{O}_{(A. acutus)} + 0.001\text{‰}$
			Predicted $\delta^{18}\text{O}$ <i>C. decoratus</i> : (‰ VPDB)	Predicted $\delta^{18}\text{O}$ <i>C. decoratus</i> : (‰ VPDB)
4	-2.914	-2.825	-2.004	-2.824
8	-2.396	-2.261	-1.525	-2.260
10	-2.426	-2.562	-1.781	-2.561
13	-2.685	-2.633	-1.841	-2.632
17	-2.316	-2.417	-1.657	-2.416
20	-2.780	-2.630	-1.839	-2.629
22	-2.848	-2.950	-2.110	-2.949
24	-2.799	-2.895	-2.064	-2.894
Mean:	-2.646	-2.647	-1.853	-2.646
Mean <sub>(C. decoratus)</sub> - Mean <sub>(A. acutus)</sub> =		0.001		
Measured versus predicted <i>C. decoratus</i> , Standard deviation (1 $\sigma$ )			0.114	0.119



**Appendix VII.:  $\delta^{13}\text{C}$  correlation of *Anomalinoidea acutus* and *Anomalinoidea zitteli***

Sample	$\delta^{13}\text{C}$ <i>A. acutus</i> (‰ VPDB)	$\delta^{13}\text{C}$ <i>A. zitteli</i> (‰ VPDB)	Best fit correlation	Best fit correlation with slope = 0
			$\delta^{13}\text{C}_{(A. acutus)} = 0.9278 * \delta^{13}\text{C}_{(A. zitteli)} - 0.3556\text{‰}$	$\delta^{13}\text{C}_{(A. acutus)} = \delta^{13}\text{C}_{(A. zitteli)} - 0.360\text{‰}$
			Predicted $\delta^{13}\text{C}$ <i>A. acutus</i> (‰ VPDB)	Predicted $\delta^{13}\text{C}$ <i>A. acutus</i> (‰ VPDB)
2	0.166	0.478	0.088	0.118
4	-1.372	-1.088	-1.365	-1.448
20	-0.008	0.271	-0.104	-0.089
22	-0.176	0.402	0.017	0.042
23	-0.132	0.213	-0.158	-0.147
Mean:	-0.304	0.055	-0.304	-0.305
Mean <sub>(A. acutus)</sub> - Mean <sub>(A. zitteli)</sub> =		-0.360		
Measured versus predicted <i>A. acutus</i> , Standard deviation ( $1\sigma$ )			0.115	0.124

**Appendix VIII.:  $\delta^{13}\text{C}$  correlation of *Cibicoides decoratus* and *Anomalinoidea zitteli***

Sample	$\delta^{13}\text{C}$ <i>C. decoratus</i> (‰ VPDB)	$\delta^{13}\text{C}$ <i>A. zitteli</i> (‰ VPDB)	Best fit correlation	Best fit correlation with slope = 0 based on <i>A. acutus</i> and <i>A. zitteli</i>
			$\delta^{13}\text{C}_{(C. decoratus)} = 0.9382 * \delta^{13}\text{C}_{(A. acutus)} - 0.1373\text{‰}$	$\delta^{13}\text{C}_{(C. decoratus)} = \delta^{13}\text{C}_{(A. zitteli)} - 0.042\text{‰}$
			Predicted $\delta^{13}\text{C}$ <i>C. decoratus</i> (‰ VPDB)	Predicted $\delta^{13}\text{C}$ <i>C. decoratus</i> (‰ VPDB)
4	-1.143	-1.088	-1.158	-1.130
20	-0.051	0.271	0.117	0.229
22	0.393	0.402	0.239	0.360
Mean:	-0.267	-0.138	-0.267	-0.180
Mean <sub>(C. decoratus)</sub> - Mean <sub>(A. zitteli)</sub> =		-0.128		
Measured versus predicted <i>C. decoratus</i> , Standard deviation ( $1\sigma$ )			0.161	0.200

**Appendix IX.:  $\delta^{18}\text{O}$  correlation of *Anomalinoides acutus* and *Anomalinoides zitteli***

			Best fit correlation	Best fit correlation with slope = 0
			$\delta^{18}\text{O}_{(A. acutus)} = 0.519 * \delta^{18}\text{O}_{(A. zitteli)} - 1.3523\text{‰}$	$\delta^{18}\text{O}_{(A. acutus)} = \delta^{18}\text{O}_{(A. zitteli)} - 0.135\text{‰}$
Sample	$\delta^{18}\text{O}$ <i>A. acutus</i> (‰ VPDB)	$\delta^{18}\text{O}$ <i>A. zitteli</i> (‰ VPDB)	Predicted $\delta^{18}\text{O}$ <i>A. acutus</i> (‰ VPDB)	Predicted $\delta^{18}\text{O}$ <i>A. acutus</i> (‰ VPDB)
2	-2.161	-2.124	-2.455	-2.259
4	-2.825	-3.143	-2.984	-3.278
20	-2.630	-2.459	-2.629	-2.594
22	-2.950	-2.535	-2.668	-2.670
23	-2.763	-2.393	-2.594	-2.528
Mean:	-2.666	-2.531	-2.666	-2.666
Mean <sub>(A. acutus)</sub> - Mean <sub>(A. zitteli)</sub> =		-0.135		
Measured versus predicted <i>C. decoratus</i> , Standard deviation (1 $\sigma$ )			0.234	0.296

**Appendix X.:  $\delta^{18}\text{O}$  correlation of *Cibicoides decoratus* and *Anomalinoides zitteli***

$\delta^{18}\text{O}_{(C. decoratus)} = \delta^{18}\text{O}_{(A. acutus)} + 0.001\text{‰}$   
 $\delta^{18}\text{O}_{(A. acutus)} = \delta^{18}\text{O}_{(A. zitteli)} - 0.135\text{‰}$   
 $\delta^{18}\text{O}_{(C. decoratus)} = \delta^{18}\text{O}_{(A. zitteli)} - 0.135\text{‰} + 0.001\text{‰}$   
 $\delta^{18}\text{O}_{(C. decoratus)} = \delta^{18}\text{O}_{(A. zitteli)} - 0.134\text{‰}$

			Best fit correlation	Best fit correlation with slope = 0 based on <i>Anomalinoides acutus</i>
			$\delta^{18}\text{O}_{(C. decoratus)} = 0.0967 * \delta^{18}\text{O}_{(A. acutus)} - 2.5395\text{‰}$	$\delta^{18}\text{O}_{(C. decoratus)} = \delta^{18}\text{O}_{(A. zitteli)} - 0.134\text{‰}$
Sample	$\delta^{18}\text{O}$ <i>C. decoratus</i> (‰ VPDB)	$\delta^{18}\text{O}$ <i>A. zitteli</i> (‰ VPDB)	Predicted $\delta^{18}\text{O}$ <i>C. decoratus</i> (‰ VPDB)	Predicted $\delta^{18}\text{O}$ <i>C. decoratus</i> (‰ VPDB)
4	-2.825	-3.143	-2.843	-3.277
20	-2.630	-2.459	-2.777	-2.593
22	-2.950	-2.535	-2.785	-2.669
Mean:	-2.802	-2.712	-2.802	-2.846
Mean <sub>(C. decoratus)</sub> - Mean <sub>(A. zitteli)</sub> =		-0.089		
Measured versus predicted <i>C. decoratus</i> , Standard deviation (1 $\sigma$ )			0.157	<b>0.377</b>

Appendix XI. The clustered species of Deprez *et al.* (2012)

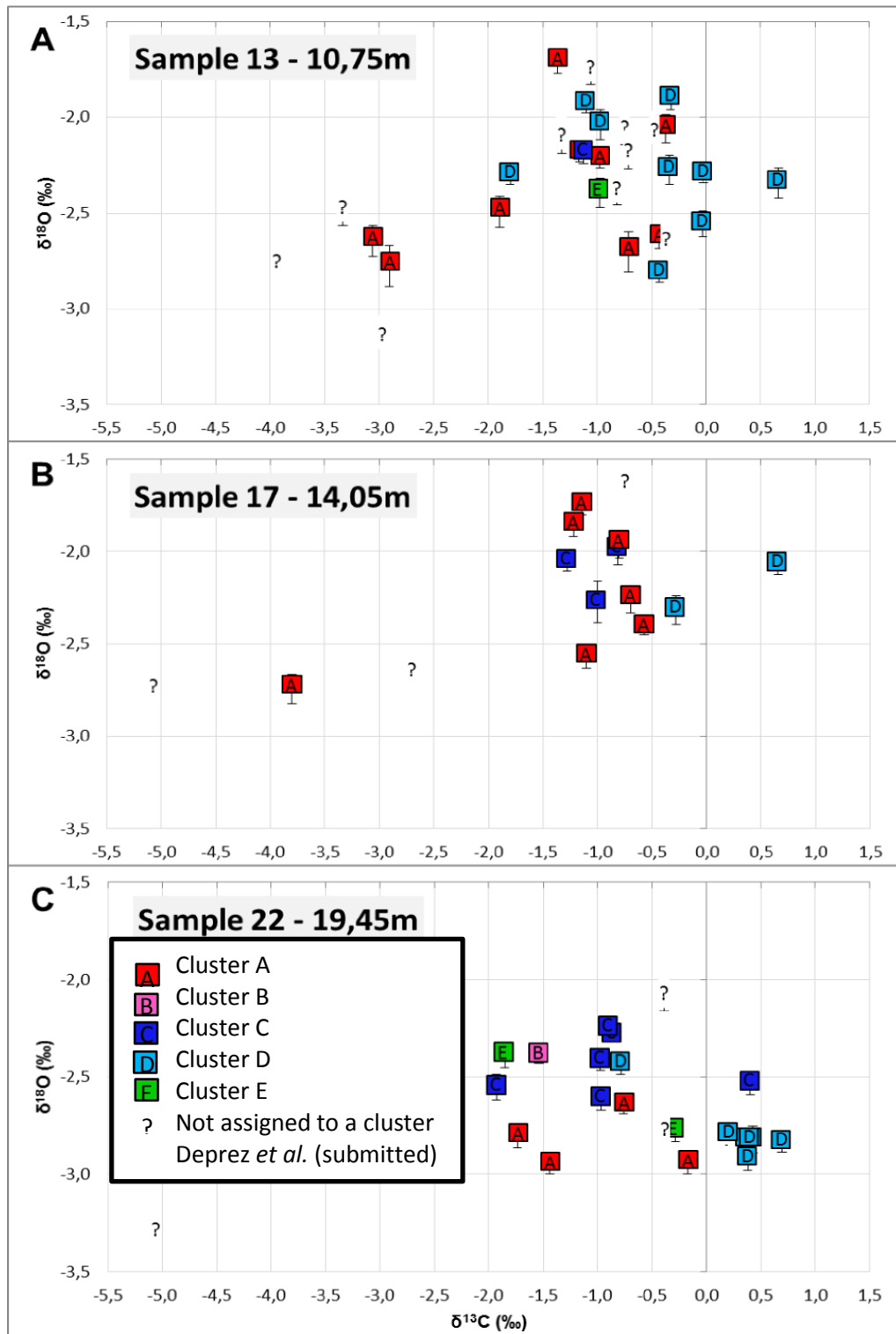


Figure 84. The figures demonstrate the  $\delta^{13}\text{C}$  and  $\delta^{18}\text{O}$  values of the species at 10.75 m (A), 14.05 m (B) and 19.45 m (C). The species were assigned to their cluster defined by Deprez *et al.* (2012). It became apparent that the clusters cannot be isotopically distinguished and that the clusters are not restricted to a specific isotopic range. The clusters were not further discussed in the study.

## Appendix XII. Taxonomy

Most of the species in this study were identified based on the taxonomic interpretation of Deprez (2012) and Deprez *et al.* (submitted). SEM images of the species are presented in Figure 85, Figure 86 and Figure 87.

Figure 85: SEM images

- |  |  |
|--|--|
| 1a, 1b: <i>Lenticulina</i> sp. 1 [13]                | 2a, 2b: <i>Lenticulina</i> sp. 2 [13]        |
| 3a, 3b: <i>Lenticulina</i> sp. 3 [13]                | 4a, 4b: <i>Lenticulina</i> sp. 4 [13]        |
| 5: <i>Nodosaria</i> sp. 1 [22]                       | 6: <i>Ramulina</i> sp. 1 [13]                |
| 7: <i>Allomorpha</i> sp. 1 [13]                      | 8a, 8b: <i>Anomalinoidea rubiginosa</i> [13] |
| 9: <i>Bulimina kugleri</i> sp. 1 [17]                | 10: <i>Stainforthia</i> sp. 1 [13]           |
| 11a, 11b, 11c: <i>Anomalinoidea cf. rigidus</i> [22] | 12: <i>Marginulinopsis</i> sp. 1 [13]        |
| 13: <i>Marginulinopsis</i> sp. 2 [17]                | 14: <i>Pyramidulina</i> sp. 1 [22]           |
| 15: <i>Cibicidoides</i> sp. 1 [25]                   | 16: <i>Percultazonaria</i> sp. 1 [22]        |

Figure 86: SEM images (Deprez *et al.*, submitted).

1) *Loxostomoides applinae* [16], 2) *Cibicidoides cf. decoratus* [14], 3) *Valvulineria scrobiculata* [16], 4) *Anomalinoidea cf. praeacutus* [15], 5) *Anomalinoidea acutus* [24], 6) *Lenticulina* spp. [14], 7) *Oridorsalis plummerae* [14], 8) *Coryphostoma* spp. [14], 9) *Valvalabamina planulata* [14], 10) *Uvigerinella? sp. 1* [24], 11) *Aragonia aragonensis* [24], 12) *Epistominella minuta* [17], 13) *Bulimina aksuatica* [17], 14) *Anomalinoidea? sp. 2* [3], 15) *Uvigerina elongata* [14], 16) *Quinqueloculina* spp. [20], 17) *Bulimina (aff.) midwayensis* [24], 18) *Anomalinoidea zitteli* [15], 19) dinoflagellate cyst [22], 20) group of dinoflagellate cysts [22].

Figure 87: SEM images (Deprez *et al.*, submitted).

1) *Dentalina* spp. [14], 2) *Stilostomella* spp. [15], 3) *Spiroplectinella esnaensis* [15], 4) *Spiroloculina* spp. [14], 5) *Cibicidoides decoratus* [15], 6) *Lagena* spp. [16], 7) *Cibicidoides rigidus* [15], 8) *Tritaxia midwayensis* [14], 9) *Nuttallides truempyi* [14], 10) *Alabamina obtusa* [14], 11) *Turrilina brevispira* [15], 12) *Paralabamina lunata* [14], 13) *Globocassidulina subglobosa* [14], 14) *Cibicidoides eocaenus* [2], 15) *Osangularia plummerae* [2], 16) *Gyroidinoidea octocameratus* [14], 17) *Pulsiphonina prima* [14], 18) *Bulimina cf. thanetensis* [16], 19) *Seabrookia lagenoides* [5], 20) *Pseudouvigerina triangularis* [2], 21) *Valvalabamina depressa?* [14].

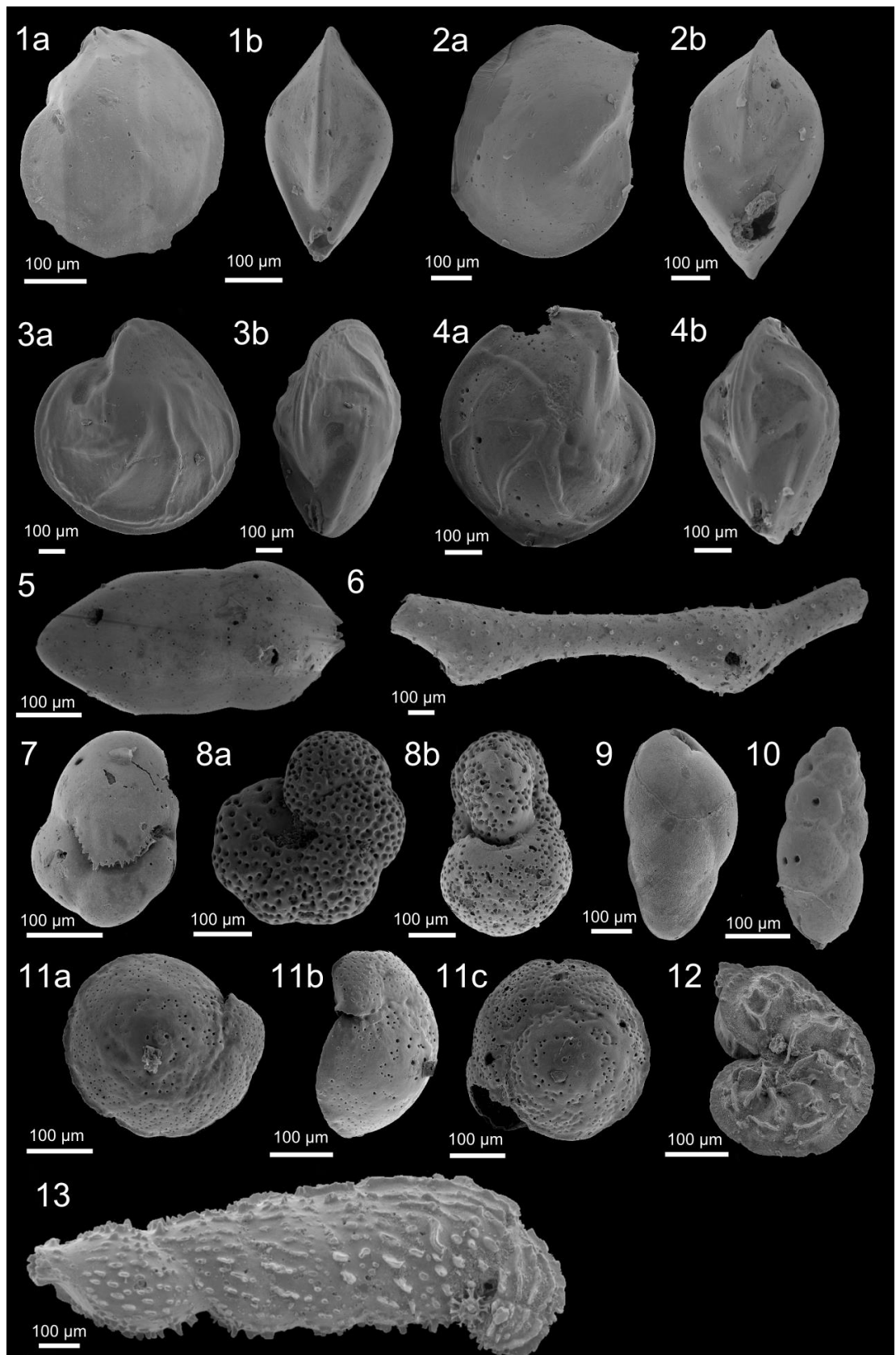


Figure 85. SEM-pictures.

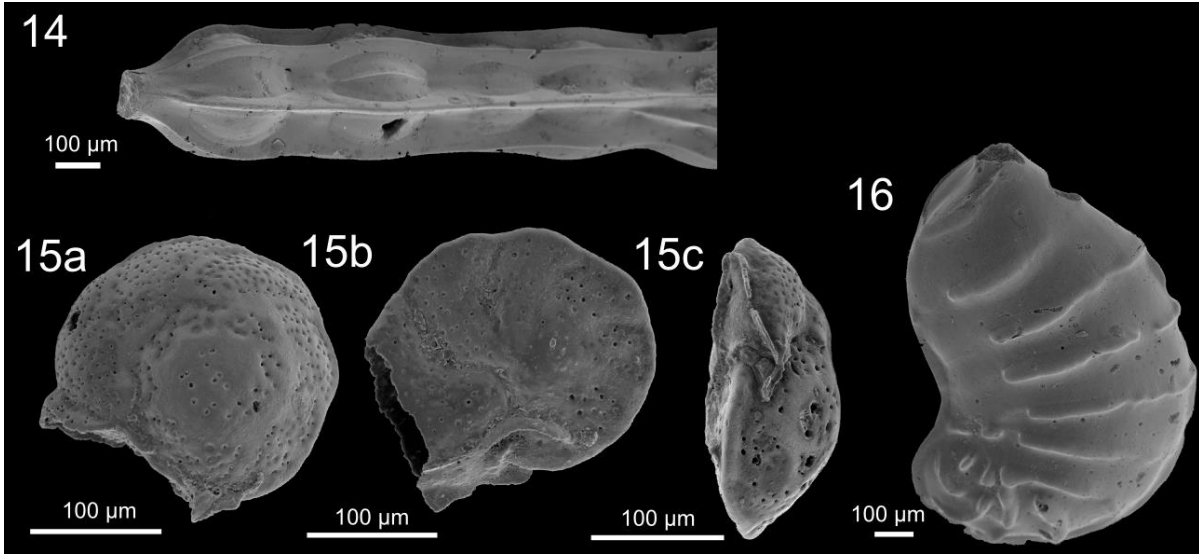


Figure 85 (continued).

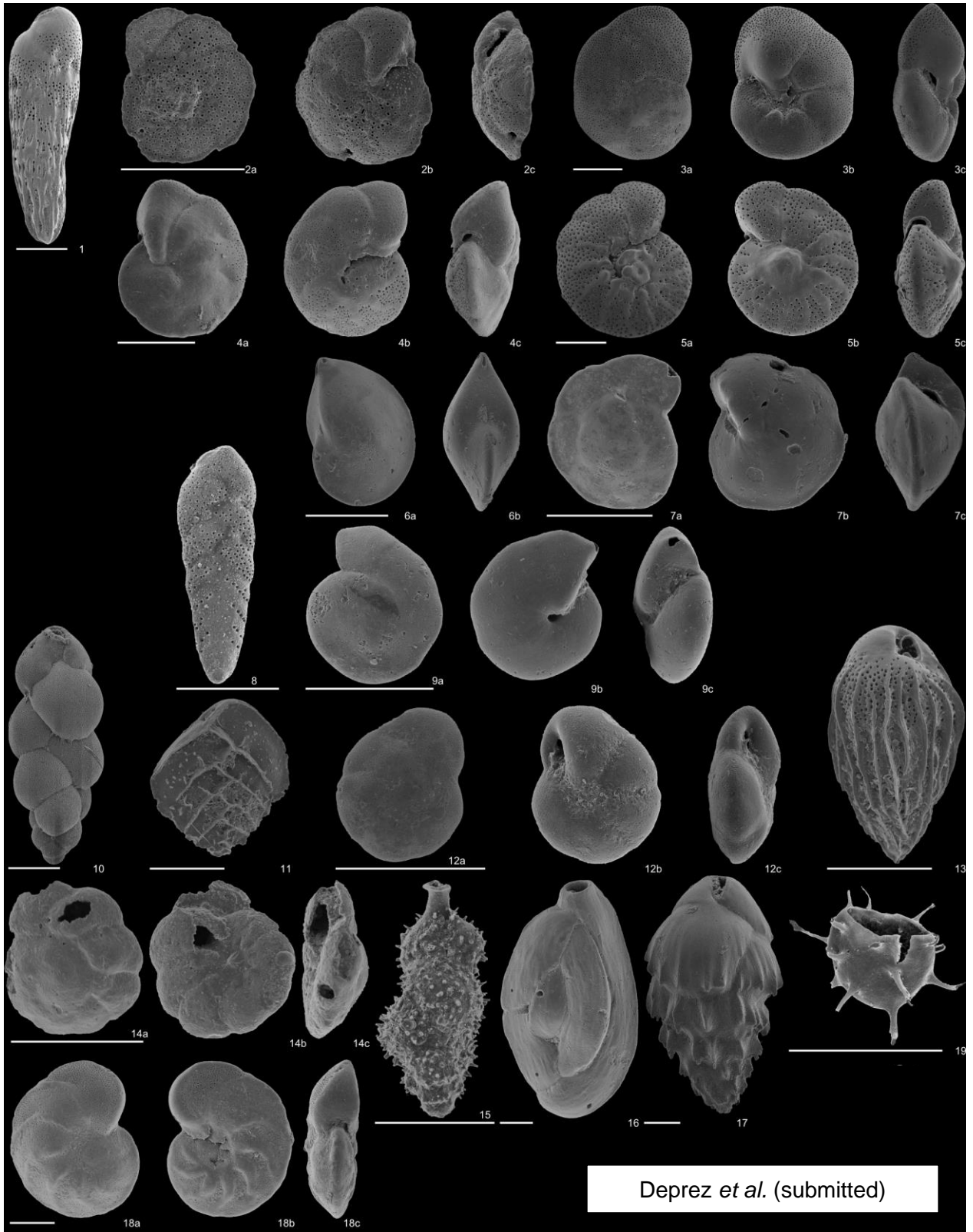


Figure 86. SEM images from Deprez *et al.* (submitted). The scale bar represents 100  $\mu\text{m}$ .

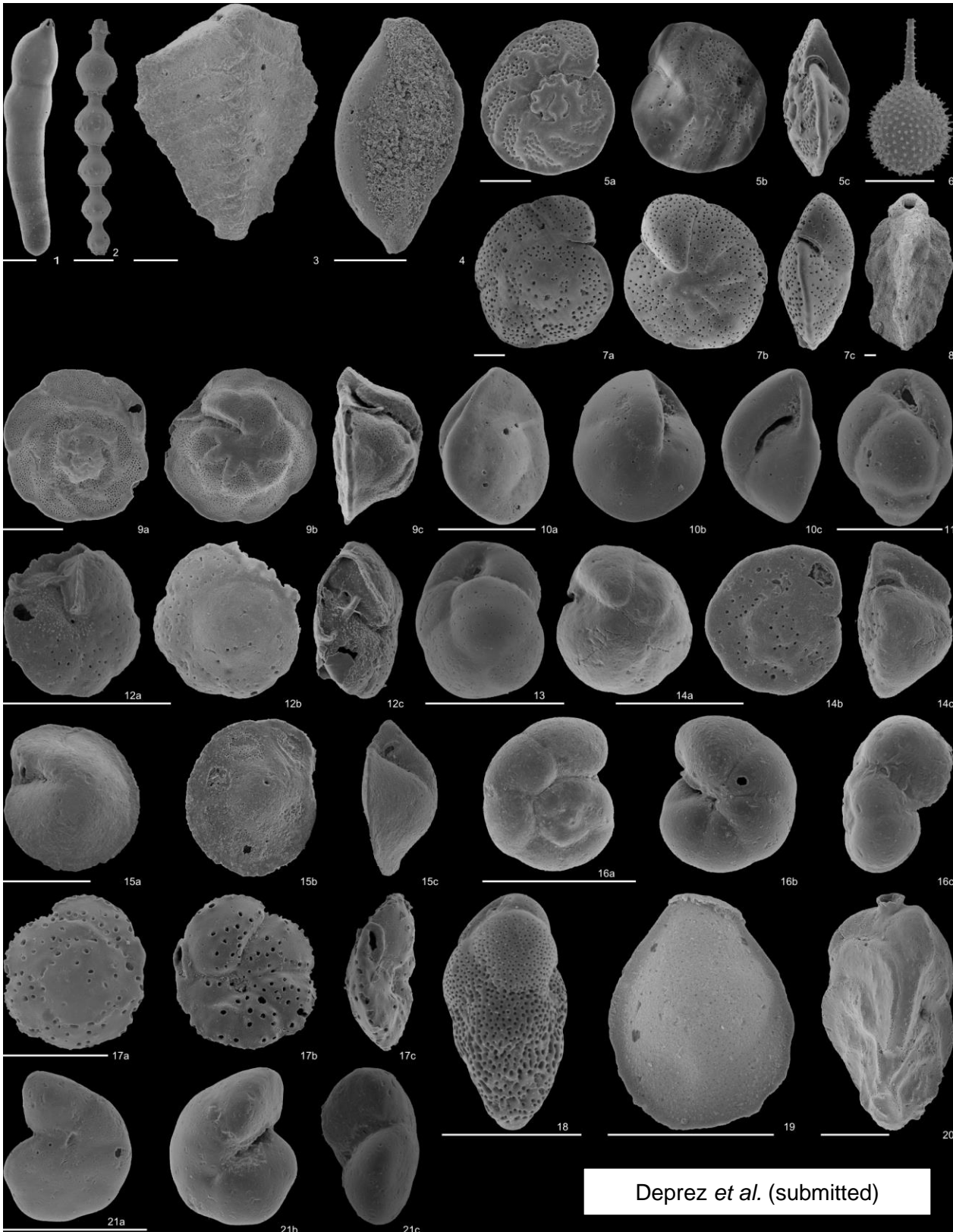


Figure 87. SEM images from Depez *et al.* (submitted). The scale bar represents 100  $\mu\text{m}$ .





**AFDELING GEOLOGIE**  
Celestijnenlaan 200 E bus 2408  
3000 LEUVEN, BELGIË  
tel. + 32 16 32 64 60  
fax + 32 16 32 29 80  
[www.kuleuven.be](http://www.kuleuven.be)

